



Final Report to the Beach Erosion Authority for Clean Oceans and Nourishment (BEACON)

Coastal Processes Study of Santa Barbara and Ventura Counties, California

By Patrick L. Barnard, David L. Revell, Dan Hoover, Jon Warrick, John Brocatus, Amy E. Draut, Pete Dartnell, Edwin Elias, Neomi Mustain, Pat E. Hart, and Holly F. Ryan



Open File Report 2009–1029

**U.S. Department of the Interior
U.S. Geological Survey**

U.S. Department of the Interior

KEN SALAZAR, Secretary

U.S. Geological Survey

Suzette M. Kimball, Acting Director

U.S. Geological Survey, Reston, Virginia: 2009

For product and ordering information:

World Wide Web: <http://www.usgs.gov/pubprod>

Telephone: 1-888-ASK-USGS

For more information on the USGS—the Federal source for science about the Earth, its natural and living resources, natural hazards, and the environment:

World Wide Web: <http://www.usgs.gov>

Telephone: 1-888-ASK-USGS

Suggested citation:

Barnard, P.L., Revell, D.L., Hoover, D., Warrick, J., Brocatus, J., Draut, A.E., Dartnell, P., Elias, E., Mustain, N., Hart, P.E., and Ryan, H.F., 2009, Coastal processes study of Santa Barbara and Ventura Counties, California: U.S. Geological Survey Open-File Report 2009-1029, 904 p. [<http://pubs.usgs.gov/of/2009/1029/>].

Any use of trade, product, or firm names is for descriptive purposes only and does not imply endorsement by the U.S. Government.

Although this report is in the public domain, permission must be secured from the individual copyright owners to reproduce any copyrighted material contained within this report.

Contents

Executive Summary of Major Findings	1
Chapter 2—Historical Changes.....	2
Chapter 3—BEACON Surveys.....	4
Chapter 4—Recent Morphological Changes.....	4
Chapter 5—Grain-Size Analysis	6
Chapter 6—The Impacts of Debris Basins on Sediment Delivery to the Santa Barbara Littoral Cell, California	7
Chapter 7—Multibeam Bathymetry	7
Chapter 8—Seismic-Reflection Images of Shallow Sedimentary Deposits	8
Chapter 9—Numerical Modeling	8
Chapter 1—Introduction.....	9
Project Summary	9
Project Objectives	10
Project Approach	10
Future Work	11
Report Outline.....	11
Project Support and Collaboration	12
Acknowledgments.....	13
References.....	13
Chapter 2—Historical Changes	15
Summary.....	15
Introduction	16
Methods	20

Historical Air Photos and Topographic Sheets	20
Lidar and GPS Surveys	22
Uncertainties and Errors.....	23
Correlation of Dredge Volumes and Beach Volumes	25
Results	26
Beach Widths	26
Beach Widths and Shoreline Orientations	28
Shoreline Changes.....	29
Case Study: Carpinteria Erosion	31
Case Study: Hope Ranch.....	33
Sand Transport and Lag Correlation Analyses.....	33
Discussion.....	36
Beach Width.....	36
Shoreline Changes.....	38
Human Alterations.....	38
Storm Event Responses.....	40
Sediment Transport and Lag Correlations.....	40
Conclusions	42
References.....	45
Chapter 3—BEACON Surveys	63
Introduction	63
Methods	63
Results	65
Recent Changes (2003-2007)	65

Recent Decadal Changes (1987-2007)	67
Other Observations	68
Shoreline-Change Rates	68
Conclusions	69
References.....	70
Chapter 4—Recent Morphological Changes	82
Introduction	82
Methods	82
Lidar	83
All-Terrain Vehicle Surveys	83
Coastal Profiling System	83
Analysis Tools	84
Results	84
Lidar	84
Lidar Shoreline Change 1998-2005.....	84
Beach Slope	86
All-Terrain Vehicle Beach-Topography Mapping	86
Ellwood/Isla Vista/Goleta	87
Carpinteria	88
Ventura/Santa Clara River Mouths	89
Coastal Profiling System Bathymetry Mapping.....	90
Ellwood/Isla Vista/Goleta	91
Carpinteria	92
Rincon Parkway.....	93

Ventura/Santa Clara River Mouths	94
Mugu Canyon	96
Offshore Wave Conditions (2005-2008)	96
Conclusions	97
References.....	99
 Chapter 5—Grain-Size Analysis	141
Introduction	141
Methods	141
Bed-Sediment Cameras	141
Box Coring	143
Results	143
Discussion.....	146
Conclusions	147
References.....	147
 Chapter 6— The Impacts of Debris Basins on Sediment Delivery to the Santa Barbara Littoral Cell, California	161
Abstract.....	161
Introduction	162
Santa Barbara Littoral Cell	163
Methods	165
Results	166
Sediment Removal from Debris Basins	166
Fate of Maintenance Material.....	168
Sediment Grain Size	168
Sediment Removal from Coastal Wetlands	169

Discussion.....	170
Conclusions	173
Acknowledgments.....	173
References.....	173
Chapter 7—Multibeam Bathymetry.....	183
Introduction	183
Results	184
Conclusions	184
References.....	185
Chapter 8—Seismic-Reflection Images of Shallow Sedimentary Deposits.....	191
Introduction	191
Conclusions	192
References.....	193
Chapter 9—Numerical Modeling Sediment Budget Analysis for the Santa Barbara Littoral Cell using Delft3D	197
Introduction	197
Methods	198
Delft3D-FLOW Module	198
Delft3D-WAVE Module.....	199
Computational Grids.....	199
Schematization of Wave Climate.....	200
Summary of Results.....	202
Conclusions	207
References.....	208
Chapter 10—Project Synthesis.....	222

Appendix A - BEACON Survey Lines224
Appendix B - Beach Mapping307
Ellwood/Isla Vista/Goleta308
Carpinteria317
Ventura/Santa Clara River Mouths324
Appendix C - Coastal Profiling System Lines333
Ellwood/isla Vista/Goleta.....	.334
Carpinteria483
Rincon Parkway568
Ventura/Santa Clara River Mouths639
Mugu Canyon.....	.744
Appendix D – Grain-Size Data.....	.763
Surficial Grain Size Data764
Box-Core Data780
Appendix E – Modeling Report785

Figures

Figure 1.1. Overview of the Santa Barbara littoral cell with the designated focus study areas.	14
Figure 2.1. The Santa Barbara and Ventura County, California, beaches analyzed for this chapter.	51
Figure 2.2. Santa Barbara (1933-2003) and Ventura (1964-2005) harbor dredge records. Data from Army Corp of Engineers, adapted from Patsch and Griggs 2007.	52
Figure 2.3. Long-term beach-width changes relative to the 2005 beach width. The earliest dates used in the calculation vary based on air photo availability (1943 for beaches updrift of Santa Barbara Harbor and 1947 for	

downdrift beaches, except 1929 for Carpinteria and Isla Vista). Negative changes indicate beach narrowing, positive changes indicate beach widening.....	52
Figure 2.4. An example of beach oscillations around UCSB and Goleta Beaches. Beaches reached maximum widths in the 1960s and 1970s while current beach widths are similar to those found in the 1930s and 1940s.	53
Figure 2.5. Beach-width (BW) variability along 70 km of coastline in southern Santa Barbara and Ventura Counties, California, throughout all available years of aerial photography (1929-2005). Areas with shoreline armoring are highlighted.	54
Figure 2.6. Shoreline armoring in the study area. Data adapted from California Coastal Commission.	54
Figure 2.7. Beach widths plotted by shoreline orientation for specific time periods from the 1940s to 2001. Data points were extracted from the same shoreline transects and have comparable numbers of data points. Radial axis is beach width in meters.	55
Figure 2.8. Shoreline-change rates (linear regression) for the wet/dry (1929-2005), back beach (1929-2005), and wet/dry with T-sheets (1829 –2005) shorelines.	55
Figure 2.9. Statistically significant shoreline-change rates for each reference feature based on the number of shorelines at each transect (generally R >0.7). LRR: Linear regression rate in m/yr.	56
Figure 2.10. Significant back-beach changes in relation to shoreline armoring. LRR: Linear regression rate.....	57
Figure 2.11. Photograph taken in 1936 after the erosion wave had passed Fernald Point en route to Carpinteria. Santa Barbara Harbor is visible in the distance; note the numerous cross-shore groins emplaced to slow erosion. Photo courtesy of the Spense Collection, UCLA.....	57
Figure 2.12. Beach-width changes in Carpinteria relative to the 1929 baseline. Shown are long-term changes from 1929 to 2006, changes immediately following the arrival of the erosion wave between 1929 and 1938, and recent changes from 1997 to 2006. The City of Carpinteria focus site is between transects 771 and 779, and Carpinteria Creek discharges between transects 791-793.....	58

Figure 2.13. Carpinteria shoreline-change linear-regression rates (LRR) for the various shoreline reference features. The red line is the back beach, the blue line is the MSL wet/dry adjusted line from air photos, and the green line is the shoreline-change rates derived by including the historical NOS T-sheets, as well as air photo and Lidar-derived shorelines. The City of Carpinteria focus site is between transects 771 and 779.	58
Figure 2.14. Carpinteria beach-width changes and recovery following <i>A</i> , 1982-83 and <i>B</i> , 1997-98 El Niño events. ...	59
Figure 2.15. Seasonal beach-width changes for the Carpinteria coastline. City Beach is located between transects 771 and 779. Shoreline armoring (revetment) occurs from transect 759 to 770.	59
Figure 2.16. Gridded sediment grain-size results for Carpinteria beach. The hotter colors represent coarser grain materials while the cooler colors represent finer grained material. <i>A</i> , Winter 2006, <i>B</i> , Summer 2006, and <i>C</i> , Winter 2007. Note the coarsening of grain sizes at the end of the revetment near the Ash Avenue erosion hotspot (red region in top panel). Figure from Barnard and others (2007).....	60
Figure 2.17. <i>A</i> , Hope Ranch, California, shoreline-change and <i>B</i> , beach-width response following the 1982-83 El Niño event. LRR: Linear regression rate.....	61
Figure 2.18. <i>A</i> , Transect volume and <i>B</i> , total beach volume above MSL from Goleta Beach to Santa Barbara Harbor following the 1982-83 erosion event at UCSB and Goleta beaches.	62
Figure 3.1. Location of BEACON survey lines, Santa Barbara and Ventura Counties, California.....	76
Figure 3.2. BEACON profile changes from November 2003 to October 2007. <i>A</i> , volume change above the given elevation to the depth of closure, and <i>B</i> , contour change (shoreline proxy) with a positive value representing accretion since 2003 and a negative value representing erosion since 2003. The “Active Zone” is the region between the mean high water (MHW) and 4 m depth contours. Santa Barbara Harbor is located between Lines 10 and 11.....	77
Figure 3.3. BEACON profile changes from November 2003 to October 2007, for lines north of the Santa Clara River mouth. <i>A</i> , volume change above the given elevation, and <i>B</i> , contour change (shoreline proxy) with a positive value representing accretion since 2003 and a negative value representing erosion since 2003. The “Active Zone” is the region between the mean high water (MHW) and 4 m depth contours.	78

Figure 3.4. BEACON profile changes from October 1987 to October 2007. <i>A</i> , volume change above the given elevation, and <i>B</i> , contour change (shoreline proxy) with a positive value representing accretion since 1987 and a negative value representing erosion since 1987. The “Active Zone” is the region between the mean high water (MHW) and 4 m depth contours.....	79
Figure 3.5. BEACON profile changes from October 1987 to October 2007 for lines north of the Santa Clara River mouth. <i>A</i> , volume change above the given elevation, and <i>B</i> , contour change (shoreline proxy) with a positive value representing accretion since 1987 and a negative value representing erosion since 1987. The “Active Zone” is the region between the mean high water (MHW) and 4 m depth contours.....	80
Figure 3.6. Shoreline-change rates based on the mean high water (MHW) position from 1987 to 2007 and from 2003 to 2007.....	81
Figure 4.1. Mean high water (MHW) shoreline-change rate in the SBLC from the 1998 and 2005 Lidar surveys. <i>A</i> , survey area with inset of Ventura/Santa Clara River Area. <i>B</i> , plot of shoreline-change rate versus alongshore distance from Point Conception, raw, and 1-km moving average.....	118
Figure 4.2. Beach slope (Mean sea level to mean high water) in the SBLC from the 2005 Lidar survey. <i>A</i> , survey area with inset of Rincon and Santa Clara River area. <i>B</i> , plot of alongshore distance from Point Conception versus beach slope, raw, and 1-km moving average.....	119
Figure 4.3. Shoreline change for the Ellwood/Isla Vista/Goleta study area from ATV topographic surveys conducted from 2005 to 2008. <i>A</i> , maximum range (all surveys) and total change (October 2005 to October 2008) for the mean sea level (MSL) and mean high water (MHW) shoreline proxies. <i>B</i> , end point and linear regression shoreline-change rates. Alongshore distance is kilometers from Point Conception. The October 2005 Lidar data was substituted for the October 2005 ATV data due to its greater accuracy and more extensive coverage area. See table 4.3 for the shoreline-analysis summary.....	120
Figure 4.4. Map view of the linear regression shoreline-change rates calculated using October mean high water shorelines from 2005 to 2008 in the Ellwood/Isla Vista/Goleta study area.....	121

Figure 4.5. Beach slope (mean sea level to mean high water) in the Ellwood/Isla Vista/Goleta study area from ATV topographic surveys conducted from 2005 to 2008. Alongshore distance is kilometers from Point Conception. The October 2005 Lidar data was substituted for the October 2005 ATV data due to its greater accuracy and more extensive coverage area. See table 4.5 for the slope-analysis summary.....	122
Figure 4.6. Shoreline change for the Carpinteria study area from ATV topographic surveys conducted from 2005 to 2008. <i>A</i> , maximum range (all surveys) and total change (October 2005 to October 2008) for the MSL and MHW shoreline proxies. <i>B</i> , end point and linear regression shoreline-change rates. Alongshore distance is kilometers from Point Conception. The October 2005 Lidar data was substituted for the October 2005 ATV data due to its greater accuracy and more extensive coverage area. See Table 4.6 for the shoreline-analysis summary.....	123
Figure 4.7. Map view of the linear regression shoreline-change rates calculated using October mean high water shorelines from 2005 to 2008 in the Carpinteria study area.	124
Figure 4.8. Beach slope (mean sea level to mean high water) in the Carpinteria study area from ATV topographic surveys conducted from 2005 to 2008. Alongshore distance is kilometers from Point Conception. The October 2005 Lidar data was substituted for the October 2005 ATV data due to its greater accuracy and more extensive coverage area. See table 4.8 for the slope-analysis summary.....	125
Figure 4.9. Shoreline change for the Ventura study area from ATV topographic surveys conducted from 2005 to 2008. <i>A</i> , maximum range (all surveys) and total change (October 2005 to October 2008) for the mean sea level (MSL) and mean high water (MHW) shoreline proxies. <i>B</i> , end point and linear regression shoreline-change rates. Alongshore distance is kilometers from Point Conception. The October 2005 Lidar data was substituted for the October 2005 ATV data due to its greater accuracy and more extensive coverage area. See table 4.9 for the shoreline-analysis summary.....	126
Figure 4.10. Map view of the linear regression shoreline-change rates calculated using October mean high water shorelines from 2005 to 2008 in the Ventura study area.	127

Figure 4.11. Beach slope (mean sea level to mean high water) in the Ventura study area from ATV topographic surveys conducted from 2005 to 2008. Alongshore distance is kilometers from Point Conception. The October 2005 Lidar data was substituted for the October 2005 ATV data due to its greater accuracy and more extensive coverage area. See table 4.11 for the slope-analysis summary.....	128
Figure 4.12. Depth of closure in the Santa Barbara littoral cell focus areas from Coastal Profiling System bathymetry data. Selected line numbers are shown for reference.....	129
Figure 4.13. Seasonal volume changes in cross-shore bathymetry profiles in the Santa Barbara littoral cell focus areas.....	130
Figure 4.14. Seasonal volume changes in cross-shore bathymetry profiles for the Goleta focus area. Selected line numbers are shown for reference.....	131
Figure 4.15. Seasonal volume changes in cross-shore bathymetry profiles for the Carpinteria focus area. Selected line numbers are shown for reference.	132
Figure 4.16. Seasonal volume changes in cross-shore bathymetry profiles for the Rincon focus area. Selected line numbers are shown for reference.....	133
Figure 4.17. Seasonal volume changes in cross-shore bathymetry profiles for the Ventura/Santa Clara river mouths focus area. Selected line numbers are shown for reference.....	134
Figure 4.18. Annual volume changes in cross-shore bathymetry profiles in the Santa Barbara littoral cell (SBLC) focus areas.....	135
Figure 4.19. Annual volume changes in cross-shore bathymetry profiles for the Goleta focus area. Selected line numbers are shown for reference.....	136
Figure 4.19. Annual volume changes in cross-shore bathymetry profiles for the Goleta focus area. Selected line numbers are shown for reference.....	136
Figure 4.20. Annual volume changes in cross-shore bathymetry profiles for the Carpinteria focus area. Selected line numbers are shown for reference.....	137

Figure 4.21. Annual volume changes in cross-shore bathymetry profiles for the Rincon focus area. Selected line numbers are shown for reference.....	138
Figure 4.22. Annual volume changes in cross-shore bathymetry profiles for the Ventura/ Santa Clara river mouths focus area. Selected line numbers are shown for reference.....	139
Figure 4.23. Offshore wave parameters during the study period (2005-2008) from the Coastal Data Information Program Harvest Buoy (Scripps, 2008). A, Significant wave height (Hs); B, Peak period (Tp), C, Peak direction (Dp).	140
Figure 5.1. Locations of beach-face samples collected with the Beachball camera and nearshore samples in 5, 10, and 20 m water depth collected with the Flying Eyeball camera	149
Figure 5.2. Locations of summer nearshore samples, summer kilometer-spaced samples, and seasonal beach-face samples collected at <i>A</i> , Goleta/Isla Vista; <i>B</i> , Carpinteria; and <i>C</i> , Ventura beaches.....	150
Figure 5.3. <i>A</i> , Beachball camera—digital camera encased in waterproof housing. <i>B</i> , Flying Eyeball—video camera encased in wrecking ball.....	151
Figure 5.4. <i>A</i> , Beachball camera image and processed image in grayscale, cropped from center and rescaled. <i>B</i> , Flying Eyeball camera image and processed image cropped from center and rescaled.	152
Figure 5.5. <i>A</i> , Beachball and <i>B</i> , Flying Eyeball calibration matrices. Legends show grain size in millimeters.	153
Figure 5.6. Box corer used in this study.....	154
Figure 5.7. Surface and lateral views of sample box core from offshore of Santa Barbara Harbor.....	155
Figure 5.8. Box-core sample locations.....	156
Figure 5.9. <i>A</i> , Location of regional beach-face samples. <i>B</i> , Beach-face mean grain size (mm) and grab-sample finest (d10). Sample locations are specified by distance from Point Conception.	157
Figure 5.10. Seasonal beach-face grain size. A, Goleta/Isla Vista. B, Carpinteria. C, Ventura. Note different scales.	158

Figure 5.11. <i>A</i> , Locations of all surficial-sediment samples. <i>B</i> , Beach-face and nearshore (5, 10, and 20 m water depth) sediment grain size results. Sample locations are plotted in <i>B</i> as distance from Point Conception.....	159
Figure 5.12. Surface-sediment map, Santa Barbara Channel. Data from this study, usSEABED (Reid and others, 2006), and BEACON (Noble Consultants, 1989). Grain sizes in legend are in mm.....	160
Figure 5.13. Box-core sample results.....	160
Figure 6.1. Study area maps for the Santa Barbara littoral cell (SBL) and its watersheds. <i>A</i> , California location map with the major mountain ranges identified: Western Transverse Range (WTR), Coastal (C), Eastern Transverse (ET), Klamath (K), Modoc and Cascade (MC), Peninsular (P) and Sierra Nevada (SN). <i>B</i> , Watershed map of the SBL. <i>C</i> , Watershed map of the small coastal drainages of the Santa Ynez Mountains, including the locations of debris basins and channel-dredging operations.....	180
Figure 6.2. Characteristics of the debris basins maintained by the Santa Barbara County Public Works Department in the Santa Ynez Mountains drainage basin. <i>A</i> , Cumulative watershed area trapped by debris basins. <i>B</i> , Cumulative debris-basin volumetric design capacity. <i>C</i> , History of the removal of sediment from these debris basins.....	181
Figure 6.3. Grain-size distribution data from the debris basins and coastal-wetland channels of the Santa Ynez Mountain coastal watersheds. Data include unpublished hand-auger samples from the basins in 1998 by the Santa Barbara County Public Works Department (SBCPWD)(All basins, SBC), a published integrated sample from the Santa Monica Creek Basin (Basin C, SL) after Simons, Li and Associates (1994), and wetland-channel (Goleta Slough) samples from 1998 by SBCWPD (Wetlands). The grain-size cutoff of the SBL (SB littoral) is after the findings of Limber and others (2008).	182
Figure 6.4. The cumulative suspended-sediment discharge during 1930-2005 from the Ventura River as assessed at USGS stream gage 11118500. Data compiled from Warrick and Mertes (in press). The shaded area represents the time for which debris-basin maintenance records are synthesized in this report.	182
Figure 7.1. All high-resolution bathymetric surveys in the Santa Barbara Channel through summer 2008.....	186
Figure 7.2. Perspective view, looking north, of the Mugu submarine canyon.....	187

Figure 7.3. Example of sea-floor character map from the Coal Oil Point area.....	188
Figure 7.4. Examples of products to be released as part of the California State Waters Mapping Projects.....	189
Figure 7.5. Coverage area for the 2005 Carpinteria offshore bathymetric survey	190
Figure 8.1. Location map of tracklines (from Sliter and others, 2008).....	194
Figure 8.2. Mini-sparker data along Line SB-148 (from Sliter and others, 2008), showing sediment (including clinoforms) overlying regional lowstand unconformity.....	195
Figure 8.3. Isopach map for the survey region.....	196
Figure 9.1. Computational grids. <i>A</i> , Wave grid. <i>B</i> , Flow grid. The flow grid is also used as a nested wave grid to ensure a high grid resolution in the surf zone.....	211
Figure 9.2. Overview of the 27 predefined transects. Bathymetry shading is at 10m intervals.....	212
Figure 9.3. <i>Top panel</i> , Comparison of the nonvalidated littoral-drift rates for the entire (green) and the reduced (yellow) wave climate. The relative root mean square error is 5.6 percent. <i>Bottom panels</i> , Individual sediment- transport contributions for each wave condition (WC) within the reduced wave climate. Negative transport values indicate north and/or westward transport.....	213
Figure 9.4. Modeled total annual sediment transport (yellow bars), and individual contributions for each wave condition in the morphologically representative wave climate (colored lines). Dredging volumes at Santa Barbara and Ventura Harbors (black bars) are shown for reference. WC, Wave condition.....	214
Figure 9.5. Residual sediment-transport vectors for the Santa Barbara Channel.....	215
Figure 9.6. Residual current patterns in the Santa Barbara littoral cell along the Gaviota Coast to Goleta Beach. <i>A</i> , Updrift segment, <i>B</i> , Middle segment, <i>C</i> , Downdrift segment. Longer arrows indicate higher potential sediment- transport rates.....	216
Figure 9.6 (cont.). Residual current patterns in the Santa Barbara littoral cell from <i>D</i> , the Santa Barbara area to <i>E</i> , Carpinteria. Longer arrows indicate higher potential sediment-transport rates.....	217

Figure 9.6 (cont.). F , Residual current patterns in the Santa Barbara littoral cell along the Rincon Parkway. Longer arrows indicate higher potential sediment-transport rates.....	218
Figure 9.6 (cont.). G , Residual current patterns in the Santa Barbara littoral cell in the Ventura/Santa Clara River mouths focus area. Longer arrows indicate higher potential sediment-transport rates.....	219
Figure 9.7. Significant wave height and direction for wave conditions 88 and 62 at <i>A</i> , Ellwood/Isla Vista/Goleta, and <i>B</i> , Santa Barbara Harbor. White arrows indicate wave direction.....	220
Figure 9.7 (cont.). C , Significant wave height and direction for wave conditions 88 and 62 at Ventura/Santa Clara River mouths. White arrows indicate wave direction.....	221
Figure A1. BEACON survey line locations. See Table 3.1 for superseded BEACON line IDs and location names..	224
Figure A2. BEACON survey line plots, lines 1 to 41. See Figure A1 for line locations.....	225
Figure A3. BEACON survey line focus (depths shallower than 5 m) plots.....	266
Figure B1. Topographic data points collected in the Ellwood/Isla Vista/Goleta study site, Oct 2007 – Oct 2008.	309
Figure B1 (cont.). Topographic data points collected in the Ellwood/Isla Vista/Goleta study site, Oct 2007 – Oct 2008.....	310
Figure B2. Topographic data gridded to 2 m cells from the Ellwood/Isla Vista/Goleta study site.....	311
Figure B2 (cont.). Topographic data gridded to 2 m cells from the Ellwood/Isla Vista/Goleta study site.....	312
Figure B3. Vertical change from the annual surveys in Ellwood/Isla Vista/Goleta.	313
Figure B3 (cont.). Vertical change from the annual surveys in Ellwood/Isla Vista/Goleta.	314
Figure B4. Vertical change from seasonal surveys in Ellwood/Isla Vista/Goleta.	315
Figure B4 (cont.). Vertical change from seasonal surveys in Ellwood/Isla Vista/Goleta.	316
Figure B5. Topographic data points collected in the Carpinteria study site.	318
Figure B5 (cont.). Topographic data points collected in the Carpinteria study site.	319
Figure B6. Topographic data gridded to 2 m cells from the Carpinteria study site.....	320
Figure B6 (cont.). Topographic data gridded to 2 m cells from the Carpinteria study site.....	321

Figure B7. Vertical change from annual surveys at the Carpinteria study site.....	322
Figure B8. Vertical change from seasonal surveys at the Carpinteria study site.....	323
Figure B9 (cont.). Topographic data points collected in the Ventura study site.....	326
Figure B10 (cont.). Topographic data gridded to 2 m cells from the Ventura study site.....	328
Figure B11 (cont.). Vertical change from the annual surveys in Ventura.....	330
Figure B12 (cont.). Vertical change from seasonal surveys in Ventura.....	332
Figure C1. All focus area Coastal Profiling System survey line locations.....	333
Figure C2. Ellwood/Isla Vista/Goleta Coastal Profiling System survey line locations.....	334
Figure C3. Ellwood/Isla Vista/Goleta Coastal Profiling System plots, survey lines 0 - 73.....	335
Figure C4. Ellwood/Isla Vista/Goleta Coastal Profiling System focus (depths shallower than 5 m) plots, survey lines 0-73	409
Figure C5. Carpinteria Coastal Profiling System survey line locations.....	483
Figure C6. Carpinteria Coastal Profiling System plots, survey lines 1-42.....	484
Figure C7. Carpinteria Coastal Profiling System focus (depths shallower than 5 m) plots, survey lines 1-42.....	526
Figure C8. Rincon Parkway Coastal Profiling System survey line locations.....	568
Figure C9. Rincon Parkway Coastal Profiling System plots, survey lines 1-35.....	569
Figure C10. Rincon Parkway Coastal Profiling System focus (depths shallower than 5 m) plots, survey lines 1-35. 604	
Figure C11. Ventura/Santa Clara River Mouths Coastal Profiling System survey line locations.....	639
Figure C12. Ventura/Santa Clara River Mouths Coastal Profiling System plots, survey lines 1-52.....	640
Figure C13. Ventura/Santa Clara River Mouths Coastal Profiling System focus (depths shallower than 5 m) plots, survey lines 1-52.....	692
Figure C14. Mugu Canyon Coastal Profiling System survey line locations.....	744
Figure C15. Mugu Canyon Coastal Profiling System plots, survey lines 72-80 (Ventura).....	745

Figure C16. Mugu Canyon Coastal Profiling System focus (depths shallower than 5 m) plots, survey lines 72-80 (Ventura).....	754
Figure D1. Eyeball and grab sediment sample locations from the study area.....	764
Figure D2. Eyeball and grab sample mean grain-size distribution of offshore samples.....	765
Figure D3. Box-core locations from the October 2007 survey.....	780
Figure D4. Box-core grain-size variation from the October 2007 survey.	781

Tables

Table 2.1. Specifications of aerial photography. [Spatial errors are the average error for the entire flightline. Sources: University of California, Santa Barbara Map and Imagery Library, California Coastal Commission, U.S. Geological Survey, and Pacific Western Aerial Surveys].....	49
Table 2.2. Summary of historical shoreline-change rates for various shoreline reference features, along with associated error estimates.....	50
Table 2.3. <i>A</i> , Shoreline-change rates of each reference feature with additional statistics on erosion and accretion transects. <i>B</i> , Shoreline-change rates associated with various types of shoreline armoring. "No Structure" sites have been additionally filtered to remove inlet-influenced transects. [BB, back beach; WD, Wet/Dry line; and WDT, Wet/Dry and T-sheet]	50
Table 2.4. Correlation coefficients between the various shoreline reference features. [All correlations are significant at the 0.1 percent level]	51
Table 3.1. Naming convention for BEACON survey lines.....	71
Table 3.2. Summary statistics of BEACON line profile changes from 2003 to 2007. [MHW: mean high water. Active zone: depth interval from -4m to MHW]	72
Table 3.3. Profile change for each of the BEACON lines from 2003 to 2007. [Volume change is calculated for the entire profile (Total) and then above the specified contours. NaN: no calculation possible due to poor profile overlap or	

poor data (for example, due to kelp beds at line 2). MHW: mean high water. Active zone: depth interval from -4m to MHW].....	73
Table 3.4. Summary statistics of BEACON line profile changes from 1987 to 2007. [MHW: mean high water. Active zone: depth interval from -4m to MHW]	74
Table 3.5. Profile change for each of the BEACON lines from 1987 to 2007. [Volume change is calculated for the entire profile (Total) and then above the specified contours. NaN: no calculation possible due to poor data (for example, due to kelp beds at line 2 or no data from 1987 survey. MHW: mean high water. Active zone: depth interval from -4m to MHW]	75
Table 4.1. Survey dates and data collected for the 5 focus areas. [T, topography data collected; B bathymetry data collected; dashes indicate no data].....	101
Table 4.2. Mean high water (MHW) shoreline-change statistics for the Santa Barbara littoral cell (SBLC), April 1998 to October 2005.....	102
Table 4.3. Shoreline-change statistics for 100-m spaced shore-normal transects in the Ellwood/Isla Vista/Goleta study area. [Topographic data are from ATV surveys conducted from 2005 to 2008 (Table 4.1), except for October 2005 where Lidar data was used due to its greater accuracy and more extensive coverage area. The end point rate (EPR) was calculated using only the October 2005 and 2008 shorelines, and the linear regression rate (LRR) was calculated using only October shorelines. MSL, mean sea level; MHW, mean high water].....	103
Table 4.4. Vertical- and volume-change statistics for the Ellwood/Isla Vista/Goleta study area from ATV topographic surveys conducted from 2005 to 2008. [The October 2005 Lidar was substituted for the October 2005 ATV data due to its greater accuracy and more extensive coverage area. Surface area is the overlapping region surveyed between the two surveys being analyzed].....	104
Table 4.4. (cont.) Vertical- and volume-change statistics for the Ellwood/Isla Vista/Goleta study area from ATV topographic surveys conducted from 2005 to 2008. [The October 2005 Lidar was substituted for the October 2005	

ATV data due to its greater accuracy and more extensive coverage area. Surface area is the overlapping region surveyed between the two surveys being analyzed]..... 105

Table 4.5. Beach slope (mean sea level to mean high water) statistics for the Ellwood/Isla Vista/Goleta study area from the ATV topographic surveys conducted from 2005 to 2008. [The October 2005 Lidar data was substituted for the October 2005 ATV data due to its greater accuracy and more extensive coverage area. All values are in percent]

..... 106

Table 4.6. Shoreline-change statistics for 100-m spaced shore-normal transects in the Carpinteria study area.

[Topographic data are from ATV surveys conducted from 2005 to 2008 (Table 4.1), except for October 2005 where Lidar data was used due to its greater accuracy and more extensive coverage area. The end point rate (EPR) was calculated using only the October 2005 and 2008 shorelines, and the linear regression rate (LRR) was calculated using only October shorelines. MSL, mean sea level; MHW, mean high water] 107

Table 4.7. Vertical- and volume-change statistics for the Carpinteria study area from ATV topographic surveys conducted from 2005 to 2008. [The October 2005 Lidar was substituted for the October 2005 ATV data due to its greater accuracy and more extensive coverage area. Surface area is the overlapping region surveyed between the two surveys being analyzed]..... 108

Table 4.8. Beach slope (mean sea level to mean high water) statistics for the Carpinteria study area from the ATV topographic surveys conducted from 2005 to 2008. [The October 2005 Lidar data was substituted for the October 2005 ATV data due to its greater accuracy and more extensive coverage area. All values are in percent]..... 109

Table 4.9. Shoreline-change statistics for 100-m spaced shore-normal transects in the Ventura study area.

[Topographic data are from ATV surveys conducted from 2005 to 2008 (Table 4.1), except for October 2005 where Lidar data was used due to its greater accuracy and more extensive coverage area. The end point rate (EPR) was calculated using only the October 2005 and 2008 shorelines, and the linear regression rate (LRR) was calculated using only October shorelines. MSL, mean sea level; MHW, mean high water] 110

Table 4.10. Vertical- and volume-change statistics for the Ventura study area from ATV topographic surveys conducted from 2005 to 2008. [The October 2005 Lidar was substituted for the October 2005 ATV data due to its greater accuracy and more extensive coverage area. Surface area is the overlapping region surveyed between the two surveys being analyzed].....	111
Table 4.10. (cont.) Vertical- and volume-change statistics for the Ventura study area from ATV topographic surveys conducted from 2005 to 2008. [The October 2005 Lidar was substituted for the October 2005 ATV data due to its greater accuracy and more extensive coverage area. Surface area is the overlapping region surveyed between the two surveys being analyzed].....	112
Table 4.11. Beach slope (mean sea level to mean high water) statistics for the Ventura study area from the ATV topographic surveys conducted from 2005 to 2008. [The October 2005 Lidar data was substituted for the October 2005 ATV data due to its greater accuracy and more extensive coverage area. All values are in percent].....	113
Table 4.12. Depth of closure (DOC) statistics for each region and for the study area as a whole. [DOCs were not calculated for Mugu Canyon due to insufficient replication (n=2). Depths are in meters].....	114
Table 4.13. Seasonal bathymetric profile volume-change statistics. [Volume changes are in m ³ /m].....	115
Table 4.14. Annual and 3-year bathymetric profile volume-change statistics. [Volume changes are in m ³ /m]	116
Table 4.15. Offshore-wave statistics for the 2005-2008 study period. [H _s , significant wave height; T _p , peak period; D _p , peak direction].....	117
Table 6.1. Characteristics of debris basins in the Santa Ynez coastal drainage basin. Totals may not equal sums due to rounding.....	179
Table 9.1. Morphological representative wave climate as derived from the Coastal Data Information Program Harvest Buoy (Station 071; Scripps Institute of Oceanography, 2008).	210
Table D1. Mean grain size data for each sample site. Additional grab sample data (for example, sorting, skewness, et cetera) are available upon request.	766
Table D2. Box-core sample grain-size data from the October 9-11, 2007, survey, sorted by latitude.	782

Coastal Processes Study of Santa Barbara and Ventura Counties, California

By Patrick L. Barnard, David L. Revell, Dan Hoover, Jon Warrick, John Brocatus, Amy E. Draut, Pete Dartnell, Edwin Elias, Neomi Mustain, Pat E. Hart, and Holly F. Ryan

Executive Summary of Major Findings

The United States Geological Survey and the University of California, Santa Cruz collaborated on a three-year project (2005-2008) to analyze sediment transport processes and identify coarse-grained, nearshore sediment bodies along the Santa Barbara and Ventura County coastline. Work described in this project was primarily supported by the California Department of Boating and Waterways through a grant from the Beach Erosion Authority for Clean Oceans and Nourishment, and was conducted in collaboration with the United States Army Corps of Engineers, Los Angeles District. This research was designed as a regional study of the Santa Barbara-Ventura County coast, complemented with five localized studies in areas of critical interest. Semi-annual surveys (October 2005 to October 2008) designed to capture maximum and minimum beach volumes and seasonal transport patterns (early fall and late winter) included topographic beach surveys using All-Terrain Vehicles, nearshore bathymetric surveys using the USGS Coastal Profiling System, and grain-size analysis using digital cameras. In addition, this project was supported by a Lidar flight in October 2005 performed by the University of Texas, numerous multibeam and side scan surveys, sub-bottom profiling, regional sediment sampling using a box core, digital still and video bed-sediment cameras, and numerical modeling using Delft3D. What follows is a summary of the key findings discussed in this report.

Chapter 2—Historical Changes

- No systematic narrowing of beach widths was found in the end point beach-width changes as was hypothesized to be associated with a reduction in sand supply. Instead, beach widths have oscillated during the 75-year record.
- Updrift of the Santa Barbara Harbor, minimum beach widths were closely related to the strong El Niño events of 1982-83 and 1997-98. Downdrift of the harbor, beach widths did not follow this El Niño pattern, suggesting that the harbor was regulating beach widths downdrift similar to a dam regulating water levels downstream.
- Beach-width envelopes provide strong evidence for stable beaches and could help in refining the current beach-monitoring program.
- The greatest narrowing of beach widths occurred (1) near Carpinteria—caused by sand impoundment by the construction of the Santa Barbara Harbor; (2) by Ventura Harbor—caused by the breaching of the beach to form the harbor; and (3) at Goleta Beach—due to the construction of the Santa Barbara airport and the loss of tidal prism at Goleta Slough.
- The greatest widening of beach widths occurred immediately updrift of Santa Barbara Harbor (>200 m) as a result of sand impoundment by the breakwater, and at the groin field in Ventura where beach widths widened by >100 m.
- The greatest shoreline changes resulted from large erosion events such as the 1982-83 El Niño and the erosion wave associated with the construction of the Santa Barbara Harbor breakwater.
- Analyses of natural beach widths and shoreline orientation demonstrate that the west-facing beaches of Ellwood (255-240 degrees) were the most stable, with beach widths ranging from 25 to 75 m. The east-facing beaches (120-105 degrees) were the most variable, ranging from 0 to 150 m in width. South-facing beaches were the narrowest.

- Beach-width and shoreline-change analyses reveal a pattern of beach narrowing attributable to shoreline armoring. Along the 70 km study area, 60 percent (41.9 km) of the shoreline has been armored with a variety of revetments and seawalls. In these areas, accretion of the back beach and erosion of the wet/dry shoreline illustrate the effects of placement loss and passive erosion.
- From 1929 to 2005, shoreline-change analyses reveal a study-area-wide accretion pattern of 10 cm/yr for the back beach and 16 cm/yr for the Mean Sea Level shoreline. From 1860 to 2005 the Mean Sea Level shoreline accreted at a rate of 8 cm/yr.
- Shoreline-change analyses show that accretion is associated with shore-protection structures, with cross-shore structures (groins and jetties) accreting the wet/dry shoreline, and shore-parallel structures (seawalls and revetments) building out the backbeach and reducing beach widths.
- Shoreline segments without shoreline armoring show mild erosion of both the back beach and wet/dry shoreline of about 2-3 cm/yr.
- Carpinteria and Hope Ranch beaches both show El Niño storm-event rotation responses that match the long-term shoreline-change pattern. This suggests that El Niño events may be driving the long-term coastal evolution.
- Sand travels alongshore as coherent pulses that are detectable at stable beaches. Evidence of alongshore sand movement can be seen subaerially in both erosion and accretion waves, with some of the sand transported below mean sea level in the nearshore.
- Lag-correlation analyses show that the movement of sediment pulses may be faster than previously thought, with potential migration rates of several kilometers per year.
- The beach-width methodology is useful when coupled with shoreline-change analyses for examining the cumulative impacts associated with shore-protection structures and the response of the shoreline to large storm events.

Chapter 3—BEACON Surveys

- There is no significant average regional change observed in the Santa Barbara littoral cell between 2003 and 2007 based on 41 BEACON survey lines.
- Significant erosion is observed in the vicinity of the Santa Barbara Harbor and Rincon Parkway between 2003 and 2007.
- From 2003 to 2007 accretion is observed at Goleta, from Summerland to La Conchita, and along most of the coastline south of the Santa Clara River mouth, including around Hueneme Harbor.
- At least 6 million m³ of sediment was delivered to the coast at the mouth of the Santa Clara River during the winter flood of 2004-2005.
- The shoreline adjacent to the Santa Clara River prograded up to 129 m as a result of the winter flood in 2004-2005.
- North of the Santa Clara River mouth the mean high water shoreline retreated an average of 6 m from 1987 to 2007.
- The shoreline south of the Santa Clara River mouth accreted an average of 34 m from 1987 to 2007.
- Approximately 5 million m³ (250,000 m³/yr) of sediment was eroded from the Rincon Parkway region (Hobson to Surfer's Point) from 1987 to 2007.

Chapter 4—Recent Morphological Changes

- Shoreline change since the 1997-98 El Niño is negligible in the Santa Barbara littoral cell, although there have been pockets of considerable accretion and lesser amounts of erosion.
- Between 1997 and 2005, the highest rates of accretion were measured just updrift of the Santa Barbara Harbor (3 m/yr) and at the mouth of the Santa Clara River (8.1 m/yr).

- Between 1997 and 2005, the highest rates of erosion were measured on the beach adjacent to Mugu Canyon, at up to -11.4 m/yr.
- Regional beach slope suggests dominantly reflective conditions, but conditions can be influenced locally by shore-protection structures.
- From 2005 to 2008, all-terrain vehicle beach mapping at Ellwood/Isla Vista/Goleta, Carpinteria, and Ventura shows that the shoreline was retreating at each of the three sites, with rates ranging from ~1 m/yr in Carpinteria to 6.3 m/yr in Ventura.
- From 2005 to 2008, shoreline-retreat rates locally exceeded 40 m/yr at the Santa Clara River mouth, likely due to a rapid return to equilibrium after the large January 2005 flood built the shoreline seaward more than 100 m.
- From 2005 to 2008, a trend of beach steeping was observed at each site, except at the mouth of the Santa Clara River.
- From 2005 to 2008, typical seasonal patterns of beach loss in the winter and recovery in the fall were observed at each focus area, except at the Santa Clara River mouth from October 2005 to March 2006.
- From 2005 to 2008, despite rapid shoreline-retreat rates, the beach south of the Santa Clara River gained more than 200,000 m³ of sediment.
- From 2005 to 2008, Goleta County Beach experienced unusual beach steeping from winter to fall each year.
- From 2005 to 2008, repeated cross-shore bathymetric surveys suggest depth-of-closure values from 1.8 to 11.3 m or more, with the deepest values occurring on the Santa Clara River delta. Values in most areas are between 2 and 8 m.

- From 2005 to 2008, semiannual bathymetry measurements outside of the Ventura/Santa Clara River study area show relatively modest (~10 to 50 m³/m) seasonal and annual volume changes. Subtidal seasonal changes occur primarily as accretion during the winter and erosion during the summer, with only a slight net loss (average -4.7 m³/m) in profiles during the study period.
- In the Santa Clara River delta area, bathymetric profiles collected from 2005 to 2008 show erosional losses both seasonally and annually, indicating continuing deflation of the delta following the major input of flood sediments in January 2005. Sediment losses from the delta during this period were much larger than anywhere else in the study region, commonly exceeding 400 m³/m per year.
- Offshore wave statistics from 2005 to 2008 show no significant mean wave-height changes, but very large waves (>6 m) occurred more frequently in the last two winters of the study, which could explain the higher beach-erosion rates observed at the focus sites during this time period.

Chapter 5—Grain-Size Analysis

- The mean grain size of swash samples in the Santa Barbara littoral cell is 0.26 mm (range 0.15 to 0.58 mm), with a littoral cut-off diameter of 0.125 mm.
- Out of 318 nearshore sample locations, only 2 percent contained mean grain sizes that exceeded fine sand (≥ 0.25 mm).
- Only 3 percent of the nearshore box-core samples collected equaled or exceeded the mean grain size of the swash samples.
- The most promising sites for further investigation of potentially large volumes of beach-compatible sediment are off of Santa Barbara Harbor and Oil Piers.
- The volume of beach-sized sediment off the Santa Clara River mouth is potentially high, but poorly resolved.

Chapter 6—The Impacts of Debris Basins on Sediment Delivery to the Santa Barbara Littoral Cell, California

- Debris basin maintenance records suggest that coastal watersheds in the Santa Ynez Mountains discharge 110,000 to 300,000 m³/yr of littoral-grade sediment into the Santa Barbara littoral cell.
- Debris basins are estimated to have reduced littoral-sediment contributions to the Santa Barbara littoral cell by 15,000 to 40,000 m³/yr, or about 15 percent of the total littoral-sediment production of the Santa Ynez Mountain coastal watersheds.
- Debris-basin maintenance has removed 1.3 to 2.0 million m³ of sediment between 1969 and 2005, the majority (~85 percent) of which is permanently removed from the downstream fluvial and littoral systems through disposal or reuse.

Chapter 7—Multibeam Bathymetry

- During the last several years the entire nearshore zone from the 10-m isobath seaward to the State 3-mile limit has been mapped using multibeam and sidescan sonar.
- Numerous map products are currently in production, highlighted by high-resolution bathymetry, habitat maps, and seamless onshore-offshore geologic maps.
- The Coal Oil Point region is dominated by thin veneers of sediment and bedrock exposures.
- The substrate offshore of Carpinteria and off of the Ventura and Santa Clara Rivers is sand-dominated.
- At Mugu Canyon, abundant, long-wavelength sand waves suggest high rates of down-canyon, sand-sized sediment transport.

Chapter 8—Seismic-Reflection Images of Shallow Sedimentary Deposits

- Major depositional centers are located off Ellwood, Goleta, Miramar/Summerland, and Rincon toward the Ventura River delta.
- Shallow bedrock (<1 m) is found off Isla Vista, Arroyo Burro, Santa Barbara Harbor, and Rincon Point.

Chapter 9—Numerical Modeling

- Local erosion and accretion patterns in the Santa Barbara littoral cell are well explained by modeled littoral-sediment transport gradients.
- Significant littoral-drift reversals at the Ventura and Channel Islands Harbors, due to western and southern wave energy, result in dredging rates that may significantly exceed the true net sediment transport rate.
- Littoral-drift acceleration at Goleta, Carpinteria, and Surfer's Point correlates with short- and long-term erosion trends in those areas.
- Deceleration of littoral-drift rates near La Conchita and the Santa Clara River mouth corresponds with the decadal-scale accretion noted in those locations.
- Geologically controlled shoreline orientation and sediment supply are the critical factors controlling local shoreline behavior.
- Rotation of beaches predicted in modeling agrees with observed trends at the Ellwood/Isla Vista/Goleta and Carpinteria focus areas.

Chapter 1—Introduction

Project Summary

The U.S. Geological Survey (USGS) and the University of California, Santa Cruz (UCSC) collaborated on a three-year project (2005-2008) to analyze sediment-transport processes and identify coarse-grained, nearshore sediment bodies along the Santa Barbara and Ventura County, California, coastline. This region, the Santa Barbara littoral cell (SBLCC), extends 150 km from Point Conception to the Mugu submarine canyon (fig. 1.1). Work described in this project was primarily supported by the California Department of Boating and Waterways (CDBW), through a grant from the Beach Erosion Authority for Clean Oceans and Nourishment (BEACON), and was conducted in collaboration with the U.S. Army Corps of Engineers (USACE), Los Angeles District.

The approach of the study has been regional, but five areas were chosen for focused, high-resolution survey work:

- Goleta/Isla Vista/Ellwood,
- Carpinteria,
- Rincon Parkway,
- Ventura/Santa Clara River Mouths, and
- Mugu Canyon.

We addressed each of the tasks as outlined in the accepted proposal of August 2005, which was designed to respond directly to the USACE Project Management Plan (PMP) for the region: “Coast of California Storm and Tidal Waves Study (CCSTWS) Ventura/Santa Barbara Counties, California PMP” (April 2004). The work at Carpinteria, having been supported through separate

funding, was completed and published in 2007 (Barnard and others, 2007). The results of this study can be found online at <http://pubs.usgs.gov/of/2007/1412/>.

Project Objectives

- Document changes in the SBLC during the last century.
- Quantify annual and seasonal nearshore sediment-transport patterns in the focus areas.
- Assess the compatibility of beach and nearshore sediment bodies.
- Assimilate data collection into a numerical modeling framework to identify the dominant sediment-transport pathways in the SBLC.
- Synthesize the results to revise the sediment budget for the SBLC and support SBLC management decisions.

Project Approach

This research was designed as a regional study of the Santa Barbara-Ventura County coast, complemented with five localized studies in areas of critical interest. Semiannual surveys (October 2005 to October 2008) designed to capture maximum and minimum beach volumes and seasonal transport patterns (early fall and late winter) included topographic beach surveys using all-terrain vehicles (ATVs), nearshore bathymetric surveys using the USGS Coastal Profiling System (CPS), and grain-size analysis using digital cameras. In addition, this project was supported by a Lidar flight performed by the University of Texas in October 2005; numerous multibeam and sidescan surveys; sub-bottom profiling; regional sediment sampling using a box core; digital still camera and video bed-sediment cameras, and numerical modeling using Delft3D.

Future Work

The USGS plans to establish a long-term monitoring presence in the region with annual surveys in October. This effort was initialized by funding from the USACE, Los Angeles District, in August 2008. The goal of this long-term monitoring program will be to analyze regional changes by using the historical BEACON survey lines that were established in 1987, as well as detailed analysis of site-specific coastal evolution in areas with specific management concerns, such as Goleta and Carpinteria (beach erosion), Rincon Parkway (various State interests), Ventura River mouth (Surfer's Point erosion/restoration and pending Matilija dam removal), Santa Clara River mouth (major littoral-sand provider), and Mugu Canyon (primary sink for sediment in littoral cell).

In addition, the Coastal Erosion task of the USGS Southern California Multi-Hazards Demonstration Project includes assessing coastal storm impacts to the SBLCC. This work is scheduled for completion in September 2011 (see http://walrus.wr.usgs.gov/coastal_processes/socalhazards/).

Report Outline

This report is designed to provide a summary of all coastal research performed by the USGS-UCSC collaboration in the Santa Barbara-Ventura County region from 2005-2008, including work not directly supported by BEACON. The report is laid out as follows:

- Executive Summary
- Chapter 1—Introduction
- Chapter 2—Historical Changes
- Chapter 3—BEACON Surveys
- Chapter 4—Recent Morphological Changes
- Chapter 5—Grain-Size Analysis
- Chapter 6—The Impacts of Debris Basins on Sediment Delivery to the Santa Barbara Littoral Cell, California
- Chapter 7—Multibeam Bathymetry
- Chapter 8—Seismic-Reflection Images of Shallow Sedimentary Deposits
- Chapter 9—Numerical Modeling Sediment Budget Analysis for the Santa Barbara Littoral Cell using Delft3D
- Chapter 10—Project Synthesis

- Appendix A—BEACON Survey Lines
- Appendix B—Beach Mapping
- Appendix C—Coastal Profiling System Lines
- Appendix D—Grain-Size Data
- Appendix E—Modeling Report

At the end of each chapter there are bullet points to emphasize the key findings—these findings are also listed in the Executive summary at the beginning of this report. A large amount of the survey data directly supported by BEACON (for example, topographic maps, bathymetric profiles, and grain-size results) is contained in the appendices. This report is designed to present the key data supported by BEACON and to introduce related data and analysis by providing links to other data and reports.

Project Support and Collaboration

The Santa Barbara and Ventura County Coastal Processes study was primarily funded by the CDBW through BEACON. However, the project and additional complementary research has also benefited greatly from internal support at the USGS, an additional grant from the CDBW through the City of Carpinteria, and funding from the USACE, as well as interactions with a number of other agencies and groups. A list of the primary collaborators is outlined below.

- USGS Support:
 - California Urban Oceans Project (Project Chief: Homa Lee)
 - Seafloor Mapping Project (Project Chief: Guy Cochrane)
- Academic Partners:
 - California State University Monterey Bay (Rikk Kvitek, Seafloor Mapping Lab)
 - University of California, Santa Barbara (Jenny Dugan, Dave Hubbard, Shane Anderson)
 - University of California, Santa Cruz (Gary Griggs)
 - Deltares (Edwin Elias)
- Government Agencies:
 - U.S. Army Corps of Engineers, Los Angeles District (Heather Schlosser, Art Shak)
 - City of Carpinteria (Matt Roberts)
 - California Department of Boating and Waterways (Kim Sterrett)
 - BEACON (Jim Bailard, Gerald Comati)
 - U.S. Environmental Protection Agency
 - Minerals Management Service
 - California Coastal Conservancy

- California State Parks (Thomas Dore)
- City of Ventura (Brian Brennan)
- County of Santa Barbara (Richard Lindley)
- Private Sector:
 - Noble Consultants (Jon Moore)

Acknowledgments

In addition to the numerous collaborators, this project also benefited from logistical support and assistance from a number of other agencies, students, and USGS employees. Tom Reiss provided GPS survey support during each of our 7 surveys in the region. Gerry Hatcher was our primary electronics technician. Jodi Eshleman, Jeff Hansen, Jackson Currie, Kate Dallas, Brian Spear, Nicole Kinsman and Diane Escobedo assisted in the field. Shane Anderson at UCSB, Matt Roberts at the City of Carpinteria, and the staff at San Buenaventura Lifeguard Headquarters generously allowed us to establish and continually reoccupy our GPS base stations on their property. The Coal Oil Point Reserve, Santa Barbara County Parks, California State Parks, City of Carpinteria, and Mugu Naval Air Station generously granted us access to survey in areas under their jurisdiction.

References

Barnard, P.L., Revell, D.L., Eshleman, J.L., and Mustain, Neomi, 2008, Carpinteria coastal processes study, 2005-2007; Final report: U.S. Geological Survey Open-File Report 2007-1412, 129 p., [<http://pubs.usgs.gov/of/2007/1412>, (last accessed March 13, 2009)].

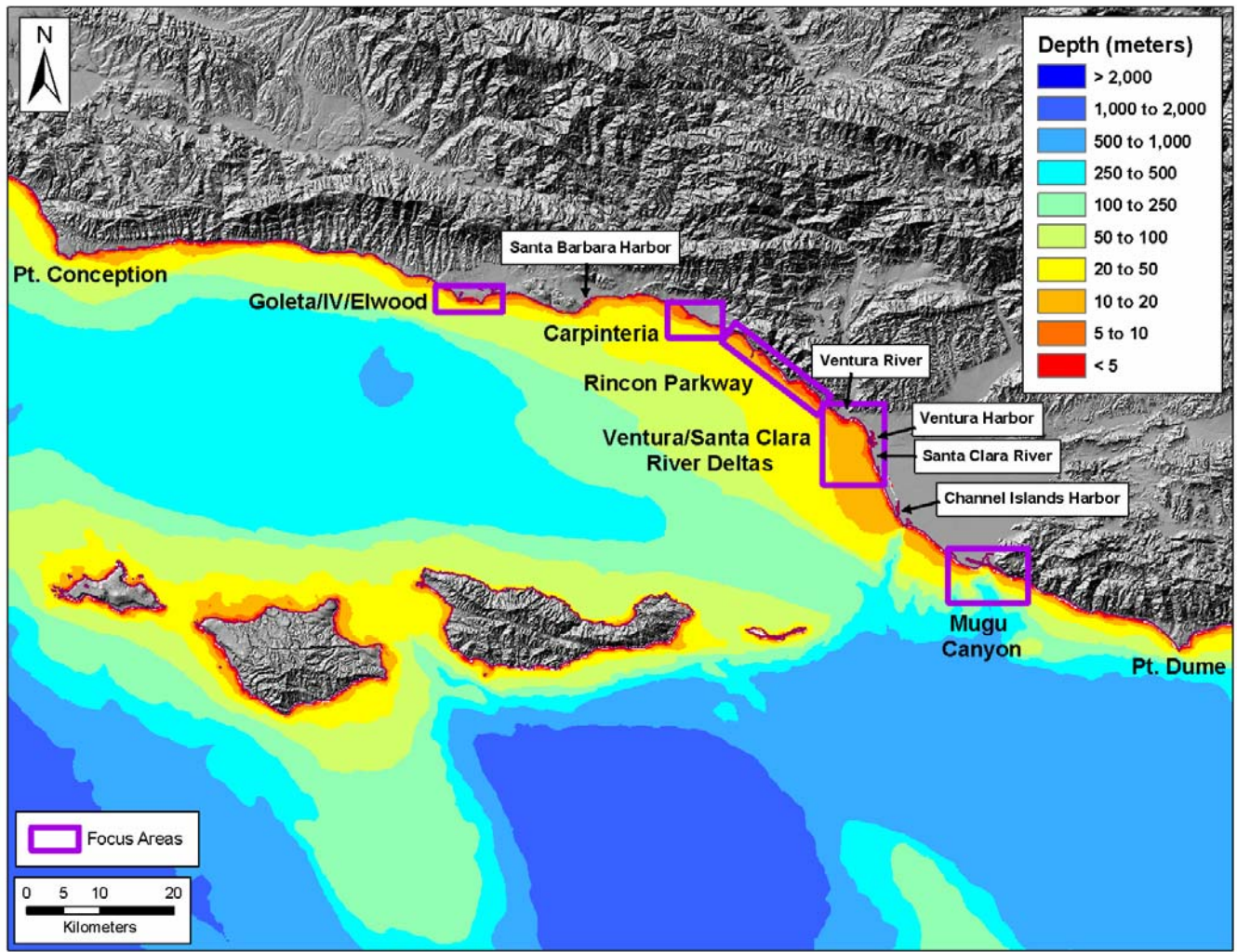


Figure 1.1. Overview of the Santa Barbara littoral cell with the designated focus study areas.

Chapter 2—Historical Changes

By David L. Revell

Summary

Beach widths and shoreline change along Santa Barbara and Ventura Counties, California, were evaluated using a 75-year record of rectified historical air photos and a 138-year record of historical maps. The analyses did not reveal any large-scale, long-term beach narrowing trends that would be associated with a reduction in sand supply caused by dam construction and/or shoreline armoring. Instead, beach widths oscillated widely across the littoral cell. Updrift of the Santa Barbara Harbor, minimum beach widths were closely related to the strong El Niño events of 1982-83 and 1997-98. Downdrift of the harbor, minimum beach widths did not follow this pattern, suggesting that the harbor regulated downdrift beach widths, although shoreline orientation and wave exposure may also play a role. The beach-width analyses did reveal a pattern of narrowing attributable to shoreline armoring. The beach-width envelopes also identified stable beaches along the study area. Along the 70 km study area, 60 percent (41.9 km) of the shoreline is armored and showed accretion of the back beach and erosion of the wet/dry shoreline (a proxy for mean sea level (MSL)), patterns consistent with the effects of placement loss and passive erosion. The largest shoreline and beach-width changes were associated with the construction of Santa Barbara Harbor in 1928.

Beach responses to large El Niño events formed a pattern of beach-width reduction of >50 percent and rotation into the dominant direction of wave attack. Long-term shoreline-change patterns show a similar pattern of shoreline rotations, providing evidence that El Niño events play an important role in long-term coastal evolution. A large volume of sand (~385,000 m³) eroded from UCSB and Goleta beaches during the 1982-83 El Niño event moved downcoast as a pulse, but is visible only along

stable beaches updrift of the Santa Barbara Harbor. Sand volumes above MSL on these stable beaches could not account for the entire eroded volume. The missing portions must have been transported alongshore below MSL, as the original volume eroded could be accounted for in subsequent Santa Barbara Harbor dredge records as an increase above average annual dredge volumes.

The application of a beach-width methodology to regional coastal-change analyses provides information on sand volumes, beach response to storm events, and the impacts of human alterations to the coast. This information can assist coastal managers in identifying cumulative impacts of shoreline armoring and quantifying impacts to sand supply.

Introduction

The Santa Barbara sandshed (the watershed and the littoral cell; Revell and others, 2007) extends 245 km from the Santa Maria River in the north, around Point Conception, where the north-south trending coast takes an abrupt turn to a west-east trending shoreline heading into the Southern California Bight (fig. 1.1). The sand on area beaches moves along the coast of southern Santa Barbara and Ventura Counties until it reaches the Mugu submarine canyon, which is believed to be the endpoint of the littoral cell.

The Santa Barbara sandshed is a relatively complex coastline with a variety of rocky outcrops, offshore reefs, and relatively narrow beaches. The beaches receive the majority of their sand inputs from four major rivers: the Santa Maria, Santa Ynez, Ventura, and Santa Clara Rivers, which drain the sedimentary rocks of the Transverse Range. Numerous small coastal drainages also provide sediment pulses during episodic rain events (Inman and Jenkins, 1999; fig. 1.1).

Point Conception to the northwest and the Channel Islands to the south create a narrow swell window that shelters much of the south-facing coast of Santa Barbara County from extreme wave events (fig. 2.1). The Mediterranean climate of southern California results in mild annual temperatures and low

precipitation punctuated by episodic and often extreme events frequently associated with El Niños.

Winds and wave heights vary seasonally, but focusing of waves into the Santa Barbara Channel drives an almost unidirectional alongshore sediment transport from west to east. Beaches narrow during the winter and spring (November to April), and widen during the summer and fall (May to October).

Alongshore transport rates for the study area are approximated by the 75-year Santa Barbara Harbor and the 44-year Ventura Harbor dredge records, which show mean annual rates of \sim 230,000 m³ and \sim 505,000 m³ of sand removed per year respectively (adapted from Patsch and Griggs 2007; pers. comm., U.S. Army Corp of Engineers, December 2007; fig. 2.2). Variability in the dredge volumes stem from sediment supply, navigational depth requirements, funding, and differences in reporting of sediment volumes. The southern coast of Santa Barbara and Ventura Counties is composed mostly of bluff-backed beaches perched on bedrock wave-cut platforms. Along this coast are a few dune-backed beaches that have formed near ephemeral creeks and sloughs, typically controlled by the complex faulting in the Western Transverse Range.

The northern end of this sandshed has been characterized as the last remaining stretch of relatively undeveloped coast in southern California; however, the area is not without human influence. Physical alterations to the Santa Barbara coastline began with the completion of the Southern Pacific Railroad in 1901. Major physical alterations to the Santa Barbara sandshed began with dam construction on major rivers: the Santa Ynez River in 1920, the Ventura River in 1955, and the Santa Clara River in 1948 (Patsch, 2004). In 1928, the Santa Barbara Harbor was constructed, and subsequent sand impoundment in the harbor provided a classic example of down-coast erosion caused by the disruption of alongshore transport (Wiegel, 2002; Barnard and others, 2007; Revell and others, 2008). Dam impoundment and shore-protection structures have been estimated to result in an approximately 40 percent reduction in sand supplied to the SBLC by the major rivers and bluff erosion, with the great

majority of the reduction from dam impoundment (Runyan and Griggs, 2003; Willis and Griggs, 2003). It was predicted that this reduction would result in a subsequent decline in sand volume dredged at the harbors in the cell. However, Patsch and Griggs (2007) used dredge records to estimate average alongshore transport of sand at Santa Barbara and Ventura Harbors (fig. 2.2), and concluded that there was no evidence of reductions in dredge volumes following major impoundments in the sandshed. One potential explanation for the lack of reductions could be that updrift beaches were narrowing and supplying the sand that had been lost due to dam impoundment.

Generally, beach widths typically remain constant (after factoring out seasonal cycles) by migrating inland or seaward depending on the amount of sand in the system (Komar, 1998). If the shoreline is eroding due to sea-level rise or some other factor, that same beach width would then be translated inland, but remain relatively constant, assuming a constant sediment supply and no shoreline armoring. However, if the sediment supply is reduced, then beaches would be expected to narrow. Additionally, in locations of shoreline armoring, the placement of a structure on the beach and subsequent erosion results in a narrowing of the beach.

This hypothesis was tested along 10 km of coast centered at Isla Vista, updrift of the Santa Barbara Harbor, where it was found that beach widths had not narrowed but instead had oscillated (Revell and Griggs, 2006). Major beach changes were related to the occurrence of large El Niño events, which elevate water levels, wave heights, and precipitation while shifting the normal storm track to the south, creating more westerly wave attack in this study area (Seymour, 1998; Storlazzi and Griggs, 2000 Inman and Jenkins; 1999, Bromirski and others; 2005, Storlazzi and Wingfield; 2005, Adams and others; 2008). The oscillations in beach width updrift of the Santa Barbara Harbor were found to coincide with different phases of the Pacific Decadal Oscillation (PDO), a climate index of sea-surface temperature with a periodicity of ~20+ years (Mantua and others, 1997). During positive PDO phases,

despite El Niño-like patterns of increased precipitation and stream flow (Inman and Jenkins, 1999), beaches narrowed; during negative and calmer, drier PDO phases, beach widths widened (Revell and Griggs, 2006). The driving mechanisms of beach changes are most likely related to the change in wave direction that shifts waves more to the west during large El Niño events (Seymour 1998; Storlazzi and Wingfield, 2005; Adams and others, 2008). A shift in wave direction over a longer period of time would preferentially affect beaches that were normally sheltered in the Southern California Bight (Graham, 2003). This PDO-related oscillation has also been observed in Kihei, Maui, where alongshore sediment transport in similarly sheltered areas was also affected by a change in wave direction (Rooney and Fletcher, 2005).

Historical regional shoreline changes have recently been calculated for this study area as part of the USGS National Shoreline Assessment Project for California. Using three historical topographic sheets (T-sheets; 1870s, 1933, and 1970s) and a more recent 1998 Lidar shoreline, Hapke and others (2006) found that for the Santa Barbara South region, average shoreline-change rates were slightly accretional (0.1 m/yr) from 1871 to 1998, while short-term rates (1970s to 1998) were erosional (-0.5 m/yr; 2006). The minimum and maximum rates were found to be mostly associated with large transportation and engineering projects.

The focus of this study has been to incorporate additional shorelines into the change analyses and to incorporate a beach-width component into the 70-km stretch of the Santa Barbara sandshed extending from Ellwood Beach to Ventura Harbor in order to evaluate the response of beaches and the shoreline to the quantified reduction in sand supply. This study also examined beach response to major El Niño events, and the impacts of human alterations to the coastline.

Methods

Historical Air Photos and Topographic Sheets

Historical aerial photographs and T-sheets provide two of the best data sources for long-term shoreline and beach-change investigations. For this study, eighteen different sets of vertical air photos were obtained for the period from 1929 to 2003 (table 2.1). Photographs selected for this study (at scale 1:24,000 or smaller) were taken during the calmer season (summer to fall) to reduce the influence of seasonal variability and to ensure that beaches were near their maximum width. Additionally, the use of historical National Ocean Service (formerly U.S. Coast and Geodetic Survey) T-sheets from the 1870s and 1933 that mapped a High Water Line (HWL) shoreline extended the shoreline-change analyses to 138 years. To minimize errors, historical imagery and topographic maps were georectified using known coordinates of ground locations (obtained through GPS surveys) and orthophotography to reduce photo distortions (Moore, 2000; Hapke and others, 2006; Moore and others, 2006).

For each rectified air photo, two shoreline reference features were digitized—the wet/dry line (identified using tonal contrasts), and the back beach or toe of the cliff, revetment, or dune. The beach width is the distance between the wet/dry line and the back-beach feature, generally the dry sand (subaerial) portion of the beach at the time of the photo. Given the short-term variability of water levels, corrections to the wet/dry proxy-based shoreline reference features were based on the tide-level portion of the total water-level model discussed in Ruggiero and others (2003). Tide-level corrections adjusted the wet/dry shorelines to Mean Sea Level (MSL; 0.83 m NAVD88) by using historical hourly water-level data at Santa Barbara Harbor (Station # 9411340; National Oceanic and Atmospheric Administration, 2007). These corrections translated the water level at the time of each historical photo onto an average summer beach slope calculated from historical profiles and more recent Lidar data sets. A similar correction was also applied to the HWL mapped on historical T-sheets, which has been shown

to be systematically offset landward of mean high water (MHW) (Hapke and others, 2006), thus adjusting the T-sheet shoreline to MSL (see additional discussion under uncertainties and errors).

The historical beach-slope averages used in the tidal correction were taken only from the historical summer profiles (June to October) and ranged from 0.036 (sand beach) to 0.11 (cobble beach). Due to the typical low energy waves found in the Santa Barbara Channel during the summer and fall, and the lack of directional hindcast wave data for most of the photography, a wave run-up adjustment was not included in the proxy-based shoreline correction.

Shoreline change and beach widths for all imagery were measured along the same 50-meter spaced transects drawn from an offshore baseline using the USGS Digital Shoreline Analysis System (DSAS; Thieler and others, 2005). All shoreline-change rates discussed in this paper were calculated using DSAS version 3.2, which uses an offshore baseline to calculate relative shoreline position and change rates. This study focused on the shoreline-change linear regressions rate (LRR) and statistics of both the wet/dry MSL shoreline and the back-beach shoreline. Using the intersection locations of the shorelines along each transect, a history of shoreline positions relative to the historical T-sheet baseline were calculated to examine temporal movement of the shoreline. The intersection of the 50-m transects and the individual wet/dry shorelines for each year were then used to calculate shoreline orientations. At the intersection points of the wet/dry shoreline and the transect lines, a straight line was drawn between transects, and an azimuth angle of this intersecting line was calculated in ArcGIS. By adding 90 degrees to this azimuth angle a shore normal or perpendicular angle to the shoreline was created. Shoreline orientations were filtered to exclude all transects in front of shore-parallel protection structures, at rocky outcrops, and near creek and river mouths to reduce the noise associated with inlet dynamics and abrupt or artificial changes in the shoreline.

Beach widths were measured for individual years, by setting the back-beach reference feature to one year after the date of the wet/dry shoreline, so that the end-point rate calculation in DSAS actually measured the beach width. Tide corrections were then applied to the beach widths following measurement with DSAS. Beach-width changes were calculated by subtracting the older beach widths from the more recent year at each transect. For example, to calculate the long-term changes between 1929 and 2006, the 1929 beach width (for example, 30 m) was subtracted from the 2006 beach width (for example, 20 m) so that any negative change would indicate beach narrowing (for example, 20 m - 30 m = -10 m).

Beach-width measurements and the average beach slopes used in the tide-level corrections were multiplied to calculate sand volumes above MSL per transect (m^3/m). Transect volumes were then multiplied by the 50-m transect spacing and summed alongshore to provide a total volume for a length of shoreline. A sensitivity analysis examined the difference in beach volumes calculated using the range of beach slopes. The use of maximum and minimum (1:10 and 1:23 respectively) beach slopes in the volume calculation led to worst-case volume differences on wide beaches of up to \pm 23 m^3/m compared to volumes obtained using the average summer beach slope.

Lidar and GPS Surveys

More recent applications of high accuracy, topographic Lidar data coupled with historical air-photo analyses enables rapid assessment of long stretches of coastline and provides additional information on beach volumes and regional shoreline changes caused by extreme storm events (Revell and others, 2002; Sallenger and others, 2003). To document changes caused by the 1997-98 El Niño event, NOAA, NASA, and the USGS partnered to conduct pre- and post-storm Lidar surveys along the Pacific coast in October 1997 and April 1998 (Sallenger and others, 1999). An additional Lidar data set

was collected in October 2005 by the University of Texas, in collaboration with the USGS, UCSC, and BEACON.

Lidar data sets were processed to extract a MSL contour and the back-beach reference feature by using visual cues in cross-shore profiles, slope, and hillshade layers. These two reference features were included in the beach-width change analyses, and the 1997 and 2005 MSL contours were included in the shoreline-change analyses. Subaerial beach volumes (above MSL 0.83 m) were calculated and reported. Changes between the various data sets were calculated by differencing the Lidar grids, showing the spatial extent of the changes between time periods.

Uncertainties and Errors

The use of air photos for accurate shoreline-change assessments requires an understanding of potential error sources. Errors inherent in air-photo interpretation can be broken down into (1) source error, (2) interpretation error, and (3) short-term natural variability errors (Morton and Speed, 1998). Source error results from photo distortion, scale, and scanning errors (Moore, 2000). Interpretation errors come from difficulty in locating shoreline reference features. Short-term variability errors arise from seasonal changes in beach profile and variations in water levels and wave run-up elevations that change the location of the shoreline reference features (Morton and Speed, 1998; Ruggiero and others, 2003). The use of historical T-sheets also introduces another level of uncertainty. Recent studies have shown that there is a systematic offset of MHW seaward when compared to HWL-derived shorelines (Ruggiero and others, 2003; Hapke and others, 2006; Moore and others, 2006). This offset varies depending on beach morphology, especially slope, but is tied primarily to water levels which are comprised of both tide-level and wave run-up components (Ruggiero and others, 2003; Moore and others, 2006).

Error estimates for the identification and absolute spatial location of the shoreline reference features associated with shoreline-change analysis are, ± 9.7 m, and ± 9.3 m for the early 1929 and 1938 photography, respectively, based on a quadrature, or sum of squares method (Hapke and others, 2006). More recent photography scanned at a higher resolution provides lower spatial errors on the order of ± 7 m (table 2.2). Errors reported in table 2.2 are an average root mean square (RMS) error of all photos used in the flight line and relate to the spatial accuracies associated with the reference features.

To reduce the errors associated with the use of historical T-sheets, given the lack of availability of historical wave data, an elevation correction of 0.46 m was applied to adjust the HWL to MHW based on estimates of average horizontal offsets found along Texas and Maryland coasts with similar beach slopes (Morton and Speed, 1998; Hapke and others, 2006). Additionally, another vertical offset of 0.45 m was applied to adjust the MHW shoreline to MSL based on the tidal records available from Santa Barbara Harbor. The overall horizontal offset seaward after these vertical adjustments were applied to the HWL T-sheet shoreline ranged from 8.3 to 25.4 m with an average of 15.8 m.

Unlike the shoreline-change analysis that depends on different images and T-sheets, the errors in beach-width measurements are spatially independent because both reference features can be seen in each image. The maximum potential error in the beach-width corrections associated with choosing one tide level and slope for the entire flight is 10.6 m, assuming a spring tide range (2.3 m) and the most dissipative mean summer slope (2 degrees). The tidal records show, however, that none of the photo flights was conducted during the maximum spring tide fluctuations, making this most likely an overestimate of the magnitude of beach-width error. Beach-width errors resulting from the use of a mean summer beach slope for all of the photos were examined by calculating beach-width corrections using the range of historical beach slopes through all seasons. The largest difference in beach-width corrections using the minimum versus maximum historical beach slope and the maximum water level

adjustment for a given year was 29.2 m. However, because the photos were selected from summer and fall, the use of a mean summer beach slope should reduce the potential errors from the use of a single slope.

Lidar data sets from the 1997-98 flights have been reported to have accuracies on the order of 1 m in the horizontal, and \pm 15 cm in the vertical (Sallenger and others, 1999, 2003). However, the 2005 Lidar flight reports a vertical error of only \pm 7 cm, and comparison with survey grade control points gathered in Carpinteria at the end of Linden and Ash Avenues coincident with the Lidar flight shows that the mean vertical error of 325 co-located points (within 0.5 m) is only 0.5 cm (Barnard and others, 2007). Comparison of control points in the 2005 Lidar and the 1997-98 flights shows a systematic offset of < 4 cm.

Correlation of Dredge Volumes and Beach Volumes

Given that alongshore transport in the SBLC is nearly unidirectional, there is an expected correlation between the various beach widths and the volumes of sand dredged at the Santa Barbara and Ventura Harbors. To examine this relationship, a lagged cross-correlation analysis was conducted between the harbor dredge records compiled from the USACE and Patsch and Griggs (2007; fig. 2.2), and the summer/fall beach-width data set for the coastline from Ellwood Beach to the Ventura Harbor. Prior to the analysis, modifications of the two data sets were necessary. First, the Santa Barbara Harbor dredge record was interpolated during the early years (1930s to 1960s) during the sporadic dredge operations. The dredge data was smoothed using a moving average between the existing volume records, producing a continuous time series of dredging. The summer/fall beach-width record, consisting of various numbers of records at each beach, collected by using the methods discussed above, was also smoothed using linear interpolation to create a continuous time series. The final alteration to the beach-width data set was the assumption that beach widths were reduced significantly following the

especially energetic 1982-83 and 1997-98 El Niño events, with similar reductions following both events. A lagged cross-correlation was then performed to examine potential transport times between changes in beach widths and volumes of sand dredged from the harbors.

Results

Beach Widths

The primary research objective was to examine the long-term changes in beach widths to ascertain whether the beaches have narrowed over time and supplied sand to the harbor dredge records, masking the reduction in fluvial-sand supply (Runyan and Griggs 2003; Willis and Griggs 2003). Figure 2.3 shows long-term beach-width changes relative to the 2005 beach widths. Overall, there is not a uniform narrowing of beach widths across the study area. It is important to note that this end point beach-width change analysis does not capture the oscillations in beach width that have been previously documented (Revell and Griggs, 2006; fig. 2.4)

The beach widths in the study area have varied widely throughout the more than 70-year aerial photographic time series (fig. 2.5). By examining the beach-width envelopes, two types of beaches can be identified—stable beaches and storage beaches. A stable beach maintains a consistent minimum beach width, and a storage beach is one that exhibits natural variability but occasionally has a zero minimum beach width. Stable beaches (for example, Ellwood, Hope Ranch and Carpinteria) provide good locations to examine storm impacts and to observe pulses of sand moving along the coast. Storage beaches have the capacity to store sand and may make better locations for potential nourishment projects. An example of a potential storage beach is UCSB, a beach that reached maximum widths (>150 m) in the 1960s and 1970s (Revell and Griggs, 2006), but has also been completely removed at times (fig. 2.4).

The beach-width envelope results demonstrated in figure 2.5 divide the study area into two parts based on the location relative to the Santa Barbara Harbor. The updrift beaches to the west of the Harbor (toward Ellwood) face more southward and exhibit a wider range of beach widths, with minimum widths following either the 1982-83 or 1997-98 El Niño event. The maximum widths for most of these beaches were reached in the 1970s. Current beach widths are similar to those found in the 1930s and 1940s for most of the study area.

The beaches downdrift of the harbor (toward Carpinteria and Pierpont groins) have smaller ranges of beach widths and are primarily armored shorelines (fig. 2.6). The minimum widths do not follow El Niño events, and maximum widths along this stretch do not fit any obvious pattern, although the lack of photo sets available prior to railroad completion in 1901 (we didn't have airplanes yet for aerial photos), extensive armoring, and highway expansion limit the analysis.

The largest beach-width changes in this study area result from transportation and engineering projects. The greatest widening and narrowing both resulted from the construction of the Santa Barbara Harbor in 1928. West Beach, immediately downdrift of the sand bypass, widened by ~150 m, while Carpinteria around Sand Point and the inlet to Carpinteria Salt Marsh showed the greatest beach narrowing (-138 m). Other large beach widening (>100 m) has occurred at the Pierpont groins in Ventura and at Ledbetter Beach due to sand impoundment updrift of the Santa Barbara Harbor (>50 m). Ellwood Beach is uniquely situated, facing west into the dominant wave direction, and is the only natural dune-backed shoreline remaining in the study area. Large beach narrowing has occurred at Goleta Beach (-50 m) as a result of the construction of the Santa Barbara airport and the loss of tidal prism at Goleta Slough (Revell and Griggs, 2006).

Beach Widths and Shoreline Orientations

Due to the irregular shape of the coastline and the near uniform wave direction, wave exposure varies greatly depending on shoreline orientation. Oscillations observed in the long-term beach-width change analysis (for example, fig. 2.4) are related to changes in the shoreline orientations that partially control beach widths due to exposure to wave attack (fig. 2.7). The shoreline-orientation results indicate that the most stable and widest beaches are those found facing SSW (255 to 210 degrees) and SSE (165 to 150 degrees). The narrowest beaches are found facing nearly due south (210 to 165 degrees), with the exception of the beach created at the end of the Santa Barbara Harbor dredge-discharge site (180 degrees). The shoreline-orientation analysis also demonstrates the impacts of cross-shore littoral barriers (for example, groins, jetties) across the study area through time.

While air photo data from the pre-harbor construction era are sparse, it appears from historical oblique photos that most of the beaches were relatively narrow. In the 1940s (data from 1943 for the area west of harbor and from 1947 for the area east of harbor), the beaches remained relatively narrow with the widest being in the east (facing 165 to 150 degrees) as a result of Santa Barbara Harbor construction and the trapping of sand to form the updrift Ledbetter Beach. Wide beaches in the west were found in the dunes of Ellwood Beach (facing 255 to 235 degrees). By 1975, a series of engineered groins were constructed at Pierpont creating wide beaches near Ventura, facing 225 to 215 degrees. The beaches in 1975 were generally wide, and the southeast facing (105 to 120 degrees) UCSB storage beach reached its maximum width. After the 1982-83 El Niño, the beach at UCSB was eroded ~100 m (Revell and Griggs, 2006). Throughout 1994 and 2001, beach widths continued to widen as they recovered from the 1982-83 El Niño and, despite the large 1997-98 El Niño, most of the beaches remained relatively wide in 2001.

Shoreline Changes

Linear regression shoreline-change rates were calculated for both the wet/dry shoreline proxy and the back-beach reference features at each transect along the entire study area (tables 2.2 and 2.3; fig. 2.8). The average change trend along the 70-km study area for all reference features is accretion. During the time period between 1929 and 2005, the wet/dry shoreline proxy accreted about 16 cm/yr, while the 1869 to 2005 time period showed accretion of 8 cm/yr. During the 1929 to 2005 time period, the back beach also accreted at an average rate of 10 cm/yr (table 2.2). The change rates summarized in table 2.2 do little to describe the smaller spatial patterns and trends associated with the different shoreline segments (figs. 2.8 and 2.9).

In the entire study area, the highest shoreline-erosion rates occur near Sandyland at the inlet to Carpinteria Salt Marsh, and north of the entrance to the Ventura Harbor, with both rates greater than -2 m/year (fig. 2.8). Maximum accretion rates are a direct result of engineered structures, with the construction of the Santa Barbara Harbor and the construction of the oil-processing facilities and highway expansion at Oil Piers resulting in accretion rates of >2.5m/yr (fig. 2.8; table 2.3A). Significant linear regressions ($r > 0.7$) shown in figure 2.9 highlight the spatial locations of erosion hotspots and accretion for each reference feature. Persistent erosion can be seen along Isla Vista, Sandyland, Carpinteria, Pitas Point, and north of the mouth of the Ventura River. Significant accretion trends can be seen both updrift and downdrift of the Santa Barbara Harbor and along Oil Piers and the Pierpont Groins (fig. 2.9).

Many of the differences in shoreline changes between the back beach and the wet/dry (and T-sheet) shorelines can be attributed to the presence of shoreline armoring (fig. 2.10; table 2.3B). The various shoreline protection structures were separated into shore-parallel (seawalls, revetments) and cross-shore (groins and breakwaters) categories to examine the relative effect on the associated

shoreline of different types of structures. Table 2.3b shows that cross-shore structures are more effective at moving the wet/dry line seaward, with accretionary-change rates around 50 to 70 cm/yr. Shore-parallel structures, including revetments and seawalls, seem more effective at advancing the back beach, with average accretion rates for the study area around 23 cm/yr, while the MSL shoreline only accreted at 12 cm/yr.

A closer spatial examination of significant regressions ($r > 0.7$) shows that in several cases, there are differences in rates between the back beach and the wet/dry reference features (figs. 2.9 and 2.10). Of particular interest to current management decisions are the accretion of the back beach at Goleta Beach and Carpinteria that correspond to a significant erosion trend of the wet/dry shoreline. This combination will be exacerbated by sea level rise leading to an eventual loss of beach. In contrast, at the two back-beach accretion locations (near Arroyo Burro and Padaro Lane—fig. 2.10), the back beach is dominated by large seacliffs whose failure is characterized by large mass wasting events. Despite their lack of armoring, these locations show accretion, indicating that as these cliffs fail the material remains, resulting in accretion of the back beach. In contrast, Ellwood, the only remaining natural dune-backed beach in this study area, has shown significant erosion of the back beach (figs. 2.9 and 2.10), while the wet/dry shoreline has accreted (fig. 2.3).

The application of a beach-width methodology to the study of Santa Barbara and Ventura County beaches permits an examination of both the foreshore and the backshore, as well as the shape of the beach over time. Along an unarmored beach, given a steady supply of sand, widths should stay relatively stable over the long term, with the beach migrating landward or seaward depending on changes in sea level. In this case, shoreline-change rates for both reference features should be similar. As can be seen in table 2.4, significant correlations exist between the change rates calculated for the various reference features, indicating a coupling of the shoreline response. The strongest correlations are found along unarmored stretches of shorelines (table 2.4). In areas of no structures, the “natural”

shoreline-change rates show the back beach and the wet/dry line having similar rates of erosion—around 2 to 3 cm/yr (table 2.3b). The similarity in rates can be expected because as the wet/dry shoreline erodes, the back beach should erode at about the same rate, maintaining a stable beach width. This similarity in rates provides some evidence that there has not yet been a large-scale reduction in sediment supply. Several case studies demonstrate the benefits of incorporating a beach-width methodology into the shoreline-change analyses.

Case Study: Carpinteria Erosion

Breakwater construction and sand impoundment at the Santa Barbara Harbor led to a well-documented erosion wave that impacted downcoast (southeast) beaches (Komar 1998, Wiegel 2002, Barnard and others 2007, Revell and others, 2008; fig. 2.11). Downdrift beaches at Sandyland and Carpinteria were impacted significantly. At Carpinteria, a recurring erosion hotspot requires regular beach maintenance and periodically threatens oceanfront property during large storm events. Using a combination of historical air photos, Lidar data, and physical measurements, historical shoreline and beach-width changes were analyzed for the last 138 years. The initial erosion wave dramatically reduced beach widths by about 50 m (fig. 2.12). The long-term beach-width and shoreline-change analyses show preferential erosion (-0.35 m/yr) at the west end of Carpinteria and accretion in the east (0.3 m/yr) (fig. 2.13). The net result has been a clockwise beach rotation with the updrift west end narrowing ~50 m while the downdrift east end of the beach has widened about 40 m during the same time period.

El Niño storm impacts from the 1982-83 and 1997-98 El Niño seasons have a similar west-end erosion and east-end accretion pattern that matches the overall trend in the long-term (138-year) shoreline-change analysis, providing evidence that strong El Niños may be driving the long-term coastal evolution (fig. 2.14). Following the 1982-83 El Niño, a revetment at the western end of the beach was

constructed. Analyses following the 1997-98 El Niño showed that the 1997-98 El Niño erosion hotspot shifted downdrift onto the City of Carpinteria beach (fig. 2.14).

Seasonal beach-width changes show that the seasonal cyclical pattern is a systematic retreat of the shoreline and narrowing of the beach width by about 20 m. The seasonal analyses show an erosion hotspot at the end of the revetment that is evidenced by increased narrowing of the beach width and loss of sand volumes (fig. 2.15). During the seasonal surveys, relatively low wave conditions dominated, with changes to the nearshore and beach occurring above 5 m water depth. Tidal currents are relatively low (<20 cm/sec) and not of sufficient velocity to move the coarse-grained sediment alongshore (Barnard and others, 2007).

Sediment sampling shows that there is a seasonal coarsening of sediments in the winter and a fining in the summer. There is alongshore variability in the winter coarsening pattern with the coarsest materials co-located with the erosion hotspot seen in the El Niño storm impacts and the seasonal beach-width changes (fig. 2.16; Barnard and others, 2007).

Finally, a significant lag correlation analysis, with a peak lag of 4 years, indicates that most of the sand dredged from Santa Barbara Harbor arrives on the beaches of Carpinteria after 4 years and may continue to supply the beaches for up to 10 years (Barnard and others, 2007; Revell and others, 2008).

The consistent pattern of shoreline rotation is visible in beach response to both major El Niño events and in the long-term shoreline-change data, suggesting that El Niños may be playing a role in driving the long-term coastal evolution. However, there are several complicating factors in Carpinteria associated with the erosion wave due to harbor construction, ongoing dredging, and shoreline armoring. These complications require us to examine another beach to assess the El Niño pattern of shoreline rotation.

Case Study: Hope Ranch

To better understand the relationship between shoreline reorientation patterns and storm responses, we examined a less altered beach. Hope Ranch is a stable, bluff-backed beach downdrift of Isla Vista and Goleta Beaches and updrift of the Santa Barbara Harbor (fig. 2.1); it can be characterized as having a relatively narrow range of beach widths (~25 m) and is notable for its lack of shoreline armoring (fig. 2.6). Hope Ranch thus can provide additional insight into patterns of long-term and storm changes, as well as sediment transport along this portion of the coast.

The 70-year long-term shoreline change of both the wet/dry and back-beach shoreline show similar rotation patterns to the shoreline changes observed at Carpinteria, with updrift erosion rates greater than those at the downdrift end (fig. 2.17). This erosion-rate pattern results in a subtle reorientation of the coast, similar to the pattern seen in Carpinteria (fig. 2.12). At Hope Ranch, the lack of armoring results in both the back beach and wet/dry shoreline showing similar reorientation patterns, with the back-beach rates slightly smaller. The Hope Ranch beach response to the 1982-83 El Niño was similar to that seen in Carpinteria, with erosion at the west end of nearly 50 m and much less erosion at the east end (~ 10 m) (fig. 2.17B). The similarity in shoreline changes and beach response at Hope Ranch and Carpinteria suggests that the complicating factors of harbor influences and shoreline armoring at Carpinteria are not the causes of the changes, and provides additional evidence that large storm events, particularly those associated with strong El Niño events, may be playing a major role in shaping the beaches along the Santa Barbara coast.

Sand Transport and Lag Correlation Analyses

To understand how sand is transported along the Santa Barbara coast, several analyses were conducted. First, observations of the pulse of sand eroded from UCSB during the 1982-83 El Niño event were examined. Second, lag correlations between the beach widths and the sand volumes dredged from

both Santa Barbara and Ventura Harbors were examined to better quantify the transport times to and from various beaches to the harbors.

The 1982-83 El Niño event reduced the beach width at UCSB by ~75 m and the volume of sand by ~385,000 m³ (-109 m³/m; Revell and Griggs, 2006). Santa Barbara Harbor dredge records from 1993-95 show an increase in the volume of dredged material (~450,000 m³) above long-term average rates (~230,000 m³/yr) that is of a similar magnitude to that eroded from UCSB and Goleta Beaches (~385,000 m³). Given the unidirectional alongshore transport and estimates for migration rates of sand pulses and erosion waves of ~1.7 km/year (Bailard and Jenkins, 1982; Wiegel, 2002), this sand would have to have been transported downcoast along the beaches of Hope Ranch (~7 km) and Ledbetter (~14 km) before being deposited in Santa Barbara Harbor. By examining the transport of this sand volume at each transect and the total volumes for the two stable beaches along this relatively unaltered coastline, we can better understand the transport dynamics (fig. 2.18).

Immediately following the 1982-83 El Niño event, beach widths and volumes along the segment of coast between UCSB and Santa Barbara Harbor were significantly reduced. Between 1983 and 1986, some recovery occurred from storm rotation, but sand volumes did not increase significantly (fig. 2.18). However, by 1989 there was significant beach accretion at Hope Ranch and counter-rotation at the eastern end of the beach that coincided with the expected arrival time of the sand pulse from UCSB and Goleta beaches (fig. 2.18). Sand eroded from Hope Ranch by the 1982-83 EL Niño event probably arrived at Ledbetter Beach in 1989, while by 1994 the pulse of sand had passed Hope Ranch and the eastern end of the beach rotated westward. At Ledbetter Beach, beach volumes that had been increasing steadily since the 1982-83 El Niño event reached their maximum of more than 400 m³/m in 1994. While the stable beaches at Hope Ranch and Ledbetter show oscillations in beach volume, the beaches in between show relatively little change during the migration of this sand pulse.

Considering that the beaches between Hope Ranch and Ledbetter did not accrete significantly, we can examine the total beach volumes above MSL for these two beaches to try to detect the sand pulse (fig. 2.18B). The pulse can be seen moving on the beach at Hope Ranch in 1989, which then decreases in width by 1994, while Ledbetter continues to accumulate sand on the beach until 1994. The sand volumes at both beaches are about equal in 1989, suggesting that the sand at Hope Ranch pre-1982-83 El Niño migrated downdrift to Ledbetter beach. The increase in beach volumes above MSL between 1983 and 1989 ($\sim 200,000 \text{ m}^3$) at Hope Ranch and Ledbetter and the magnitude of sand lost from UCSB Beach and Goleta beaches ($\sim 385,000 \text{ m}^3$) are different. Since the beaches between the two beaches did not accrete significantly, and assuming that the beach slopes did not change significantly, the implication is that some of the sand was deposited offshore and moved alongshore below MSL.

The lag-correlation analyses yielded some significant results, however, the sporadic air photo record (table 2.1) and the resulting need to interpolate data for years with no photos creates some uncertainty in the results, so the calculated transport times must be considered only as approximations. In general, the beaches around Isla Vista and Carpinteria that had the most shoreline data had the most significant correlations. Beach widths at Ellwood, Isla Vista, UCSB, and Goleta were all significantly correlated with each other at the 5 percent level (95 percent confidence interval). Significant lag times indicate that transport between those beaches, as measured through beach width changes, ranged from 2-5 years. UCSB beach widths were significantly correlated, at the 0.02 percent level, with the Santa Barbara Harbor dredge volumes at a peak lag time of 5 years. This correlation was significant at the 5 percent level for lag times from 2-7 years. Downdrift of the Santa Barbara Harbor, beach widths at Sandyland and Carpinteria were both significantly correlated with Santa Barbara Harbor dredge volumes. The peak lag time for Sandyland was at 9 years, matching the arrival time of the erosion wave following harbor construction. A secondary peak at Sandyland matched the 4-year lag-time result at

Carpinteria, which was significant at the 0.1 percent level. The significant 4-year lag between beach width changes at Carpinteria matches the lag estimated by Barnard and others (2007) based on changes in Carpinteria beach volumes and Santa Barbara Harbor dredge volumes. At the downdrift end of the study area, beach widths at San Buenaventura and the Pierpont groins were correlated with the Ventura Harbor dredge records with lags of 1-3 years that were significant at the 2 percent level. Finally, a lag correlation analysis comparing the Santa Barbara and Ventura Harbor dredge records did not produce any statistically significant relationships.

Discussion

Beach Width

A beach-width methodology, when used in conjunction with shoreline-change analyses, provides information on the shape of the beach, response of the beach to storm events, and additional information for assessing changes in beach volumes. The motivation for selecting a beach-width methodology was to determine if there was a long-term narrowing of the beaches that could explain the discrepancy between a sediment-supply reduction (Runyan and Griggs 2003; Willis and Griggs, 2003) and the relatively stable long-term average dredge volume recorded at Santa Barbara Harbor (Patsch and Griggs, 2007). The endpoint beach-width change analyses did not identify any systematic long-term narrowing that could be attributable to sediment-supply reductions. Because the harbor plays a role in regulating beach widths downcoast, we would not expect to see narrowing downcoast without first finding a drop in the harbor dredge records—unless there was substantial sediment coming into the harbor from the east such as that described by Bailard (2007). An endpoint analysis is susceptible to extremely wide or narrow beach widths at either one of the two reference points in time, although it seems most likely that the photo sets were obtained at intermediate beach conditions which prevail most

of the time. Due to the prevalence of narrow beaches with widths near zero, beach-width narrowing would best be detected at stable beaches. There is also some evidence of beach-width narrowing occurring at Hope Ranch, where long-term shoreline-change rates differed between the back beach and wet/dry shorelines. The difference would result in long-term narrowing of the beach, but back beach and wet/dry shoreline-change rates did not differ in a consistent way across the study area. Another possibility exists in this alongshore-transport dominated system—that a sediment-supply reduction would not manifest as a systematic narrowing of beaches, but rather as a rotation with the updrift beaches narrowing more than the downdrift ends of beaches. There is some evidence of rotation at Carpinteria, Hope Ranch, and Isla Vista, but the data are not sufficient to determine whether rotation alone can explain the apparent mismatch between sediment supply to the SBLC and beach response. Current modeling efforts by the USGS and the University of Florida may provide additional insights in this area.

The limited findings supporting a beach narrowing updrift of the harbor must be interpreted cautiously because the reductions were only slightly larger than the uncertainty in the beach-width analysis (\pm 5m). Regional analyses were complicated by the limited availability of air photos early in the record and the irregular spacing in time (1929, 1938, 1943, and 1947). Further complicating the analyses were beach changes associated with a variety of human alterations that pre-dated air photos. Ideally, a set of air photos taken at a lower tide during the late summer, prior to railroad construction (circa 1900), and a 1928 set (before harbor construction) would be used with the existing photo sets to better examine the question of long-term narrowing. The use of historical T-sheets is not applicable for beach-width analyses due to the lack of a delineated back-beach feature and the artistic license in the 1870s maps.

Shoreline Changes

Shoreline-change rates calculated for the wet/dry shorelines in the study area are comparable to the long-term average erosion and accretion rates calculated by Hapke and others (2006). The short-term rates calculated by Hapke and others (2006) are near the minimum/maximum erosion/accretion rates calculated in this study. However, the short-term rates seem on the high side given that very few of the rates determined in this study were greater than 1.0, or less than -1.0 m/yr . The short-term results in Hapke and others (2006) may have been biased by the dates chosen for the end-point rate analyses, with the first date in the 1970s occurring at a time when many of the beaches were at their maximum width, while the 1998 Lidar data was collected following a major El Niño storm event that narrowed beaches significantly. These endpoints thus may have resulted in unusually high values for short-term erosion rates. More recent studies that used 2005 as the recent endpoint documented recovery of most of the beaches affected by the 1997-98 El Niño event (Barnard and others, 2007; Revell and others, 2008).

The shoreline-change rates in this study were based on linear-regression analyses that assume that the documented shoreline changes can be explained based on a linear relationship. As has been documented in Revell and Griggs (2006) and in this present study, many of the study-area beaches actually have oscillated throughout the historical record, indicating that a more robust technique capable of dealing with changes in signs and rates over time may yield additional insights into beach dynamics in the SBLCA.

Human Alterations

Although the long-term beach-width change analysis did not reveal any systematic long-term narrowing attributable to sediment-supply reductions, the analysis did reveal a pattern of beach narrowing attributable to shoreline armoring. In the 70 km study area, 60 percent (42 km) of the shoreline was armored with a variety of revetments and seawalls. Along these armored sections,

accretion of the back beach and erosion of the wet/dry shoreline illustrate the effects of placement loss and passive erosion (Griggs, 2005). These two effects dominate the large-scale pattern of beach-width changes. Another ten kilometers (14 percent) of the shoreline is altered by groins, breakwaters, or other littoral barriers. These areas showed accretion of the wet/dry shoreline and a relatively stable back beach. With high rates of littoral transport, the cross-shore structures are effective at increasing beach widths, while shore parallel structures, such as revetments and seawalls, have resulted in placement loss and passive erosion, reducing beach widths. Once a structure fixes the back beach and the placement loss occurs, the rate of back-beach shoreline change becomes irrelevant (fig. 2.5), however the beach-width methodology can provide a tool for coastal managers interested in quantifying and assessing the cumulative impacts of shoreline armoring on broad spatial scales.

At smaller spatial scales, differences between accretion of the back beach and erosion of the wet/dry shoreline could be used to identify locations of placement loss and passive erosion, while changes associated with intervals when shoreline armoring was emplaced could be used to examine active erosion and the location of erosion hot spots at more site-specific scales. For instance, the shift in the 1982-83 and 1997-98 El Niño erosion hotspots in Carpinteria coincided with the construction of the revetment and may be evidence that active erosion and flanking erosion is occurring at the end of the structure.

Beach-width envelopes (minimums and maximums) helped to identify locations of stable beaches—those with greater minimum widths, and storage beaches—those that exhibit extreme natural variability in widths and thus could potentially be good candidates for beach nourishment. Stable beaches were critical to identify because they provide a natural control for examining sediment-transport dynamics along the coastline, as well as the coastal response to storm events. Minimum beach widths showed a distinct difference between beaches updrift of the Santa Barbara Harbor and those

downdrift. Updrift beaches were narrowest following the major El Niño events of 1982-83 and 1997-98, while downdrift beach widths were not obviously linked to major El Niño events. Although the apparent decoupling may partially be explained by limitations in the available photo coverage, it also seems likely that the Santa Barbara Harbor regulates beaches downdrift, much like a dam regulates river levels downstream.

Storm Event Responses

Beach-width responses to large El Niño events match the long-term shoreline-change patterns of shoreline rotation at both Carpinteria and Hope Ranch beaches. The air photos available to examine the effects of the 1982-83 El Niño event at both beaches are not ideal and were obtained several years after the event; however, the similarity in patterns between beaches, and between El Niño events, is striking. If the beach conditions at Carpinteria in 1989 were the result of the 1982-83 El Niño event, then the 1982-83 event had a longer-lasting impact on the coast than did the 1997-98 event. The similarity in beach responses along these west-facing beaches to the two major El Niño events suggests that there may be a predictable pattern of El Niño storm response, in which beach widths are reduced by more than 50 percent and beaches rotate clockwise. This knowledge could be useful to coastal managers and emergency responders tasked with deciding where, and for how long, they should permit emergency structures, build sand berms, or nourish beaches.

Sediment Transport and Lag Correlations

While several authors have estimated sediment pulse migration rates in the SBLC at ~1.7 km/yr (Bailard 1982; Barnard and others, 2007; Revell and others, 2008), the physical response of beaches during pulse migration has not been well characterized. The lag correlation results obtained in this study suggest migration rates that may be twice as fast or more—on the order of several km/yr. It is likely that

sediment transport along this coast is extremely episodic, with much of the annual transport occurring during the few largest storm events of the year. During calmer years, sediment transport would likely be reduced compared to energetic years with more frequent and severe storm events.

The erosion of a large sand volume from UCSB and Goleta Beaches following the 1982-83 El Niño event provided an opportunity to examine sediment transport. The beach-volume changes and observations of pulse effects at both Hope Ranch and Ledbetter beaches indicate that sand does travel as a relatively cohesive pulse (Hicks, 1985), but the pulse is only detectable at stable beaches and not along the entire length of shoreline. Visibility of the pulse in specific areas may be related to gradients in alongshore transport, or to shoreline orientation. The volume of sand lost from UCSB and Goleta beaches can be accounted for in dredge records at Santa Barbara (fig. 2.2), but cannot be entirely accounted for in beach volumes (above MSL) between these sites, indicating that a significant portion of the alongshore transport occurs offshore. The lag-correlation analyses provided some additional insights into sand-transport timing from various beaches to harbors; however, the sporadic air photo record limits the utility of this approach in forecasting arrival times of sand on downcoast beaches.

The lag correlation between the Santa Barbara and Ventura Harbor dredge records was found to be not significant. Several possible explanations could account for this finding. One explanation could be that travel times exceed the lengths of the time series (75 years at Santa Barbara versus 44 years at Ventura). Another potential explanation is that there are several steep coastal creeks, and the Ventura River, along the 40-km stretch between the harbors. Sediment inputs from these sources may mask significant correlations. Finally, the close proximity of the Santa Clara River to the Ventura Harbor, and the potential for sediment transport reversals in the Ventura area, could complicate interpretation of the Ventura Harbor dredge records. Overall, while the analyses performed in this study may facilitate regional sediment management (for example, nourishment locations) and should provide a better

understanding of cumulative impacts of human alterations on beaches (for example, habitat loss, placement loss), most of the management decisions directly affecting long-term beach widths (for example, setbacks, flood control) and recreational and economic opportunities happen at smaller scales that will require an understanding of regional and local processes to minimize impacts.

Conclusions

- No systematic narrowing of beach widths was found in the end point beach-width changes as was hypothesized to be associated with a reduction in sand supply. Instead, beach widths have oscillated during the 75-year record.
- Updrift of the Santa Barbara Harbor, minimum beach widths were closely related to the strong El Niño events of 1982-83 and 1997-98. Downdrift of the harbor, beach widths did not follow this El Niño pattern, suggesting that the harbor was regulating beach widths downdrift similar to a dam regulating water levels downstream.
- Beach-width envelopes provide strong evidence for stable beaches and could help in refining the current beach-monitoring program.
- The greatest narrowing of beach widths occurred (1) near Carpinteria—caused by sand impoundment by the construction of the Santa Barbara Harbor; (2) by Ventura Harbor—caused by the breaching of the beach to form the harbor; and (3) at Goleta Beach—due to the construction of the Santa Barbara airport and the loss of tidal prism at Goleta Slough.
- The greatest widening of beach widths occurred immediately updrift of Santa Barbara Harbor (>200 m) as a result of sand impoundment by the breakwater, and at the groin field in Ventura where beach widths widened by >100 m.

- The greatest changes to the shoreline resulted from large erosion events such as the 1982-83 El Niño and from the erosion wave associated with the construction of the Santa Barbara Harbor breakwater.
- Analyses of natural beach widths and shoreline orientation demonstrate that the west-facing beaches of Ellwood (255-240 degrees) were the most stable, with beach widths ranging from 25 to 75 m. The east-facing beaches (120-105 degrees) were the most variable, ranging from 0 to 150 m in width. South-facing beaches were the narrowest.
- Beach-width and shoreline-change analyses reveal a pattern of beach narrowing attributable to shoreline armoring. Along the 70 km study area, 60 percent (41.9 km) of the shoreline has been armored with a variety of revetments and seawalls. Along these armored sections, accretion of the back beach and erosion of the wet/dry shoreline illustrate the effects of placement loss and passive erosion.
- From 1929 to 2005, shoreline-change analyses reveal a study-area-wide accretion pattern of 10 cm/yr for the back beach and 16 cm/yr for the Mean Sea Level shoreline. From 1860 to 2005 the Mean Sea Level shoreline accreted at a rate of 8 cm/yr.
- Shoreline-change analyses show that accretion is associated with shore-protection structures, with cross-shore structures (for example, groins, jetties) accreting the wet/dry shoreline by trapping sand and shore-parallel structures (for example, seawalls, revetments) building out the backbeach and reducing beach widths.
- Shoreline segments without shoreline armoring show mild erosion of both the back beach and wet/dry shoreline of about 2-3 cm/yr.

- Carpinteria and Hope Ranch beaches both show El Niño storm-event rotation responses that match the long-term shoreline-change pattern. This suggests that El Niño events may be driving the long-term coastal evolution.
- Sand travels alongshore as coherent pulses that are detectable at stable beaches. Evidence of alongshore sand movement can be seen subaerially in both erosion and accretion waves, with some of the sand transported below Mean Sea Level in the nearshore.
- Lag-correlation analyses show that the movement of sediment pulses may be faster than previously thought, with potential migration rates of several kilometers per year.
- The beach-width methodology is useful when coupled with shoreline-change analyses for examining the cumulative impacts associated with shore-protection structures and the response of the shoreline to large storm events.

References

- Adams, P., Inman, D.L., and Graham, N.E., 2008, Southern California deep-water wave climate: characterization and application to coastal processes: *Journal of Coastal Research*, v. 24, no. 4, p. 1022-1035.
- Bailard, J., and Jenkins, S.A., 1982, City of Carpinteria beach erosion and pier study—Final report to the City of Carpinteria: Bailard/Jenkins Consultants, 292 p.
- Bailard, J., 2007, Improving sand bypassing at Santa Barbara Harbor, CA., In: Smith, J.M. ed., *Coastal Engineering 2006*, Proceedings of the 30th International Conference, Conference Proceedings, San Diego, CA, USA, 3-8 September 2006, v. 4, p. 3823-3834.
- Barnard, P.L., Revell, D.L., Eshleman, J.L., and Mustain, N., 2007, Carpinteria coastal processes study, 2005-2007—Final report: U.S. Geological Survey Open-File Report 2007-1217, 130 p., [<http://pubs.usgs.gov/of/2007/1412/> (last accessed March 13, 2009)].
- Bromirski, P.D., Cayan, D.R., and Flick, R.E. 2005, Wave spectral energy variability in the northeast Pacific. *Journal of Geophysical Research*, v. 110, 2005 American Geophysical Union.
- Graham, N.E., 2003, Variability in the Wave Climate of the North Pacific – Links to Inter-Annual and Inter-Decadal Variability. *Proceedings of OCEANS 2003*. v. 2, p. 969-972.
- Griggs G.B., 2005, The impacts of coastal armoring. *Shore and Beach*, v. 73, no.1, p. 13–22.
- Hapke, C.J, and Reid, D., Richmond, B.M., Ruggiero, P., and List, J., 2006, National Assessment of Shoreline Change Part 3. Historical Shoreline Change and Coastal Land Loss Along Sandy Shorelines of the California Coast. USGS Open File Report 2006-1219.
- Hicks, D.M., 1985, Sand dispersion from an ephemeral river delta on the wave dominated central California coast. PhD Dissertation University of California, Santa Cruz. 210 p.

- Inman, D.L., and Jenkins, S.A., 1999, Climate change and the episodicity of sediment flux of small California rivers. *Journal of Geology*, v. 107, p. 251-270.
- King, P., and Symes, D., 2004, Potential loss in GNP and GSP from a failure to maintain California's beaches. *Shore and Beach* v. 72, no.1, p. 3-8.
- Komar, P.D., 1998, Beach Processes and Sedimentation. Prentice Hall, Inc., Simon & Schuster, Upper Saddle River, N.J., 544 p.
- Mantua, N.J, Hare, S.R., Zhang, Y., Wallace, J.M., and Francis, R.C., 1997, A Pacific interdecadal climate oscillation with impacts on salmon production. *Bulletin of the American Meteorological Society*, v. 78, p. 1069-1079.
- Morton, R.A., and Speed, F.M., 1998, Evaluation of shorelines and legal boundaries controlled by water levels on sandy beaches. *Journal of Coastal Research*, v. 18, Issue 2, p. 329-337.
- Moore, L.J., 2000, Shoreline Mapping Techniques. *Journal of Coastal Research*, v. 16, no.1, p. 111-124.
- Moore, L.J., Ruggiero, P., and List, J.H., 2006, Comparing mean high water and high water line shorelines: Should proxy-datum offsets be incorporated in shoreline change analysis? *Journal of Coastal Research*, v. 22, Issue 4, p. 894-905.
- National Oceanic and Atmospheric Administration (NOAA), 2007, Tides & Currents, Center of Operational Products and Services, [<http://tidesandcurrents.noaa.gov/> (last accessed March 13, 2009)].
- Patsch, K., 2004, Littoral Cells of California. PhD Dissertation, University of California, Santa Cruz Earth Science Department.
- Patsch, K., and Griggs, G.B., 2007, Development of sand budgets for California's major littoral cells. Report to the California Coastal Sediment Management Working Group. 105 p.
[<http://dbw.ca.gov/csmw/csmwhome.htm> (last accessed March 13, 2009)].

- Revell, D.L., Komar, P.D., and Sallenger, A.H., 2002, An Application of Lidar to analyses of El Niño erosion in the Netarts littoral cell. *Journal of Coastal Research* v. 18, no.4, p. 792-801
- Revell, D. L., and Griggs, G.B., 2006, Beach Width and Climate Oscillations Along Isla Vista, Santa Barbara, California. *Shore and Beach*, v. 74, no.3, p. 8-16.
- Revell, D.L., Marra, J.J., and Griggs, G.B., 2007, Sandshed Management. Special Issue-Journal of Coastal Research – Proceedings of ICS 2007. Gold Coast, Australia.
- Revell, D.L., Barnard, P., Mustain, N., and Storlazzi, C.D., 2008, Influence of Harbor Construction on Downcoast Morphological Evolution: Santa Barbara, California. Published in Coastal Disasters '08 Conference, North Shore, HI.
- Rooney, J.J., and Fletcher, C.H., 2005, Shoreline Change and Pacific Climate Oscillations in Kihei, Maui, Hawaii. *Journal of Coastal Research* v. 21, no.3, p. 535-548.
- Ruggiero, P., Kaminsky, G.M., and Gelfenbaum, G., 2003, Linking Proxy-Based and Datum-Based Shorelines on a high Energy Coastline: Implications for Shoreline Change Analyses. *Journal of Coastal Research* v. 38, p. 57-82.
- Runyan, K.B., and Griggs, G.B., 2002, Implications of harbor dredging for the Santa Barbara littoral cell. *Proceedings California and the World Oceans 2002*, Santa Barbara, CA. ASCE.
- Runyan, K.B., and Griggs, G.B., 2003, The Effects of Armoring Seacliffs on the Natural Sand Supply to the Beaches of California. *Journal of Coastal Research* v. 19, no.2, p. 336-347.
- Sallenger A.H., Krabill, W., Brock, J., Swift, R., Jansen, M., Manizade, S., Richmond, B., Hampton, M., and Eslinger, D., 1999, Airborne laser study quantifies El Niño induced coastal change. *EOS*, American Geophysical Union, v. 80, p. 92-93.
- Sallenger A.H., Krabill, W., Swift, R., Brock, J., List, J., Jansen, M., Holman, R.A., Manizade, S., Sontag, S., Meredith, A., Morgan, K., Yunkel, J.K., Frederick, E.B. and Stockdon, H.F., 2003,

- Evaluation of airborne topographic lidar for quantifying beach changes. *Journal of Coastal Research*, v. 19, Issue 1, p. 125-133.
- Seymour, R.J., 1998, Effects of El Niños on the west coast wave climate. *Shore and Beach*, v. 66, no.3, p. 3-6.
- Storlazzi, C.D., and Wingfield, D.K., 2005, Spatial and Temporal Variations in Oceanographic and Meteorological Forcing Along the Central California Coast 1980-2002. USGS Scientific Investigations Report 2005-5085.
- Storlazzi, C.D., and Griggs, G.B., 2000, The influence of El Niño-Southern Oscillation, ENSO events on the evolution of central California's shoreline. *Geological Society of America Bulletin*, v. 112, no.2, p. 236-249.
- Thieler, E.R., Himmelstoss, E.A., Zichichi, J.L., Miller, T.L., 2005, Digital Shoreline Analysis System (DSAS) version 3.0: An ArcGIS extension for calculating shoreline change: U.S. Geological Survey Open-File Report 2005-1304.
- Wiegel, R.L., 2002, Seawalls, seacliffs, beachrock: What beach effects? Part 2. *Shore and Beach*. v. 70, no.2, p. 13-22.
- Willis, C.W., and Griggs, G.B., 2003, Reductions in fluvial sediment discharge by coastal dams in California and implications for beach sustainability. *Journal of Geology* v. 111, p.167-182.

Table 2.1. Specifications of aerial photography. [Spatial errors are the average error for the entire flightline.
Sources: University of California, Santa Barbara Map and Imagery Library, California Coastal Commission, U.S. Geological Survey, and Pacific Western Aerial Surveys]

Year	Date	Scale	Isla Vista	Carpinteria	Santa Barbara	Ventura	Spatial error, in meters
1929	NA	15,840		x			9.7
1938	NA	24,000	x	x			9.3
1943	9/22/1943	20,000	x		x		9.3
1945	11/13/1945	14,400				x partial	8.7
1947	8/20 and 8/21/1947	24,000	x	x		x	9.3
1959	11/23/1959	15,600	x	x			8.4
1959	8/22 and 11/5/1959	16,000				x partial	8.4
1966	9/23 and 10/18/1966	12,000	x	x			8.4
1966	7/5/1966	12,000				x partial	8.2
1968	7/22/1968	30,000				x	9.2
1969	10/30/1969	12,000	x	x			8.3
1971	6/1/1971	12,000	x				8.2
1973	8/23/1973	12,000	x				8.1
1975	7/29/1975	24,000	x	x	x	x	7.2
1981	6/15/1981	24,000				x	7.5
1983	10/26/1983	24,000	x		x		6.1
1986	10/31/1986	24,000	x		x		6.5
1989	5/22 and 5/23/1989	24,000	x	x	x	x	6.4
1992	9/1/1992	24,000				x	6.6
1994	9/9/1994	24,000	x	x	x	x	5.0
2001	9/25/2001	12,000	x	x	x	x	6.3
2003	6/25/2003	6,000	x	x			5.4

Table 2.2. Summary of historical shoreline-change rates for various shoreline reference features, along with associated error estimates.

Shoreline Change (m/yr)	All Transects N=1403	No Structures N=613	Structures N=780
1929-2005 Back Beach	.10 ± .014	.03 ± .022	.15 ± .016
1929-2005 Wet/Dry	.16 ± .013	.04 ± .021	.24 ± .016
1869 –2005 Wet/Dry and T-sheet	.08 ± .013	-.08 ± .021	.15 ± .016

Table 2.3. A, Shoreline-change rates of each reference feature with additional statistics on erosion and accretion transects. B, Shoreline-change rates associated with various types of shoreline armoring. “No Structure” sites have been additionally filtered to remove inlet-influenced transects. [BB, back beach; WD, Wet/Dry line; and WDT, Wet/Dry and T-sheet]

A	All (n=1403)			Erosion			Accretion		
	BB	WD	WDT	BB (n=667)	WD (n=668)	WDT (n=652)	BB (n=736)	WD (n=735)	WDT (n=749)
Mean	0.10	0.16	0.08	-0.18	-0.24	-0.18	0.35	0.52	0.30
Max	2.83	2.58	1.79				2.83	2.55	1.79
Min	-1.33	-2.02	-1.43	-1.33	-3.07	-3.07			
B	Structure – Parallel n=681			Structure – Cross shore n= 99			No Structure n=596		
	BB	WD	WDT	BB	WD	WDT	BB	WD	WDT
Mean	0.23	0.22	0.12	0.07	0.67	0.47	-0.03	0.02	-0.02
Max	2.83	2.13	1.79	2.66	2.55	1.71	1.19	1.71	0.43
Min	-1.33	-1.95	-1.38	-0.89	-3.07	-3.07	-1.15	-2.02	-1.43

Table 2.4. Correlation coefficients between the various shoreline reference features. [All correlations are significant at the 0.1 percent level]

Shoreline-change correlations (r)	All transects N=1403	No structures N=754	Only structures N=649
Wet/dry versus back beach 1929-2005 versus 1929-2005	0.66 0.69		0.43
Wet/dry & T-sheet versus back beach 1869-2005 versus 1929-2005	0.46 0.37		0.20
Wet/dry & T-sheet versus wet/dry 1869-2005 versus 1929-2005	0.68 0.56		0.53

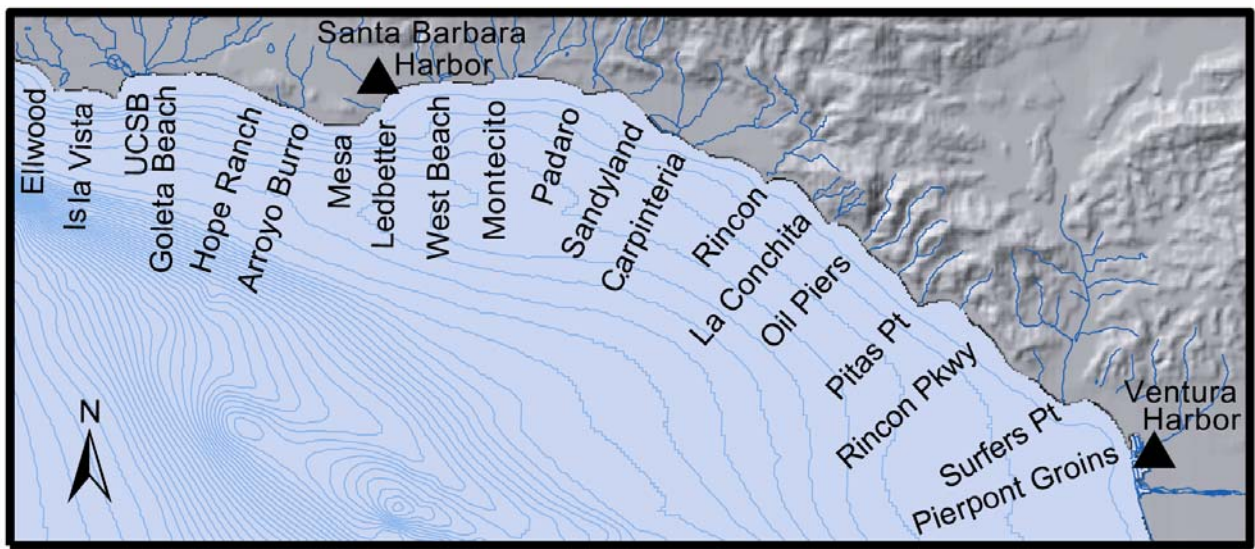


Figure 2.1. The Santa Barbara and Ventura County, California, beaches analyzed for this chapter.

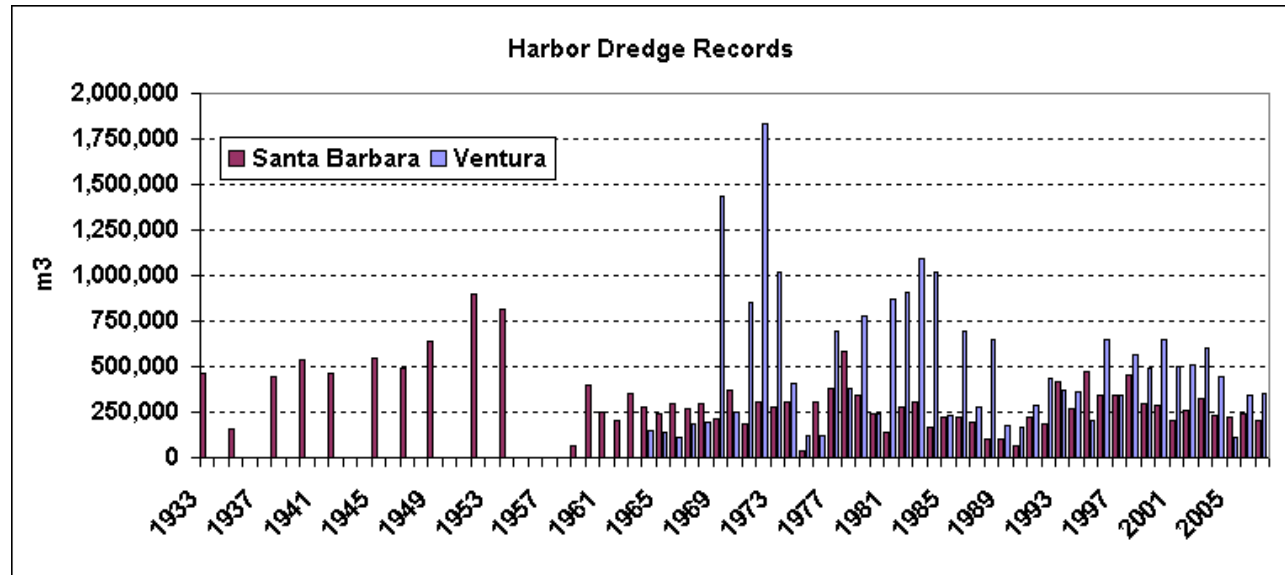


Figure 2.2. Santa Barbara (1933-2003) and Ventura (1964-2005) harbor dredge records. Data from Army Corp of Engineers, adapted from Patsch and Griggs 2007.

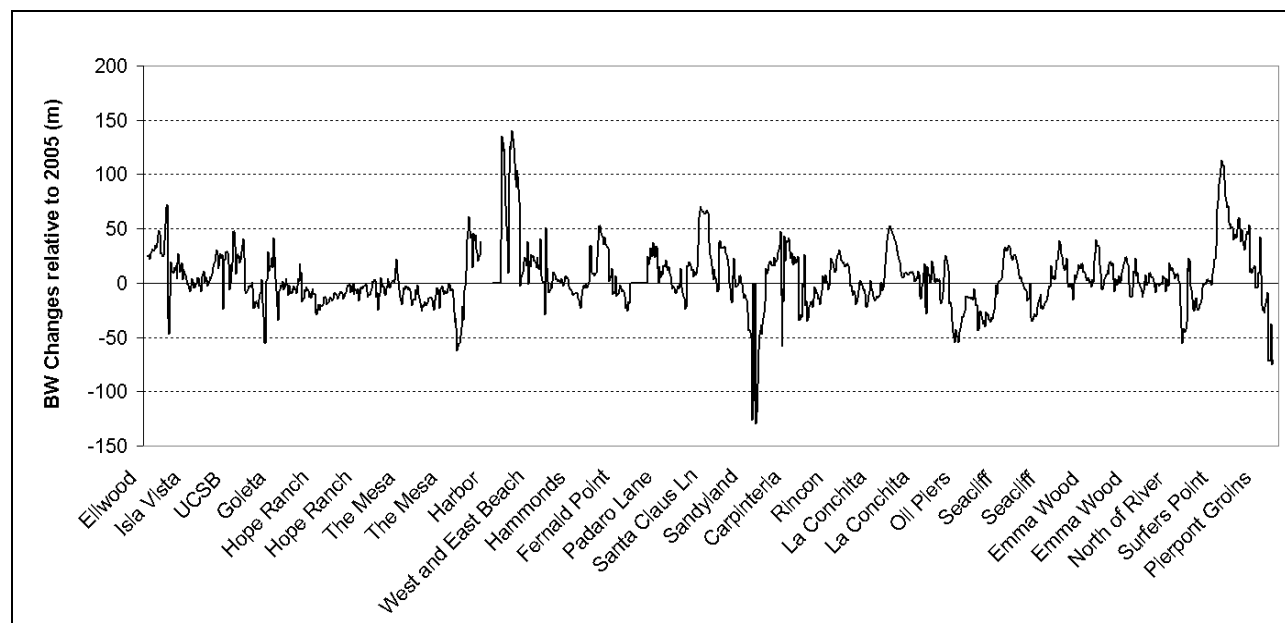


Figure 2.3. Long-term beach-width changes relative to the 2005 beach width. The earliest dates used in the calculation vary based on air photo availability (1943 for beaches updrift of Santa Barbara Harbor and 1947 for downdrift beaches, except 1929 for Carpinteria and Isla Vista). Negative changes indicate beach narrowing, positive changes indicate beach widening.



Figure 2.4. An example of beach oscillations around UCSB and Goleta Beaches. Beaches reached maximum widths in the 1960s and 1970s while current beach widths are similar to those found in the 1930s and 1940s.

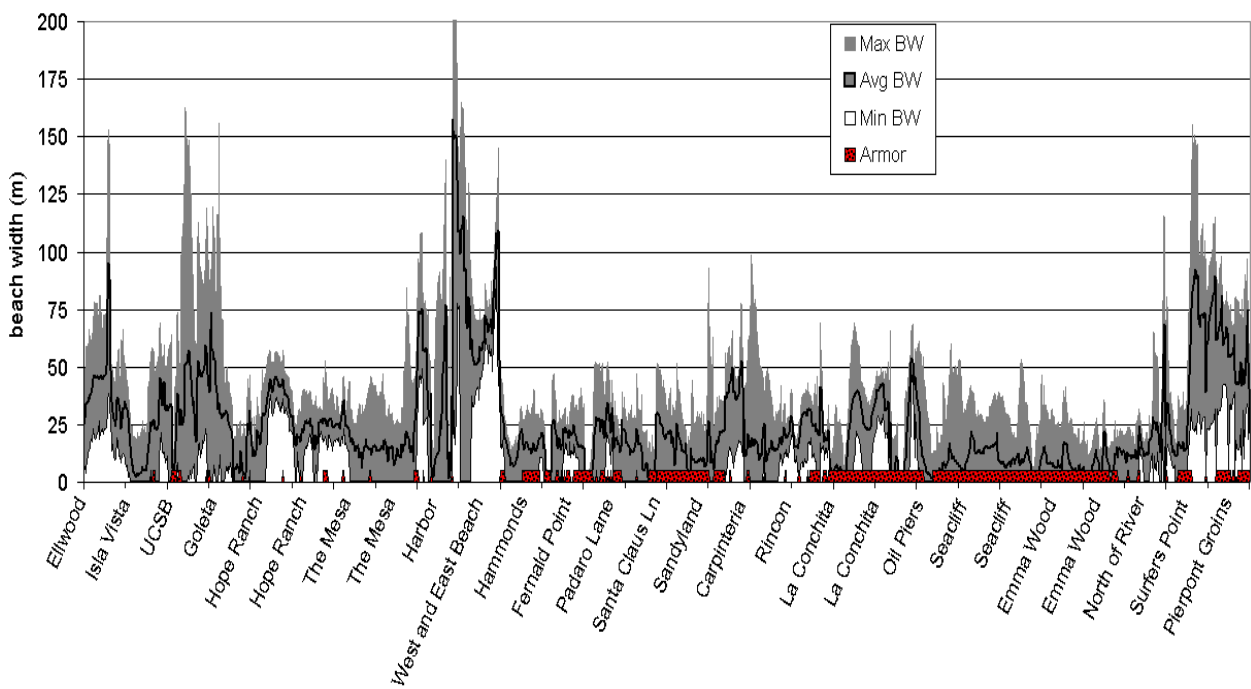


Figure 2.5. Beach-width (BW) variability along 70 km of coastline in southern Santa Barbara and Ventura Counties, California, throughout all available years of aerial photography (1929-2005). Areas with shoreline armoring are highlighted.

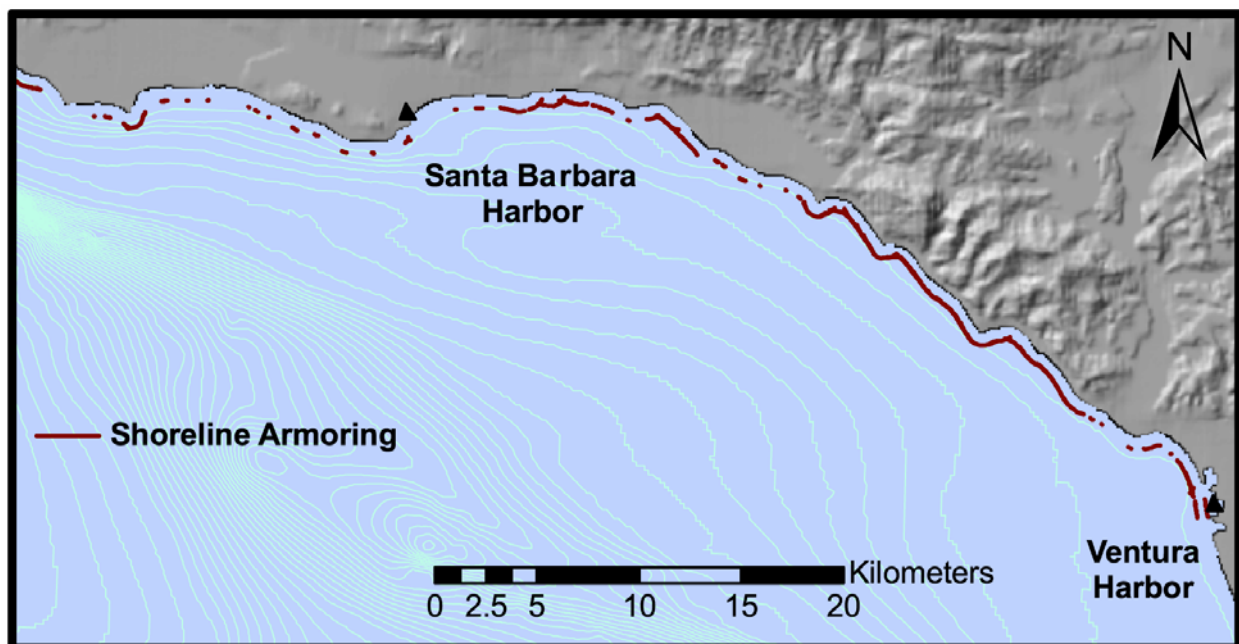


Figure 2.6. Shoreline armoring in the study area. Data adapted from California Coastal Commission.

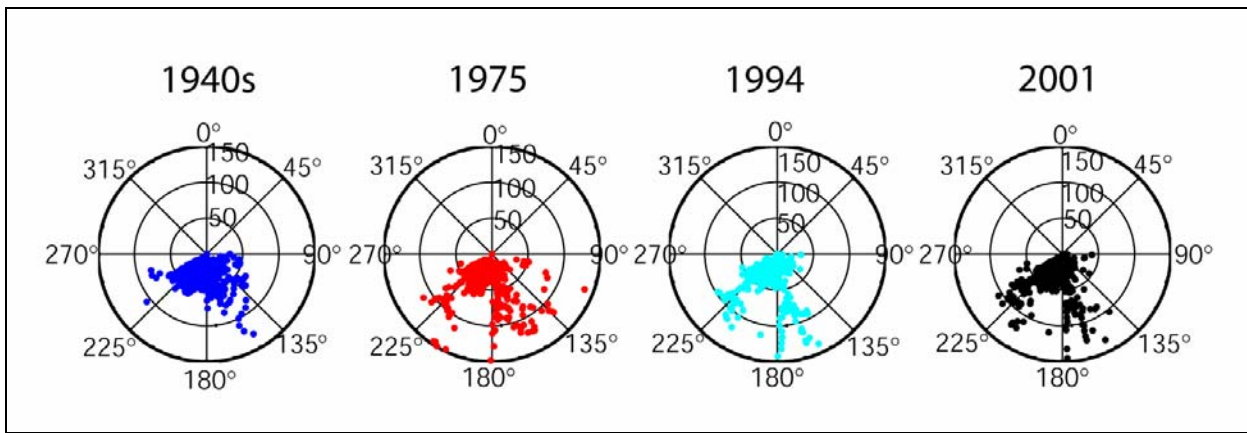


Figure 2.7. Beach widths plotted by shoreline orientation for specific time periods from the 1940s to 2001. Data points were extracted from the same shoreline transects and have comparable numbers of data points. Radial axis is beach width in meters.

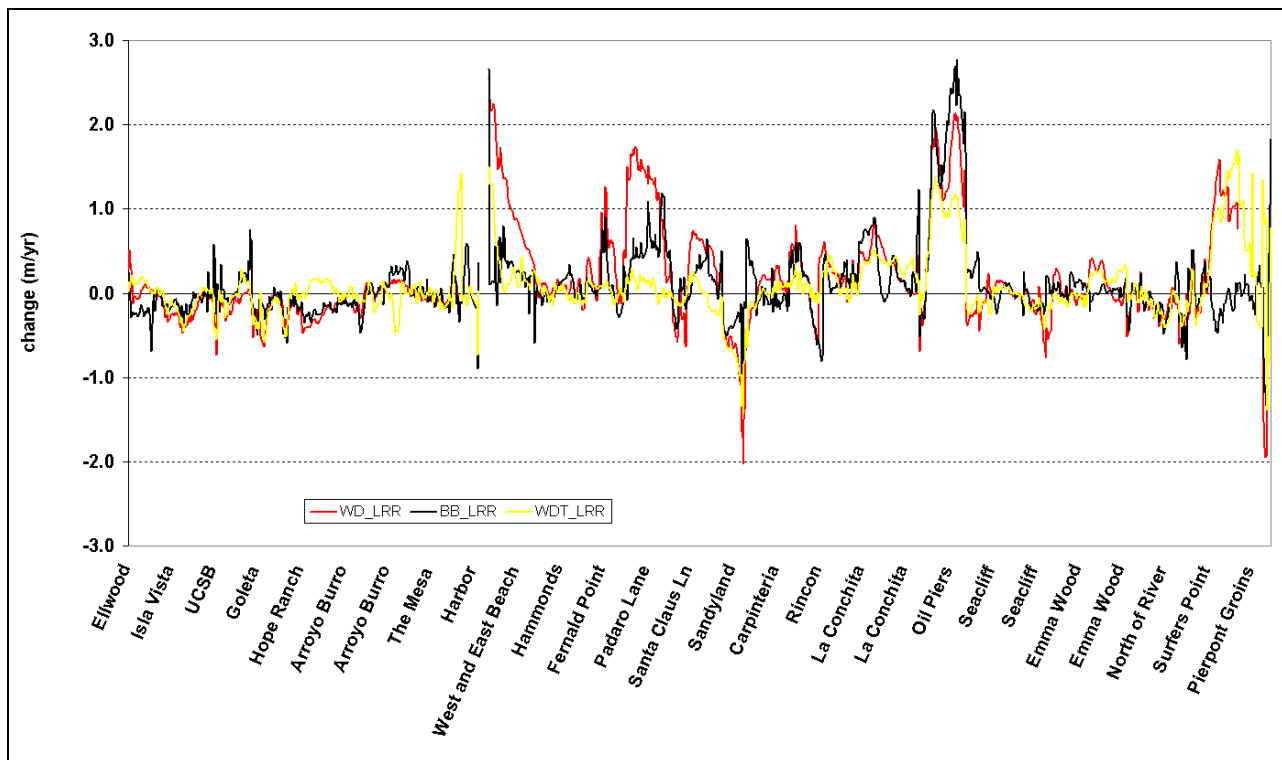


Figure 2.8. Shoreline-change rates (linear regression) for the wet/dry (1929-2005), back beach (1929-2005), and wet/dry with T-sheets (1829 –2005) shorelines.

Significant Shoreline Change Rates for Ellwood to Ventura Harbor

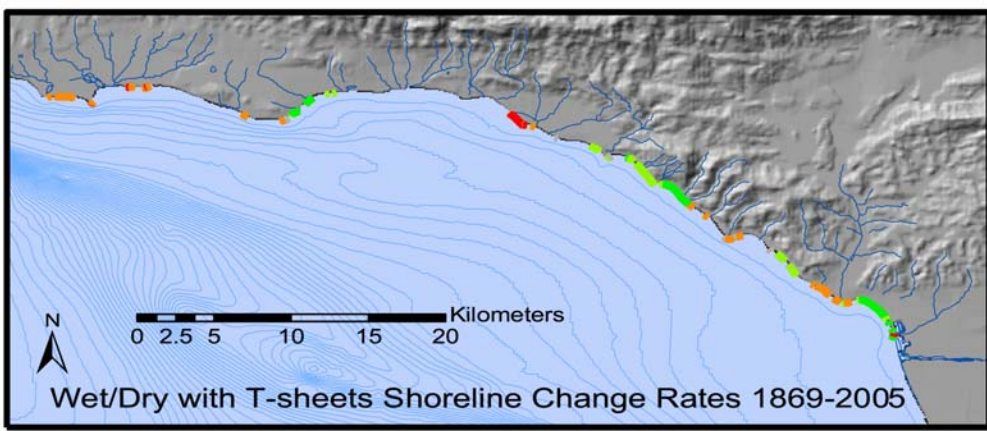
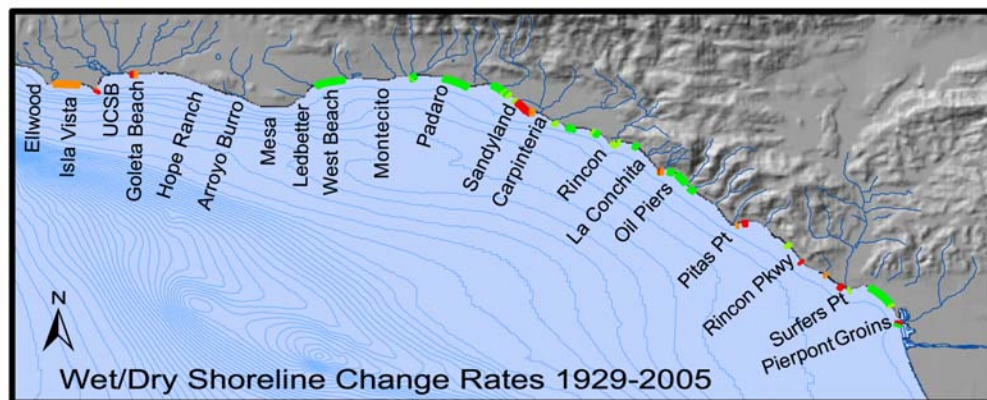
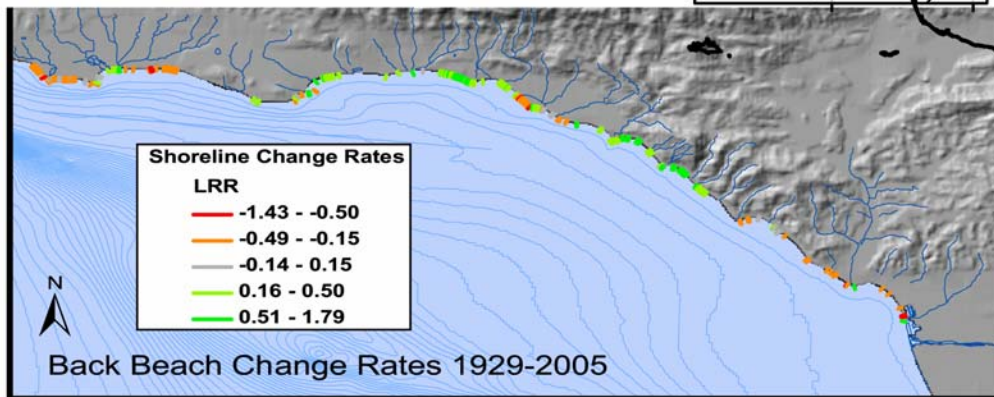


Figure 2.9. Statistically significant shoreline-change rates for each reference feature based on the number of shorelines at each transect (generally $R > 0.7$). LRR: Linear regression rate in m/yr.

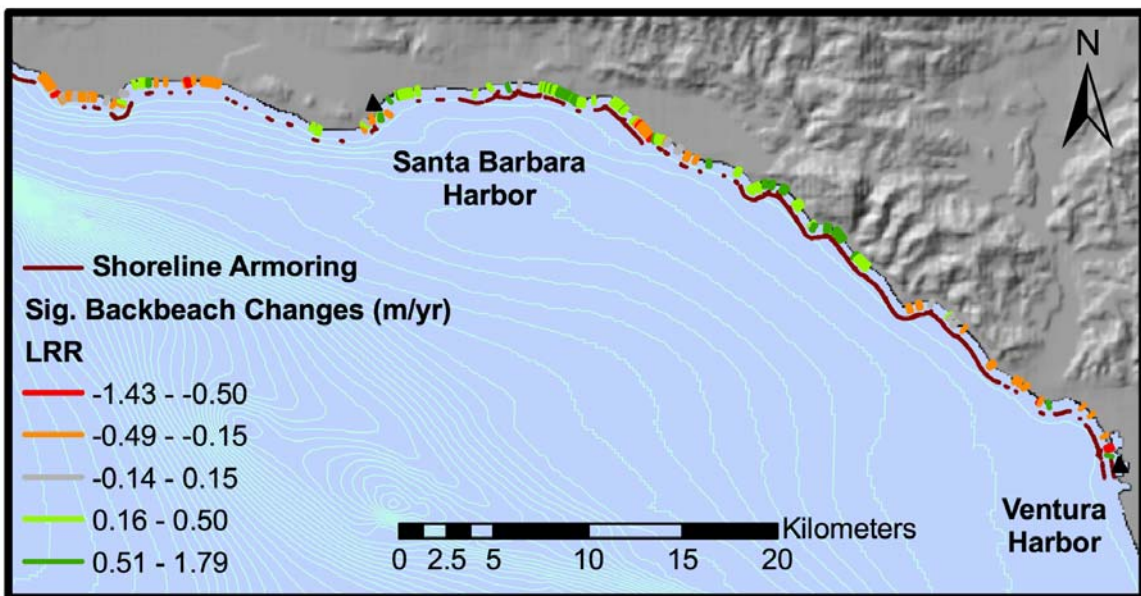


Figure 2.10. Significant back-beach changes in relation to shoreline armoring. LRR: Linear regression rate.



Figure 2.11. Photograph taken in 1936 after the erosion wave had passed Fernald Point en route to Carpinteria. Santa Barbara Harbor is visible in the distance; note the numerous cross-shore groins emplaced to slow erosion. Photo courtesy of the Spence Collection, UCLA.

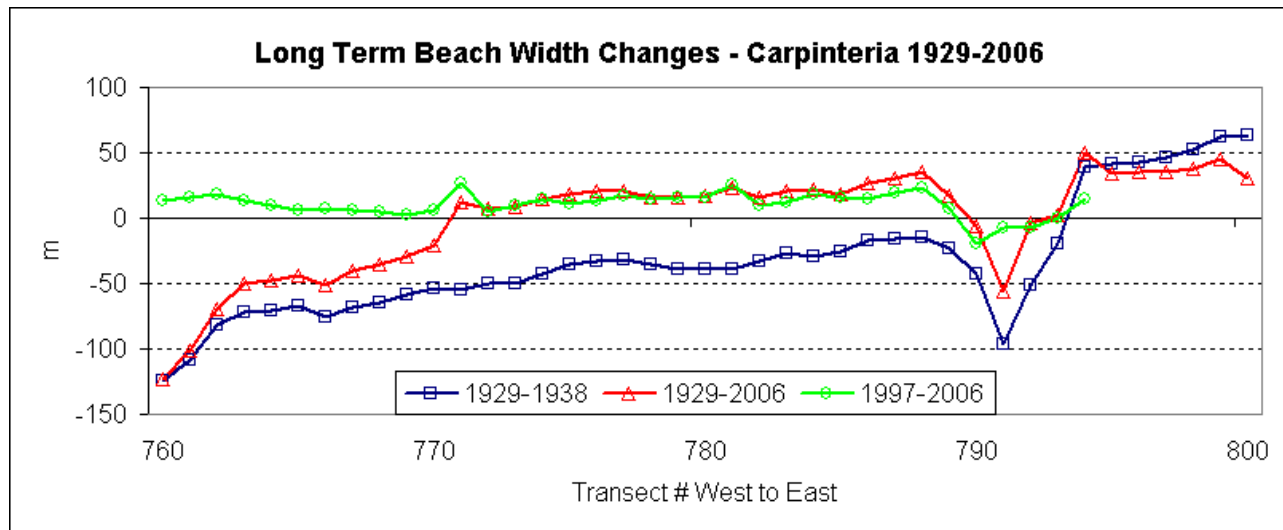


Figure 2.12. Beach-width changes in Carpinteria relative to the 1929 baseline. Shown are long-term changes from 1929 to 2006, changes immediately following the arrival of the erosion wave between 1929 and 1938, and recent changes from 1997 to 2006. The City of Carpinteria focus site is between transects 771 and 779, and Carpinteria Creek discharges between transects 791-793.

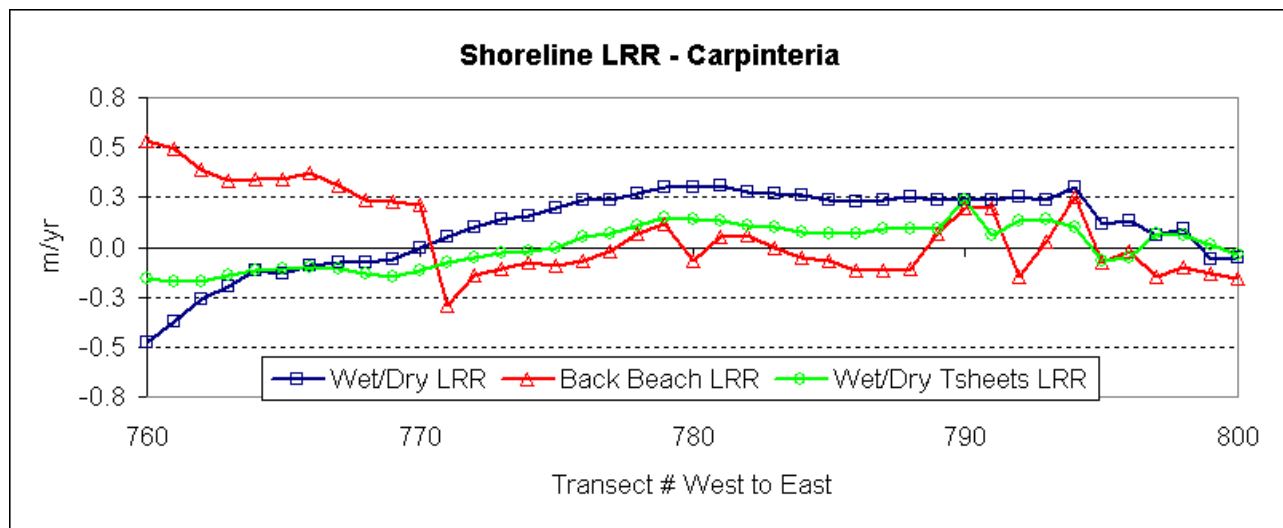


Figure 2.13. Carpinteria shoreline-change linear-regression rates (LRR) for the various shoreline reference features. The red line is the back beach, the blue line is the MSL wet/dry adjusted line from air photos, and the green line is the shoreline-change rates derived by including the historical NOS T-sheets, as well as air photo and Lidar-derived shorelines. The City of Carpinteria focus site is between transects 771 and 779.

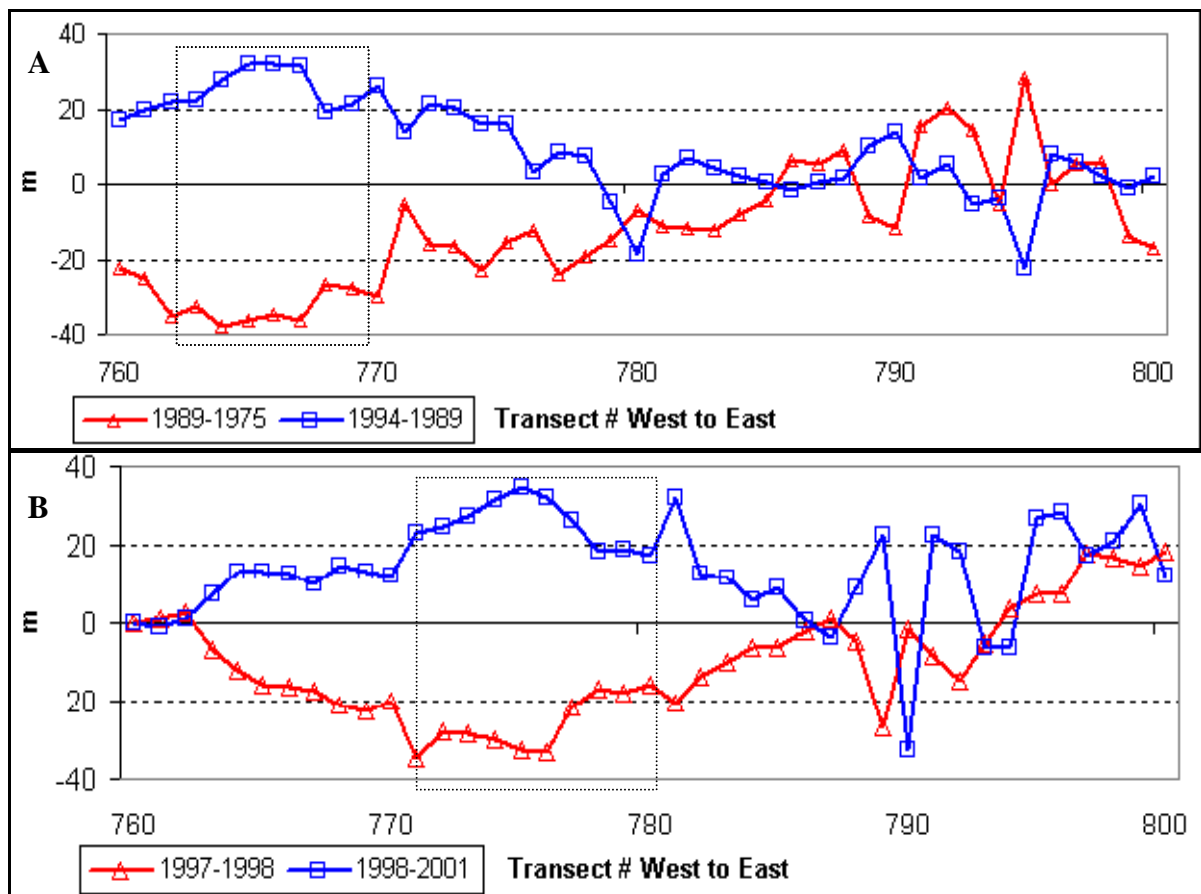


Figure 2.14. Carpinteria beach-width changes and recovery following *A*, 1982-83 and *B*, 1997-98 El Niño events.

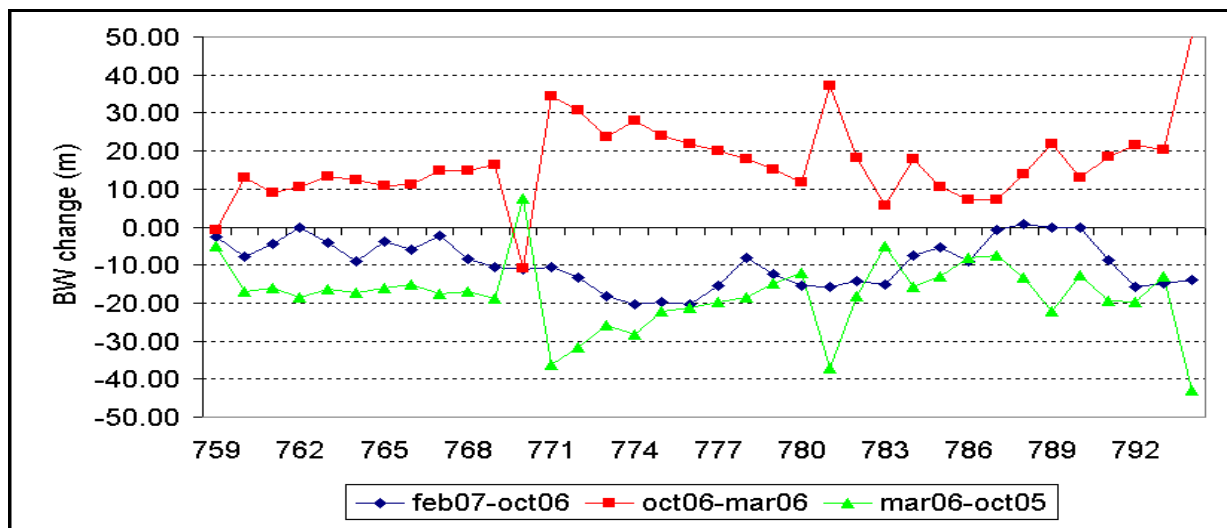
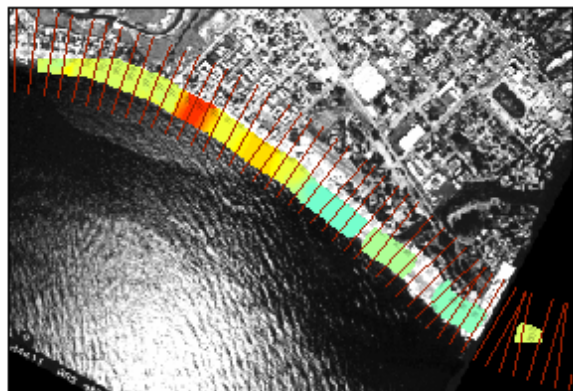
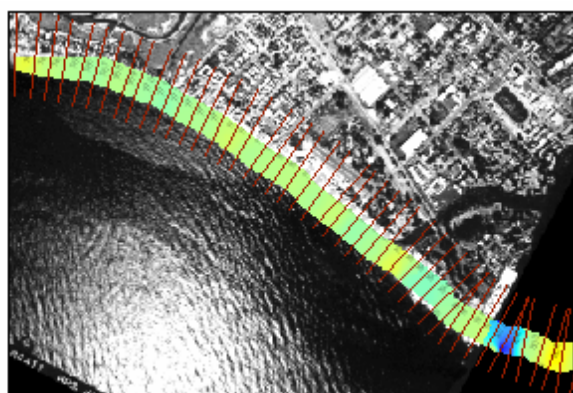


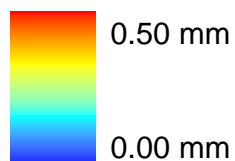
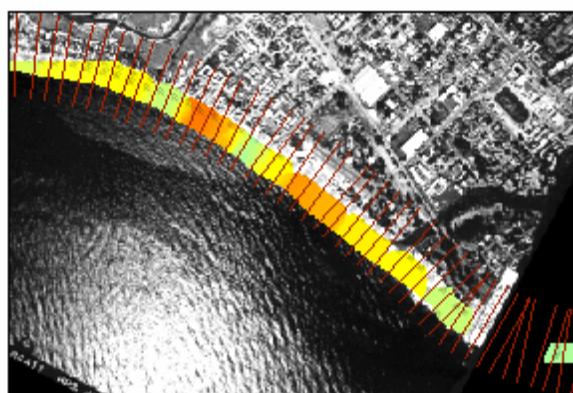
Figure 2.15. Seasonal beach-width changes for the Carpinteria coastline. City Beach is located between transects 771 and 779. Shoreline armoring (revetment) occurs from transect 759 to 770.



Winter 2006



Summer 2006



Winter 2007

Figure 2.16. Gridded sediment grain-size results for Carpinteria beach. The hotter colors represent coarser grain materials while the cooler colors represent finer grained material. *A*, Winter 2006, *B*, Summer 2006, and *C*, Winter 2007. Note the coarsening of grain sizes at the end of the revetment near the Ash Avenue erosion hotspot (red region in top panel). Figure from Barnard and others (2007).

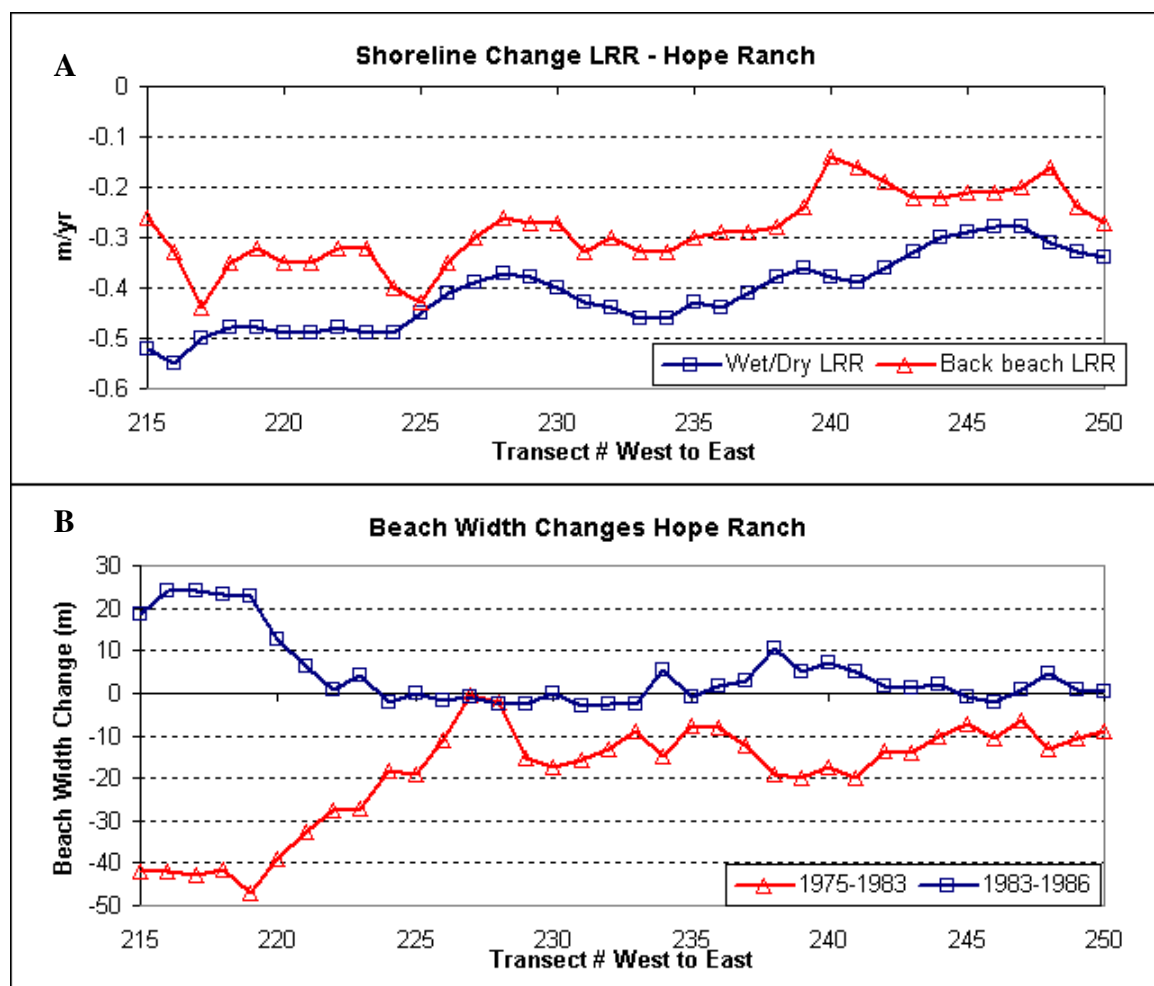


Figure 2.17. *A*, Hope Ranch, California, shoreline-change and *B*, beach-width response following the 1982-83 El Niño event. LRR: Linear regression rate.

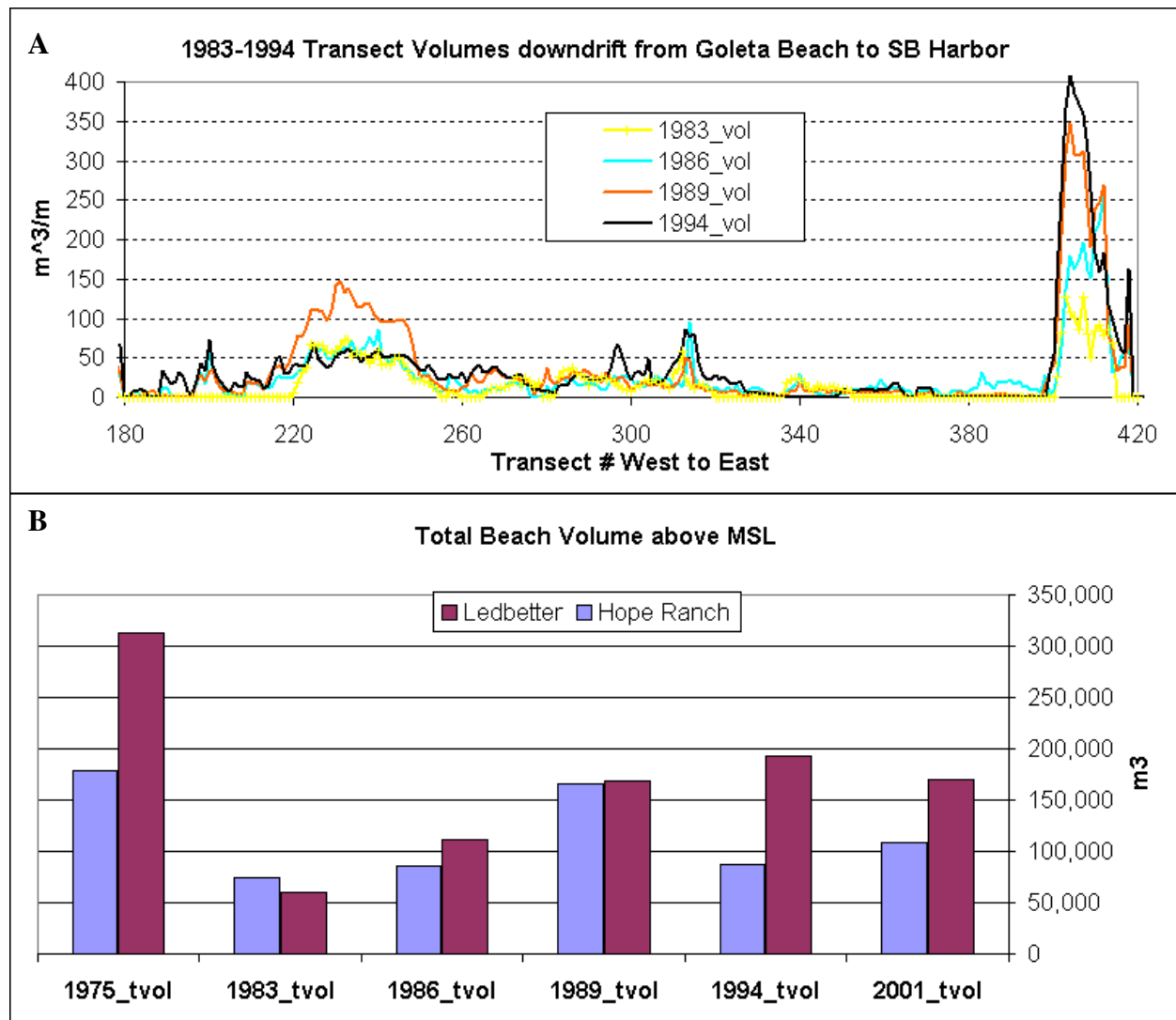


Figure 2.18. A, Transect volume and B, total beach volume above MSL from Goleta Beach to Santa Barbara Harbor following the 1982-83 erosion event at UCSB and Goleta beaches.

Chapter 3—BEACON Surveys

By Patrick L. Barnard

Introduction

In 1987, a long-term monitoring program consisting of 25 cross-shore beach survey lines in a variety of coastal locations within the SBLC was established for BEACON. The objective was to assess long- and short-term changes in shoreline position and profile area change from the back beach to beyond the depth of closure. Additional lines have been added since 1987 based on management needs, including six lines at Goleta Beach and seven lines on the Santa Clara River delta, for a current total of 41 lines (fig. 3.1). The USGS resurveyed each of these 41 lines in October 2007 to quantify changes along these historical transects. This chapter summarizes the results of this recent USGS survey and compares them with the prior complete survey from November 2003 and the first BEACON survey in 1987.

Methods

The October 2007 survey of the BEACON lines was conducted using a Real Time-Kinematic Global Positioning System (RTK-GPS). The portion of the survey lines above the water line was surveyed on foot with the GPS antenna mounted on a 2 m survey rod, while the below-water portion of the profiles was surveyed using the Coastal Profiling System (see Chapter 4, Methods). All horizontal positions were referenced to the Universal Transverse Mercator (UTM) projection North American Datum 1983 (NAD83), Zone 11 North (meters). All vertical positions were referenced in meters to the North American Vertical Datum 1988 (NAVD88), which is 2.9 cm above MLLW at the Santa Barbara tide station (National Oceanic and Atmospheric Administration, 2008).

Most of the historical survey data was horizontally referenced in NAD83, Cal Zone 5 (US Survey Feet), with elevation (feet) referenced to MLLW tidal epoch 1983-2001 (Coastal Frontiers, 2004). For comparison purposes all of the historical data was converted to meters in UTM NAD83, Zone 11 North, and NAVD88 using ArcGIS transformation tools and datums from National Oceanic and Atmospheric Administration (2008). The naming convention of the BEACON survey lines also was simplified to avoid confusion caused by the variety of prefixes introduced over the years—lines were renumbered from 1 to 41, west to east (table 3.1; fig. 3.1). The compilation of all BEACON survey lines can be found in the Appendix (figs. A1-A82). All current and historical survey data is available from the author upon request.

Line comparisons were performed using tools in the Regional Morphology Analysis Package (RMAP) module in the Coastal Engineering Design and Analysis System (CEDAS; 2008). Volume changes (m^3/m) were calculated for each time interval (for example, 2003 to 2007 or 1987 to 2007) for all portions of the line where data were available, as well as above mean high water (MHW, +1.384 m NAVD88), above 0 m, above -4 m, and between MHW and the -4 m contour, labeled the “active zone”. Volume-change calculations for the entire profile are tenuous as very small systematic errors in echosounder accuracy and speed of sound corrections at depth (below -5 m), can lead to large volume changes (for example, a 10 cm systematic offset over 1 km results in a volume change of 100 m^3/m). Because we have no way of verifying exactly how error estimates and speed of sound corrections for BEACON surveys prior to October 2007 were performed, the total volume calculations should be interpreted with caution. However, the October 1987 lines seem more consistent spatially than those gathered in 2003. In two instances [line 2 (Isla Vista) and line 16 (Carpinteria north)] kelp prevented accurate bathymetric data collection, so the data from those areas was discarded. Extensive accretion at the mouth of the Santa Clara River prevented volume-change calculations in several instances because

surveys did not overlap. For example, at line 28 the river mouth had migrated so far seaward by 2007 that there was no profile overlap, and volume change above MHW could not be determined. In some instances the back-beach area was clipped where coarse survey coverage introduced obvious bias.

Shoreline proxy contours were determined for each survey line at MHW, 0 m, and -4 m elevations, and the horizontal position difference was calculated between each set of surveys for the respective contours. Positive values designate shoreline progradation (accretion), and negative values designate shoreline recession (erosion).

Results

Recent Changes (2003-2007)

The results of the survey comparison between 2003 and 2007 are summarized in tables 3.2-3.3 and figures 3.2-3.3. The average of all lines show a trend of net accretion in the SBLC, with each of the three contours (MHW, 0 m and -4 m) migrating seaward between 11 and 23 m. However, the overall signal is completely dominated by the extensive accretion at the mouth of the Santa Clara River (lines 27-35) where total volume change averaged $1,341 \text{ m}^3/\text{m}$ and the shorelines prograded, on average, between 43 and 84 m. With the Santa Clara River delta lines removed, net accretion on the remaining BEACON lines is negligible, with the MHW and 0 m contours prograding only $\sim 1 \text{ m}$, or $\sim 0.25 \text{ m/yr}$. If only lines north of the Santa Clara River (lines 1-26) are included, net change is even more negligible, with 0 to 1 m of change for all contours. Lines south of the Santa Clara River accreted substantially, with all contours migrating at least 29 m seaward.

Despite the lack of an obvious regional trend, throughout the BEACON survey area there are fairly continuous pockets of erosion and accretion. Erosion, especially in the nearshore, or “active zone”, is prevalent in lines 1-3 (Ellwood to West Goleta Beach), 8-13 (east Goleta Beach to Miramar,

especially around Santa Barbara Harbor), and 19-24 (Rincon, Oil Piers to Surfers Point). Accretion was observed in lines 4-7 (Goleta Beach), 14-18 (Summerland to La Conchita), 27-35 (Santa Clara River delta), 37-39 (adjacent to Hueneme Harbor), and 41 (Point Mugu). No significant change was noted for lines 25-26 (adjacent to Ventura Harbor), 36 (Hollywood Beach), and 40 (Ormond Beach).

The Santa Clara River delta region (lines 27-35) shows significant vertical accretion and shoreline progradation since 2003. Clearly, there was a major amount of sediment input to the system as a result of the winter 2004-2005 flood, with 1 to 2 m of vertical accretion in surveyed water depths ranging from 0 to 12 m, and shoreline progradation and transect volume increases as high as 129 m and 3,074 m³/m, respectively. The average volume change of shore-normal lines 27, 29, and 32-35, which are each about 1 km apart, is +1,067 m³/m. Thus, along this 6 km stretch of coastline, at least 6.4 million m³ of sediment was delivered to the survey area alone. The actual volume delivered from the January 2005 Santa Clara River flood must have been far higher, however, as we have observed continuing losses of sediment from the Santa Clara River delta based on our semiannual monitoring from 2005-2008 (see Chapter 4), and because there is still up to 2 m of accretion at the seaward extreme of the survey lines at the mouth of the Santa Clara River compared to the 2003 survey (for example, see fig. A32, line 32). However, the sediment grain size declines offshore, so the estimate of ~6 million m³ of littoral-sized sand delivered from the 2004-2005 flood may be a reasonable, albeit crude, estimate.

The portion of the Ellwood (line 1) profile in the nearshore (fig. A42) shows considerable erosion, but the offshore component shows accretion. This profile is adjacent to the mouth of the creek draining near Bacara where paleochannels may be intermittently active. Additionally, this is one of only a few locations that Mustain (2007) identified as consisting of coarse- to medium-sand.

Recent Decadal Changes (1987-2007)

Two decades of change are captured by the comparison of the 25 original BEACON profiles from 1987 to the recent survey in 2007 (tables 3.4-3.5; figs. 3.4-3.5). Due to the massive amount of sediment input from the Santa Clara River, especially during the 2004-2005 winter flood, there is a clear distinction between lines north and south of the Santa Clara River. Summary statistics show that the lines north of the Santa Clara River show net erosion, with an average shoreline change of -6 m and volume-change rates for the total profile and the “active zone” of -115 and -29 m^3/m , respectively. Conversely, south of the Santa Clara River the average shoreline change was 34 m and volume change rates for the total profile and the “active zone” were 725 and 133 m^3/m , respectively.

Erosion is prevalent in all profiles from Ellwood to Miramar (lines 1 to 13, MHW shoreline and “active zone”), with the exception of East Beach (line 11) where there is negligible change. Erosion dominates from Carpinteria (line 17) to Surfer’s Point (line 24), with the exception of La Conchita (line 18) where there is accretion in the “active zone”. Erosion is prevalent at Marina Park (line 26). As in the 2003 to 2007 comparison, there is clear accretion at Summerland (line 14), Padaro Lane (line 15), La Conchita (line 18) and at nearly every profile south of the Santa Clara River, except for Hueneme Pier (line 39). There is also a smaller amount of accretion noted at San Buenaventura State Beach (line 25).

The large erosion signal in the Rincon Parkway area is noteworthy. Alongshore averaging for the total profile volume change from Hobson (line 20) to Surfer’s Point (line 24) is $-410 \text{ m}^3/\text{m}$ from 1987-2007. Extrapolating this value to the entire 12 km stretch of coastline amounts to a total volume loss of ~ 5 million m^3 , or an average of $\sim 250,000 \text{ m}^3/\text{yr}$. The “active zone” lost about 750,000 m^3 during this 20 year period.

Other Observations

Looking qualitatively at pre-2003 surveys, there is continued profile loss noted at Ellwood (line 1), Ledbetter (line 10), East Beach (line 11), and Surfer's Point (line 24). Recent and/or continued profile gain is recognized at Padaro (line 15), La Conchita (line 18), San Buenaventura (line 25), and Hueneme North and South (lines 37-38).

Goleta Beach profiles from January 2005 show the development of a nearshore bar at around 1 to 2 m depth that seems to be followed by accretion of the shoreface and dry-sand beach. This scenario fits the standard conceptual model of beach behavior, with a sand pulse arriving from updrift in the winter, then moving up the profile in subsequent surveys throughout the year and remaining there until the most recent surveys. Meanwhile, Arroyo Burro (fig. A9) downdrift suffered erosion observationally and anecdotally. The higher temporal and spatial resolution of the Goleta profiles enable a better understanding of the evolution of this beach and illustrates some of the benefits of a more robust monitoring program.

On average, beach slope (calculated between the MHW and 0 m contours) decreased north of the Santa Clara River and increased south of the Santa Clara River. This is consistent with a gradual fining of the littoral sediment supply to the north due to a limited supply, and coarsening to the south, likely due to the influx of coarse sediment from the Santa Clara River delta flood in 2004-2005 and to increased wave energy in this location due to focusing by the delta.

Shoreline-Change Rates

Figure 3.6 shows the long- and short-term MHW shoreline-change rates along the BEACON lines as determined from the 1987-2007 and 2003-2007 survey pairs. The long-term (20 yr, 1987-2007) rate for all lines north of the Santa Clara River is ~ -0.3 m/yr, while lines to the south accreted at a rate of ~ 1.7 m/yr. Rates on individual lines north of the Santa Clara River all are modest, with most less

than ± 1 m/yr. The highest long-term rate is at line 32 (McGrath State Beach) with 5.3 m/yr of accretion, although this may be strongly biased by the extensive accretion caused by the flood in winter 2004-2005. Shore protection structures along the Rincon Parkway keep the shoreline position relatively stable (lines 16-24).

Short-term (4 yr, 2003-2007) rates are far more variable, with rates in the western portion of the study area ranging from +7.7 m/yr at Goleta (line 6) to -7.9 m/yr at East Beach (line 11). At the mouth of the Santa Clara River, accretion rates reached up to 20.4 m/yr (line 31), with significant but reduced accretion on lines south of the rivermouth as well. However, lines immediately north of the Santa Clara River (19-26) exhibited little net shoreline change.

Conclusions

- There is no significant average regional change observed in the SBLC between 2003 and 2007 based on 41 BEACON survey lines.
- Significant erosion is observed in the vicinity of the Santa Barbara Harbor and Rincon Parkway between 2003 and 2007.
- From 2003 to 2007 accretion is observed at Goleta, from Summerland to La Conchita, and along most of the coastline south of the Santa Clara River mouth, including areas adjacent to Hueneme Harbor.
- At least 6 million m³ of sediment was delivered to the coast at the mouth of the Santa Clara River during the winter flood of 2004-2005.
- The shoreline adjacent to the Santa Clara River prograded up to 129 m as a result of the winter flood in 2004-2005.
- North of the Santa Clara River mouth the MHW shoreline retreated an average of 6 m from 1987 to 2007.

- The shoreline south of the Santa Clara River mouth accreted an average of 34 m from 1987 to 2007.
- Approximately 5 million m³ (250,000 m³/yr) of sediment was eroded from the Rincon Parkway region (Hobson to Surfer's Point) from 1987 to 2007.

References

Coastal Engineering Design and Analysis System (CEDAS), 2008, Regional morphology analysis package (RMAP) in CEDAS Version 4.03: Vicksburg, Mississippi, Veri-Tech Inc., U.S. Army Corps of Engineers.

Coastal Frontiers, 2004, Fall 2003 BEACON Regional Beach Profile Survey. 46 p.

National Oceanic and Atmospheric Administration (NOAA), 2008, Tides & Currents, Center of Operational Products and Services,

[http://tidesandcurrents.noaa.gov/data_menu.shtml?unit=1&format=Apply+Change&stn=9411340+Santa+Barbara%2C+CA&type=Datums (last accessed March 13, 2009)].

Table 3.1. Naming convention for BEACON survey lines.

USGS line #	Old BEACON ID	Alt. ID	Name
1 B	CN01		Ellwood
2	BCN02		Isla Vista
3 GB	06		Goleta Beach #6
4 GB	01		Goleta Beach #1
5 GB	02	BN01	Goleta Beach #2
6 GB	03		Goleta Beach #3
7 GB	05		Goleta Beach #5
8 GB	04		Goleta Beach #4
9 BCN03			Arroyo Burro
10 B	CN04		Ledbetter Beach
11 BCN05			East Beach
12 BCN06			Biltmore
13 BCN0	7		Miramar
14 B	CN08		Summerland
15 B	CN09		Padaro Lane
16 BN02			Carpinteria (north)
17 BCN1	0		Carpinteria (south)
18 B	CN11		La Conchita
19 B	N03		Oil Piers
20 B	CN12		Hobson
21 B	CN13		Faria
22 B	CN14		Solimar
23 BCN	15		Emma Wood
24 BCN16			Surfer's Point
25	BCN17		San Buenaventura State Beach
26 B	CN18		Marina Park
27	BD01		Santa Clara River Delta #1
28	BD02		Santa Clara River Delta #2
29	BD03		Santa Clara River Delta #3
30	BD04		Santa Clara River Delta #4
31	BD05		Santa Clara River Delta #5
32	BCN19	BD06	McGrath State Beach/ SC Delta #6
33	BD07		Santa Clara River Delta #7
34	BCN20	BD08	Oxnard Shores/ SC Delta #8
35	BD09		Santa Clara River Delta #9
36 BCN21			Hollywood Beach
37 BCN	22		Silver Strand
38	BN04		Hueneme Beach (North of Pier)
39	BCN23		Hueneme Beach (South of Pier)
40 BCN24			Ormond Beach
41	BCN25		Point Mugu

Table 3.2. Summary statistics of BEACON line profile changes from 2003 to 2007. [MHW: mean high water. Active zone: depth interval from -4m to MHW]

	Volume change, in m ³ /m					Contour change, in meters		
	Total	MHW	0 m	- 4 m	Active zone	MHW	0 m	-4 m
All lines								
Average	392 3		13	62	17	11	13	23
Maximum	3,074 57		187	488	434	81	93	129
Minimum	-413 -	145	-154	-269	-191	-32	-32	-34
Std Deviation	722 38		63	177	103	27	31	41
Excluding Santa Clara River delta (lines 27-35)								
Average	108 3		4	4	1	1	1	6
Maximum	460 56		90	133	145	31	26	70
Minimum	-413 -	77	-122	-269	-191	-32	-32	-34
Std Deviation	221 28		42	84	63	13	16	23
Santa Clara River delta (lines 27-35)								
Average	1,341 -3		58	261	112	43	54	84
Maximum	3,074 57		187	488	434	81	93	129
Minimum	337 -1	45	-154	-223	-96	-8	0	42
Std Deviation	992 84		123	263	221	37	36	31
North of Santa Clara River mouth (lines 1-26)								
Average	99 0		-1	-10	-9	0	1	0
Maximum	364 56		90	119	85	31	26	57
Minimum	-413 -	77	-122	-269	-191	-32	-32	-34
Std Deviation	226 28		45	84	60	14	16	19
South of Santa Clara River mouth (lines 27-41)								
Average	861 9		41	182	75	29	33	62
Maximum	3,074 57		187	488	434	81	93	129
Minimum	-103 -	145	-154	-223	-96	-8	-27	-1
Std Deviation	975 56		86	225	151	34	39	39

Table 3.3. Profile change for each of the BEACON lines from 2003 to 2007. [Volume change is calculated for the entire profile (Total) and then above the specified contours. NaN: no calculation possible due to poor profile overlap or poor data (for example, due to kelp beds at line 2). MHW: mean high water. Active zone: depth interval from -4m to MHW]

Line #	Volume change in m ³ /m					Contour change in meters		
	Total	MHW	0 m	-4 m	Active zone	MHW	0 m	-4 m
1 18	7	-12	-33	-75	-62	-9	-19	-6
2 NaN		8	11	NaN	NaN	4	3	NaN
3 77		-35	-40	-82	-47	-5	-2	6
4 28	5	10	32	66	56	15	14	57
5 28	3	12	40	96	85	22	19	5
6 36	4	56	90	119	63	31	20	37
7 26	3	12	36	94	82	17	21	-1
8 20	1	-15	-26	-23	-8	-11	-7	11
9 34	2	-19	-23	-20	-1	-8	-1	-7
10 -2	64	-23	-29	-69	-46	-9	-8	-11
11 -	263	-77	-122	-269	-191	-32	-32	-33
12 29	8	-31	-54	-55	-24	-16	0	-2
13 -5	1	-34	-62	-117	-84	-26	-15	-9
14 28	6	48	57	65	17	8	3	-3
15 14	8	28	44	79	51	11	10	5
16 NaN		28	39	8	-20	7	7	-8
17 70		12	16	21	9	3	0	-12
18 30	3	18	37	69	51	9	26	7
19 60		0	-6	-29	-29	-4	0	-5
20 10		-4	8	10	14	-1	23	-5
21 -4	13	1	10	-17	-18	3	18	-34
22 -3	70	-10	-34	-70	-60	-9	-30	-21
23 19	4	-10	-25	-56	-46	-3	-23	4
24 23	1	-8	-10	-41	-33	0	1	4
25 10	6	34	29	37	3	1	-4	2
26 37		0	-3	8	8	-4	2	17
27 33	7	-14	18	207	221	14	42	57
28 1,	172	NaN	187	455	NaN	71	74	85
29 1,	445	NaN	NaN	429	NaN	68	86	87
30 2,	069	NaN	NaN	465	NaN	71	89	104
31 2,	436	NaN	NaN	457	NaN	81	93	125
32 3,	074	55	170	488	434	77	67	129
33 67	2	-145	-154	-223	-78	-8	0	73
34 47	2	34	53	-62	-96	14	11	42
35 39	5	57	72	137	79	1	21	52
36 26	9	25	13	18	-7	-1	-13	70
37 46	0	29	38	62	33	7	15	27
38 56		-12	19	133	145	21	23	49
39 -1	03	7	14	78	72	11	5	14
40 -7	1	22	4	-16	-38	4	-27	19
41 23	2	45	59	107	62	7	13	-1

Table 3.4. Summary statistics of BEACON line profile changes from 1987 to 2007. [MHW: mean high water. Active zone: depth interval from -4m to MHW]

	Volume change in m ³ /m					Contour change in meters		
	Total	MHW	0 m	- 4 m	Active Zone	MHW	0 m	-4 m
All lines								
Average	130 23		27	42	18	5	1	11
Maximum	2,738 24	0	377	736	496	107	85	131
Minimum	-697 -5	6	-85	-131	-106	-20	-23	-35
Std Deviation	676 70		105	192	125	29	22	40
Excluding Santa Clara River delta (lines 27-35)								
Average	-32 5		0	-7	-12	-2	-4	1
Maximum	653 11	2	121	153	85	35	24	79
Minimum	-697 -5	6	-85	-131	-106	-20	-23	-35
Std Deviation	328 38		52	92	60	14	12	24
Santa Clara River delta (lines 27-35)								
Average	1,906 22	2	332	574	351	88	57	118
Maximum	2,738 24	0	377	736	496	107	85	131
Minimum	1,074 20	5	287	411	206	70	28	104
Std Deviation	1,177 25		63	230	205	26	40	19
North of Santa Clara River mouth (lines 1-26)								
Average	-115 -7		-16	-36	-29	-6	-5	-7
Maximum	295 51		61	97	71	10	24	15
Minimum	-697 -5	6	-85	-131	-106	-20	-23	-35
Std Deviation	292 24		35	76	56	9	12	15
South of Santa Clara River mouth (lines 27-41)								
Average	725 98		136	231	133	33	17	53
Maximum	2,738 24	0	377	736	496	107	85	131
Minimum	-129 -2	1	-44	-19	2	-20	-9	2
Std Deviation	971 94		146	258	173	43	33	52

Table 3.5. Profile change for each of the BEACON lines from 1987 to 2007. [Volume change is calculated for the entire profile (Total) and then above the specified contours. NaN: no calculation possible due to poor data (for example, due to kelp beds at line 2 or no data from 1987 survey. MHW: mean high water. Active zone: depth interval from -4m to MHW]

Line #	Volume change in m ³ /m					Contour change in meters		
	Total	MHW	0 m	- 4 m	Active Zone	MHW	0 m	-4 m
1	-100 -5	6	-85	-131 -7	6	-20	-20	-6
2	NaN NaN	4	2	NaN	NaN	1	-5	NaN
3	NaN NaN		NaN	NaN NaN		NaN	NaN	NaN
4	NaN NaN		NaN	NaN NaN		NaN	NaN	NaN
5	NaN NaN		NaN	NaN NaN		NaN	NaN	NaN
6	NaN NaN		NaN	NaN NaN		NaN	NaN	NaN
7	NaN NaN		NaN	NaN NaN		NaN	NaN	NaN
8	NaN NaN		NaN	NaN NaN		NaN	NaN	NaN
9	114 -2	8	-45	-79 -5	1	-18	-9	-3
10	-381 -2	2	-35	-100 -7	8	-10	-13	-28
11	52	1	0	14	13	1	-1	15
12	29	5	-19	-29	-27	-9	-7	8
13	26 -3	3	-51	-83 -5	0	-16	-10	-8
14	202 51		61	87 36		9	3	0
15	-4 35		51	97 62		10	11	6
16	NaN NaN		NaN	NaN NaN		NaN	NaN	NaN
17	-371 -1	1	-16	-77 -6	6	-5	-7	-19
18	15	4	9	0	55	47	-1	-9
19	NaN NaN		NaN	NaN NaN		NaN	NaN	NaN
20	-82 -1	1	-22	-59 -4	9	-13	4	-2
21	-2	00	-2	11	-59	-58	2	24
22	-6	97	2	-13	-25	-27	0	-22
23	-599 -1	1	-29	-78 -6	6	-9	-23	-6
24	-4	70	-22	-39	-129	-106	-14	-7
25	122 11		2	82 71		-3	3	12
26	-21 -1	8	-46	-107 -8	9	-12	-19	-5
27	NaN NaN		NaN	NaN NaN		NaN	NaN	NaN
28	NaN NaN		NaN	NaN NaN		NaN	NaN	NaN
29	NaN NaN		NaN	NaN NaN		NaN	NaN	NaN
30	NaN NaN		NaN	NaN NaN		NaN	NaN	NaN
31	NaN NaN		NaN	NaN NaN		NaN	NaN	NaN
32	2,738 24	0	377	736 49	6	107	85	131
33	NaN NaN		NaN	NaN NaN		NaN	NaN	NaN
34	1,074 20	5	287	411 20	6	70	28	104
35	NaN NaN		NaN	NaN NaN		NaN	NaN	NaN
36	653 69		104	153 85		35	19	79
37	41	5	112	121	140	28	17	-8
38	NaN NaN		NaN	NaN NaN		NaN	NaN	NaN
39	-1	29	-21	-44	-19	2	-20	-6
40	57 30		49	95 65		21	-9	33
41	266 52		61	101 49		5	8	3

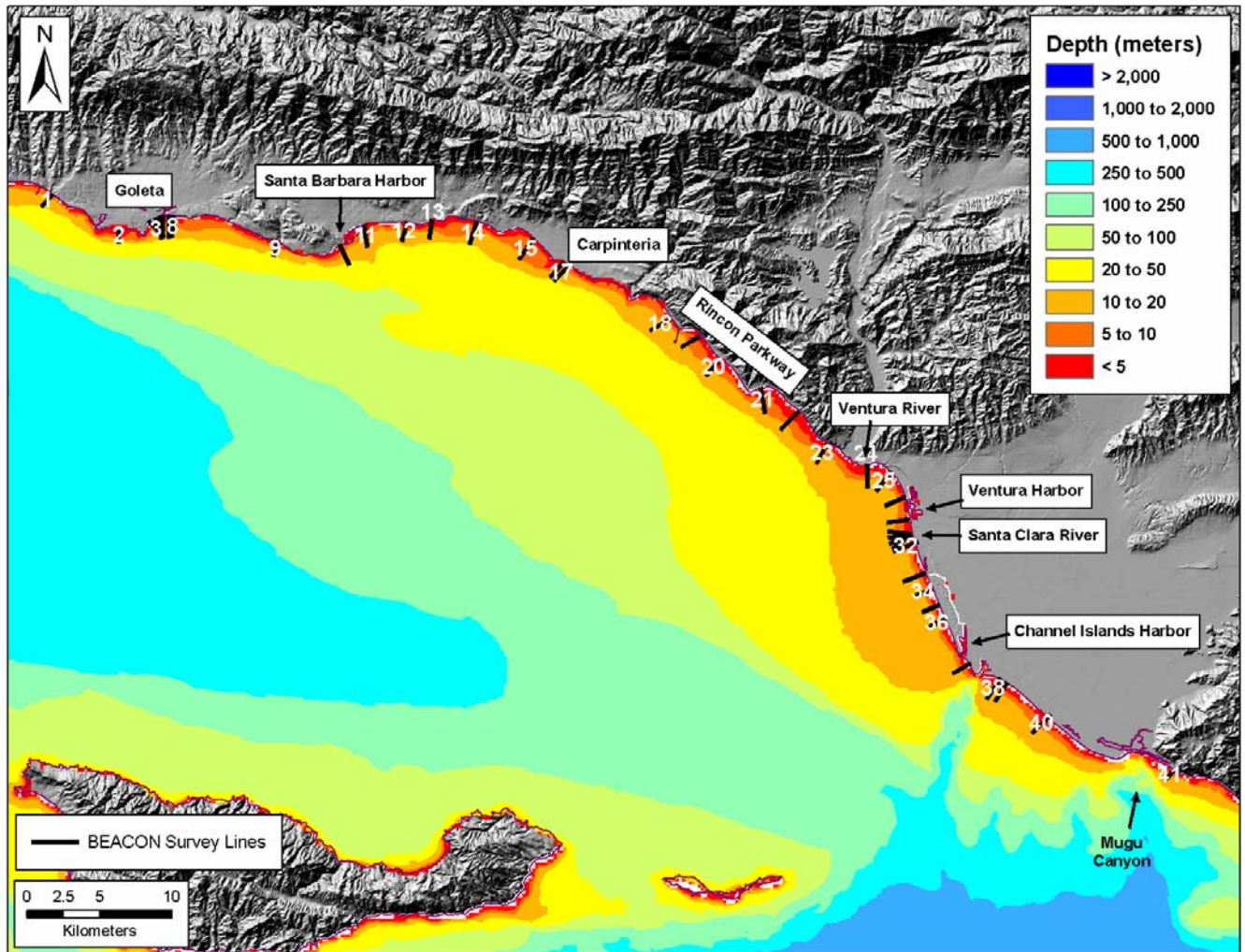


Figure 3.1. Location of BEACON survey lines, Santa Barbara and Ventura Counties, California.

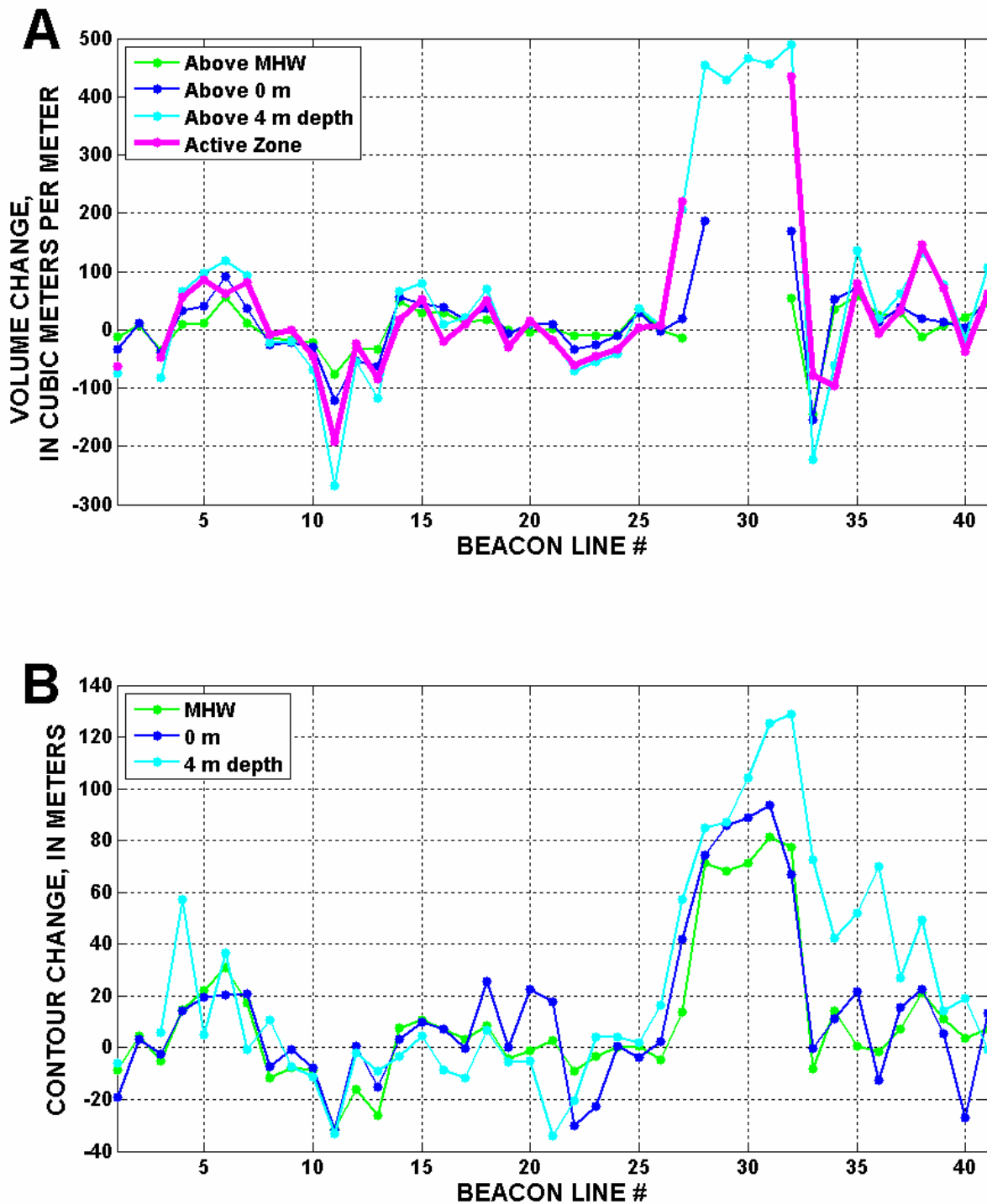


Figure 3.2. BEACON profile changes from November 2003 to October 2007. *A*, volume change above the given elevation to the depth of closure, and *B*, contour change (shoreline proxy) with a positive value representing accretion since 2003 and a negative value representing erosion since 2003. The “Active Zone” is the region between the mean high water (MHW) and 4 m depth contours. Santa Barbara Harbor is located between Lines 10 and 11.

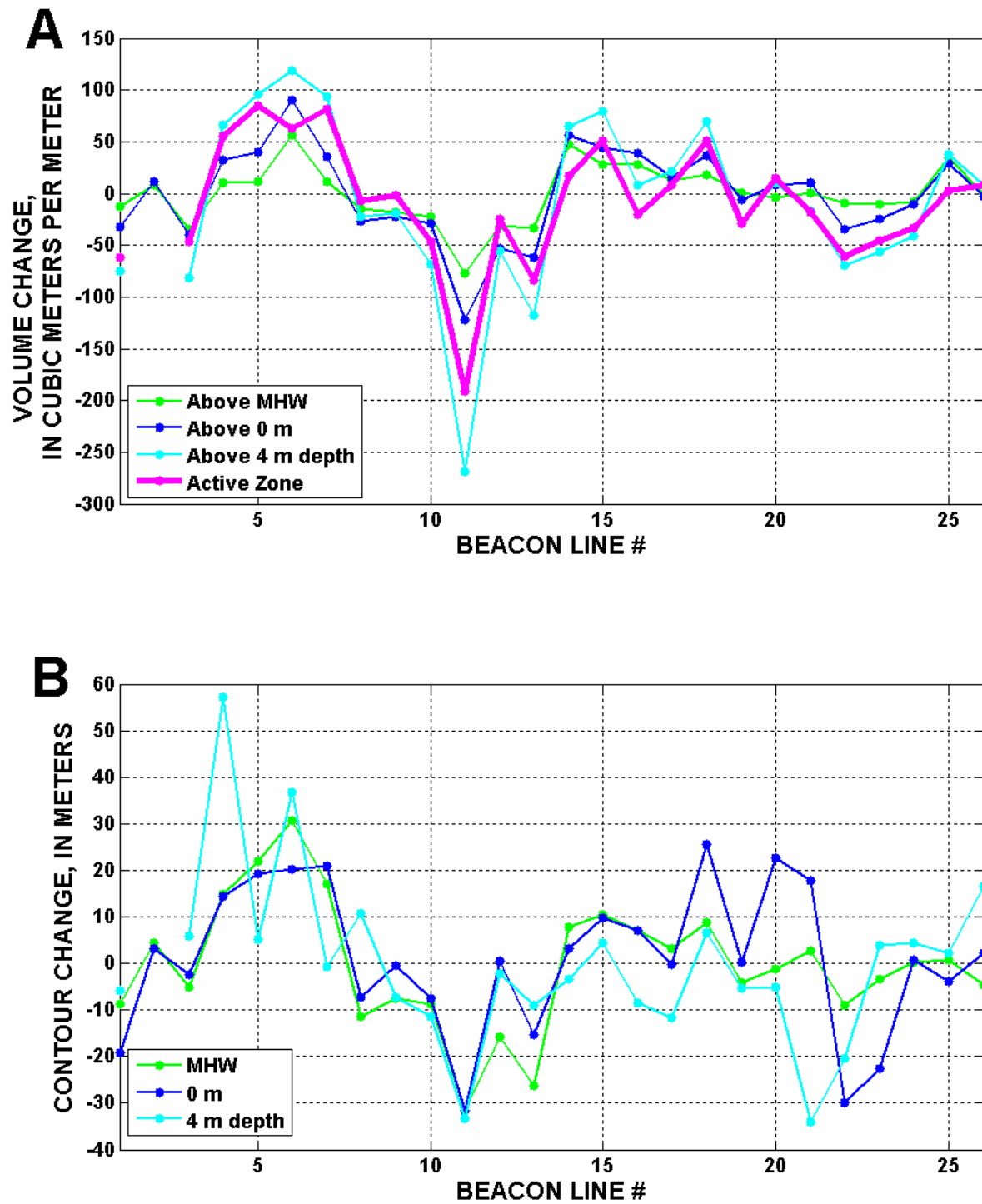


Figure 3.3. BEACON profile changes from November 2003 to October 2007, for lines north of the Santa Clara River mouth. *A*, volume change above the given elevation, and *B*, contour change (shoreline proxy) with a positive value representing accretion since 2003 and a negative value representing erosion since 2003. The “Active Zone” is the region between the mean high water (MHW) and 4 m depth contours.

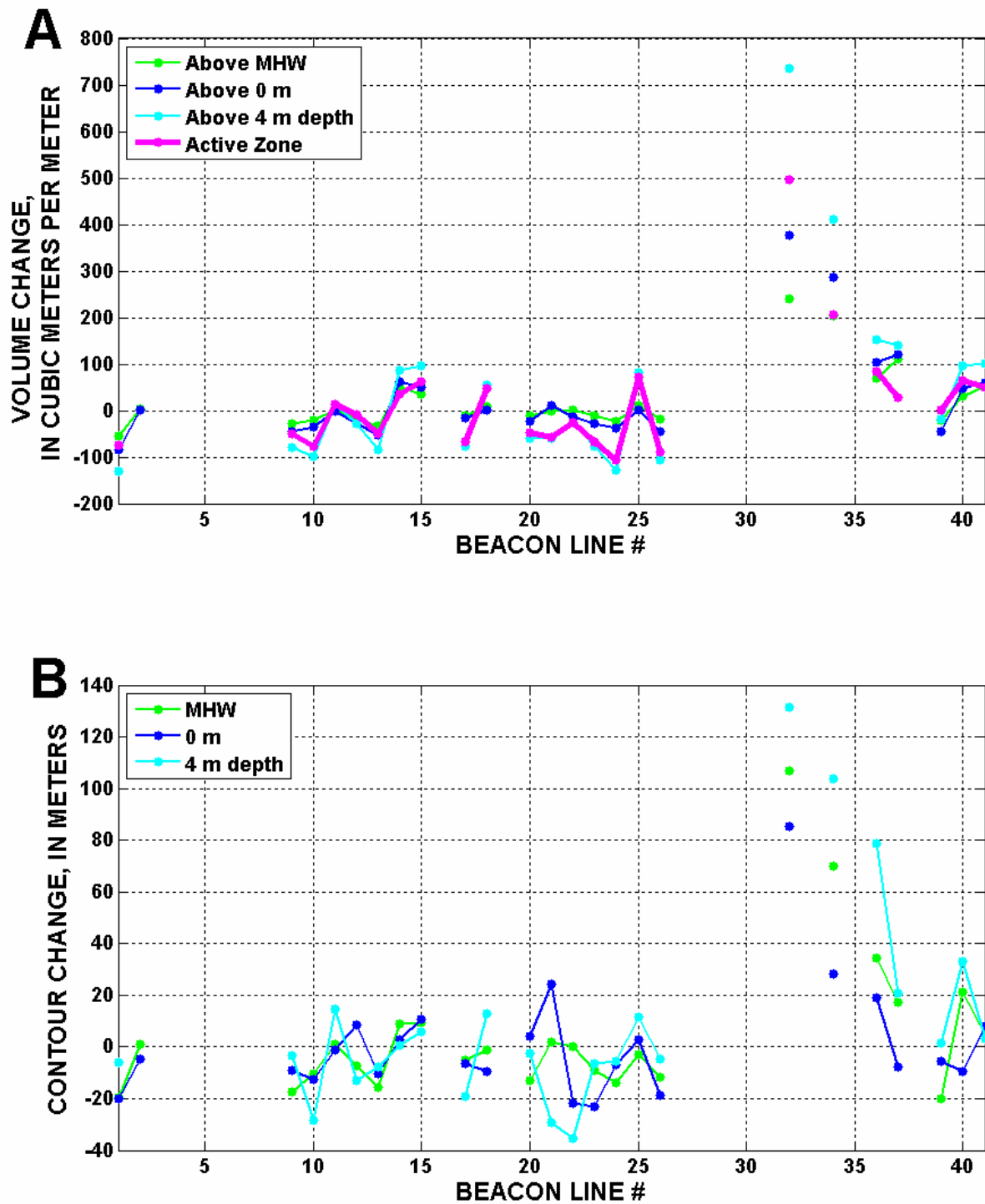


Figure 3.4. BEACON profile changes from October 1987 to October 2007. *A*, volume change above the given elevation, and *B*, contour change (shoreline proxy) with a positive value representing accretion since 1987 and a negative value representing erosion since 1987. The “Active Zone” is the region between the mean high water (MHW) and 4 m depth contours.

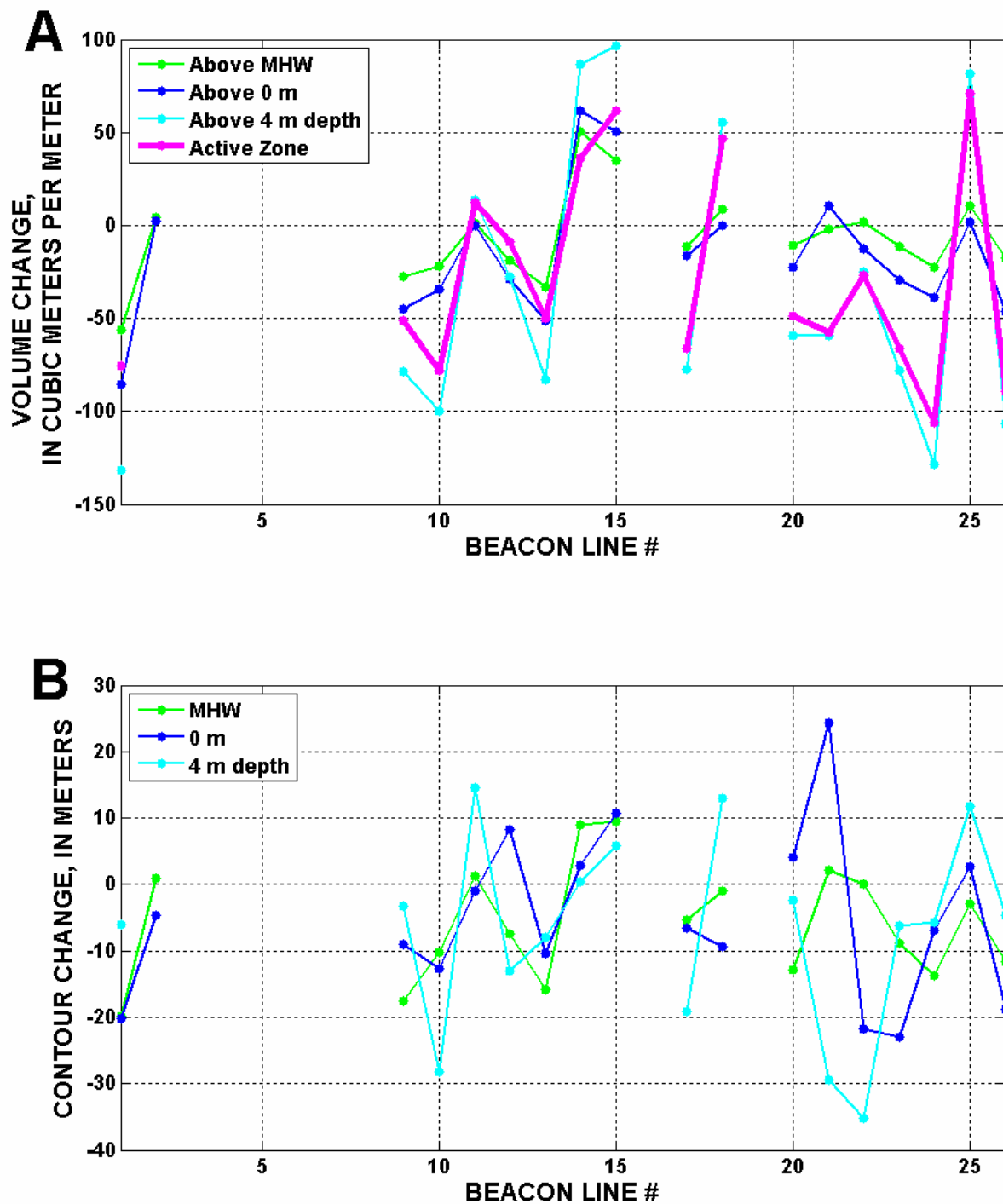


Figure 3.5. BEACON profile changes from October 1987 to October 2007 for lines north of the Santa Clara River mouth. *A*, volume change above the given elevation, and *B*, contour change (shoreline proxy) with a positive value representing accretion since 1987 and a negative value representing erosion since 1987. The “Active Zone” is the region between the mean high water (MHW) and 4 m depth contours.

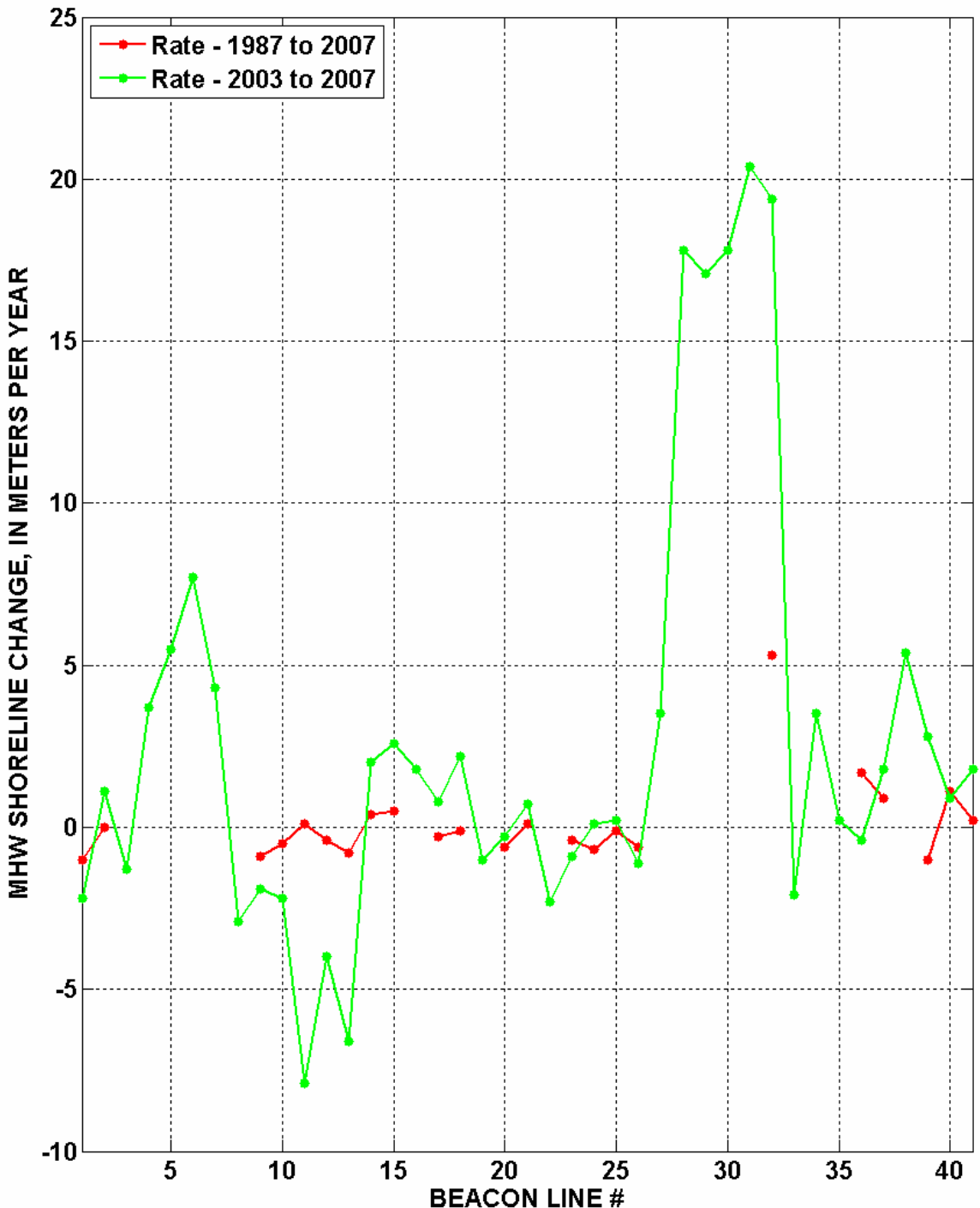


Figure 3.6. Shoreline-change rates based on the mean high water (MHW) position from 1987 to 2007 and from 2003 to 2007.

Chapter 4—Recent Morphological Changes

By Patrick L. Barnard and Daniel Hoover

Introduction

Semiannual (early fall and late winter) high-resolution topographic and bathymetric surveys were conducted at the focus areas of Ellwood/Isla Vista/Goleta, Carpinteria, Rincon Parkway, Ventura/Santa Clara River mouths and Mugu Canyon from October 2005 through October 2008 (fig. 1.1; table 4.1). The purpose of these surveys was to assess:

- Seasonal transport patterns, including the magnitude of cross-shore transport and shoreline change,
- Annual changes in sediment volume and shoreline position,
- Alongshore transport of accretion and erosion waves, and
- Net sediment-volume change during the 3-year study period.

Additionally, an airborne Lidar (light detection and ranging) survey of the entire SBLC coastline was performed on October 15, 2005. This survey enabled regional calculations of the effects of the strong 1997–98 El Niño event on shoreline position and beach slope in the SBLC when compared to the 1998 Lidar survey of the region (Hapke and others, 2006).

Methods

Barnard and others (2007) provide detailed descriptions of the methods applied to collecting and analyzing the Lidar, ATV topographic mapping, and Coastal Profiling System (CPS) mapping; this section provides a brief summary of those methods.

Lidar

Lidar survey data were collected on October 15, 2005, in partnership with BEACON, CDBW, USGS, UC Santa Cruz, and the University of Texas Bureau of Economic Geology. The data set includes point data from a strip of Southern California coastline (including water, beach, cliffs, and cliff tops) from Point Conception in Santa Barbara County to Point Mugu in Ventura County. The data were collected for comparison to previous data sets to determine rates of shoreline change along the coastlines of Santa Barbara and Ventura Counties. The October 2005 Lidar data can be downloaded at http://Lidar.cr.usgs.gov/Lidar_Viewer/viewer.php.

All-Terrain Vehicle Surveys

Subaerial beach surveys were conducted semiannually using ATVs at Ellwood/Isla Vista/Goleta, Carpinteria, and Ventura/Santa Clara River mouth (table 4.1, see Appendix B for coverage areas) and Ashtech dual-channel GPS receivers to collect data using the Differential Global Positioning System (DGPS) or Real-Time Kinematic (RTK) GPS. The differential correction was calculated at nearby base stations, and the correction was applied to the ATV data in real time (RTK) or after the survey (DGPS). All surveys were collected and processed in UTM, NAD83, Zone 11 North as the horizontal coordinate system. All elevations are relative to the North American Vertical Datum 1988 (NAVD 88), which is 2.9 cm above MLLW at the Santa Barbara Harbor Tide Station (Station # 9411340: National Oceanic and Atmospheric Administration, 2008).

Coastal Profiling System

The CPS, a hydrographic surveying system mounted on a personal watercraft, was used to collect bathymetric data at each of the focus areas (see table 4.1 for survey times and locations). The CPS combines the high accuracy positioning of RTK-GPS and the mobility of a personal watercraft to

collect rapid and precise bathymetric profiles. The CPS has traditionally been used to survey cross-shore profiles (approximately perpendicular to the shoreline) from approximately 15 m depth to 1 m depth (NAVD 88), depending on weather, tide, and surf conditions. A more complete discussion of specifics regarding the CPS is provided by Ruggiero and others (2005) and MacMahan (2001). Ashtech GPS equipment was used to collect position data. All bathymetric survey data was collected in the UTM horizontal coordinate system, Zone 11 North, and referenced to NAVD 88.

Analysis Tools

Beach slope was extracted from the 2005 Lidar data on shoreline normal transects located every 100 m alongshore in the SBLC and was measured from MSL (0.82 m NAVD88) to MHW (1.384 m NAVD88) using the Digital Shoreline Analysis System (DSAS, see Chapter 2). DSAS was also used for analyzing shorelines extracted from the ATV-collected topographic data. ArcGIS tools were used to filter and grid topographic data, as well as to calculate elevation and volume change between surveys. Custom built MATLAB scripts were used to process and analyze the bathymetry data.

Results

Data points and grids for each ATV topography survey are included in Appendix B. Profile locations and all profiles collected by the CPS system are included in Appendix C.

Lidar

Lidar Shoreline Change 1998-2005

The position of the MHW line between the April 1998 (Hapke and others, 2006) and October 2005 Lidar flights were compared to assess shoreline recovery since the El Niño winter of 1997-98 (table 4.2; fig. 4.1). Because this analysis is comparing different seasonal shorelines (early spring and late fall) without accounting for the typical summer shoreline progradation signal, the intent is only to

identify stretches of the SBLC that have clearly not regained their immediate post-El Niño position. That is, if the 2005 MHW line, even after the typical summer of progradation (April 2005 to October 2005), has not reached the April 1998 position, then it is clearly erosional.

On the basis of 1,281 transects, the average MHW position in October 2005 was 7.1 m seaward of its April 1998 position, accreting at a rate of 0.9 m/yr. However, the rate is extremely variable alongshore, ranging from accretion of 31.4 m/yr at the Santa Clara River mouth (125.9 km alongshore in fig. 4.1) to erosion of 11.4 m/yr at Mugu (149.6 km alongshore). The overall average, as with the BEACON lines analyzed in Chapter 3, is biased by the massive signal at the Santa Clara River mouth, which averaged 8.1 m/yr of accretion, with transects south of the Santa Clara River averaging 2.9 m/yr of accretion. North of the Santa Clara River, accretion was marginal at 0.5 m/yr (4 m total). Given that the seasonal shoreline migration is within this envelope (see Chapter 4), the change since April 1998 is negligible north of the Santa Clara River.

Higher rates (>3 m/yr) of accretion and erosion are associated with the updrift (75 km alongshore in fig. 4.1B) and downdrift (77 km alongshore) sides of the Santa Barbara Harbor, respectively. Other pockets of accretion are noted at Ellwood (55 km alongshore), Miramar (82 km alongshore), Summerland (85 km alongshore), Padaro (89 km alongshore), updrift of Rincon Point (96 km alongshore), La Conchita (100 km alongshore), between Hobson and Faria (107 km alongshore), Solimar (113 km), San Buenaventura State Beach to Hollywood (122 to 133 km alongshore), Silver Strand (135 km), south Hueneme to Ormond Beach (140 to 143 km alongshore), and western Mugu (146 km). Other notable pockets of erosion are at the Biltmore in Santa Barbara (80 km alongshore), Loon Point (87 km alongshore), downdrift of Rincon Point (98 km alongshore), Surfer's Point (119 km alongshore), north of Channel Islands Harbor (133 km alongshore), North Hueneme Beach (137 km

alongshore), south of Ormond Beach (144 km alongshore), and Mugu Canyon (148 and 150 km alongshore).

Beach Slope

Beach slope shows no significant alongshore trend in the SBLC (fig. 4.2). The average beach slope is 8 percent, with a standard deviation of 11 percent. Average beach slope in the SBLC is 1 percent higher east of Santa Barbara Harbor than it is to the west. However, this slight increase in slope appears to be related to the higher incidence of shore-protection structures and not to an obvious physical factor, such as grain size, as there is no significant correlation between beach slope and grain size ($r^2=0.02$) in the SBLC (based on 296 co-located (< 100 m apart) grain-size and beach-slope measurements). Areas with noticeable spikes in beach slope occur along the Gaviota Coast (27 to 31 km alongshore in fig. 4.2), around Rincon Parkway shore-protection structures (98 to 116 km alongshore), at the mouth of the Santa Clara River (125 km alongshore), and at Mugu Canyon (149 km alongshore). The higher beach slopes at the mouth of the Santa Clara River (~10 percent) are likely a result of a short alongshore spike in coarse grain sizes adjacent to the Santa Clara River mouth, as well as wave focusing on the river delta. Some of the lowest beach slopes (< 4 percent) in the region can be found just west of the Santa Barbara Mesa (67 to 73 km alongshore), at Sandyland/Carpinteria (92 to 95 km alongshore), and just north of the Channel Islands Harbor (~134 km alongshore). As a whole the SBLC beach slopes represent reflective conditions according to the Wright and Short (1984) classification, with a shoreface dominated by a single bar system (see CPS Bathymetry Mapping, this chapter) and short-period wave energy.

All-Terrain Vehicle Beach-Topography Mapping

The results presented in this section are based on ATV beach-topography mapping at each of the focus areas from October 2005 to October 2008 (table 4.1), except that the October 2005 Lidar survey

data was substituted at each focus area for the October 2005 ATV data because of its far more extensive spatial coverage and greater accuracy. Shoreline-change rates are based on the end point rate (EPR) and linear regression rate (LRR) of both the MSL and MHW shorelines. The EPR was calculated using only the October 2005 and October 2008 shorelines, and the LRR was calculated using only the fall shorelines (October 2005, 2006, 2007, and 2008).

Ellwood/Isla Vista/Goleta

A summary of the beach topography analysis for the Ellwood/Isla Vista/Goleta study area from 2005 to 2008 is presented in tables 4.3 to 4.5 and figures 4.3 to 4.5.

Shoreline-change analysis using DSAS shows this focus area to be slightly erosional at 0.4 to 2.3 m/yr of shoreline retreat based on the EPR and LRR of both the MSL and MHW shorelines. However, the local position of the shoreline varies up to 82 m, with the highest values occurring in the lee of Coal Oil Point (56.3 km; fig. 4.3) and Campus Point (59.6 km; fig. 4.3). Each of the three subareas (Ellwood, Isla Vista and Goleta) separated by Coal Oil and Campus points showed an average shoreline position range of ~20 m. Isla Vista shows the highest mean erosion rate at >2 m/yr. Within each subarea, and in the focus area as a whole, the MSL shoreline is retreating faster than the MHW line, indicating a steepening of the beach. Figure 4.4 shows the LRR of the MHW shoreline for the entire study area, with mostly continuous sections of erosion or accretion that typically exceed 500 m alongshore. Erosion is prevalent for the western half of Ellwood, almost all of Isla Vista, a small stretch in the lee of Campus Point, and the western half of Goleta County Beach. Accretion is prevalent immediately updrift and downdrift of Coal Oil Point, just updrift of Campus Point, along a small stretch in the lee of Campus Point, and on the eastern half of Goleta County Beach. Due to the severe erosion at Isla Vista the LRR often could not be calculated as the MHW line is on the cliff face.

A strong seasonal trend is documented by the vertical and volume change statistics in table 4.4, with 60,000 to 120,000 m³ of seasonal sand-volume variation, or up to 23 m³/m. Maximum annual volume change never exceeded 70,000 m³, or 11 m³/m. The winter of 2007-2008 showed the highest net loss of beach sediment (110,000 m³), compounded by poor summer recovery—Ellwood was the only subarea that recovered fully from that winter. The Goleta subarea alone lost close to 60,000 m³ of sediment from October 2007 to October 2008.

Beach slope did not show the typical steeping trend in the winter, with the exception of Ellwood (table 4.5). Overall, the mean beach slope of 7 percent was relatively constant between winter and fall. However, there was significant local steepening at Goleta County Beach each fall, while the winter slope became more gradual. There also was a noticeable reduction in beach slope regionally during the 2007-2008 winter.

Carpinteria

Summaries of the 2005-2008 beach topography analyses for the Carpinteria study area are presented in tables 4.6 to 4.8 and figures 4.6 to 4.8.

Shoreline analysis shows the Carpinteria area as erosional, averaging 0.7 to 2.4 m/yr of shoreline retreat. The Carpinteria City Beach is clearly erosional during the three year monitoring period, with a mean shoreline-retreat rate of 2.5 to 3.8 m/yr and no DSAS transect showing a MHW shoreline-retreat rate of less than 1 m/yr (see ~91.5 km in fig. 4.6). The MSL shoreline is retreating twice as fast as the MHW line, indicating an overall steepening of the beach. Erosion is prevalent over almost the entire study area, from the mid-point of the revetment downdrift of Sand Point through most of the State Park shoreline. Small pockets of relatively minor accretion are found at the ends of the study area, near Sand Point in the west and the asphaltum outcrop in the east. The local position of the shoreline varies up to 37 m, but averages just 11 m overall.

A strong seasonal trend is documented by the vertical- and volume-change statistics in table 4.7, with up to 76,000 m³ of seasonal sand-volume variation, or up to 28 m³/m. Maximum annual volume change never exceeded 38,000 m³ or 18 m³/m. As in the shoreline trend, the City Beach shows the highest seasonal variation (50 m³/m) and the largest overall volume loss (26 m³/m).

Beach slope broadly shows a steepening trend of up to two-fold from fall to winter [for example, October 2005 (4.7 percent) to March 2006 (9.1 percent)], with an overall mean of 5.3 to 7.8 percent. The City Beach did steepen from February 2008 to October 2008, but interpretation of slope changes in this area is compromised by the extensive beach scraping that is performed here.

Ventura/Santa Clara River Mouths

Summaries of the 2005-2008 beach topography analyses for the Ventura/Santa Clara River mouths study area are presented in tables 4.9 to 4.11 and figures 4.9 to 4.11.

Shoreline-change analysis shows this focus area overall to be erosional , averaging 4.6 to 6.3 m/yr of shoreline retreat. However, the overall average is dominated by the area around the Santa Clara River mouth, which is retreating at rates up to 45 m/yr (see 125.2 km in fig. 4.9). Shoreline retreat around the Santa Clara River mouth is a result of the rapid return of the shoreline to its equilibrium state after flood-induced shoreline progradation of at least 100 m in winter 2004-2005 (see Chapter 3). In the subarea north of the Ventura Harbor (122.5 km in fig. 4.9), the shoreline is retreating, but at a rate of only 1.5 to 2.8 m/yr, compared to 7 to 9.6 m/yr of retreat south of the harbor. Overall, shoreline position varies by a mean of 40 m, with a maximum of more than 100 m of movement at the Santa Clara River mouth. Shoreline position trends along San Buenaventura State Beach are variable, but erosion is prevalent downdrift of Surfer's Point for 1.6 km, and again for 2.5 km adjacent to the Santa Clara River mouth (fig. 4.10). Accretion is prevalent on both sides of the Ventura Harbor and downcoast of the massive erosion signal at the Santa Clara River mouth, where shoreline progradation rates peak at

around 20 m/yr. North of the Ventura Harbor, the MHW shoreline retreated more slowly than the MSL shoreline, indicating overall profile steeping, while the opposite occurred to the south.

Typical seasonal trends occurred throughout the northern portion of the study area, with beach volume changing seasonally by up to 75,000 m³, or 24 m³/m. South of the Ventura Harbor, seasonal trends were similar to those north of the harbor, except for 145,000 m³ of sediment that accreted (30 m³/m) from October 2005 to March 2006. This abnormal pattern is presumably a result of recently deposited flood sediments from the Santa Clara River delta migrating onto the beach. During the entire three-year study period, the beach north of the Ventura Harbor lost nearly 50,000 m³, while more than 200,000 m³ of sediment accreted to the south.

Beach slope shows the typical steeping trend in the winter, from a mean of 7.2 to 10.5 percent. However, mean beach slope is far steeper at the Santa Clara River mouth (10.5 percent) than in the rest of the study area (~ 8 percent).

Coastal Profiling System Bathymetry Mapping

Bathymetric profiles (Appendix C) show substantial variation across the study area, reflecting alongshore changes in regional geology and local sediment supply and retention. These variations affect sediment transport and retention, both on- and off-shore and alongshore. Depth of closure (DOC, the region below which seasonal and annual bathymetry changes are unresolvable, defined in this study to be < 10 cm of change during the monitoring period) varies from 1.8 to at least 11.3 m (table 4.12; fig. 4.12) and depends on a number of factors, including proximity to sediment sources (for example, the Santa Clara River mouth), profile shape (for example, shallow shelf vs. smoothly sloping or concave upward), and coastline orientation (for example, exposed vs. sheltered). Seasonal (October to February/March, and February/March to October) profile volume changes above the DOC typically were less than 100 m³ per m of profile width (m³/m), except in the Ventura region where changes of up

to 470 m³/m occurred around the Santa Clara River mouth (table 4.13; fig. 4.13). Throughout most of the study area, seasonal changes in the subtidal region were apparent as accretion during the winter and erosion during the summer, opposite of but consistent with the normal pattern observed on beaches, as sand moves from subtidal areas onto beaches in the summer and is eroded off of beaches and accumulates in shallow subtidal regions in winter. In the Ventura region, a different pattern occurred, with erosion dominating in both summer and winter due to progressive deflation of the Santa Clara River delta, although the seasonal effects of sediment exchange with the adjacent beaches still were visible in winter losses that were smaller than summer losses. Average annual volume differences for the entire study area were negative for all years due largely to the effects of losses from the Santa Clara River delta (fig. 4.18). Outside of the Ventura region, average annual volume changes were negative for the first two analyses (-4.2 m³/m for October 2005 to October 2006 and -20.6 m³/m for March 2006 to February 2007), positive for the subsequent two analyses (4.7 m³/m for October 2006 to October 2007 and 21.2 m³/m for February 2007 to February 2008), and slightly negative for the fifth analysis (-3.2 m³/m for October 2007 to October 2008. The magnitudes of the negative and positive differences were nearly equal, resulting in only a small average loss (-4.7 m³/m) in most of the study area from October 2005 to October 2008.

Ellwood/Isla Vista/Goleta

The Ellwood/Isla Vista/Goleta (E/IV/G) region is complex, with a dune-backed beach at Ellwood that is exposed to significant wave energy from the west, a rocky shelf fronting Isla Vista, and a sheltered, nearly east-facing beach fronting UC Santa Barbara that becomes progressively more exposed as it becomes south-facing at Goleta (Appendix C, fig. C2). Depths of closure in the E/IV/G region vary from 2.0 to 10.6 m, with the deepest values off of Ellwood, shallow to moderate and highly variable values off of Isla Vista, and shallow to moderate but relatively consistent values in the sheltered

region offshore of UCSB and Goleta Beach (fig. 4.12; table 4.12). Seasonal subtidal volume differences mostly were positive in the winter and negative in the summer, with the average for the region ranging from -17.2 to 14.1 m³/m (table 4.13). Consistent seasonal shifts were evident in several areas, with lines 44-49 in the Ellwood area frequently showing substantial accretion in the winter and erosion in the summer, and a number of smaller regions throughout the area (for example, around lines 6, 25-29, and 35) showing similar behavior (fig. 4.14). Annual subtidal volume differences mostly were less than 50 m³/m, with the average for the region ranging from -17.1 to 7.6 m³/m (table 4.14). A local peak in erosion offshore of the small beach at the west end of Isla Vista (lines 37-39) is evident from October 2005 to October 2006, followed in the subsequent year by accretion of comparable magnitude. Additionally, there was an unusual juxtaposition of accretion and erosion peaks off of Goleta Beach (lines 4-8) from October 2005 to October 2006; this area showed little change in the subsequent year but then showed the reverse of the first-year pattern in the third year (fig. 4.19). For the entire study period, profiles in the Goleta area were characterized by slight losses averaging -4.2 m³/m.

Carpinteria

The Carpinteria region includes the Sandyland coast, where the SBLC coastline shifts from predominantly south-facing to more southwest-facing Carpinteria Beach, which has a history of erosion (Barnard and others, 2007; Revell and others, 2008), and the section of coastline between Carpinteria and Rincon (Appendix C; fig. C5). Depths of closure in the Carpinteria region vary from 3.7 to 7.9 m, with moderate to shallow values off Sandyland and around the point at the west end of Carpinteria beach, with steadily deeper values moving eastward along Carpinteria beach to near-maximum values at lines 9 and 10. Values shallow abruptly at the east end of the beach and along the first portion of the ensuing rocky coastline, but deepen again at line 4 and remain at moderate to deep depths at lines 1 to 3 (fig. 4.12; table 4.12). Seasonal volume differences mostly were positive in the winter and negative in

the summer, with the average for profiles in the region ranging from -44.8 to 38.8 m³/m (table 4.13). The area off the central portion of Carpinteria Beach (lines 10-19) showed substantial accretion during the winter and erosion during the summer, except in winter 2006 when almost no change was observed. Lines 26-33 off of Sandyland beach, at and immediately north of the point at the west end of Carpinteria Beach, also showed mostly accretion during the winter and erosion during the summer, but local (line to line) variability was higher. Lines 1-5 in the section of coastline between Carpinteria and Rincon also appear to have experienced winter accretion and summer erosion, but fewer surveys were conducted in that area, making it difficult to examine patterns (fig. 4.15). Annual volume differences mostly were less than 50 m³/m, with the average for lines in the region ranging from -27.3 to 38.1 m³/m (table 4.14). A broad peak in erosion offshore of Carpinteria Beach at lines 9-20 is evident from March 2006 to February 2007, persisting into the next overlapping year (October 2006–October 2007) due to the lack of accretion noted previously in winter 2006. However, net accretion in the area in February 2007–February 2008 roughly balanced erosion seen in the previous year and was still visible in the October 2006–October 2007 data (fig. 4.20). For the entire study period, profiles in the Carpinteria area were characterized by slight losses averaging -5.0 m³/m.

Rincon Parkway

The Rincon region contains mostly southeasterly trending coastline interrupted by 3 prominent points that provide shelter to downdrift southerly- to southeasterly-facing coastline segments (Appendix C, fig. C8). Nearshore processes in this area also are impacted strongly by coastal armoring that protects Highway 101, which prevents beach development in this area. Depth-of-closure and volume-change results in this area are limited, and results are less robust than in other areas for a number of reasons: the area was not included in the first two surveys (table 4.1), not all lines were surveyed on subsequent dates, and radio coverage in the area is spotty making it difficult to obtain good RTK corrections to GPS

positions. Depth of closure values in the region vary from 1.8 to 7.7 m, with the deepest values at lines 28–30 along the exposed section of coastline downdrift of Solimar. Values throughout the rest of the region are moderate and show no obvious pattern relative to coastline geometry (fig. 4.12). Average seasonal volume differences were positive in winter 2006 and slightly negative in the ensuing summer, but no clear line-specific or regional patterns are evident in the data (fig. 4.16). The annual volume difference from October 2006 to October 2007 was positive (average $18.5 \text{ m}^3/\text{m}$), with local peaks in accretion around lines 12 and 25, and possibly line 34, all of which are immediately in the lee of points. One peak in erosion was seen at line 30 (fig. 4.21). The annual volume difference from October 2007 to October 2008 also was slightly positive at $3.6 \text{ m}^3/\text{m}$, but many of the regions characterized by accretion and erosion in 2006-2007 had reversed by 2007-2008 (fig. 4.21). Because the Rincon area was not surveyed in the first year of the program, data from this area can not be compared directly to the 3-year record available from other areas. However, it is notable that from October 2006 to October 2008 lines in the Rincon area generally appear to have been accumulating sediment at a modest rate, while lines in Goleta and Carpinteria showed slight net losses.

Ventura/Santa Clara River Mouths

The Ventura/Santa Clara River Mouths region includes a complex reach of coastline where coastline orientation shifts from predominantly southwest-facing to nearly west-facing. Two major rivers discharge in the region, the Ventura River in the north (~line 30) and the Santa Clara River in the south (~line 8). The point at the Ventura River discharge shelters an adjacent downdrift segment of south-facing beach (lines 23-25), and the Ventura Harbor is located immediately north of the Santa Clara River, between lines 15 and 16 (Appendix C, fig. C11). Depth of closure values in the region vary from 4.0 to 11.3 m or more and are noticeably deeper than in most of the rest of the study area, with most values deeper than 6 m and an overall average of 8.4 m. Values off of the Santa Clara River delta

may be even deeper as significant variability in profiles occurred even at the deepest portions of the profiles measured (Appendix C). Deep DOC values off of the Ventura River mouth (lines 28-35) shallow fairly rapidly to the east to the shallowest value in the region at line 23, in the sheltered region in the lee of the point, then deepen steadily to around 10 m near Ventura Harbor. Depth of closure values off of the Santa Clara River mouth and to the south mostly are in the 8—10 m range (fig. 4.12; table 4.12). Both winter and summer seasonal volume differences averaged across the region were negative, but values were less negative in winter (-7.1 to -25.3 m³/m) than in summer (-45.3 to -123 m³/m), indicating seasonal exchange with adjacent beaches superimposed on an overall erosional trend (table 4.13). Most of the erosion occurred on the Santa Clara River delta where several profiles lost 250 to 500 m³/m in the winters of 2005, 2006, and 2007, and 50 to 250 m³/m in the summers of 2006 and 2007 (fig. 4.17). Seasonal volume changes greater than 100 m³/m also were observed on a number of lines downdrift of the Santa Clara River delta and around Ventura Harbor (lines 15 and 16). More modest seasonal accretion and erosion similar to that observed in other portions of the study area were observed on lines north of the Ventura River (lines 34-39) and on lines 17-20 north of Ventura Harbor. Lines 22-25, in the lee of the point at the Ventura River Mouth, generally showed erosion in the winter and accretion in the summer, the opposite of the pattern observed at most other sites in the study area. Seasonal volume changes on lines on the Ventura River delta (lines 26-33) were comparable in magnitude to the relatively modest changes seen throughout most of the study area and exhibited no clear seasonal pattern, with one large erosional peak on line 31 in February – October 2008 that may be due to bad bathymetry data (Appendix C). Annual volume differences in the region overall were much higher than in other regions, but values for individual lines mostly were less than 100 m³/m, with the average for all lines in the region ranging from -51.4 to -127.8 m³/m (table 4.14). Erosion losses from lines on the Santa Clara River delta were much larger than anywhere else in the region, commonly

exceeding $300 \text{ m}^3/\text{m}$, and with some losses as high as $670 \text{ m}^3/\text{m}$ (table 4.14; fig. 4.22). Lines to the south (downdrift) of the eroding delta showed significant accretion from March 2006 – February 2008, suggesting that eroded delta sediments may have accumulated in this region before being transported out of the area. Annual volume differences at lines 15 and 16, on either side of Ventura Harbor, mostly were on the order of $100 \text{ m}^3/\text{m}$ or more, and generally were positive, indicating net accretion in this area consistent with the trapping effect expected by the design of the harbor entrance. The area off of the Ventura River Mouth (~lines 28-33) showed consistent erosion, but magnitudes generally were much smaller than off the Santa Clara River, typically $50 – 150 \text{ m}^3/\text{m}$ per year. Annual volume differences up-and down-drift of the Ventura River generally were very small (fig. 4.22). During the entire study period, lines in the Ventura/Santa Clara River Mouths region lost an average of $-280 \text{ m}^3/\text{m}$, with lines on the Santa Clara River delta losing up to $1,600 \text{ m}^3/\text{m}$.

Mugu Canyon

Bathymetric profiles in the Mugu Canyon area were collected in October 2007 and October 2008. More surveys would be required to estimate depth of closure values and profile-volume changes in this area as little change was seen in cross-shore profiles during this one-year period (Appendix C). Some changes were seen in alongshore profiles 78-80, including possible accretion and erosion in line 78 and a roughly 200 m shift in the position of the deep trench approaching shore in line 79. These changes suggest possible reorganization of sediments around the head of the offshore submarine canyon without significant regional erosion or accretion in this time period.

Offshore Wave Conditions (2005-2008)

Between October 2005 and October 2008, the regional offshore-wave climate, as measured by the Coastal Data Information Program Harvest Buoy (Station 071; Scripps Institute of Oceanography, 2008), varied considerably, with wave heights ranging from less than 1 m to nearly 10 m (fig. 4.23).

There does not appear to be considerable year-to-year variability in the bulk statistics—the mean winter (October 1 to March 30) offshore significant wave height ranged from 2.35 to 2.62 m; if the entire water year is considered (October 1 to September 30), the mean values range from 2.14 to 2.32 m (table 4.15). Year-to-year mean values are also similar for offshore peak period and direction. The greatest variability in wave height is seen if extreme values are considered. The winters of 2004/05 and 2005/06 each have only two recorded significant wave-height values greater than 6 m, with each record indicating the peak of a storm event, while the winter of 2006/07 has numerous values greater than 6 m from three discrete storm events, with several records greater than 8.5 m. Although the winter of 2007/08 does not have the highest mean significant wave height, four discrete storm events produced wave heights greater than 6 m, and wave heights from one event in February of 2008 approached 10 m (fig. 4.23). Thus, while the mean wave parameters from year to year did not vary greatly, the magnitude and frequency of storm events appear to have increased during the study period. The relative prevalence of large storm events during the winter of 2007/08 may explain the erosion observed at the regional beaches.

Conclusions

- Shoreline change since the 1997-98 El Niño is negligible in the SBLC, although locally there have been pockets of considerable accretion and lesser amounts of erosion.
- Between 1997 and 2005, the highest rates of accretion were measured just updrift of the Santa Barbara Harbor (3 m/yr) and at the mouth of the Santa Clara River (8.1 m/yr).
- Between 1997 and 2005, the highest rates of erosion were measured on the beach adjacent to Mugu Canyon, at up to -11.4 m/yr.
- Regional beach slope suggests dominantly reflective conditions, but conditions can be influenced locally by shore-protection structures.

- From 2005 to 2008, all-terrain vehicle beach mapping at Ellwood/Isla Vista/Goleta, Carpinteria, and Ventura shows that the shoreline was retreating at each of the three sites, with rates ranging from ~1 m/yr in Carpinteria to 6.3 m/yr in Ventura.
- From 2005 to 2008, shoreline-retreat rates locally exceeded 40 m/yr at the Santa Clara River mouth, likely due to a rapid return to equilibrium after the large winter 2004-2005 flood built the shoreline seaward more than 100 m.
- From 2005 to 2008, a trend of beach steeping was observed at each site, except at the mouth of the Santa Clara River.
- From 2005 to 2008, typical seasonal patterns of beach loss in the winter and recovery in the fall were observed at each focus area, except at the Santa Clara River mouth from October 2005 to March 2006.
- From 2005 to 2008, despite rapid shoreline-retreat rates, the beach south of the Santa Clara River gained more than 200,000 m³ of sediment.
- From 2005 to 2008, Goleta County Beach experienced unusual beach steeping from winter to fall each year.
- From 2005 to 2008, repeated cross-shore bathymetric surveys suggest depth-of-closure values from 1.8 to 11.3 m or more, with the deepest values occurring on the Santa Clara River delta. Values in most areas are between 2 and 8 m.
- From 2005 to 2008, semiannual bathymetry measurements from areas other than the Ventura/Santa Clara River study area show relatively modest (typically on the order of 10 to 50 m³/m) seasonal and annual volume changes. Subtidal seasonal changes occur primarily as accretion during the winter and erosion during the summer, with only a slight net loss (average - 4.7 m³/m) in profiles during the study period.

- In the Santa Clara River delta area, bathymetric profiles collected from 2005 to 2008 show erosional losses both seasonally and annually, indicating continuing deflation of the delta following the major input of flood sediments in January 2005. Sediment losses from the delta from 2005 to 2008 were much larger than anywhere else in the study region, commonly exceeding 400 m³/m per year.
- Offshore-wave statistics from 2005 to 2008 show no significant mean wave-height changes, but very large waves (>6 m) occurred more frequently in the last two winters of the study, which could explain the higher beach-erosion rates observed at the focus sites during this time period.

References

- Barnard, P.L., Revell, D.L., Eshleman, J.L., and Mustain, N., 2007, Carpinteria coastal processes study, 2005-2007—Final report: U.S. Geological Survey Open-File Report 2007-1217, 130 p., [<http://pubs.usgs.gov/of/2007/1412/> (last accessed March 13, 2009)].
- Hapke, C., Reid, D., Richmond, B., Ruggiero, P., and List, J., 2006, National assessment of shoreline change part 3: Historical shoreline change and associated coastal land loss along sandy shorelines of the California coast: USGS Open-File Report 2006-1219, 72 p.
- MacMahan, J., 2001, Hydrographic surveying from a personal watercraft: Journal of Surveying Engineering, v. 127, no.1, p. 12-24.
- National Oceanic and Atmospheric Administration (NOAA), 2008, Tides & Currents, Center of Operational Products and Services, [<http://tidesandcurrents.noaa.gov/> (last accessed March 13, 2009)]
- Revell, D.L., Barnard, P.L., Mustain, N., and Storlazzi, C.D., 2008, Influence of harbor construction on downcoast morphological evolution, Santa Barbara, California—Solutions to coastal disasters

conference, Oahu, Hawaii, April 13-16, 2008: Conference Proceedings, American Society of Civil Engineers, p. 630-642..

Ruggiero, P., Kaminsky, G.M., Gelfenbaum, G., and Voigt, B., 2005, Seasonal to interannual morphodynamics along a high-energy dissipative littoral cell: Journal of Coastal Research, v. 21, no.3, p. 553-578.

SCRIPPS Institution of Oceanography, 2008, The coastal data information program: San Diego, Integrative Oceanography Division, Scripps Institution of Oceanography, [<http://cdip.ucsd.edu> (last accessed March 13, 2009)].

Wright, L.D., and Short, A.D., 1984, Morphodynamic variability of surf zones and beaches: A synthesis: Marine Geology, v. 56, Issues 1-4, p. 93-118.

Table 4.1. Survey dates and data collected for the 5 focus areas. [T, topography data collected; B bathymetry data collected; dashes indicate no data]

Site	Oct 2005		Mar 2006		Oct 2006		Feb 2007		Oct 2007		Feb 2008		Oct 2008	
	T	B	T	B	T	B	T	B	T	B	T	B	T	B
Ellwood/Isla Vista/Goleta x		x	x	x	x x x			x x x x			x x		x x	x
Carpinteria	x	x	x	x	x x x			x	-	x x		x x		x
Rincon Parkway	-	-	-	-	-	x -		x -		x -		x -		x
Ventura/Santa Clara River Mouths	x	x	x	x	x x x			x x x x			x x		x x	x
Mugu Canyon	-	-	-	-	-	-	--	-	x	--	-	-	-	x

Table 4.2. Mean high water (MHW) shoreline-change statistics for the Santa Barbara littoral cell (SBLCC), April 1998 to October 2005.

	Change, in m/yr	Total change, in m
All transects		
Average 0.9		7.1
Maximum 31.4		235.6
Minimum -11.4		-85.6
Standard Dev.	3.4	25.3
Excluding Santa Clara River area		
Average 0.5		4.0
Maximum 13.3		99.7
Minimum -11.4		-85.6
Standard Dev.	2.2	16.2
North of Santa Clara River		
Average 0.5		3.5
Maximum 8.8		65.8
Minimum -9.8		-73.9
Standard Dev.	1.6	12.1
South of Santa Clara River		
Average 2.9		21.8
Maximum 31.4		235.6
Minimum -11.4		-85.6
Standard Dev.	6.5	48.9
Santa Clara River area		
Average 8.1		60.6
Maximum 31.4		235.6
Minimum -5.2		-39.2
Standard Dev.	8.6	64.8

Table 4.3. Shoreline-change statistics for 100-m spaced shore-normal transects in the Ellwood/Isla Vista/Goleta study area. [Topographic data are from ATV surveys conducted from 2005 to 2008 (Table 4.1), except for October 2005 where Lidar data was used due to its greater accuracy and more extensive coverage area. The end point rate (EPR) was calculated using only the October 2005 and 2008 shorelines, and the linear regression rate (LRR) was calculated using only October shorelines. MSL, mean sea level; MHW, mean high water]

	Range, in m		Total change, in m		EPR, in m/yr		LRR, in m/yr	
	MSL	MHW	MSL	MHW	MSL	MHW	MSL	MHW
All Ellwood/Isla Vista/Goleta transects								
Mean	22.3	21.6	-6.8	-3.8	-2.3	-1.3	-1.4	-0.4
Max	82.2	81.2	8.7	11.4	2.9	3.8	23.9	20.0
Min	0.2	0.3	-24.3	-29.2	-8.1	-9.7	-6.8	-6.5
Std. Dev.	14.8	13.8	7.4	8.9	2.5	3.0	3.3	3.2
Ellwood (transects 1 - 127)								
Mean	20.5	19.0	-4.6	1.1	-1.5	0.4	-2.0	0.8
Max	43.9	31.2	5.3	11.4	1.8	3.8	1.7	4.6
Min	0.2	8.1	-19.6	-19.4	-6.5	-6.5	-6.8	-6.5
Std. Dev.	9.2	4.7	6.7	8.0	2.2	2.7	2.4	2.9
Isla Vista (transects 128 - 261)								
Mean	22.2	22.0	-9.9	-6.9	-3.3	-2.3	-1.5	-1.2
Max	66.5	73.7	1.5	9.3	0.5	3.1	23.9	5.7
Min	2.5	0.3	-20.8	-20.8	-6.9	-6.9	-6.7	-6.0
Std. Dev.	13.7	16.1	6.1	8.5	2.0	2.8	4.3	2.9
Goleta (transects 262 - 422)								
Mean	23.9	23.5	-4.3	-4.2	-1.4	-1.4	-0.9	-0.3
Max	82.2	81.2	8.7	9.2	2.9	3.1	3.6	20.0
Min	0.9	2.3	-24.3	-29.2	-8.1	-9.7	-5.6	-5.2
Std. Dev.	19.5	16.1	7.9	8.5	2.6	2.8	2.0	3.4
Goleta Beach (transects 321 - 355)								
Mean	15.7	19.3	-4.4	-4.7	-1.5	-1.6	-1.0	-0.8
Max	26.8	32.8	5.6	7.2	1.9	2.4	3.5	4.3
Min	4.1	8.2	-18.7	-18.7	-6.2	-6.2	-5.6	-5.1
Std. Dev.	4.9	5.3	7.8	7.9	2.6	2.6	2.5	2.6

Table 4.4. Vertical- and volume-change statistics for the Ellwood/Isla Vista/Goleta study area from ATV topographic surveys conducted from 2005 to 2008. [The October 2005 Lidar was substituted for the October 2005 ATV data due to its greater accuracy and more extensive coverage area. Surface area is the overlapping region surveyed between the two surveys being analyzed]

	Mean elevation change, in m	Surface area, in m ²	Shoreline length, in m	Total volume change, in m ³	Total volume change, in m ³ /m
Entire beach - Seasonal					
Oct 05 to Mar 06	-0.39	154,892	3,235	-60,732	-19
Mar 06 to Oct 06	0.56	137,664	3,303	76,866	23
Oct 06 to Feb 07	-0.34	281,316	7,424	-96,287	-13
Feb 07 to Oct 07	0.53	226,076	6,434	120,548	19
Oct 07 to Feb 08	-0.64	170,256	6,500	-109,608	-17
Feb 08 to Oct 08	0.37	184,388	7,211	67,991	9
Annual					
Oct 05 to Oct 06	-0.08	273,244	7,988	-22,833	-3
Mar 06 to Feb 07	0.19	160,920	3,237	31,211	10
Oct 06 to Oct 07	0.25	222,328	6,337	55,664	9
Feb 07 to Feb 08	-0.16	234,896	7,532	-38,593	-5
Oct 07 to Oct 08	-0.36	192,468	6,347	-70,073	-11
Total change					
Oct 05 to Oct 08	-0.20	249,912	7,211	-48,777	-7
Ellwood - Seasonal					
Oct 05 to Mar 06	-0.48	38,960	335	-18,776	-56
Mar 06 to Oct 06	0.92	15,288	335	14,116	42
Oct 06 to Feb 07	-0.51	74,896	1,755	-38,173	-22
Feb 07 to Oct 07	0.69	27,848	657	19,175	29
Oct 07 to Feb 08	-1.12	13,804	657	-15,459	-24
Feb 08 to Oct 08	0.80	54,764	1,550	43,929	28
Annual					
Oct 05 to Oct 06	-0.07	81,944	2,303	-5,871	-3
Mar 06 to Feb 07	0.45	16,060	335	7,228	22
Oct 06 to Oct 07	0.19	31,220	657	5,868	9
Feb 07 to Feb 08	-0.25	62,544	1,755	-15,669	-9
Oct 07 to Oct 08	-0.08	27,464	657	-2,326	-4
Total change					
Oct 05 to Oct 08	-0.02	78,540	1,550	-1,423	-1

Table 4.4. (cont.) Vertical- and volume-change statistics for the Ellwood/Isla Vista/Goleta study area from ATV topographic surveys conducted from 2005 to 2008. [The October 2005 Lidar was substituted for the October 2005 ATV data due to its greater accuracy and more extensive coverage area. Surface area is the overlapping region surveyed between the two surveys being analyzed]

	Mean elevation change in m	Surface area in m ²	Shoreline length in m	Total volume change in m ³	Total volume change in m ³ /m
Isla Vista - Seasonal					
Oct 05 to Mar 06	-0.82	7,932	285	-6,482	-23
Mar 06 to Oct 06	0.84	8,992	519	7,524	14
Oct 06 to Feb 07	-0.28	94,156	3,220	-26,716	-8
Feb 07 to Oct 07	0.43	94,076	3,293	40,327	12
Oct 07 to Feb 08	-0.30	74,568	3,293	-22,671	-7
Feb 08 to Oct 08	0.10	67,480	3,293	6,732	2
Annual					
Oct 05 to Oct 06	-0.33	100,240	3,236	-33,336	-10
Mar 06 to Feb 07	0.01	9,152	418	117	0
Oct 06 to Oct 07	0.19	94,668	3,231	18,120	6
Feb 07 to Feb 08	0.11	83,816	3,293	9,134	3
Oct 07 to Oct 08	-0.15	86,572	3,293	-12,960	-4
Total change					
Oct 05 to Oct 08	-0.35	92,856	3,293	-32,264	-10
Goleta - Seasonal					
Oct 05 to Mar 06	-0.33	107,952	2,615	-35,180	-13
Mar 06 to Oct 06	0.48	113,372	2,449	54,550	22
Oct 06 to Feb 07	-0.28	112,136	2,449	-31,310	-13
Feb 07 to Oct 07	0.59	104,016	2,484	61,254	25
Oct 07 to Feb 08	-0.88	81,796	2,550	-71,892	-28
Feb 08 to Oct 08	0.29	62,084	2,368	17,794	8
Annual					
Oct 05 to Oct 06	0.17	90,860	2,449	15,753	6
Mar 06 to Feb 07	0.17	135,704	2,484	23,742	10
Oct 06 to Oct 07	0.33	96,244	2,449	32,047	13
Feb 07 to Feb 08	-0.37	88,476	2,484	-32,434	-13
Oct 07 to Oct 08	-0.70	78,304	2,397	-55,178	-23
Total change					
Oct 05 to Oct 08	-0.19	78,384	2,368	-15,215	-6

Table 4.5. Beach slope (mean sea level to mean high water) statistics for the Ellwood/Isla Vista/Goleta study area from the ATV topographic surveys conducted from 2005 to 2008. [The October 2005 Lidar data was substituted for the October 2005 ATV data due to its greater accuracy and more extensive coverage area. All values are in percent]

All Ellwood/Isla Vista/Goleta								Mean		
	Oct05	Mar06	Oct06	Feb07	Oct07	Feb08	Oct08	All	Fall	Winter
Mean	5.9 8	2	7.3	7.4	9.1	6.1	8.5 7	1	7.2	7.1
Maximum	25.2	66.9 79	.0	64.9	39.1	18.9	28.8 39	.0	30.3	39.0
Minimum	1.1 0	9	2.0	2.0	2.1	1.4	3.4 3	1	1.9	0.9
Std. Deviation	1.9 8	5	7.9	6.7	6.3	2.3	3.6 3	0	3.1	4.2
Ellwood (Transects 1 - 127)								Mean		
	Oct05	Mar06	Oct06	Feb07	Oct07	Feb08	Oct08	All	Fall	Winter
Mean	4.9 14	.9	3.4	5.5	6.4	6.3	8.9	5.8	5.5	6.7
Maximum	8.4 66	.9	8.9	31.5	28.6	18.9	16.2	13.3	10.3	25.2
Minimum	2.8 3	3	2.1	2.2	3.4	3.4	3.5 3	1	2.8	3.1
Std. Deviation	1.0 20	.2	1.6	5.5	5.0	2.8	2.9	1.6	1.4	4.1
Isla Vista (Transects 128- 261)								Mean		
	Oct05	Mar06	Oct06	Feb07	Oct07	Feb08	Oct08	All	Fall	Winter
Mean	5.6 13	.6	6.1	6.5	7.1	6.3	8.2	7.0	6.8	6.8
Maximum	13.3	39.0 14	.4	15.9	28.2	15.7	28.8 39	.0	13.7	39.0
Minimum	3.5 4	6	2.2	2.7	3.4	3.4	3.7 4	1	3.9	3.0
Std. Deviation	1.6 12	.0	2.3	3.0	4.6	1.9	3.7	3.4	2.0	3.8
Goleta (Transects 262 - 422)								Mean		
	Oct05	Mar06	Oct06	Feb07	Oct07	Feb08	Oct08	All	Fall	Winter
Mean	7.0 6	8	12.1	10.3	12.4	5.6	8.4 8	3	8.9	7.5
Maximum	25.2	32.3 79	.0	64.9	39.1	9.5	24.5 25	.2	30.3	32.3
Minimum	1.1 0	9	2.3	2.0	2.2	1.4	3.4 4	5	4.7	0.9
Std. Deviation	2.2 3	7	11.8 9	6	6.9	2.1	3.8 3	2	3.8	4.6
Goleta Beach (Transects 321 - 355)								Mean		
	Oct05	Mar06	Oct06	Feb07	Oct07	Feb08	Oct08	All	Fall	Winter
Mean	7.4 6	6	8.8	7.6	15.3	4.6	8.4 8	3	9.9	6.3
Maximum	8.7 13	.0	15.7 17	.6	25.2	8.7	15.6	12.2	15.1	14.0
Minimum	2.6 2	7	2.3	3.0	7.7	2.5	4.2 5	0	5.9	2.7
Std. Deviation	1.3 2	3	3.5	3.9	5.4	1.6	2.2 1	8	2.2	2.3

Table 4.6. Shoreline-change statistics for 100-m spaced shore-normal transects in the Carpinteria study area. [Topographic data are from ATV surveys conducted from 2005 to 2008 (Table 4.1), except for October 2005 where Lidar data was used due to its greater accuracy and more extensive coverage area. The end point rate (EPR) was calculated using only the October 2005 and 2008 shorelines, and the linear regression rate (LRR) was calculated using only October shorelines. MSL, mean sea level; MHW, mean high water]

Range, in m		Total change, in m		EPR, in m/yr		LRR, in m/yr	
MSL	MHW	MSL	MHW	MSL	MHW	MSL	MHW
All Carpinteria							
Mean	17.2	11.4	-6.1 -2 1	-2.0 -0.7	-2.4		-1.2
Max	37.6	28.9	18.8 8.8	6.3 2.9	6.0		1.7
Min	2.3	0.9	-17.3 -9 9	-5.8 -3.3	-6.3		-3.9
Std. Dev.	7.4	7.1	6.1 5.1	2.0 1.7	2.1		1.6
City Beach (Transects 76 to 92)							
Mean	27.0	24.5	-10.5 -7 5	-3.5 -2.5	-3.8		-2.8
Max	32.5	28.9	-8.9 -2 4	-3.0 -0.8	-3.3		-1.2
Min	20.0	19.3	-13.2 -9 5	-4.4 -3.2	-4.5		-3.6
Std. Dev.	3.5	2.2	1.2 1.9	0.4 0.6	0.3		0.6

Table 4.7. Vertical- and volume-change statistics for the Carpinteria study area from ATV topographic surveys conducted from 2005 to 2008. [The October 2005 Lidar was substituted for the October 2005 ATV data due to its greater accuracy and more extensive coverage area. Surface area is the overlapping region surveyed between the two surveys being analyzed]

	Mean elevation change, in m	Surface area, in m ²	Shoreline length, in m	Total volume change, in m ³	Total volume change, in m ³ /m
Entire beach - Seasonal					
Oct 05 to Mar 06	-0.49	131,896	2,677	-64,753	-24
Mar 06 to Oct 06	0.54	141,632	2,677	76,078	28
Oct 06 to Feb 07	-0.21	176,496	3,400	-37,601	-11
Feb 08 to Oct 08	0.37	105,412	2,847	38,725	14
Annual					
Oct 05 to Oct 06	0.10	175,556	4,011	17,923	4
Mar 06 to Feb 07	0.27	139,589	2,047	37,689	18
Feb 07 to Feb 08	-0.20	103,620	2,210	-20,694	-9
Total change					
Oct 05 to Oct 08	-0.22	132,212	2,837	-29,505	-10
City Beach - Seasonal					
Oct 05 to Mar 06	-0.64	27,844	410	-17,882	-44
Mar 06 to Oct 06	0.66	30,752	410	20,319	50
Oct 06 to Feb 07	-0.21	30,212	410	-6,405	-16
Feb 08 to Oct 08	0.61	22,944	410	13,983	34
Annual					
Oct 05 to Oct 06	0.06	27,832	410	1,742	4
Mar 06 to Feb 07	0.40	34,456	410	13,919	34
Feb 07 to Feb 08	-0.48	24,912	410	-12,060	-29
Total change					
Oct 05 to Oct 08	-0.39	27,012	410	-10,646	-26

Table 4.8. Beach slope (mean sea level to mean high water) statistics for the Carpinteria study area from the ATV topographic surveys conducted from 2005 to 2008. [The October 2005 Lidar data was substituted for the October 2005 ATV data due to its greater accuracy and more extensive coverage area. All values are in percent]

All Carpinteria								Mean		
	Oct05	Mar06	Oct06	Feb07	Oct07	Feb08	Oct08	All	Fall	Winter
Mean	4.7	9.1	4.9	7.6	NaN	8.0	7.2	6.1	5.3	7.8
Maximum	22.8	43.9	17.9	35.5	NaN	31.6	21.7	22.8	22.8	28.5
Minimum	2.1	2.5	2.1	1.6	NaN	3.6	3.0	2.7	2.7	1.6
Std. Deviation	1.7	6.4	2.1	4.9	NaN	4.2	3.4	2.3	1.9	3.8
City Beach (Transects 76 to 92)								Mean		
	Oct05	Mar06	Oct06	Feb07	Oct07	Feb08	Oct08	All	Fall	Winter
Mean	4.5	9.4	5.9	9.1	NaN	5.6	6.2	6.8	5.5	8.0
Maximum	5.1	13.8	17.9	15.8	NaN	8.8	10.0	8.8	8.8	12.7
Minimum	3.7	4.8	3.8	4.2	NaN	3.6	4.5	4.7	4.2	4.5
Std. Deviation	0.4	3.0	3.6	4.4	NaN	1.3	1.5	1.1	1.2	2.1

Table 4.9. Shoreline-change statistics for 100-m spaced shore-normal transects in the Ventura study area.
 [Topographic data are from ATV surveys conducted from 2005 to 2008 (Table 4.1), except for October 2005 where Lidar data was used due to its greater accuracy and more extensive coverage area. The end point rate (EPR) was calculated using only the October 2005 and 2008 shorelines, and the linear regression rate (LRR) was calculated using only October shorelines. MSL, mean sea level; MHW, mean high water]

	Range, in m		Total change, in m		EPR, in m/yr		LRR, in m/yr	
	MSL	MHW	MSL	MHW	MSL	MHW	MSL	MHW
All Ventura								
Mean	41.2 41	.2	-13.8	-16.4	-4.6	-5.5	-5.5	-6.3
Max	144.9	141.2 61	.8	65.6	20.6	21.9	18.7 19	.3
Min	0.4 1.	1	-132.5	-132.7	-44.2	-44.2	-42.6	-45.3
Std. Dev.	34.3 37	.3	42.0	46.8 14	.0	15.6	13.5	15.7
North of Ventura Harbor (Transects 1-265)								
Mean	22.2 16	0	-7.1	-4.9	-2.4 -1	.6	-2.8	-1.5
Max	54.4 52	.4	11.1	12.0	3.7	4.0	3.8	3.9
Min	1.3 1.	7	-32.0	-33.7	-10.7	-11.2	-10.9	-9.9
Std. Dev.	10.4 11	.0	11.0	10.2	3.7	3.4	3.4	3.2
South of Ventura Harbor (Transects 266-499)								
Mean	54.9 58	.5	-21.0	-24.0	-7.0	-8.0	-8.3	-9.6
Max	144.9	141.2 61	.8	65.6	20.6	21.9	18.7 19	.3
Min	0.4 1.	1	-132.5	-132.7	-44.2	-44.2	-42.6	-45.3
Std. Dev.	38.7 39	.2	58.6	58.6 19	.5	19.5	18.9	19.6
Santa Clara River Mouth (Transects 330-385)								
Mean	102.1 10	5.1	-99.0	-100.6	-33.0	-33.5	-32.7	-34.8
Max	144.9 14	1.2	-48.3	-33.1	-16.1	-11.0	-17.6	-10.8
Min	12.9 33	.1	-132.5	-132.7	-44.2	-44.2	-42.6	-45.3
Std. Dev.	34.4 29	.2	24.5	29.4	8.2	9.8	8.0	10.2

Table 4.10. Vertical- and volume-change statistics for the Ventura study area from ATV topographic surveys conducted from 2005 to 2008. [The October 2005 Lidar was substituted for the October 2005 ATV data due to its greater accuracy and more extensive coverage area. Surface area is the overlapping region surveyed between the two surveys being analyzed]

	Mean elevation change, in m	Surface area, in m ²	Shoreline length, in m	Total volume change, in m ³	Total volume change, in m ³ /m
Entire beach - Seasonal					
Oct 05 to Mar 06	0.18	544,668	8,183	99,276	12
Mar 06 to Oct 06	0.29	429,720	7,856	124,683	16
Oct 06 to Feb 07	-0.35	211,020	3,119	-74,446	-24
Feb 07 to Oct 07	0.25	170,188	3,032	42,552	14
Oct 07 to Feb 08	-0.34	219,492	5,498	-74,105	-13
Feb 08 to Oct 08	0.18	295,848	6,199	52,954	9
Annual					
Oct 05 to Oct 06	0.32	603,872	8,691	194,186	22
Mar 06 to Feb 07	-0.06	212,840	3,259	-13,520	-4
Oct 06 to Oct 07	-0.25	285,364	6,295	-72,613	-12
Feb 07 to Feb 08	0.12	131,148	3,160	15,109	5
Oct 07 to Oct 08	-0.14	325,512	6,647	-44,439	-7
Total change					
Oct 05 to Oct 08	0.29	566,904	8,658	165,744	19
Ventura North - Seasonal					
Oct 05 to Mar 06	-0.21	224,780	3,355	-48,160	-14
Mar 06 to Oct 06	0.26	186,176	3,202	48,466	15
Oct 06 to Feb 07	-0.35	211,020	3,119	-74,602	-24
Feb 07 to Oct 07	0.25	170,188	3,032	42,923	14
Oct 07 to Feb 08	-0.17	123,772	3,089	-21,077	-7
Feb 08 to Oct 08	0.13	135,520	3,560	17,406	5
Annual					
Oct 05 to Oct 06	-0.03	256,244	3,716	-8,768	-2
Mar 06 to Feb 07	-0.07	212,840	3,259	-14,075	-4
Oct 06 to Oct 07	-0.13	163,960	3,604	-21,735	-6
Feb 07 to Feb 08	0.12	131,148	3,160	15,636	5
Oct 07 to Oct 08	-0.10	184,296	3,603	-17,980	-5
Total change					
Oct 05 to Oct 08	-0.18	265,604	3,753	-48,647	-13

Table 4.10. (cont.) Vertical- and volume-change statistics for the Ventura study area from ATV topographic surveys conducted from 2005 to 2008. [The October 2005 Lidar was substituted for the October 2005 ATV data due to its greater accuracy and more extensive coverage area. Surface area is the overlapping region surveyed between the two surveys being analyzed]

	Mean elevation change in m	Surface area in m ²	Shoreline length in m	Total volume change in m ³	Total volume change in m ³ /m
Ventura South - Seasonal					
Oct 05 to Mar 06	0.45	319,888	4,828	144,577	30
Mar 06 to Oct 06	0.32	243,544	4,654	79,112	17
Oct 06 to Feb 07	N/A	N/A	0	N/A	N/A
Feb 07 to Oct 07	N/A	N/A	0	N/A	N/A
Oct 07 to Feb 08	-0.55	95,720	2,409	-52,987	-22
Feb 08 to Oct 08	0.22	160,328	2,639	35,536	13
Annual					
Oct 05 to Oct 06	0.59	347,628	4,975	203,985	41
Mar 06 to Feb 07	N/A	N/A	0	N/A	N/A
Oct 06 to Oct 07	-0.41	121,404	2,691	-49,995	-19
Feb 07 to Feb 08	N/A	N/A	0	N/A	N/A
Oct 07 to Oct 08	-0.19	141,216	3,044	-26,604	-9
Total change					
Oct 05 to Oct 08	0.71	301,300	4,905	213,853	44

Table 4.11. Beach slope (mean sea level to mean high water) statistics for the Ventura study area from the ATV topographic surveys conducted from 2005 to 2008. [The October 2005 Lidar data was substituted for the October 2005 ATV data due to its greater accuracy and more extensive coverage area. All values are in percent]

All Ventura								Mean		
	Oct05	Mar06	Oct06	Feb07	Oct07	Feb08	Oct08	All	Fall	Winter
Mean	7.1	7.0	6.7	11	.3	6	3	11.6	6.7	7.8
Maximum	36.5	24.1	56.2	57	.7	13	.6	31.9	15.1	36.5
Minimum	1.0	2.7	0.8	3.	5	2.	8	1.5	2.9	1.3
Std. Deviation	3.5	3.2	5.3	8.	5	2.	5	6.3	2.4	3.3
North of Ventura Harbor (Transects 1-265)								Mean		
	Oct05	Mar06	Oct06	Feb07	Oct07	Feb08	Oct08	All	Fall	Winter
Mean	6.3	6.6	4.2	11	.3	6	3	11.1	5.7	7.5
Maximum	36.5	24.1	56.2	57	.7	13	.6	31.0	15.1	36.5
Minimum	1.3	2.7	1.7	3.	5	2.	8	3.9	2.9	1.3
Std. Deviation	3.9	3.0	5.3	8.	5	2.	5	5.0	2.1	3.7
South of Ventura Harbor (Transects 266-499)								Mean		
	Oct05	Mar06	Oct06	Feb07	Oct07	Feb08	Oct08	All	Fall	Winter
Mean	8.0	8.	0	8.3	NaN	NaN	12.3	7.9	8.3	8.0
Maximum	26.5	16.7	24.7	NaN	NaN	31	.9	14.2	18	.1
Minimum	1.0	2.	7	0.8	NaN	NaN	1.5	3.3	4.0	2.7
Std. Deviation	2.8	3.	7	4.6	NaN	NaN	7.9	2.2	2.7	2.5
Santa Clara River Mouth (Transects 330-385)								Mean		
	Oct05	Mar06	Oct06	Feb07	Oct07	Feb08	Oct08	All	Fall	Winter
Mean	9.8	5.	9	10.9	NaN	NaN	12.1	9.4	10.5	10.0
Maximum	26.5	11.4	24.7	NaN	NaN	31	.9	14.2	18	.1
Minimum	1.0	2.	7	5.7	NaN	NaN	1.5	5.7	5.3	5.7
Std. Deviation	3.3	2.	6	4.5	NaN	NaN	8.5	2.1	2.9	2.3

Table 4.12. Depth of closure (DOC) statistics for each region and for the study area as a whole. [DOCs were not calculated for Mugu Canyon due to insufficient replication (n=2). Depths are in meters]

Area	Number of lines	Mean DOC	Minimum DOC	Maximum DOC
Ellwood/Isla Vista/Goleta	55	4.74	2.01	10.56
Carpinteria	33	5.72	3.72	7.92
Rincon Parkway	28	4.67	1.75	7.72
Ventura/Santa Clara River	39	8.40	3.96	11.32
All Areas	155	5.85	1.75	11.32

Table 4.13. Seasonal bathymetric profile volume-change statistics. [Volume changes are in m³/m]

	Goleta					
	10/05-3/06	3/06-10/06	10/06-2/07	2/07-10/07	10/07-2/08	2/08-10/08
Maximum	77.2 33	.7 50	.8 75	.1 98	.6 45	.7
Minimum	-114.1 -9	5.9 -5	6.0 -7	8.3 -4	7.9 -6	0.6
Mean	13.5 -1	7.2	1.3	-6.3	14.1 -1	6.6
Median	7.4 -1	5.4	6.2	-9.2	19.0	-21.9
Std Deviation	33.8 25	.4 19	.6 28	.5 34	.9 29	.9
Std Error	5.2 3.	4 2.	6 3.	8 5.	8 5.	0
n	43 56 56	55 36 35				
% positive	65% 25	% 57	% 44	% 69	% 37	%
	Carpinteria					
Maximum	77.2	-0.7 62	.9 99	.5	124.0	10.6
Minimum	-11.6 -7	8.4 -1	6.8 -9	8.5 -5	4.3	-138.9
Mean	32.3 -3	7.2	15.9 -1	3.3	38.8	-44.8
Median	19.8 -2	9.3	13.8 -3	4.8	23.1	-44.2
Std Deviation	27.4 22	.9 21	.5 63	.7 59	.1	28.3
Std Error	5.1 4.	2 3.	8	19.2	17.1	5.4
n	29 30 32	11 12				28
% positive	93%	0%	75% 45	% 75	%	4%
	Rincon					
Maximum			83.9	67.5		
Minimum			-63.5	-63.1		
Mean			15.1	-2.4		
Median						
Std Deviation			34.1	31.2		
Std Error			6.4	5.9		
n		13		15		
% positive		77	%	53%		
	Ventura					
Maximum	255.7 21	6.1 19	9.1 19	7.2 33	1.5	125.05
Minimum	-383.5 -	160.4 -	406.3 -	268.9 -	196.2	-472.8
Mean	-8.6	-47.8 -2	5.3 -4	5.3	-7.1	-123.04
Median	-16.2 -4	6.5	3.8 -3	6.3 -1	4.6	-87.00
Std Deviation	129.0 67	.8	123.5	104.1 97	.0	143.08
Std Error	20.7 10	.8 19	.8 16	.7 15	.5	22.91
n	35 39 38	38 37				36
% positive	49% 10	% 53	% 34	% 43	%	8%
	All sites					
Maximum	255.7 21	6.1 19	9.1 19	7.2 33	1.5	125.1
Minimum	-383.5 -	160.4 -	406.3 -	268.9 -	196.2	-472.8
Mean	11.4 -3	1.6	-1.3 -1	9.1	8.5	-63.3
Median	13.8 -2	6.1	8.25	-11.9	15.8	-38.0
Std Deviation	79.0 44	.7 68	.6 67	.5 72	.5	100.1
Std Error	7.6 4.	0 5.	8 6.	2 7.	9	10.1
n	107 12	5 13	9 11	9	85	99
% positive	68% 14	% 62	% 42	% 59	% 17	%

Table 4.14. Annual and 3-year bathymetric profile volume-change statistics. [Volume changes are in m³/m]

Goleta						
	10/05-10/06	3/06-2/07	10/06-10/07	2/07-2/08	10/07-10/08	10/05-10/08
Maximum	88.5 22	.0	102.2	65.3	72.0	69.7
Minimum	-112.9	-76.0 -6	0.5 -4	2.2	-99.2	-67.6
Mean	-2.7 -1	7.1	-1.3	7.6	-8.6	-4.2
Median	-4.8 -1	8.2	-1.1	8.1	-8.2	-4.3
Std Deviation	33.0	19.8 27	.7 22	.6	33.0	27.2
Std Error	5.0	2.7 3.	7 3.	8	4.8	4.7
n	43	55 56 36			47	34
% positive	44%	16% 46	% 69	% 38	%	38%
Carpinteria						
Maximum	37.4 30	.5	114.0	108.3	99.8	75.0
Minimum	-56.3	-87.3 -8	9.4 -2	9.2	-85.3	-108.5
Mean	-6.5 -2	7.3	0.7	38.1	0.9	-5.0
Median	-6.6 -2	5.2	-0.6	38.6	-20.6	-4.1
Std Deviation	18.3	31.3 64	.3 33	.3	63.2	34.9
Std Error	3.4 5.	8	18.6	6.2	18.2	6.7
n	29	29 12 29			12	27
% positive	24%	17% 50	% 90	%	42%	48%
Rincon						
Maximum			111.0		127.7	
Minimum			-101.7		-98.3	
Mean			18.5		3.6	
Median			23.4		4.5	
Std Deviation			42.9		42.0	
Std Error			8.1		7.7	
n			28		30	
% positive		71	%	57	%	
Ventura						
Maximum	189.8	178.3 31	7.3 20	8.0	99.7	110.4
Minimum	-669.8	-497.7 -	650.7 -	373.9	-584.1	-1568.8
Mean	-70.0	-51.4 -6	3.9 -5	2.2	-127.8	-278.2
Median	-43.5 -2	2.2	0.9	-19.0	-102.7	-137.1
Std Deviation	160.2	138.3 21	1.2 13	5.0	147.7	398.7
Std Error	27.1	22.4 33	.8 22	.5	24.3	68.4
n	35	38 39 36			37	34
% positive	29%	34% 51	% 42	% 16	%	12%
All sites						
Maximum	189.8	178.3 31	7.3 20	8.0	127.7	110.4
Minimum	-669.8	-497.7 -	650.7 -	373.9	-584.1	-1568.8
Mean	-25.8 -3	0.2	-15.1	-4.9	-39.8	-80.9
Median	-9.7	-19.55 1.	9 13	.9	-16.0	-11.3
Std Deviation	98.5 80	.4	121.2	90.9	103.5	243.4
Std Error	9.5 7.	3	10.4	9.0	9.2	22.0
n	107	122 13	5 10	1	126	122
% positive	33%	23% 53	% 65	% 36	%	35%

Table 4.15. Offshore-wave statistics for the 2005-2008 study period. [Hs, significant wave height; Tp, peak period; Dp, peak direction]

Water year means (10/1-9/30)				
Year	Hs(m)	St dev Hs (m)	Tp (s)	Dp (°)
2004/2005	2.14	0.80	12.09	286.29
2005/2006	2.32	0.84	12.19	287.63
2006/2007	2.28	0.95	11.62	292.57
2007/2008	2.28	0.94	12.02	283.02
Winter means (10/1-3/30)				
Year	Hs(m)	St dev Hs (m)	Tp (s)	Dp (°)
2004/2005	2.35	0.83	13.08	290.72
2005/2006	2.62	0.91	13.28	293.35
2006/2007	2.47	1.09	12.71	295.88
2007/2008	2.55	1.02	13.16	286.99

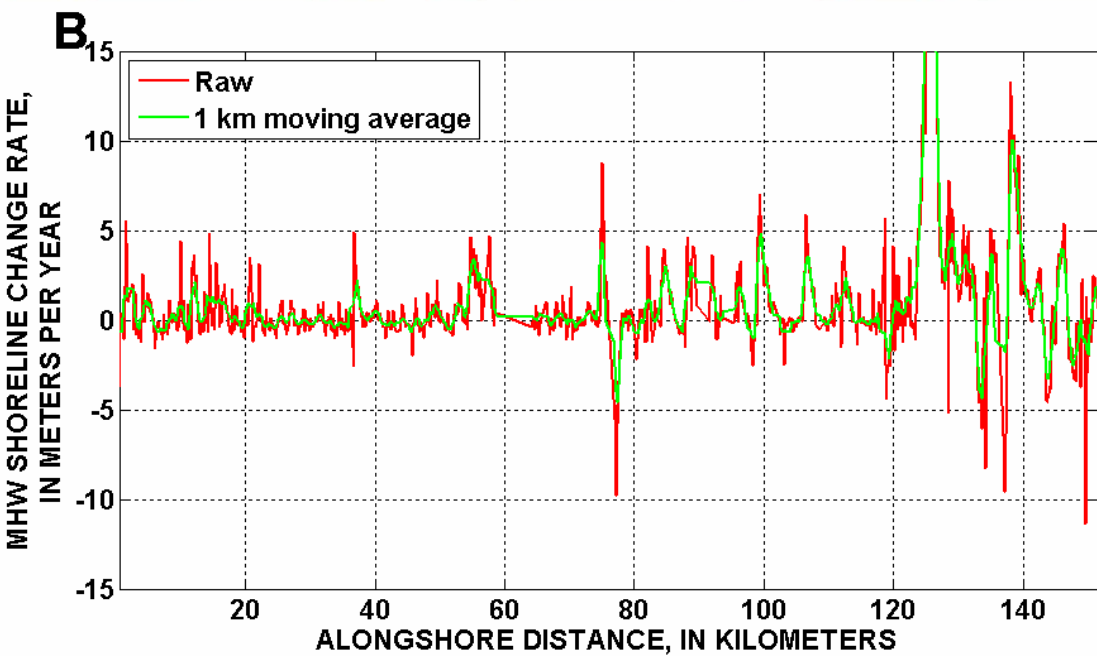
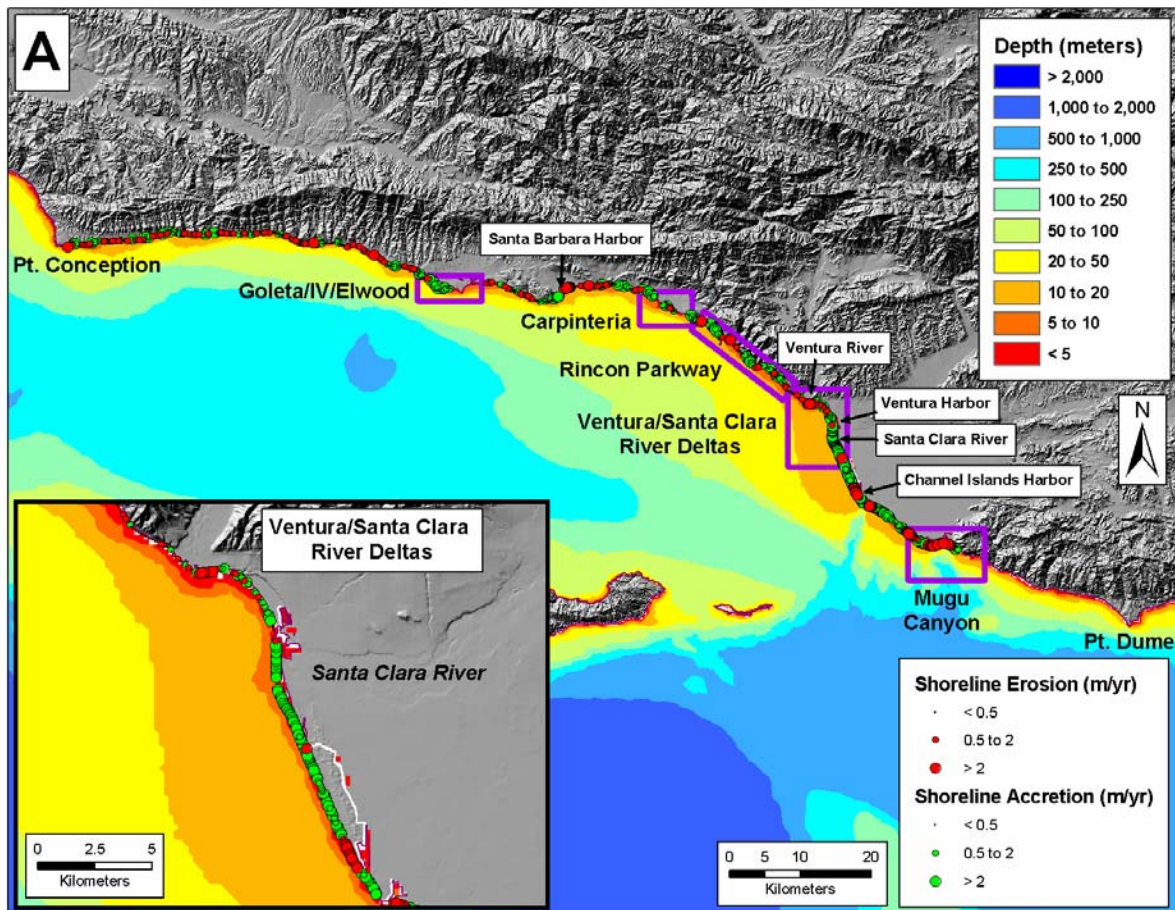


Figure 4.1. Mean high water (MHW) shoreline-change rate in the SBLC from the 1998 and 2005 Lidar surveys. *A*, survey area with inset of Ventura/Santa Clara River Area. *B*, plot of shoreline-change rate versus alongshore distance from Point Conception, raw, and 1-km moving average.

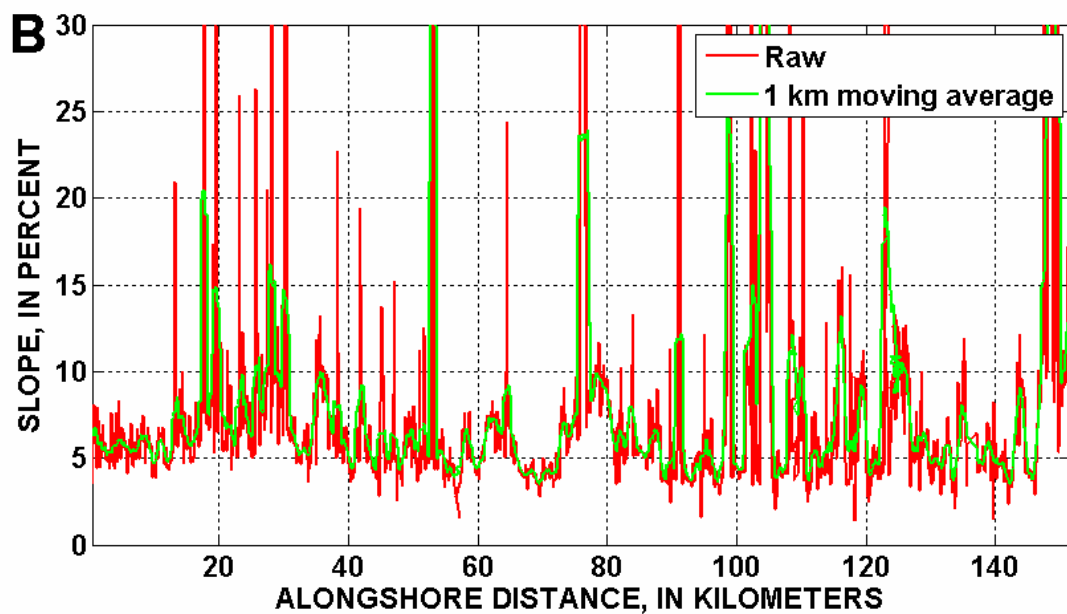
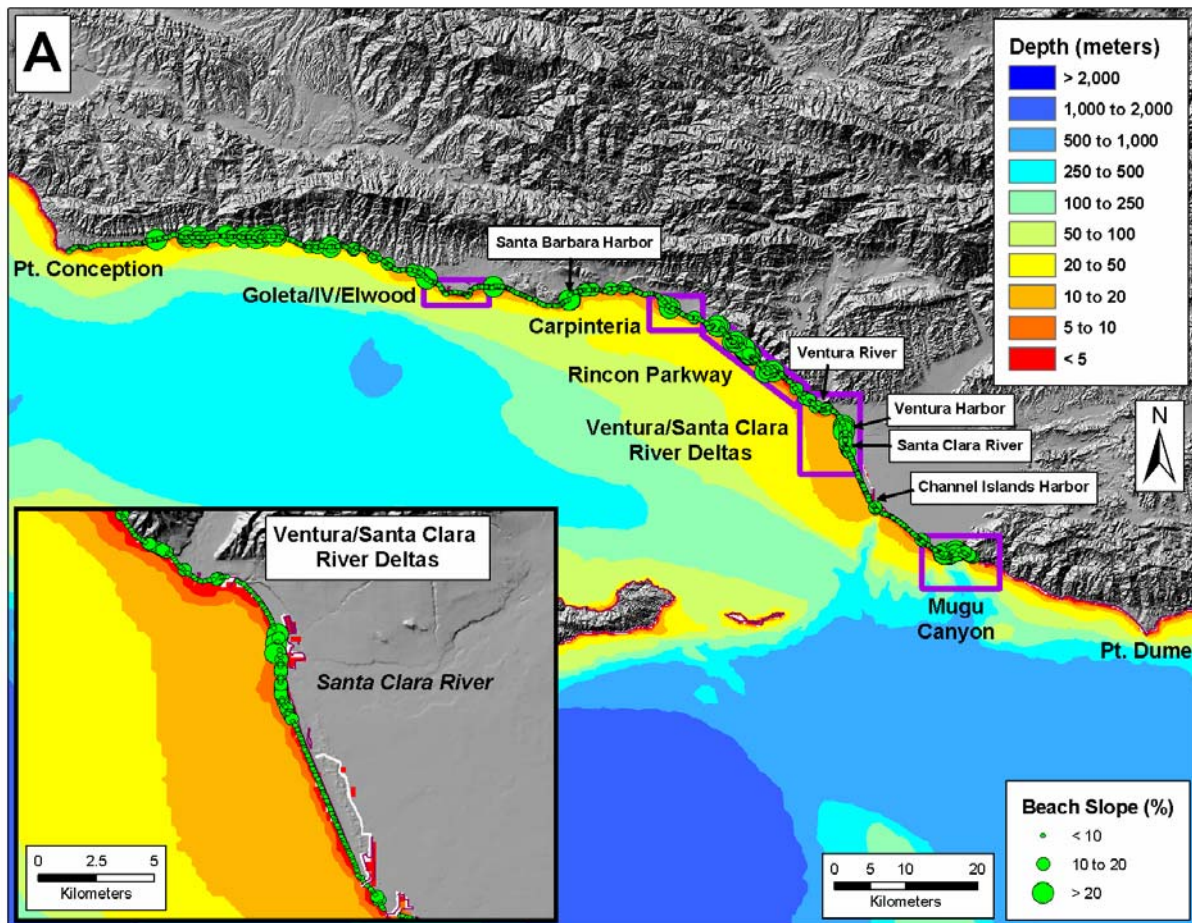


Figure 4.2. Beach slope (Mean sea level to mean high water) in the SBLC from the 2005 Lidar survey. *A*, survey area with inset of Rincon and Santa Clara River area. *B*, plot of alongshore distance from Point Conception versus beach slope, raw, and 1-km moving average.

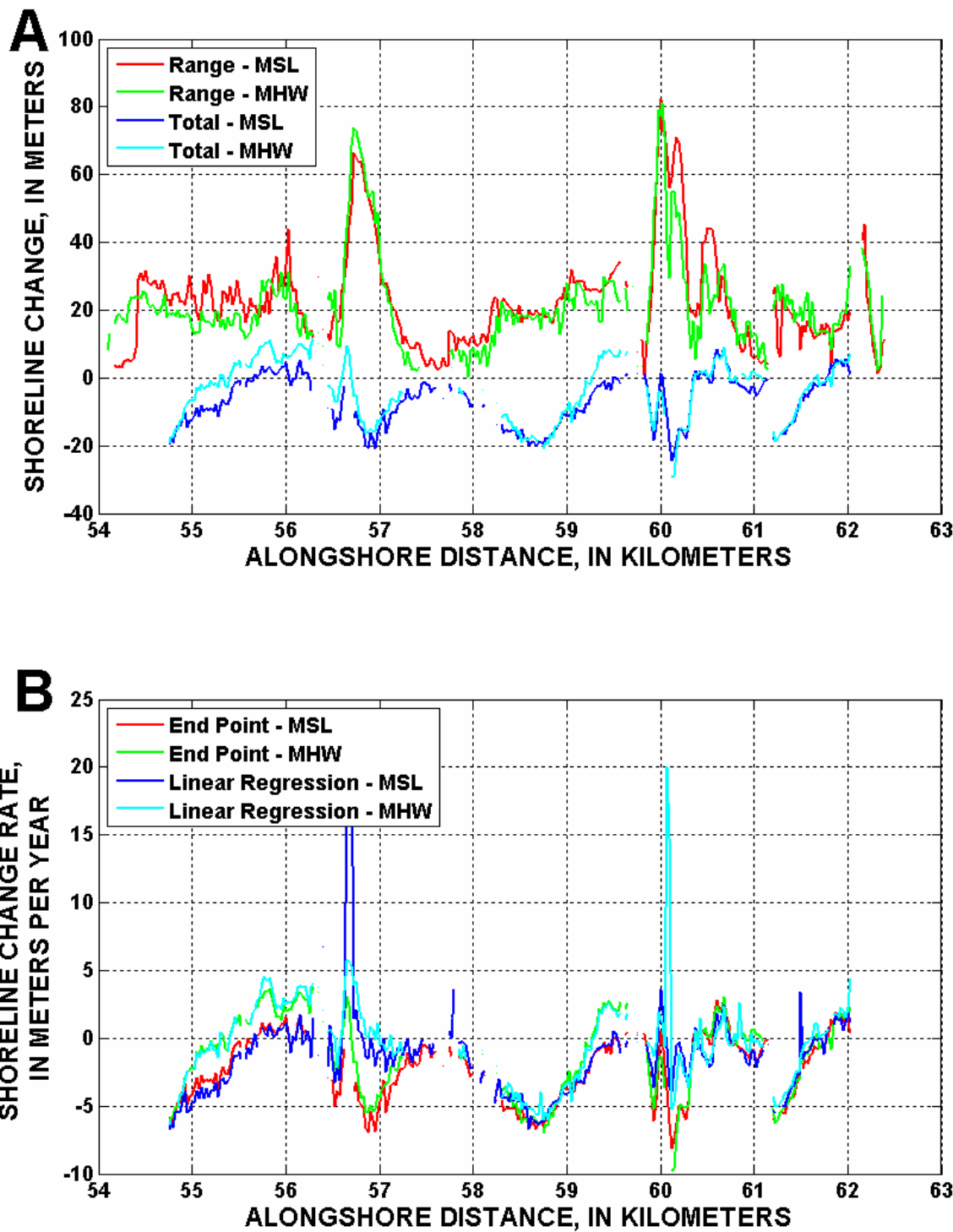


Figure 4.3. Shoreline change for the Ellwood/Isla Vista/Goleta study area from ATV topographic surveys conducted from 2005 to 2008. *A*, maximum range (all surveys) and total change (October 2005 to October 2008) for the mean sea level (MSL) and mean high water (MHW) shoreline proxies. *B*, end point and linear regression shoreline-change rates. Alongshore distance is kilometers from Point Conception. The October 2005 Lidar data was substituted for the October 2005 ATV data due to its greater accuracy and more extensive coverage area. See table 4.3 for the shoreline-analysis summary.

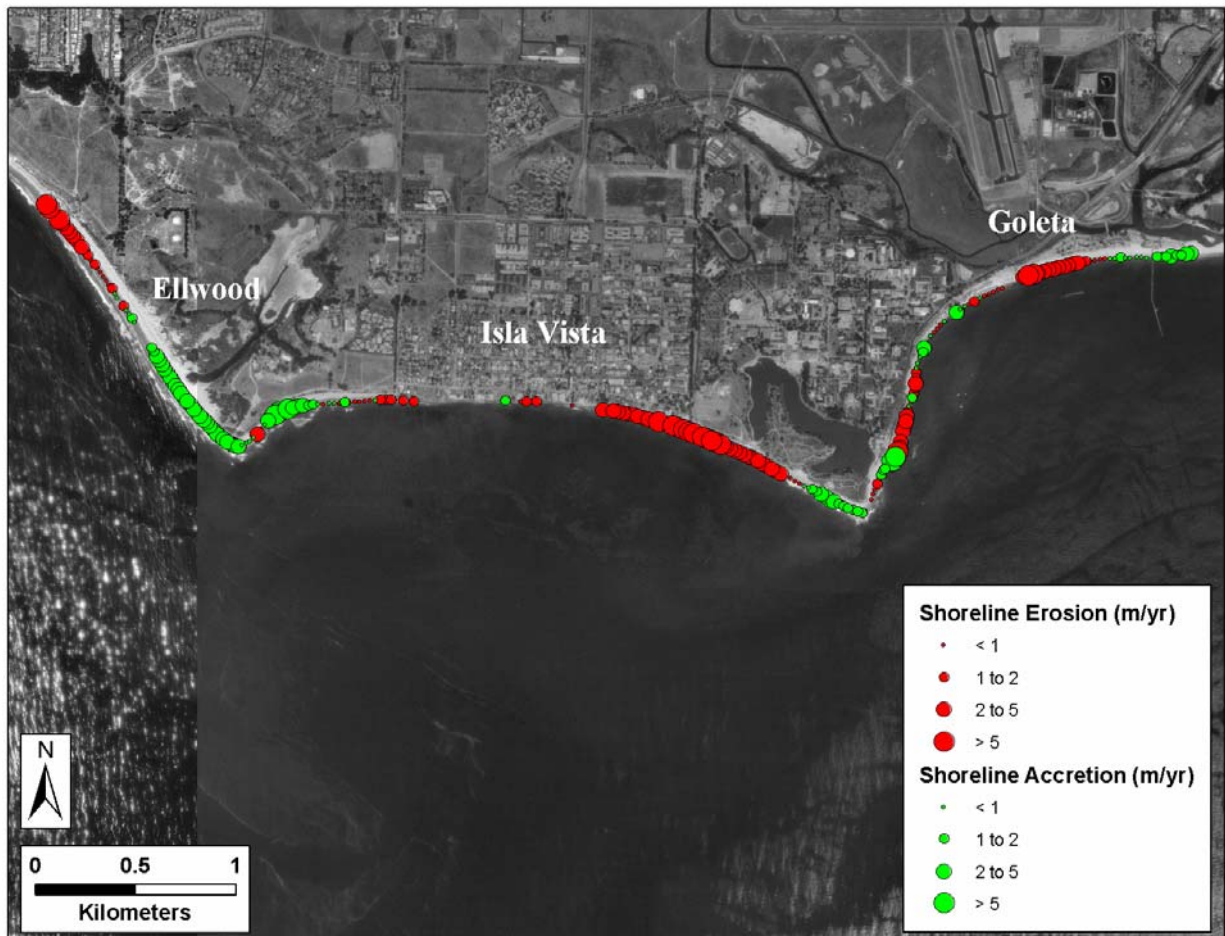


Figure 4.4. Map view of the linear regression shoreline-change rates calculated using October mean high water shorelines from 2005 to 2008 in the Ellwood/Isla Vista/Goleta study area.

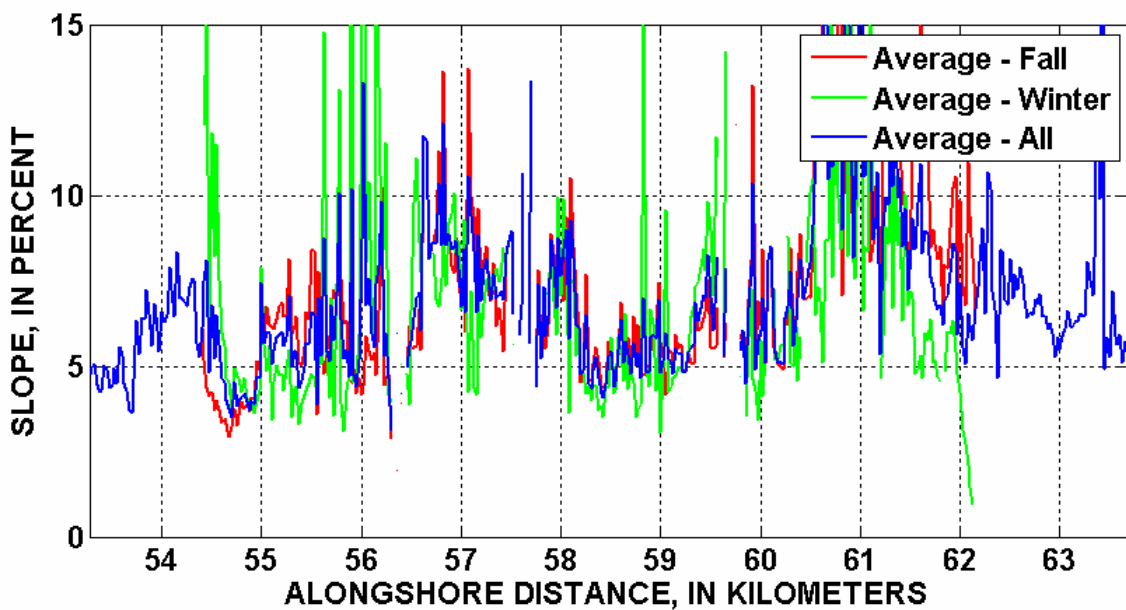


Figure 4.5. Beach slope (mean sea level to mean high water) in the Ellwood/Isla Vista/Goleta study area from ATV topographic surveys conducted from 2005 to 2008. Alongshore distance is kilometers from Point Conception. The October 2005 Lidar data was substituted for the October 2005 ATV data due to its greater accuracy and more extensive coverage area. See table 4.5 for the slope-analysis summary.

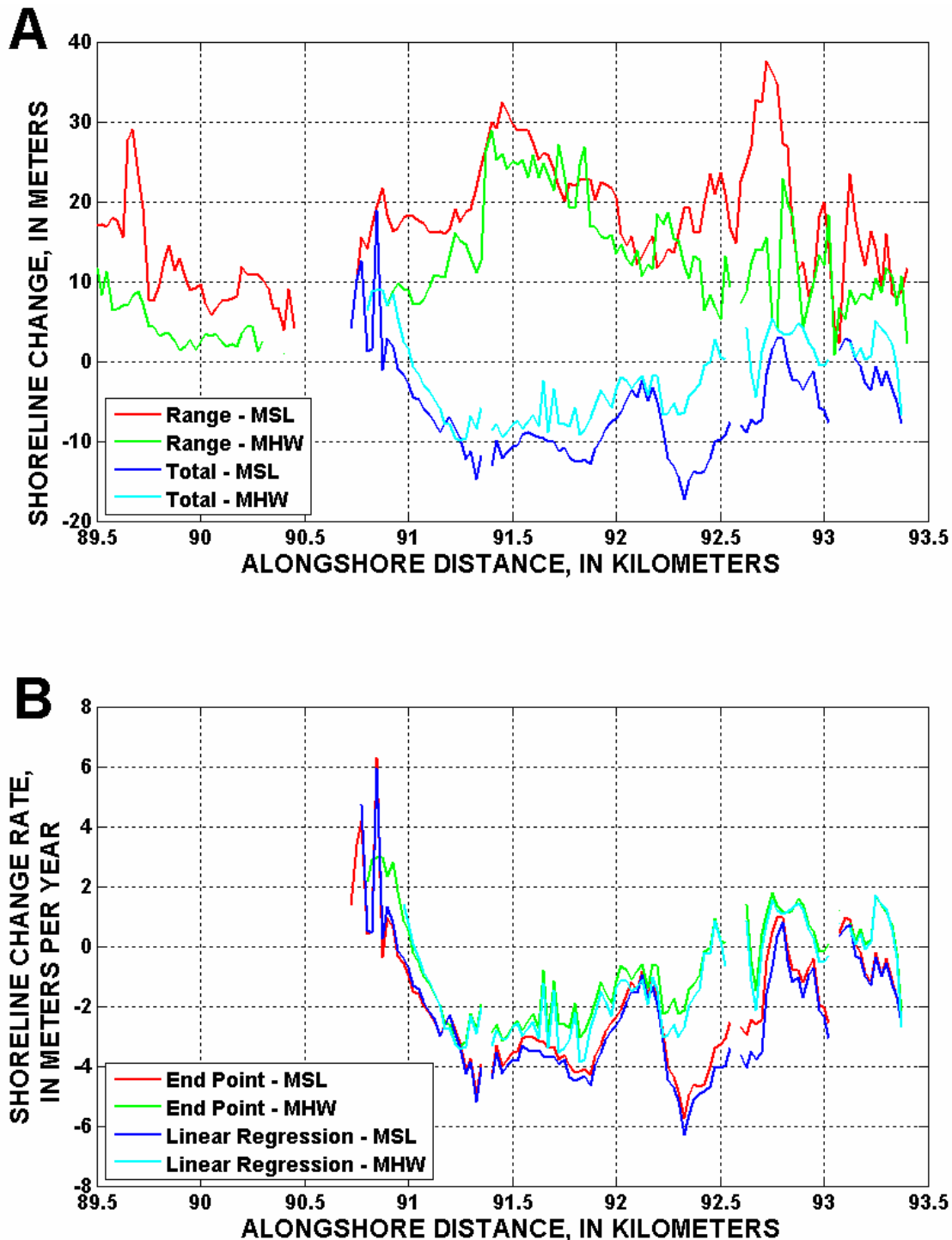


Figure 4.6. Shoreline change for the Carpinteria study area from ATV topographic surveys conducted from 2005 to 2008. *A*, maximum range (all surveys) and total change (October 2005 to October 2008) for the MSL and MHW shoreline proxies. *B*, end point and linear regression shoreline-change rates. Alongshore distance is kilometers from Point Conception. The October 2005 Lidar data was substituted for the October 2005 ATV data due to its greater accuracy and more extensive coverage area. See Table 4.6 for the shoreline-analysis summary.



Figure 4.7. Map view of the linear regression shoreline-change rates calculated using October mean high water shorelines from 2005 to 2008 in the Carpinteria study area.

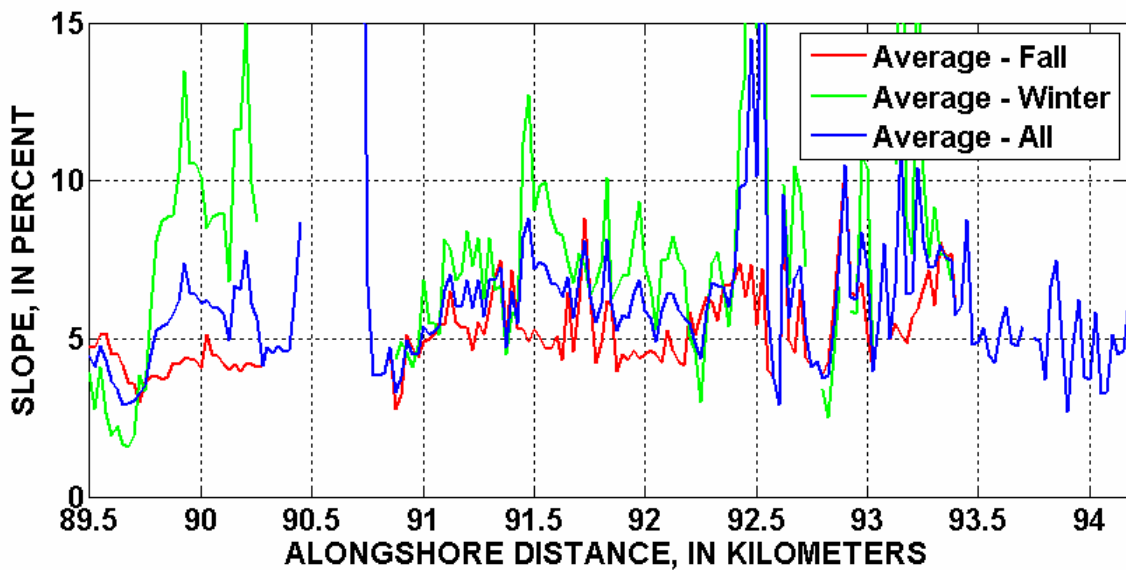


Figure 4.8. Beach slope (mean sea level to mean high water) in the Carpinteria study area from ATV topographic surveys conducted from 2005 to 2008. Alongshore distance is kilometers from Point Conception. The October 2005 Lidar data was substituted for the October 2005 ATV data due to its greater accuracy and more extensive coverage area. See table 4.8 for the slope-analysis summary.

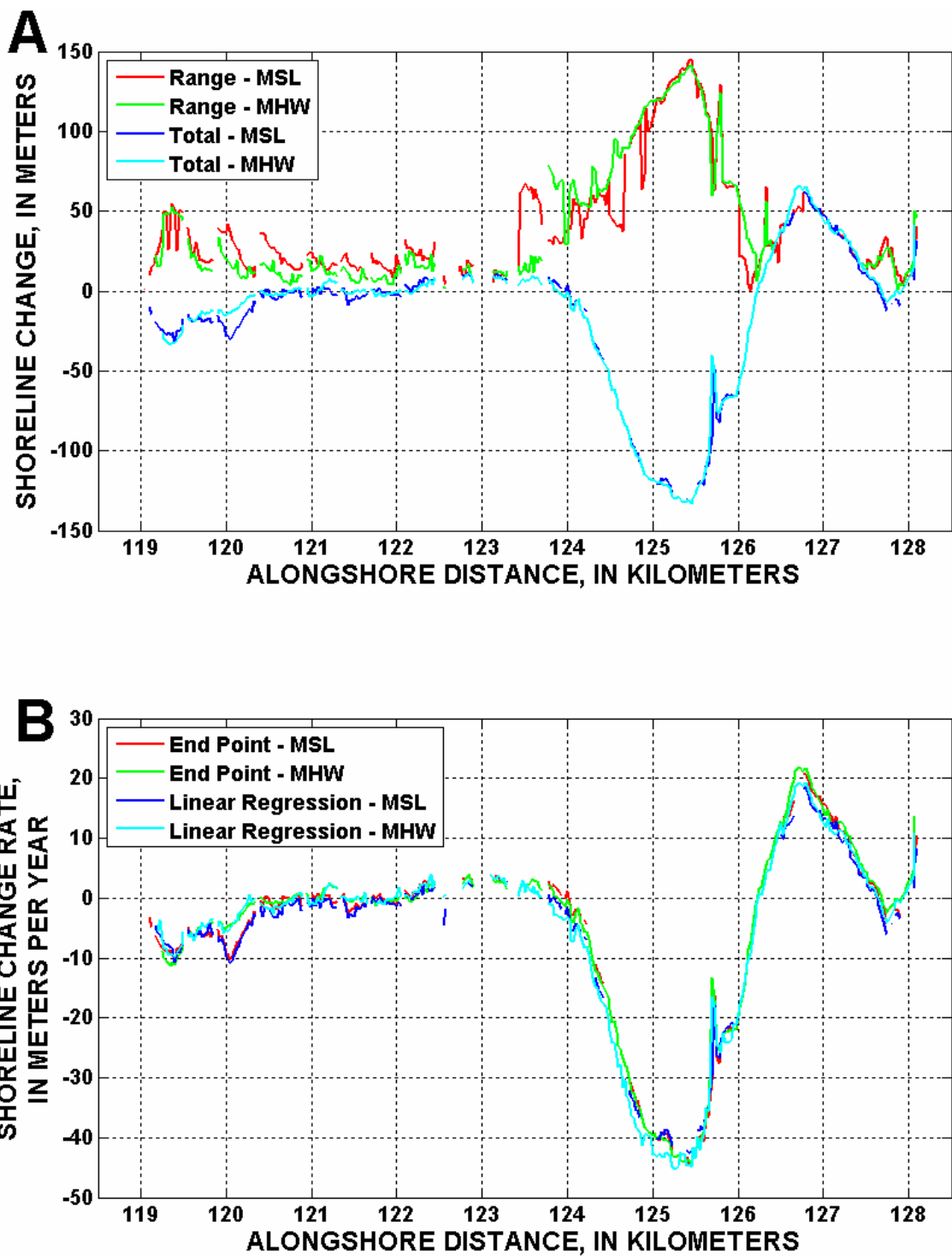


Figure 4.9. Shoreline change for the Ventura study area from ATV topographic surveys conducted from 2005 to 2008. *A*, maximum range (all surveys) and total change (October 2005 to October 2008) for the mean sea level (MSL) and mean high water (MHW) shoreline proxies. *B*, end point and linear regression shoreline-change rates. Alongshore distance is kilometers from Point Conception. The October 2005 Lidar data was substituted for the October 2005 ATV data due to its greater accuracy and more extensive coverage area. See table 4.9 for the shoreline-analysis summary.

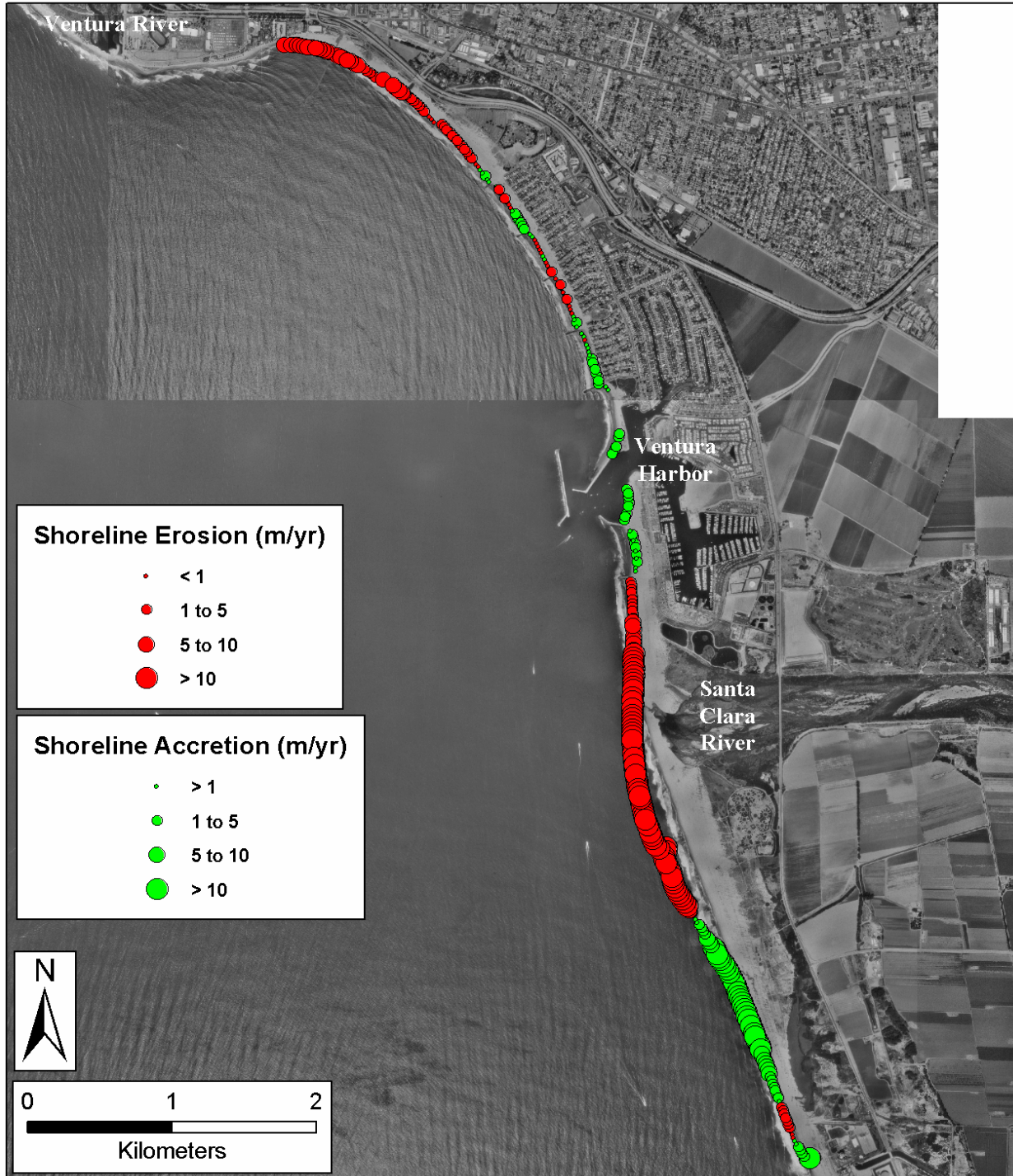


Figure 4.10. Map view of the linear regression shoreline-change rates calculated using October mean high water shorelines from 2005 to 2008 in the Ventura study area.

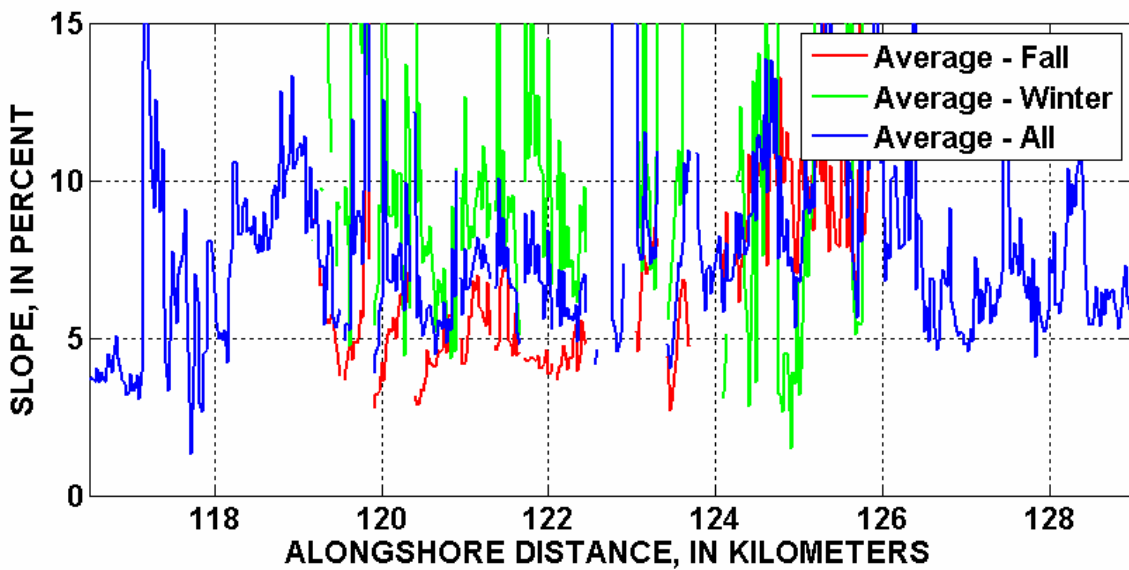


Figure 4.11. Beach slope (mean sea level to mean high water) in the Ventura study area from ATV topographic surveys conducted from 2005 to 2008. Alongshore distance is kilometers from Point Conception. The October 2005 Lidar data was substituted for the October 2005 ATV data due to its greater accuracy and more extensive coverage area. See table 4.11 for the slope-analysis summary.

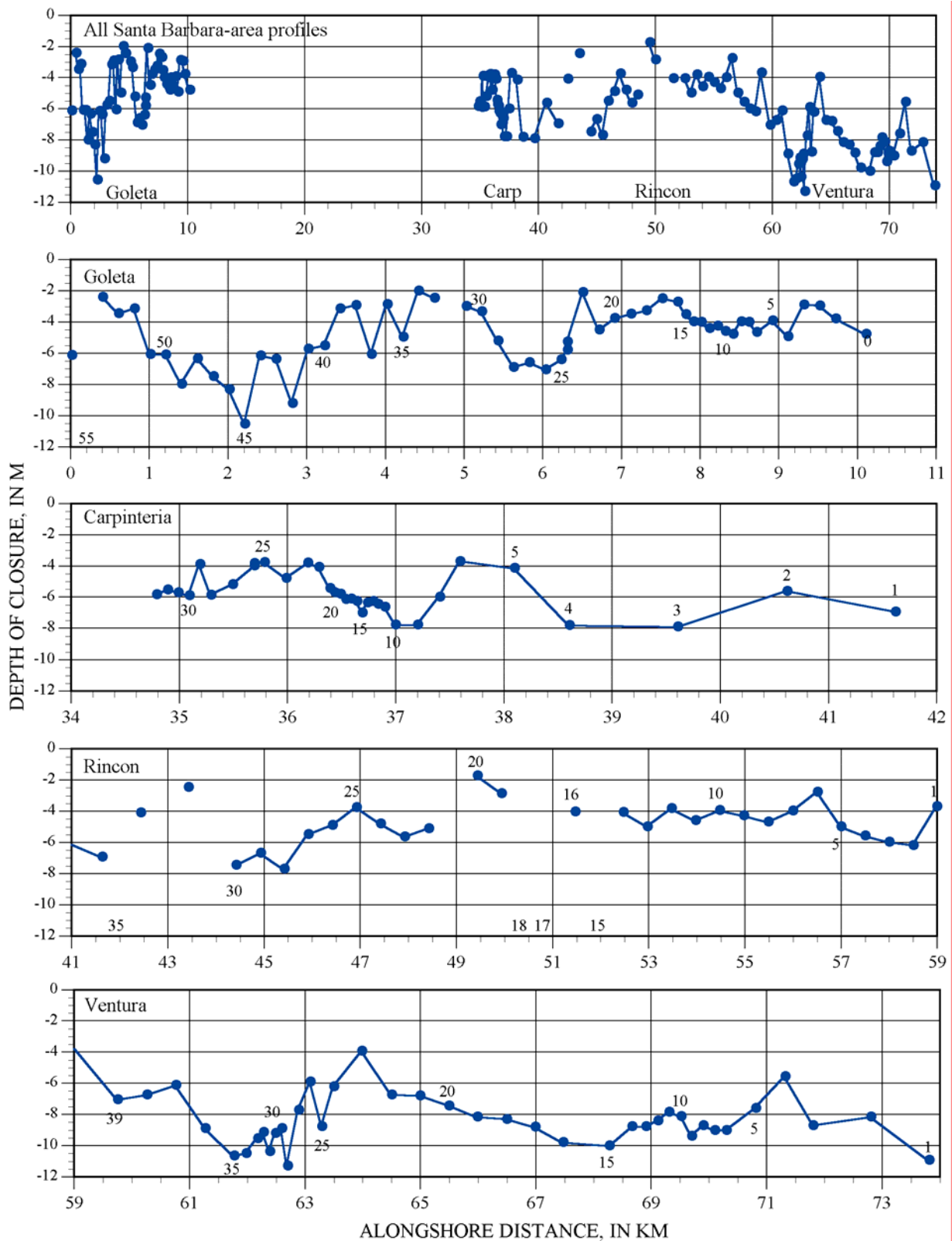


Figure 4.12. Depth of closure in the Santa Barbara littoral cell focus areas from Coastal Profiling System bathymetry data. Selected line numbers are shown for reference.

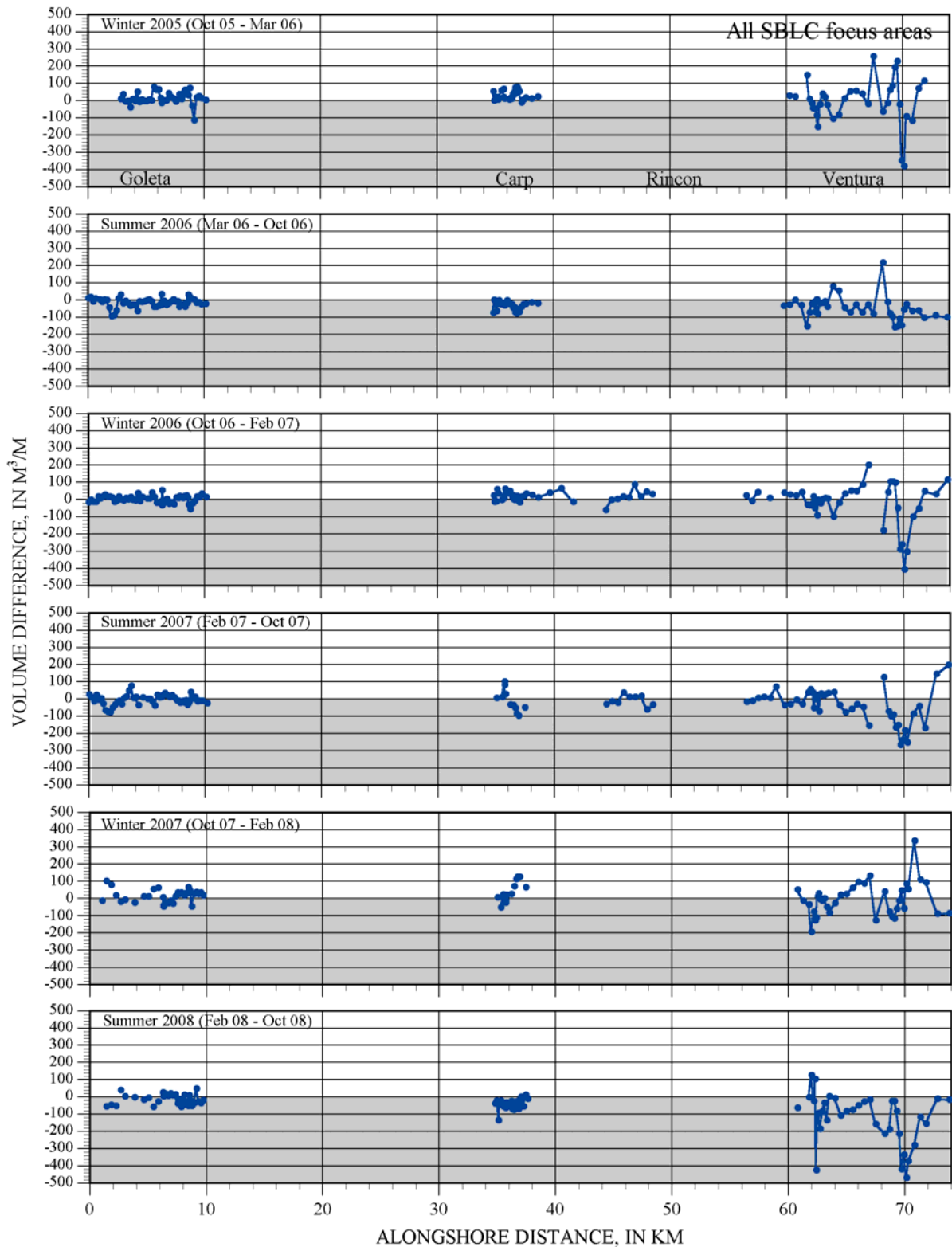


Figure 4.13. Seasonal volume changes in cross-shore bathymetry profiles in the Santa Barbara littoral cell focus areas.

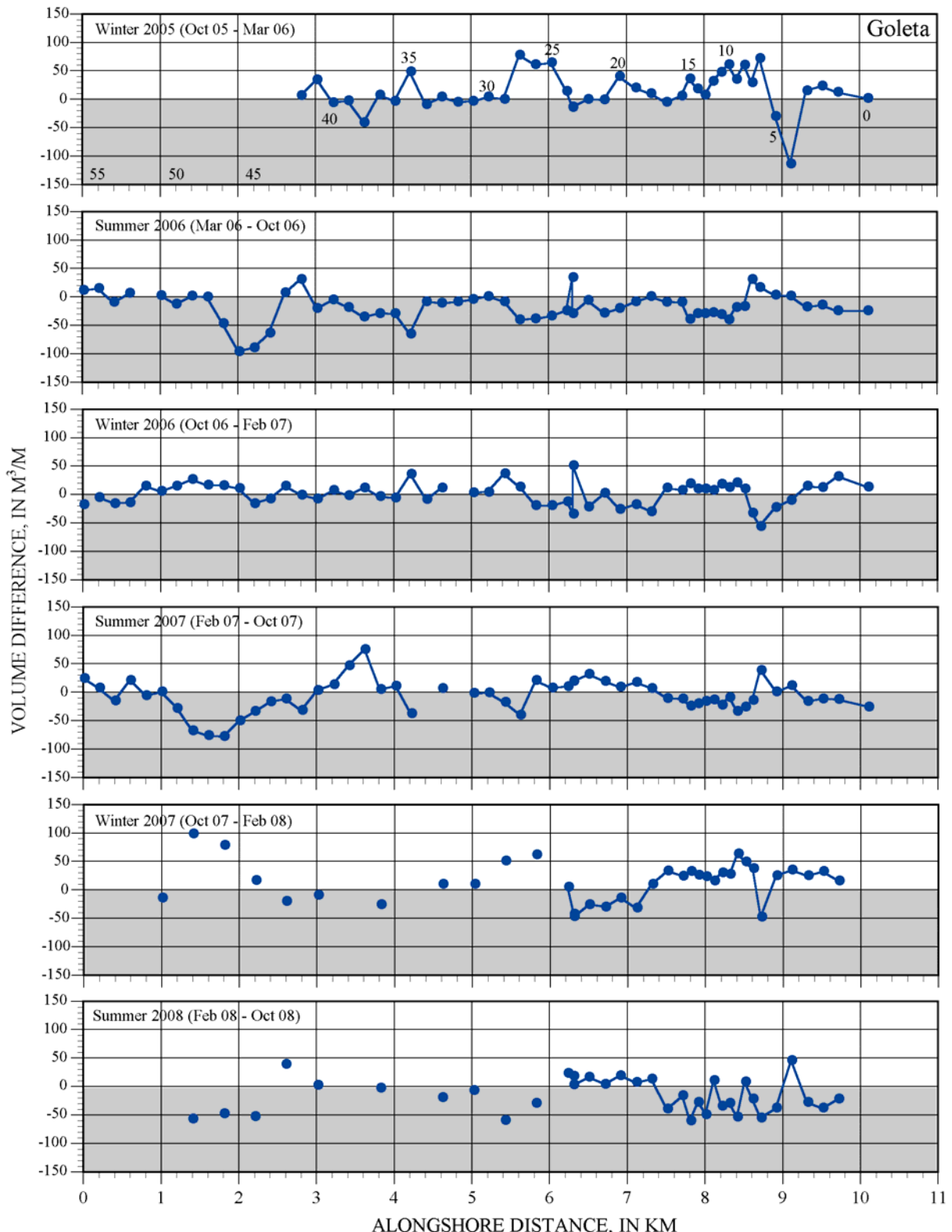


Figure 4.14. Seasonal volume changes in cross-shore bathymetry profiles for the Goleta focus area. Selected line numbers are shown for reference.

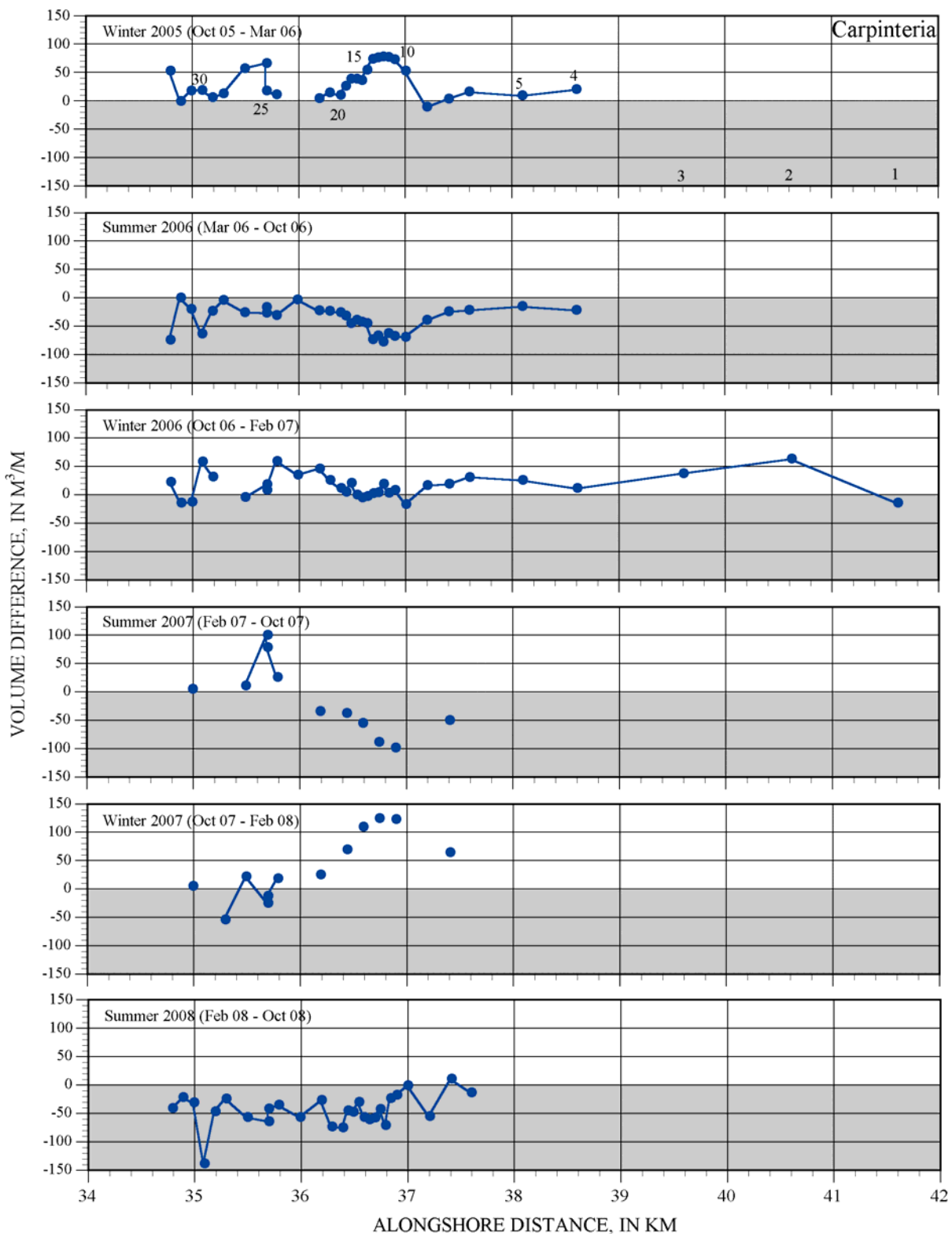


Figure 4.15. Seasonal volume changes in cross-shore bathymetry profiles for the Carpinteria focus area. Selected line numbers are shown for reference.

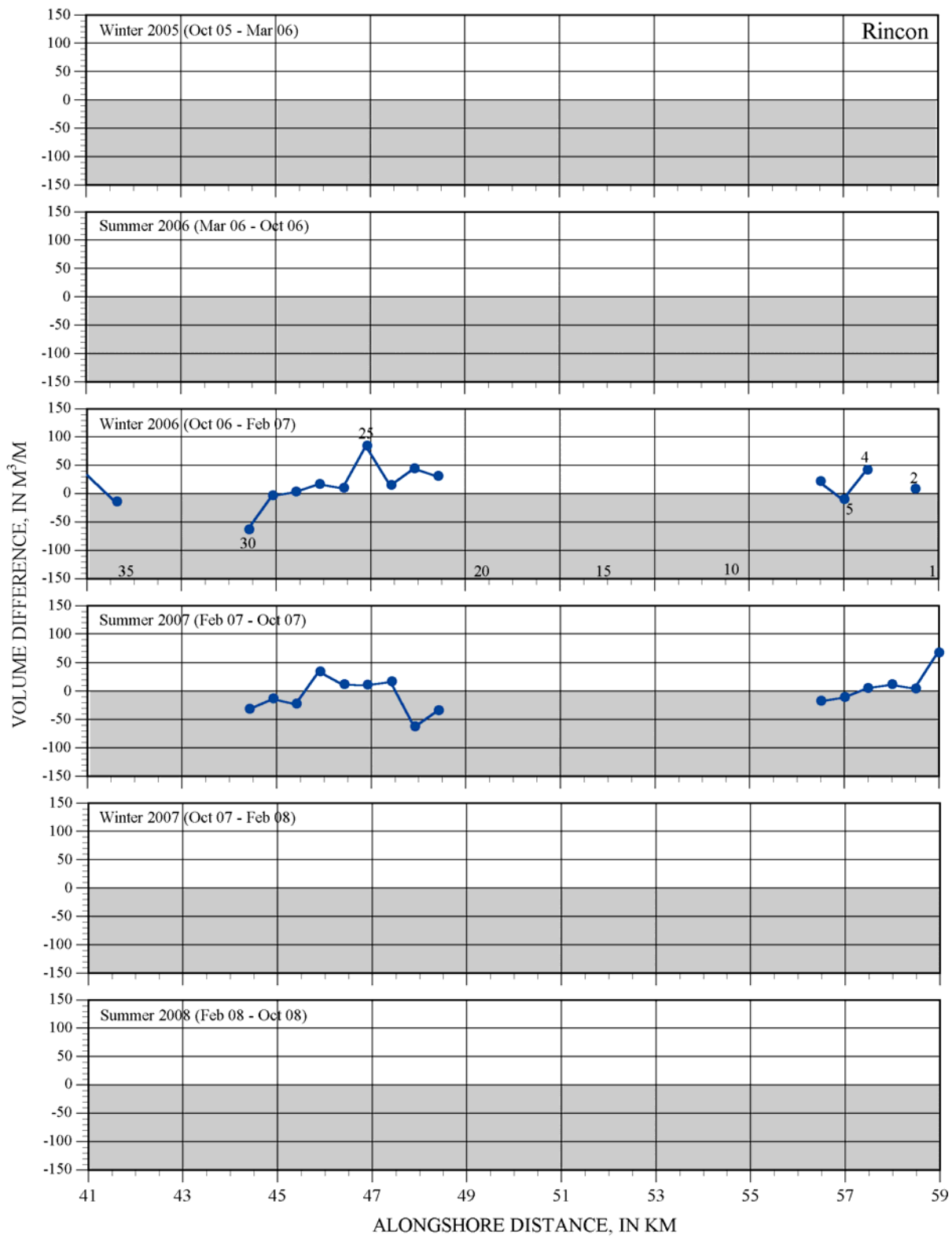


Figure 4.16. Seasonal volume changes in cross-shore bathymetry profiles for the Rincon focus area. Selected line numbers are shown for reference.

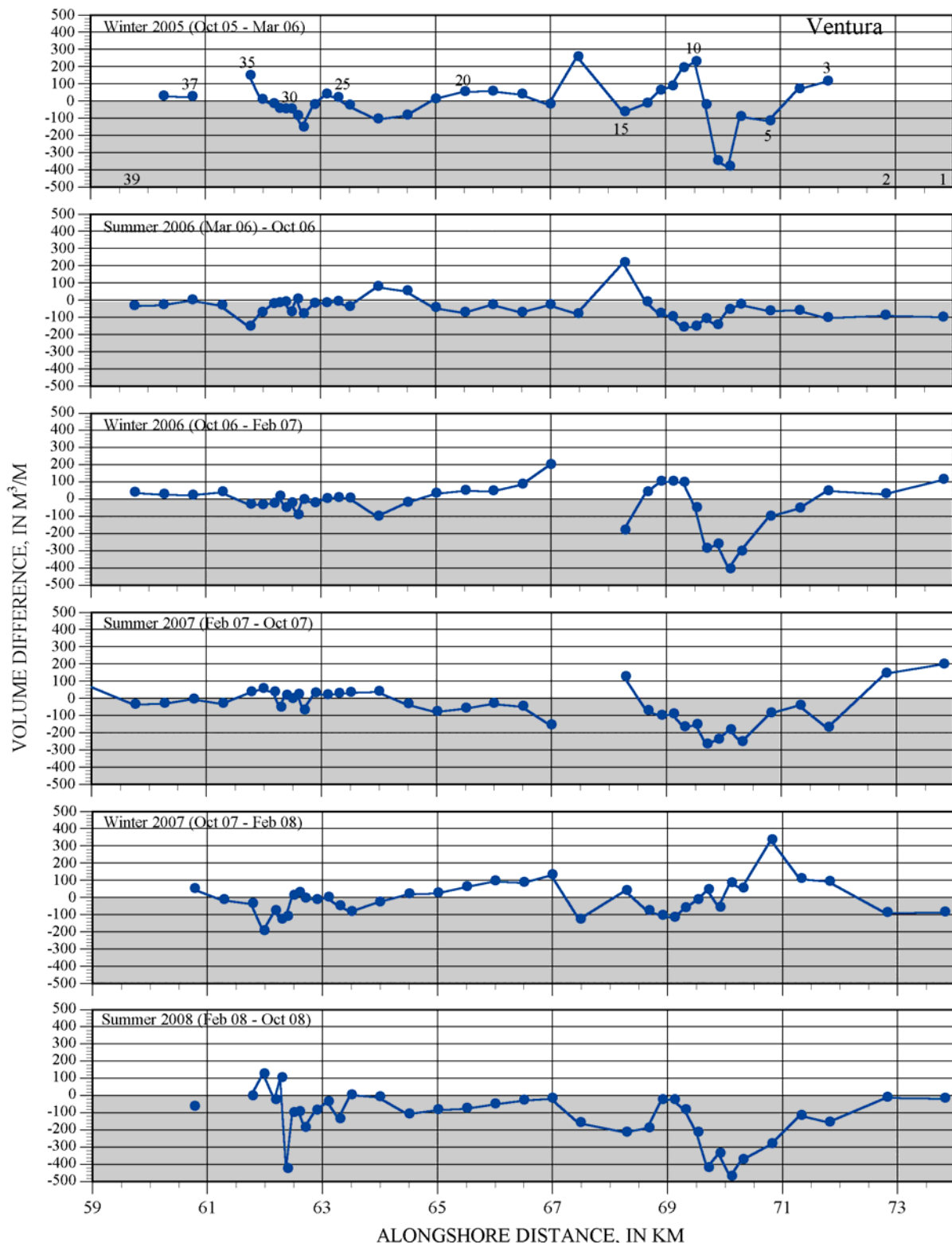


Figure 4.17. Seasonal volume changes in cross-shore bathymetry profiles for the Ventura/Santa Clara river mouths focus area. Selected line numbers are shown for reference.

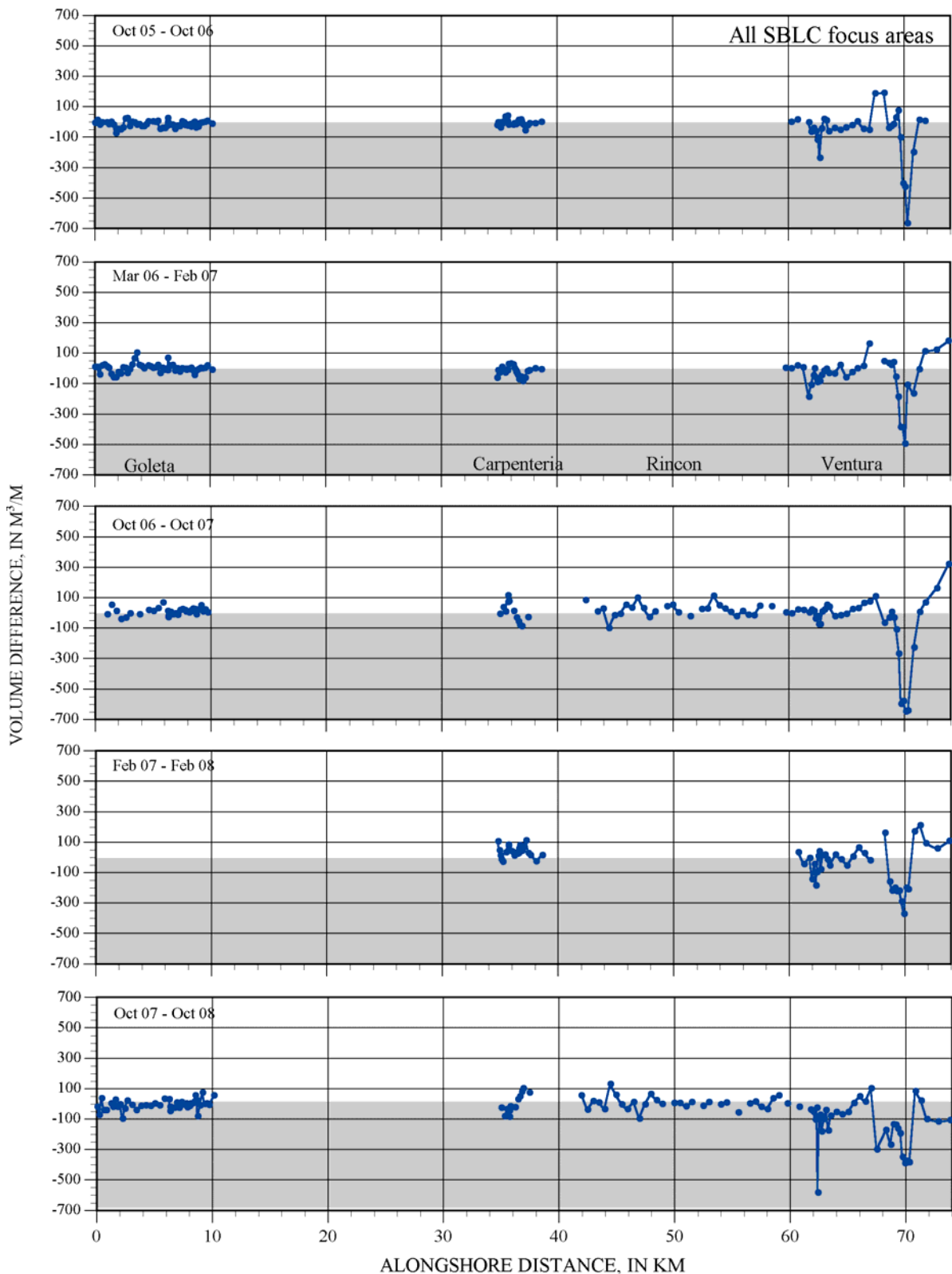


Figure 4.18. Annual volume changes in cross-shore bathymetry profiles in the Santa Barbara littoral cell (SBLC) focus areas.

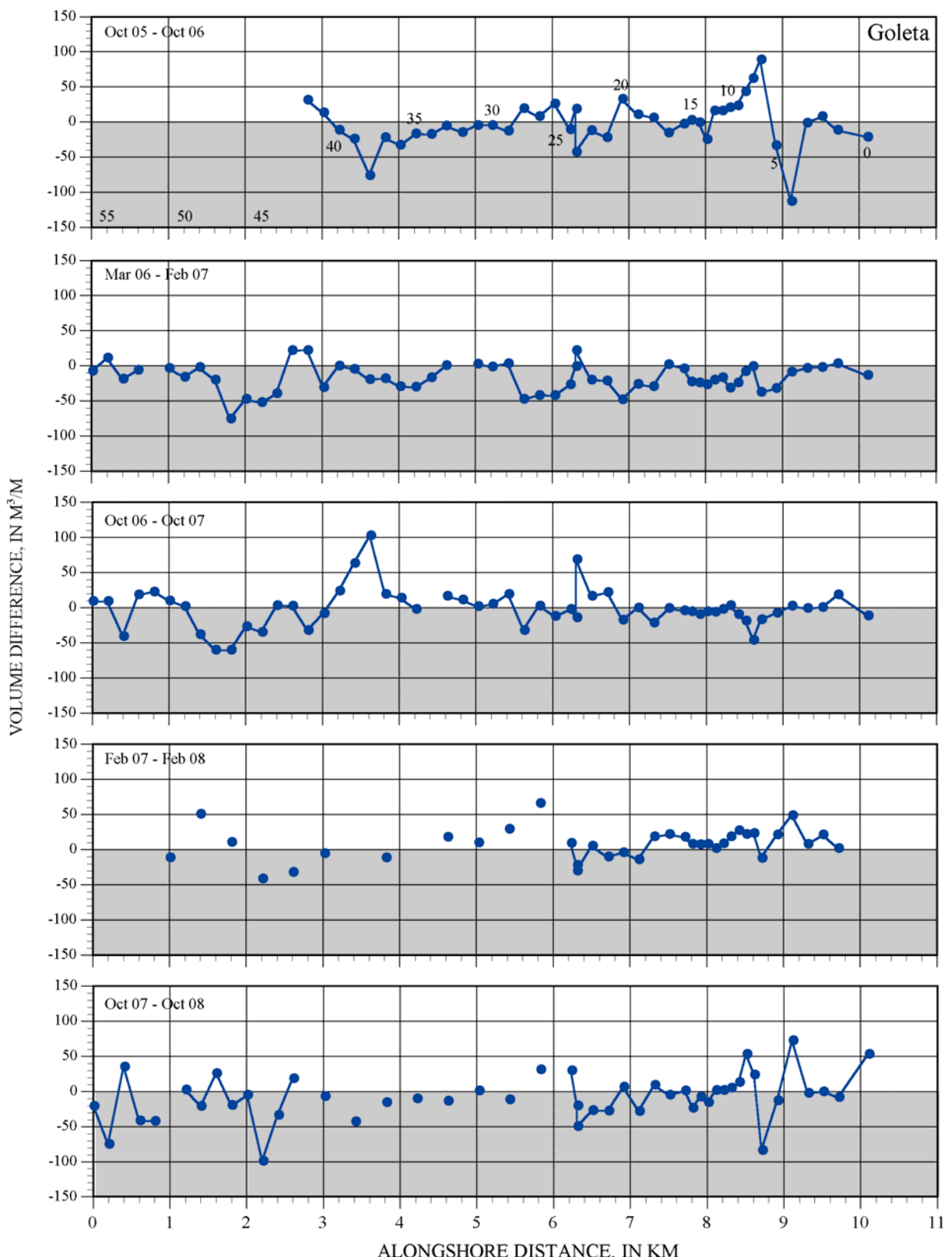


Figure 4.19. Annual volume changes in cross-shore bathymetry profiles for the Goleta focus area. Selected line numbers are shown for reference.

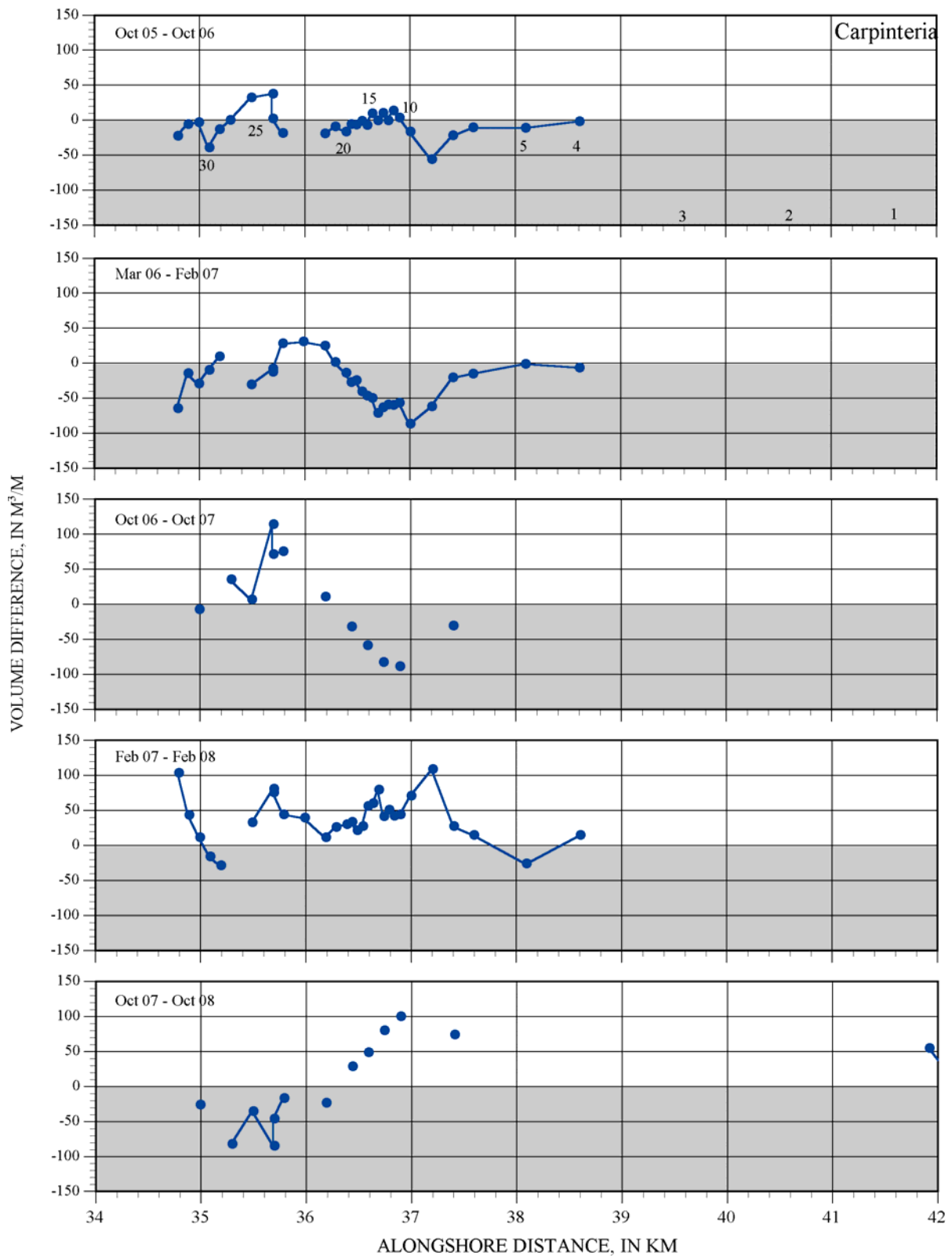


Figure 4.20. Annual volume changes in cross-shore bathymetry profiles for the Carpinteria focus area. Selected line numbers are shown for reference.

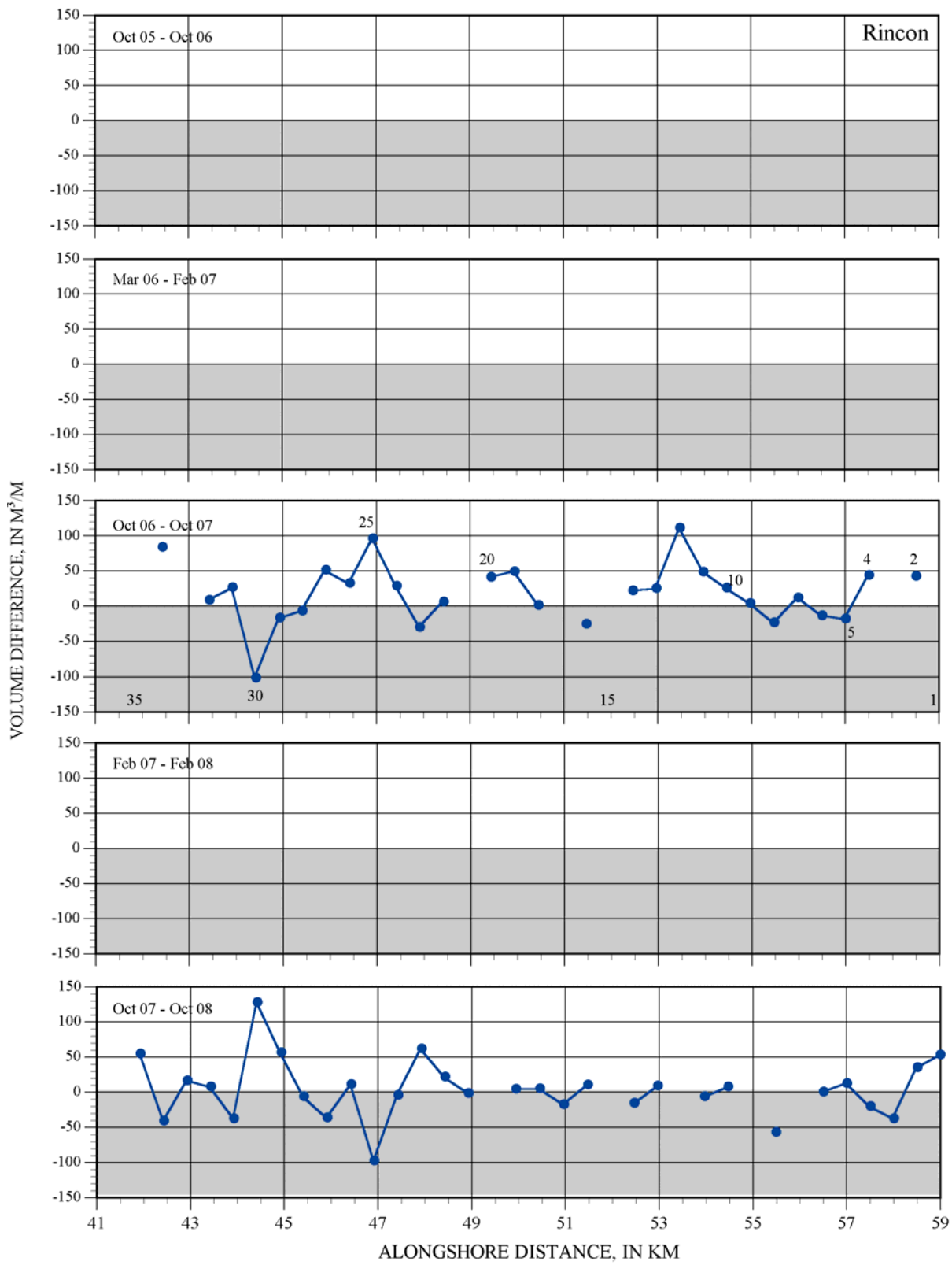


Figure 4.21. Annual volume changes in cross-shore bathymetry profiles for the Rincon focus area. Selected line numbers are shown for reference.

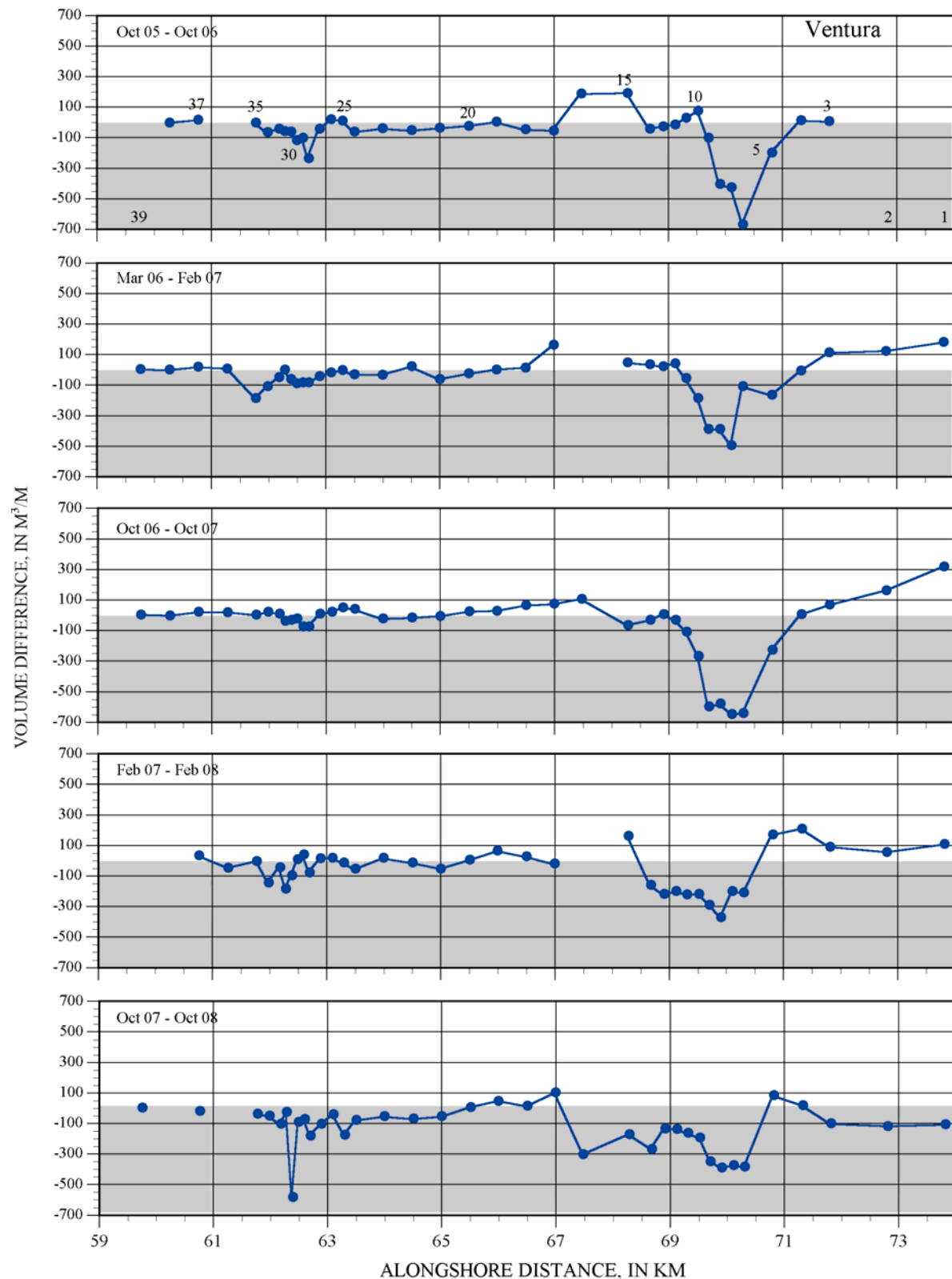


Figure 4.22. Annual volume changes in cross-shore bathymetry profiles for the Ventura/ Santa Clara river mouths focus area. Selected line numbers are shown for reference.

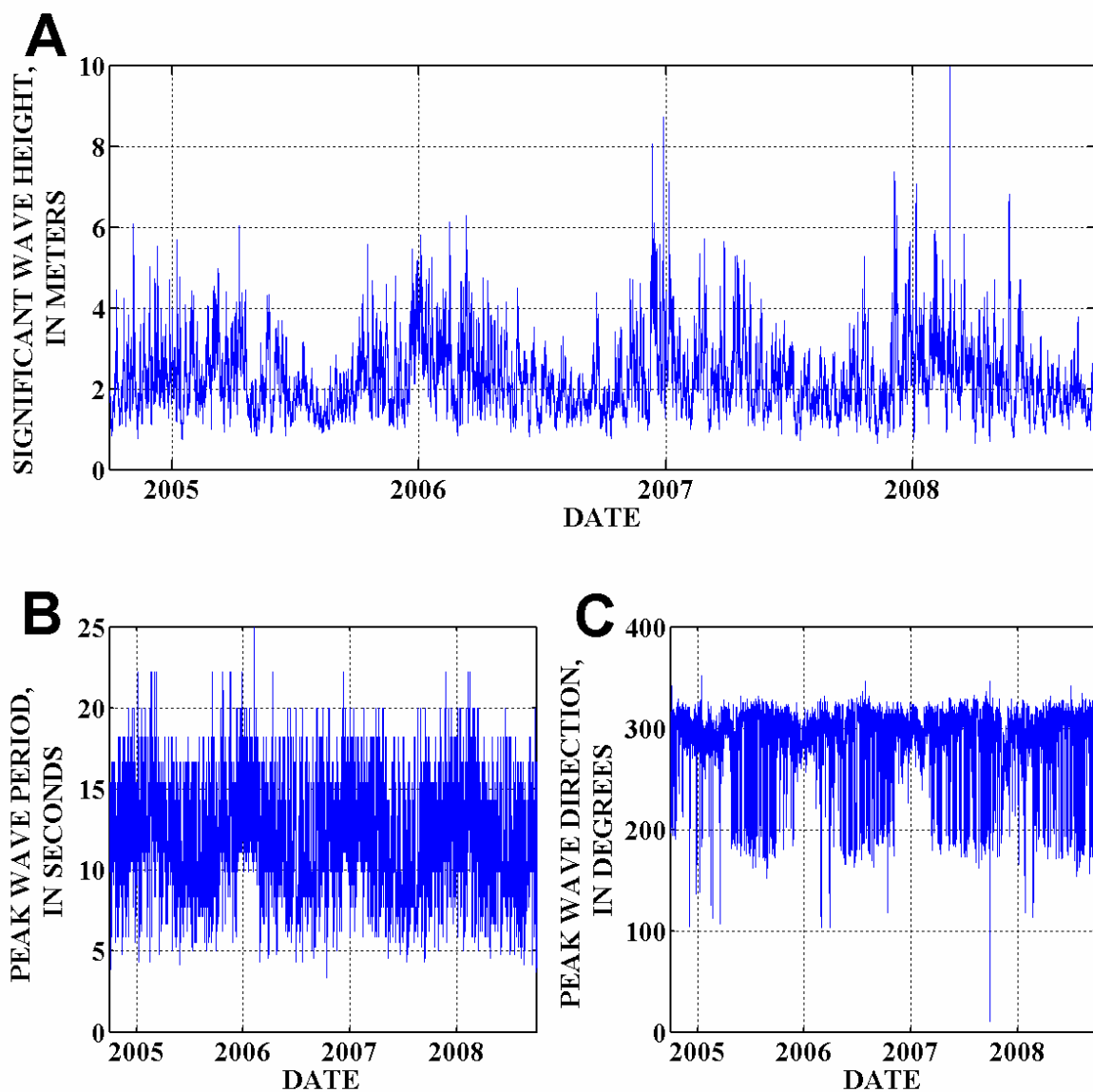


Figure 4.23. Offshore wave parameters during the study period (2005-2008) from the Coastal Data Information Program Harvest Buoy (Scripps, 2008). A, Significant wave height (Hs); B, Peak period (Tp), C, Peak direction (Dp).

Chapter 5—Grain-Size Analysis

By Neomi Mustain and Patrick L. Barnard

Introduction

An extensive surficial and shallow-subsurface sampling program was conducted on the beaches and nearshore in the SBLC to identify potential grain-size compatibility between nearshore and onshore sites for potential beach-nourishment investigations. Sediment grain size was established using both grab samples and USGS-developed bed-sediment cameras. Box coring that penetrated up to 20 cm was done following surface sampling in the nearshore to ground truth camera-derived grain-size data, as well as to determine if there is consistency between surface and shallow-subsurface grain size.

The surficial grain-size work presented here is from Mustain (2007), Mustain and others (2007), Barnard, Revell, and others (2007), and Barnard, Rubin, and others (2007). The work in all of these publications was at least partially supported by BEACON. These reports can be downloaded at:

http://walrus.wr.usgs.gov/coastal_processes/sbventura/links.html

This chapter provides a summary of the surficial grain-size work described in the above publications.

Methods

Bed-Sediment Cameras

The field survey was designed to collect samples along a cross-shore profile from the beach face and the nearshore at 5, 10, and 20 m water depth (that is, within the economic dredging limit), with transects spaced at least every kilometer alongshore throughout the entire SBLC (fig. 5.1). To compare seasonal grain-size variations, winter (March 2006 and February 2007) and fall (October 2006) beach samples were collected at a higher spatial resolution along the Ellwood/Isla Vista/Goleta, Carpinteria,

and Ventura shorelines (fig. 5.2). The Carpinteria results are described in detail in Barnard, Revell, and others (2007) at <http://pubs.usgs.gov/of/2007/1412/>.

Two different Eyeball camera systems were used to collect digital-image samples. Beach-face samples were collected with the Beachball camera, a 5-megapixel digital camera encased in a waterproof housing (fig. 5.3; Rubin and others, 2006). To sample the beach, the camera is placed flush against the sediment, which is illuminated by a ring of LED lights. Camera settings, such as aperture, shutter speed, zoom, focus, and pixel resolution of the image, are held constant. Nearshore samples were collected with the underwater Eyeball version, the Flying Eyeball, which is a video camera illuminated by LED lights encased in a wrecking ball (fig. 5.3; Rubin and others, 2006). Live video is reviewed on deck while the instrument is repeatedly raised and lowered to the seafloor to collect digital video samples. The clearest frames of video are then captured as still images and processed for grain size (fig. 5.4). For both systems, multiple images are taken at each location and later averaged to produce a grain-size result. Images that do not pass quality-control checks (for example, those that are overexposed, out of focus, or contain a coarse lag deposit, uneven sediment surface or air bubbles) are not included.

Images are processed by running a Matlab script that uses a spatial autocorrelation algorithm developed by Rubin (2004) that was extensively tested in the SBLC in Barnard, Rubin, and others (2007). This algorithm determines the correlation (as measured by pixel intensities) between a pixel and subsequent pixels at increasing distances. Grain size of an image is then interpolated by comparing the spatial autocorrelation result to a calibration matrix (fig. 5.5). The calibration matrix contains spatial autocorrelation results of calibrated sample images and was produced by imaging $\frac{1}{4}$ phi-interval sieved sediment collected from throughout the study area with the same equipment and camera settings as used in the field. In addition, for Flying Eyeball samples, point-counted images were also used to produce the calibration matrix. Each calibration matrix created is valid only for sediment of similar size, shape, and

mineralogy as the sediment initially sieved and imaged. A full description of the procedures for extracting grain size in this manner can be found in Mustain (2007). Barnard, Rubin, and others (2007) showed a more than 90 percent correlation with mean grain size determined with the autocorrelation method compared to point counting. In the SBLC, 576 images were taken at 192 beach-sample locations, and 1,590 images were taken from 318 nearshore sites.

Box Coring

Samples were extracted using a Naval Electronics Laboratory-style spade box corer equipped with a removable box (fig 5.6). The corer weighs 1,500 lbs and measures 20 cm deep by 30 cm wide by 42.5 cm high. Total depth of penetration, however, due to the predominantly sandy substrate, rarely exceeded 20 cm. When the core is recovered to the ship's deck, the box is detached, the seawater is drained, and the box is opened. The sediment surface is photographed, and one wall of the box is peeled off and a picture of the sediment cross-section is taken (fig. 5.7). The quality of the water in the box and the sediment surface is recorded, along with other important characteristics (for example, bioturbation, storm layers, oxidation state). Subsamples for grain-size analysis were extracted approximately every 5 cm vertically. Grain size was determined using a laser Coulter Counter for laser-diffraction particle-size analysis. Forty-seven sites were visited, and 123 sediment samples were extracted. Water depths at sampling sites ranged from 5 to 21 m (fig. 5.8).

Results

The key grain-size parameters of every sample measured in this study can be found in Appendix D. The mean grain size of 93 summer beach-face samples taken from throughout the SBLC ranged from 0.15 to 0.42 mm (fine- to medium-grained sand; fig. 5.9). The mean of one sample, just north of the Port Hueneme Harbor, was 0.58 mm, or coarse sand. The average of all samples was 0.26 mm. In most

cases, grab samples were very well sorted. Samples were also normally distributed, so mean and median values were essentially the same. Thus, beach samples are well represented by the mean. The finest sediment on the beach (d_{10}) varied from location to location, but followed the mean well (that is, when the mean increased so did d_{10}). Very fine-grained sand was not found on the beach in any significant amount anywhere throughout the cell (fig. 5.9).

Seasonal beach-face samples were collected throughout the focus area beaches of Ellwood/Isla Vista/Goleta, Carpinteria, and Ventura. Mean grain sizes of summer beach samples were smaller than winter beach samples throughout the focus study areas and varied by as much as a factor of two or more (fig. 5.10). On average, in Goleta and Carpinteria, grain size fluctuated from medium sand to fine sand, while in Ventura grain size fluctuated from a coarser-grained medium sand to a finer-grained medium sand.

Throughout the SBLCS, 318 nearshore locations (water depths less than 20 m) were examined, although some areas were cobble or bedrock reefs, which did not allow for grain-size determination. Mean grain size was determined for about 100 samples at each water depth (5, 10, and 20 m). Grain size generally decreased moving from the beach offshore (fig. 5.11). Only 2 percent of all samples were medium sand, 28 percent were fine sand and 70 percent were very fine sand or smaller. The coarsest samples were found in shallow depths: 78 percent of all samples coarser than very fine sand were located in 5 m water depth. Only 10 percent of Flying Eyeball samples in 10 or 20 m water depth (20 samples) were coarser than very fine sand. Some of these coarser, deep samples were located near major headlands, such as Point Conception and Point Mugu, near exposed reefs, such as west of Coal Oil Point and off Sand Point in Carpinteria, or offshore of rivers and streams, such as Gaviota Creek and Rincon Creek. Samples coarser than very fine sand not located near headlands were likely to be fine

sand (92 percent) rather than medium or coarse sand (8 percent). Grab samples were mostly well sorted, but occasionally were very well sorted or moderately sorted.

Figure 5.12 shows a surficial-sediment grain-size map of the Santa Barbara Channel that was created with regional data from the usSEABED database (Reid and others, 2006), beach and nearshore data from this study, and various nearshore cores collected by Noble Consultants (1989). The majority of offshore sediments are very fine-grained or smaller; relatively coarser sediments are mostly found only in the very nearshore and on the beach. A few locations, for example, those along the western edge of the Santa Barbara Channel, indicate coarser sediment (fine and medium sands) further offshore; however, these areas are represented by very few sediment samples, so this depiction of coarser sediment could be an artifact of the interpolation method.

The median grain size (d_{50}) of all the box-core subsamples averaged 0.095 mm (very fine sand), with a maximum of 0.72 mm and a minimum of 0.015mm (fig. 5.13). Of the 123 subsamples from the box cores, only 4 (~3 percent) contained median grain size that was comparable to the average of the beach samples (that is, 0.26 mm or greater), and only 10 samples (~ 8 percent) exceeded the finest mean grain size found on the adjacent beaches (0.15 mm or greater). Three of the four coarsest samples, with median grain sizes of 0.72, 0.32, and 0.29 mm, are offshore of the Santa Barbara Harbor (samples SB117, SB-A2, and SB-A1, respectively); the fourth, with a median grain size of 0.32 mm, is just south of Oil Piers (sample SB196B). Of the remaining samples with a median grain size greater than 0.15 mm, only two are found outside of the Santa Barbara Harbor or Oil Piers areas: one offshore of Goleta Beach (sample SB84, $d_{50}=0.20$ mm) and one offshore of Hueneme Beach (sample SB295, $d_{50}=0.15$ mm). Further, most samples decrease sharply with depth, such as at Oil Piers where surface samples from SB196B and SB198 decrease from 0.32 and 0.18 mm at the surface to 0.17 and 0.15 mm just 5 cm below the surface, respectively. It should also be noted that the coarse samples off the Santa Barbara

Harbor contain large volumes of shell debris, as a result the larger grain sizes may not be reflective of larger mineral grains.

Discussion

Overall, nearshore surface sediments in the SBLC are generally fine-grained and thus are not suitable for beach-nourishment projects. Although it is possible that coarser sediments may exist in the subsurface, the mean grain sizes of samples from sediment cores and box cores were almost always equivalent to, or finer than, surficial samples and surficial Eyeball analysis, indicating that surface samples are commonly consistent with shallow subsurface sediments.

The coarsest offshore sediments are found in 5 m water depth, within the depth of closure or area of active seasonal offshore/onshore transport (see Chapter 4). Deeper offshore sediments are mostly very fine-grained sands, or even finer. Some coarser deposits exist in deeper water, for example, offshore Naples, Coal Oil Point, the Santa Barbara Mesa, and Carpinteria, but it is unclear whether they are part of a thick deposit of suitable nourishment material, or simply a thin, coarser deposit within bedrock/reef pockets. Offshore Rincon Point-Mussel Shoals and Gaviota, relatively coarser sediments were found; these sites require further investigation.

Of the potential borrow sites identified prior to this study, the deposits off Santa Barbara Harbor seem most likely to contain potential beach-compatible sand. Together with previously collected cores, this current analysis confirms that coarser sediments suitable for beach nourishment probably do not exist in large quantities along the previously identified potential borrow areas offshore Goleta and Carpinteria, or the large deposit offshore Ventura and Oxnard. Surface sampling and box coring do suggest that the Oil Piers region might be another site for further investigation. The Santa Clara River delta was poorly sampled due to high swell conditions, but massive amounts of sediment were deposited in this region during the 2004-2005 winter flood (see chapters 3 and 4), so it is possible that coarser

sediment exists at depth in this region, and the sheer volume of sediment deposited warrants further investigation.

Conclusions

- The mean grain size of swash samples in the Santa Barbara littoral cell is 0.26 mm (range 0.15 to 0.58 mm), with a littoral cut-off diameter of 0.125 mm.
- Out of 318 nearshore sample locations, only 2 percent contained mean grain sizes that exceeded fine sand (≥ 0.25 mm).
- Only 3 percent of the nearshore box-core samples collected equaled or exceeded the mean grain size of the swash samples.
- Based on the sampling results of this project, the most promising sites for further investigation of potentially large volumes of beach-compatible sediment would be off Santa Barbara Harbor and Oil Piers.
- The volume of beach-sized sediment off the Santa Clara River mouth is potentially high, but poorly resolved.

References

Barnard, P.L., Revell, D.L., Eshleman, J.L., and Mustain, N., 2007, Carpinteria coastal processes study, 2005-2007—Final report: U.S. Geological Survey Open-File Report 2007-1217, 130 p., [<http://pubs.usgs.gov/of/2007/1412/> (last accessed March 13, 2009)].

Barnard, P.L., Rubin, D.M., Harney, J., and Mustain, N., 2007, Field test comparison of an autocorrelation technique for determining grain size using a digital ‘beachball’ camera versus traditional methods. *Sedimentary Geology*, v. 201, no.1-2, p. 180-195,

- [<http://dx.doi.org/10.1016/j.sedgeo.2007.05.016> (last accessed March 13, 2009)].
- Mustain, Neomi, 2007, Grain size distribution of beach and nearshore sediments of the Santa Barbara littoral cell: Implications for beach nourishment: Santa Cruz, University of California, master's thesis, 107 p.
- Mustain, N., Griggs, G., and Barnard, P.L., 2007, A rapid compatibility analysis of potential offshore sand sources for beaches of the Santa Barbara littoral cell *in* Kraus, N.C., Rosati, J.D., eds., Coastal sediments '07: Proceedings of the 6th International Symposium on Coastal Engineering and Science of Coastal Sediment Processes, American Society of Civil Engineers, New Orleans, Louisiana, v. 3, p. 2501-2514.
- Noble Consultants, 1989, Coastal sand management plan Santa Barbara / Ventura County coastline. Prepared for BEACON, Beach Erosion Authority for Control Operations and Nourishment, Santa Barbara, California.
- Reid, J.A., Reid, J.M., Jenkins, C.J., Zimmermann, M., Williams, S.J., and Field, M.E., 2006, usSEABED: Pacific Coast (California, Oregon, Washington) Offshore Surficial-sediment Data Release. U.S. Geological Survey Data Series, no.182, [<http://pubs.usgs.gov/ds/2006/182/> (last accessed March 13, 2009)].
- Rubin, D.M., 2004, A Simple Autocorrelation Algorithm for Determining Grain Size from Digital Images of Sediment. Journal of Sedimentary Research, v. 74, no.1, p. 160-165.
- Rubin, D.M., Chezar, H., Harney, J.N., Topping, D.J., Melis, T.S., and Sherwood, C.R., 2006, Underwater Microscope for Measuring Spatial and Temporal Changes in Bed-sediment Grain Size. U.S. Geological Survey Open-file Report, no.2006-1360, 15 p.

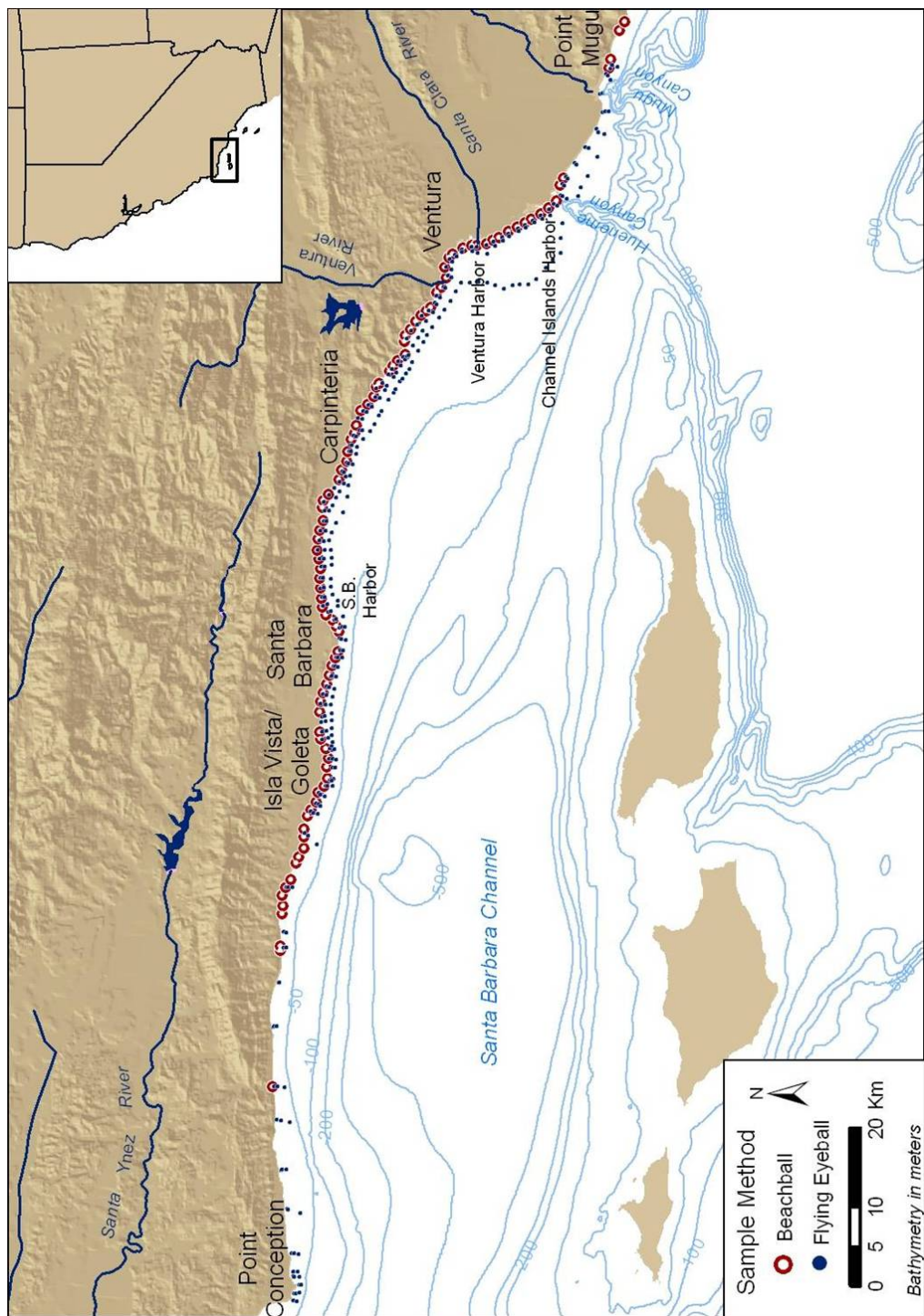


Figure 5.1. Locations of beach-face samples collected with the Beachball camera and nearshore samples in 5, 10, and 20 m water depth collected with the Flying Eyeball camera .

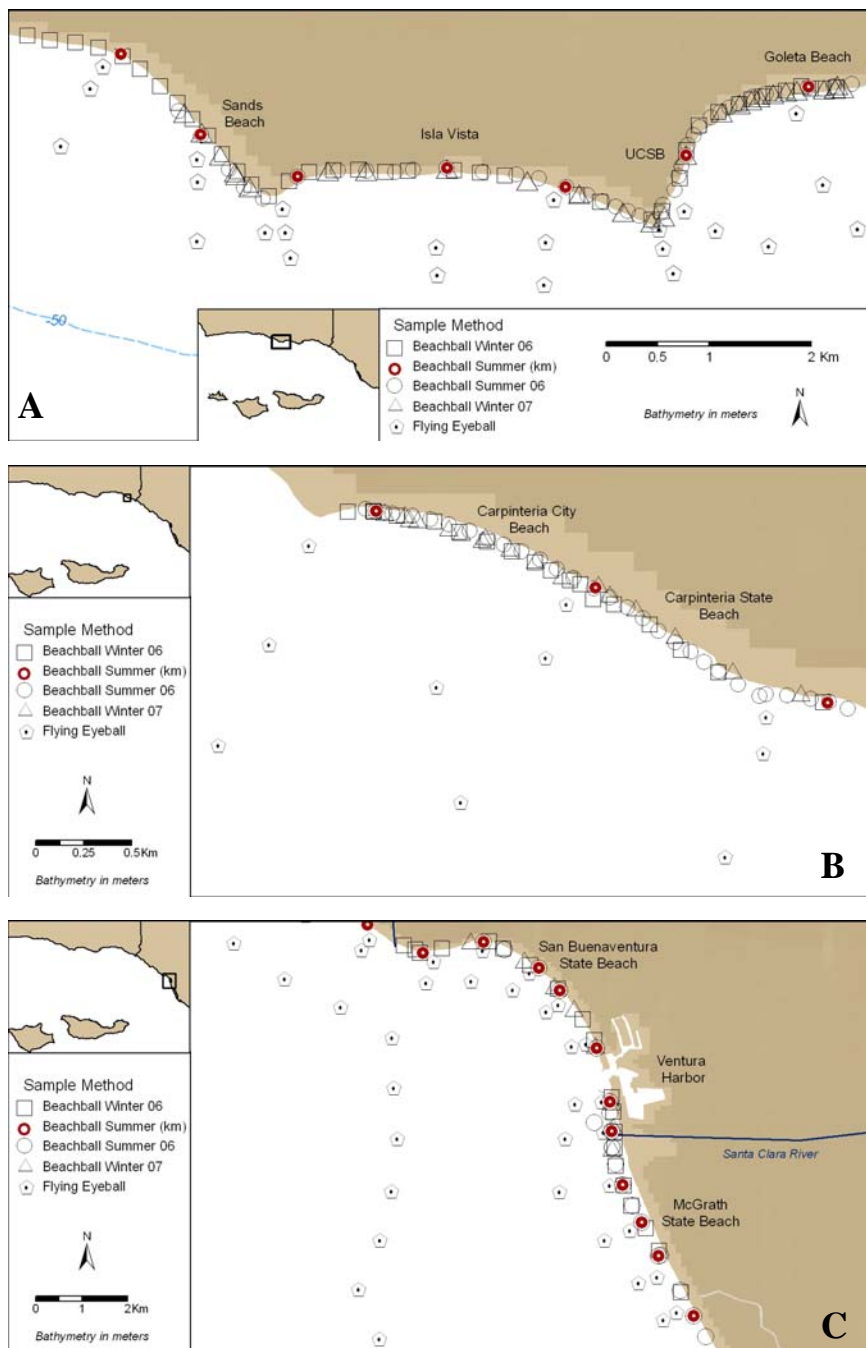


Figure 5.2. Locations of summer nearshore samples, summer kilometer-spaced samples, and seasonal beach-face samples collected at A, Goleta/Isla Vista; B, Carpinteria; and C, Ventura beaches.

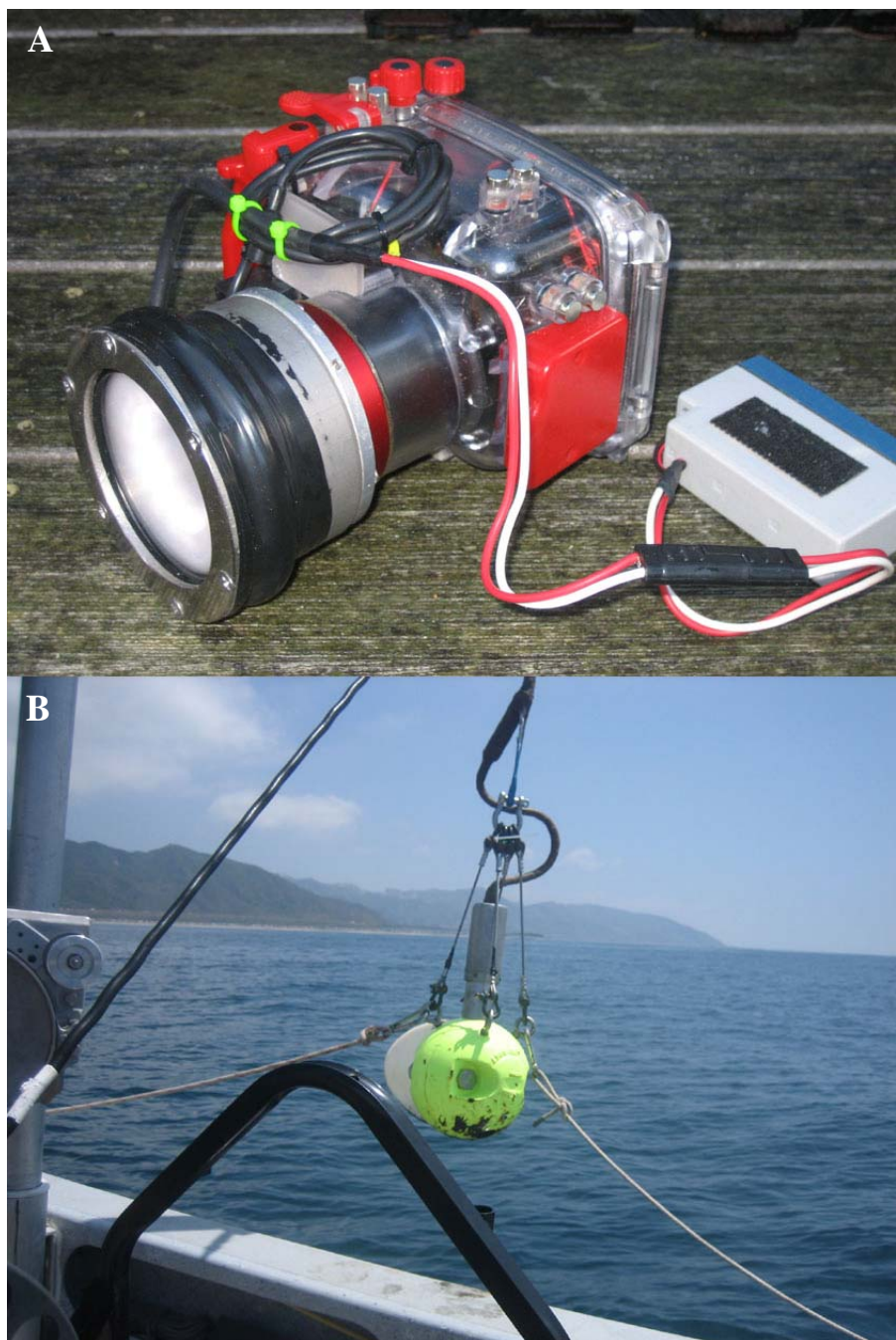


Figure 5.3. *A*, Beachball camera—digital camera encased in waterproof housing. *B*, Flying Eyeball—video camera encased in wrecking ball.

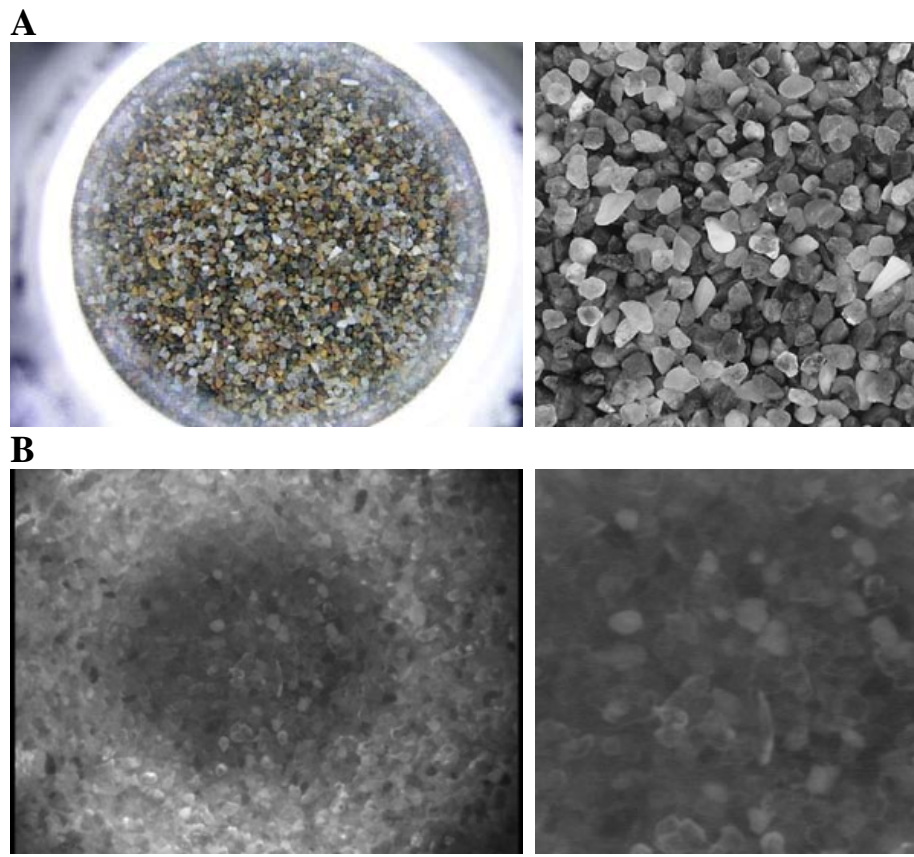


Figure 5.4. *A*, Beachball camera image and processed image in grayscale, cropped from center and rescaled. *B*, Flying Eyeball camera image and processed image cropped from center and rescaled.

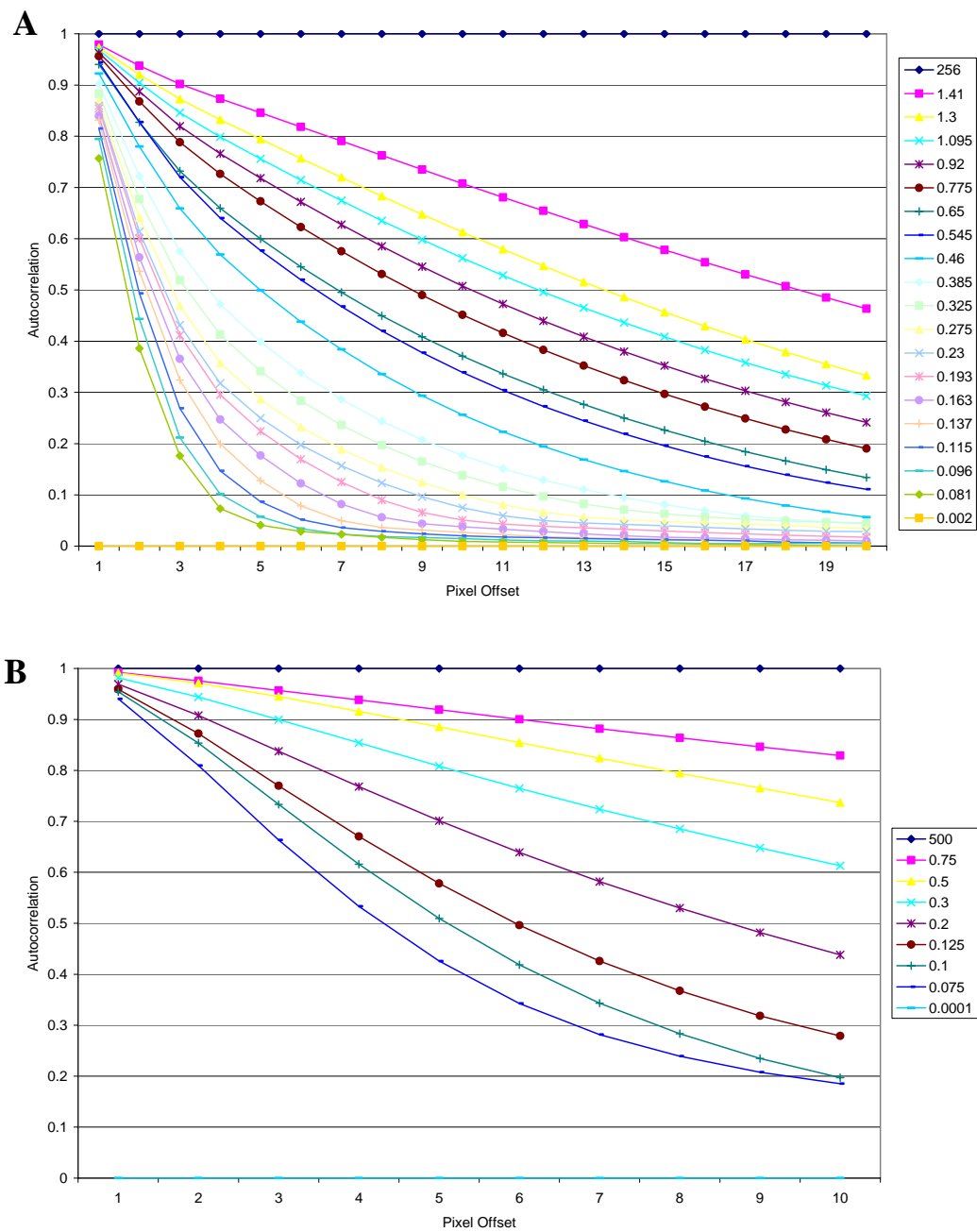


Figure 5.5. *A*, Beachball and *B*, Flying Eyeball calibration matrices. Legends show grain size in millimeters.

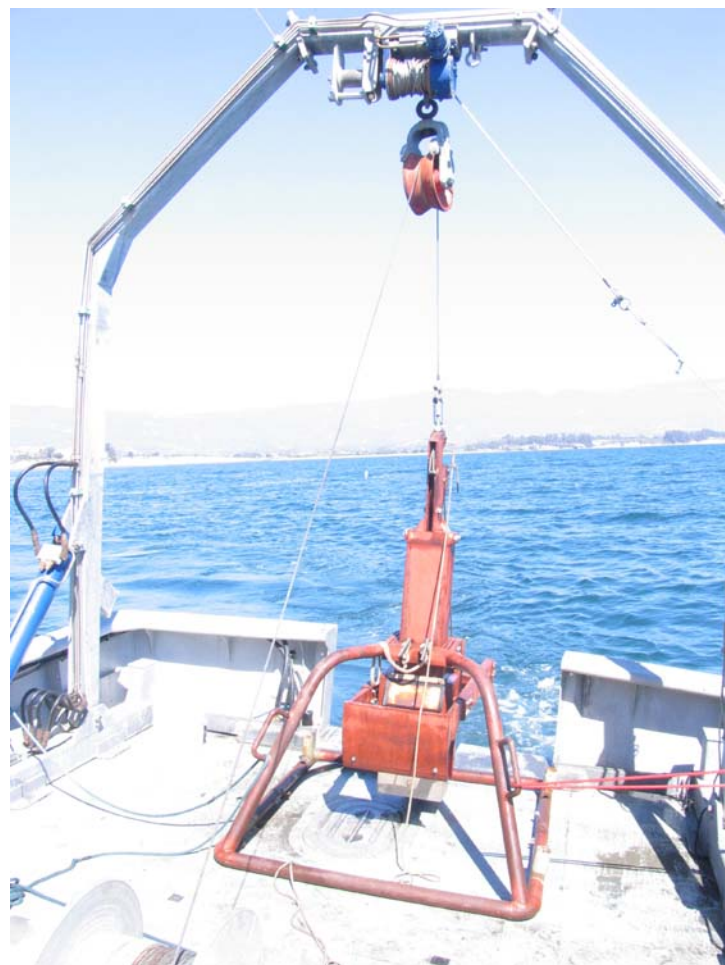


Figure 5.6. Box corer used in this study.

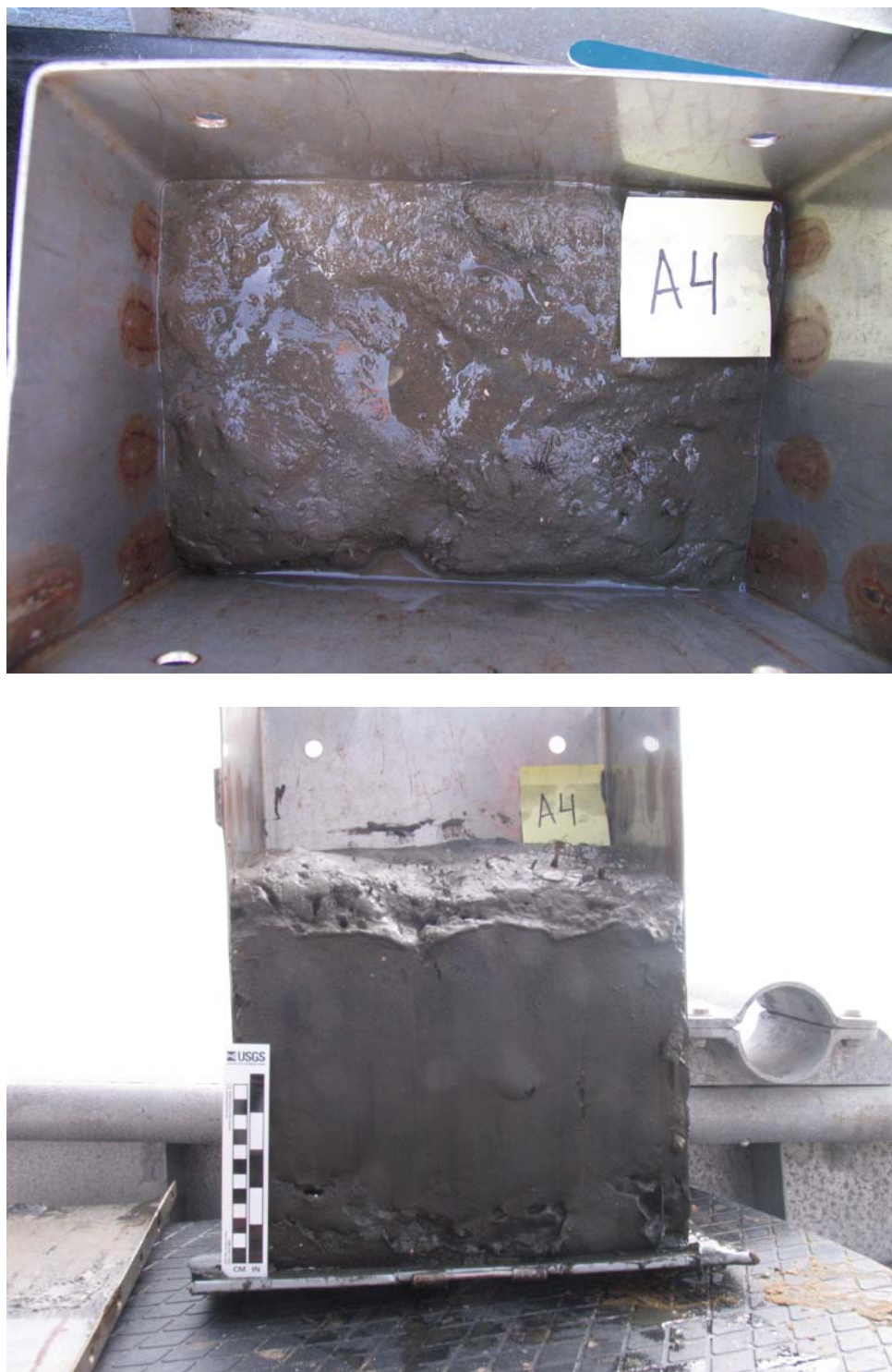


Figure 5.7. Surface and lateral views of sample box core from offshore of Santa Barbara Harbor.

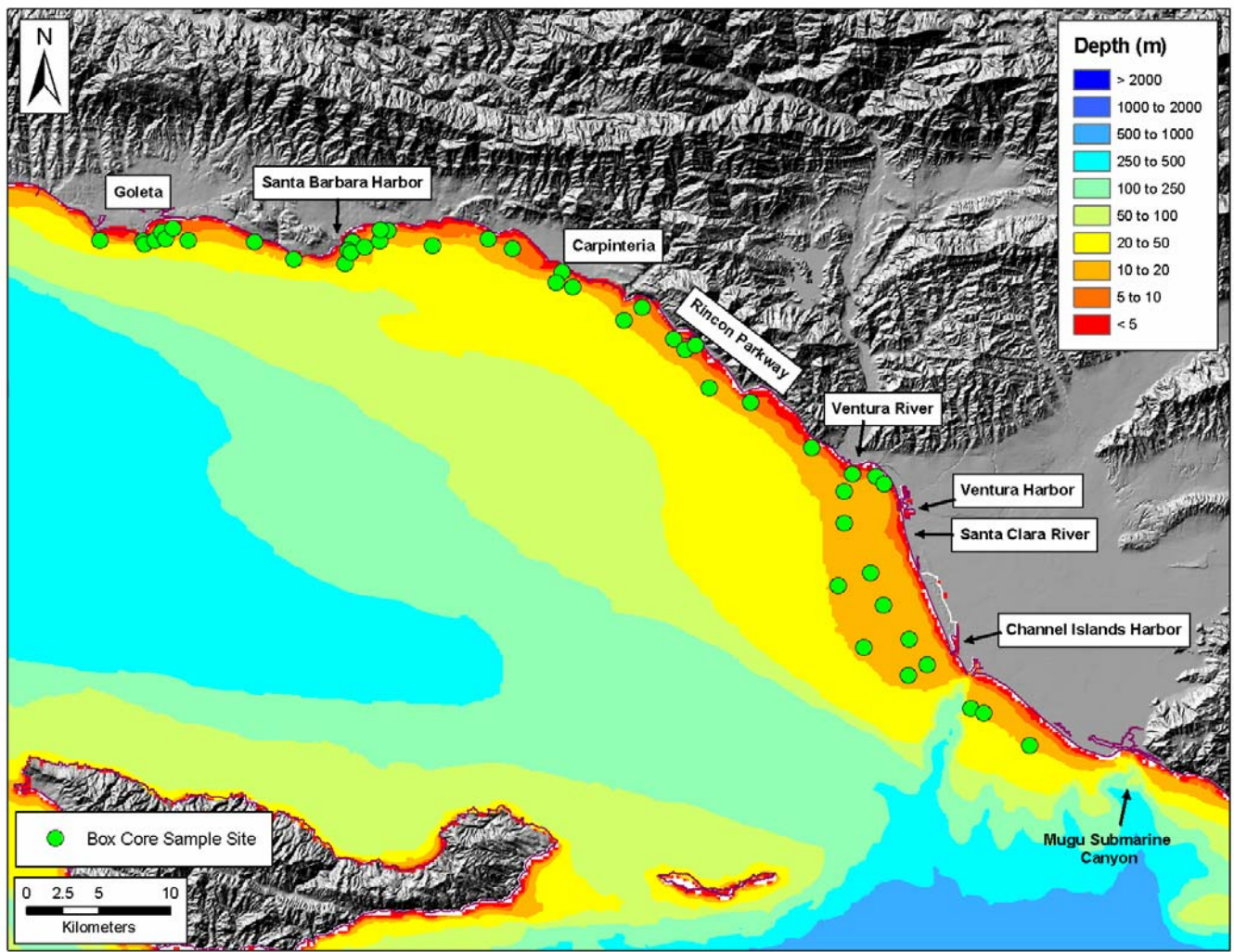


Figure 5.8. Box-core sample locations.

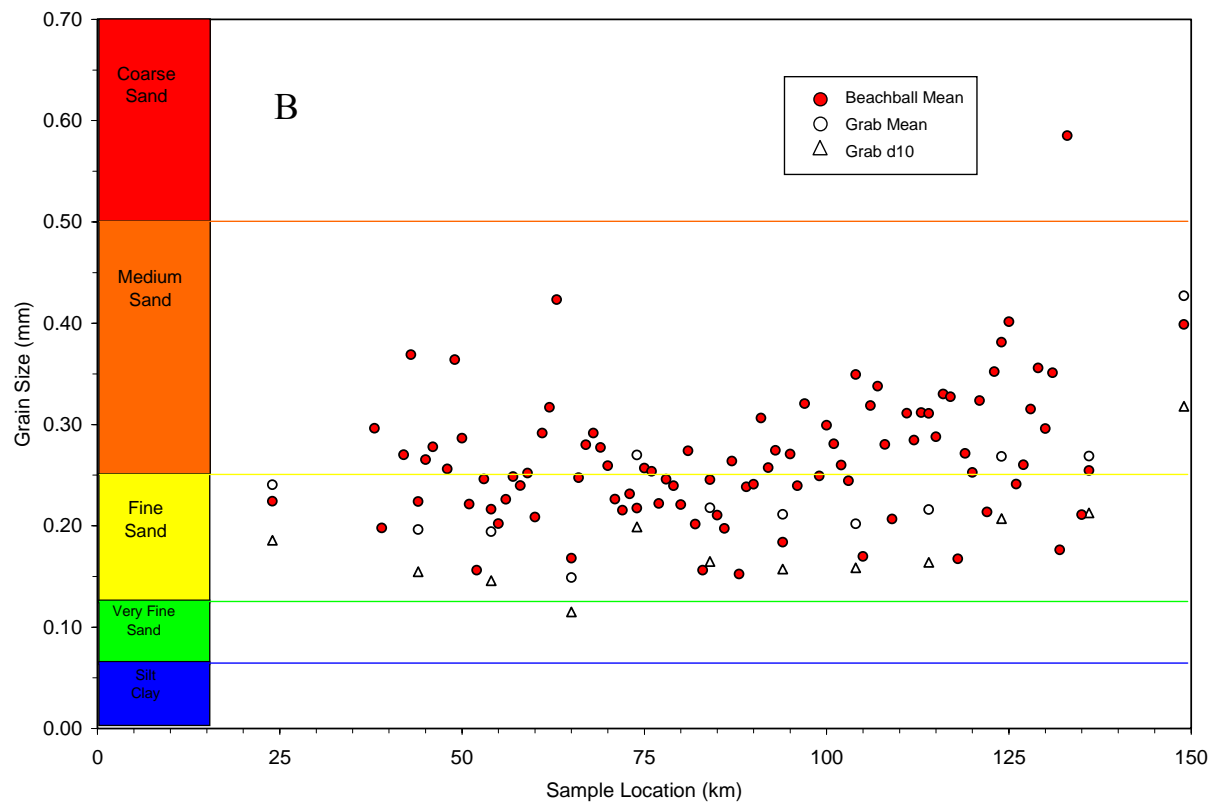
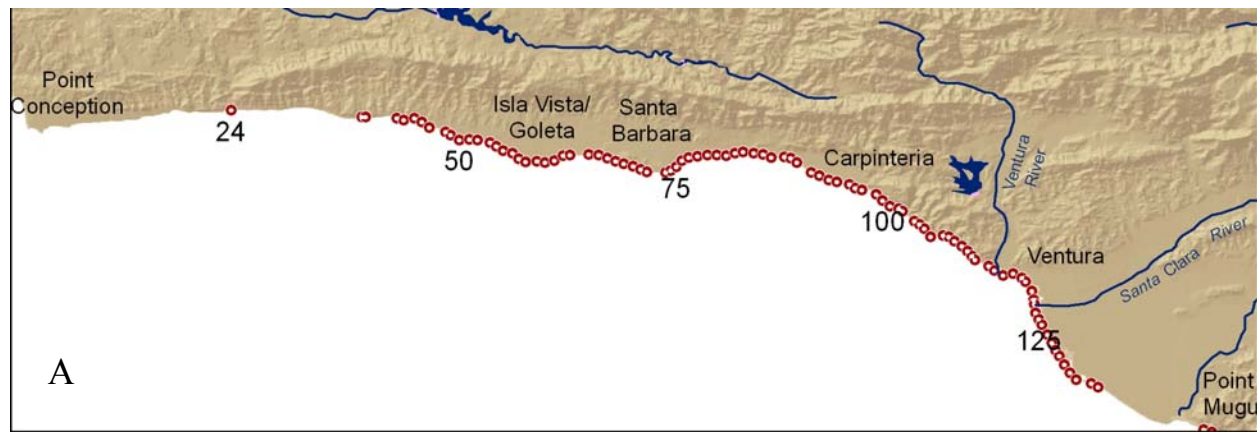


Figure 5.9. A, Location of regional beach-face samples. B, Beach-face mean grain size (mm) and grab-sample finest (d10). Sample locations are specified by distance from Point Conception.

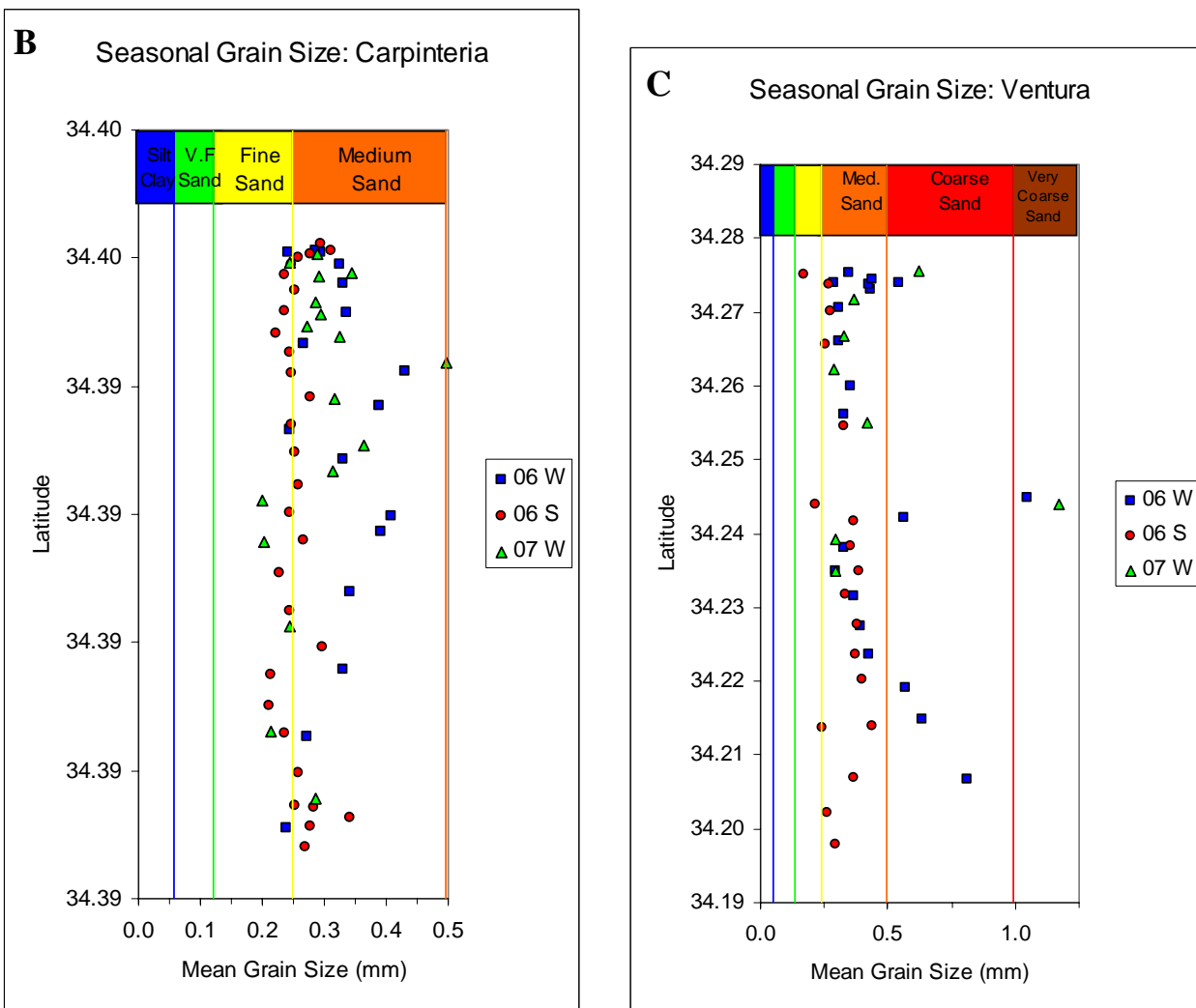
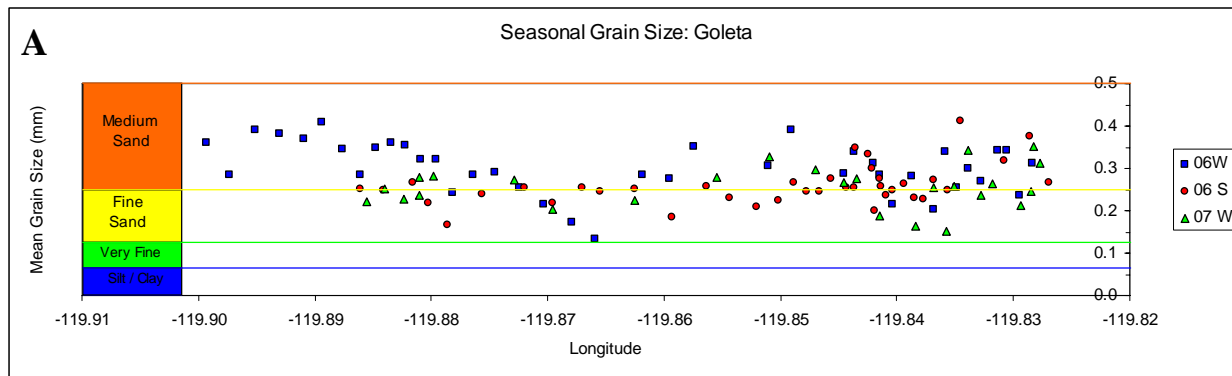


Figure 5.10. Seasonal beach-face grain size. A, Goleta/Isla Vista. B, Carpinteria. C, Ventura. Note different scales.

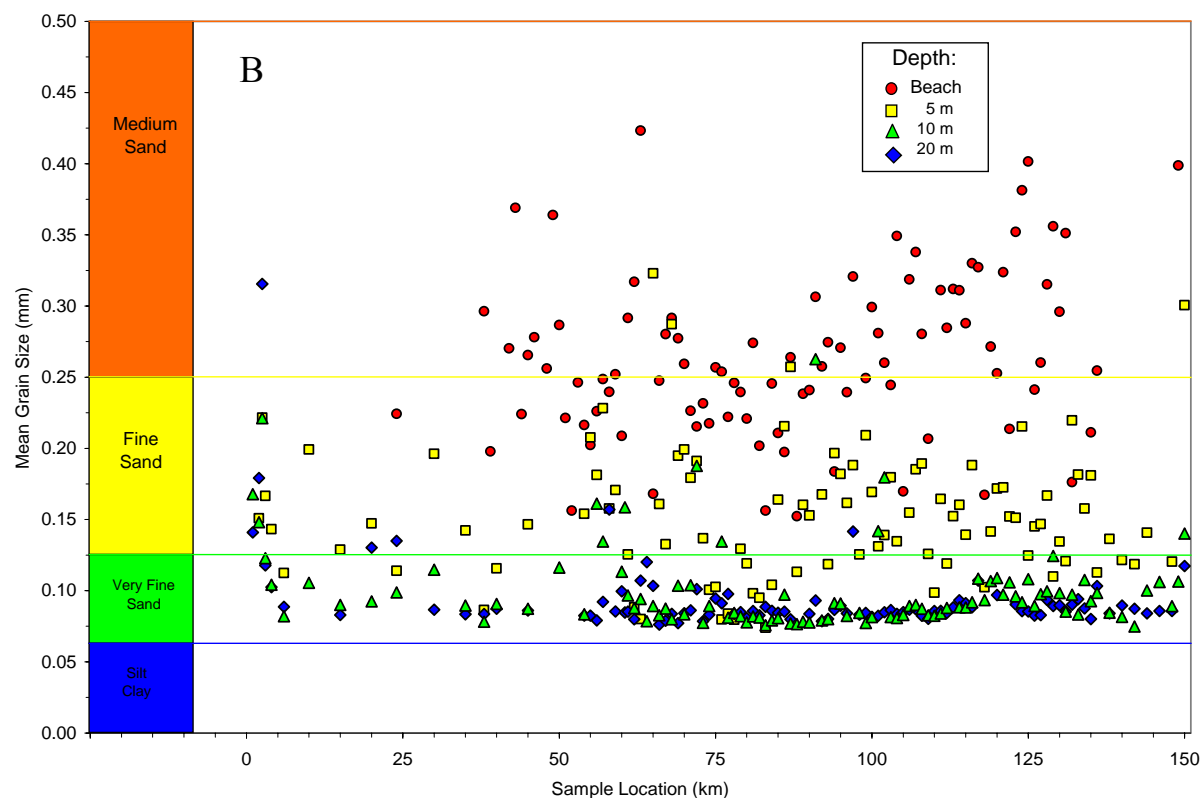
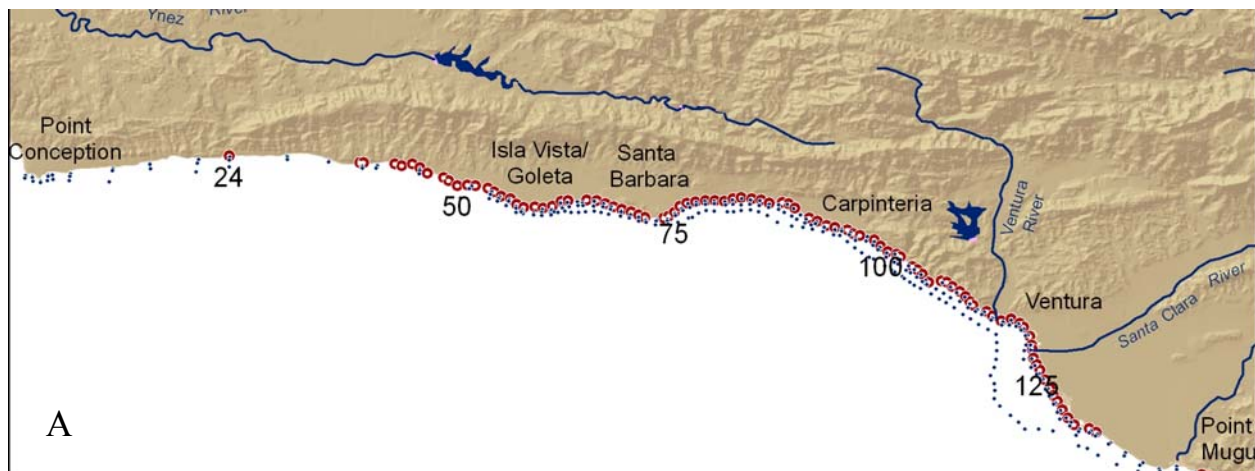


Figure 5.11. A, Locations of all surficial-sediment samples. B, Beach-face and nearshore (5, 10, and 20 m water depth) sediment grain size results. Sample locations are plotted in B as distance from Point Conception.

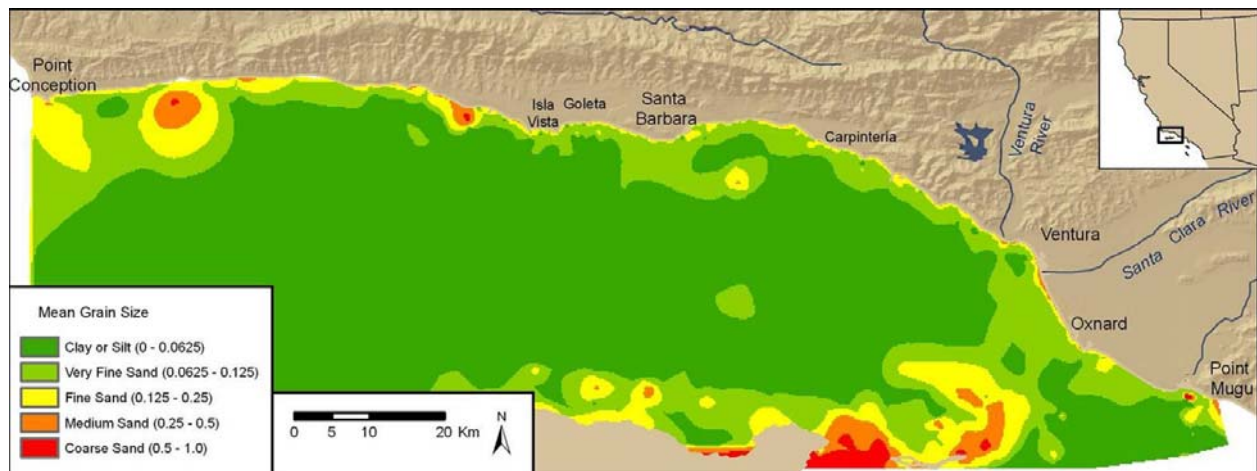


Figure 5.12. Surface-sediment map, Santa Barbara Channel. Data from this study, usSEABED (Reid and others, 2006), and BEACON (Noble Consultants, 1989). Grain sizes in legend are in mm.

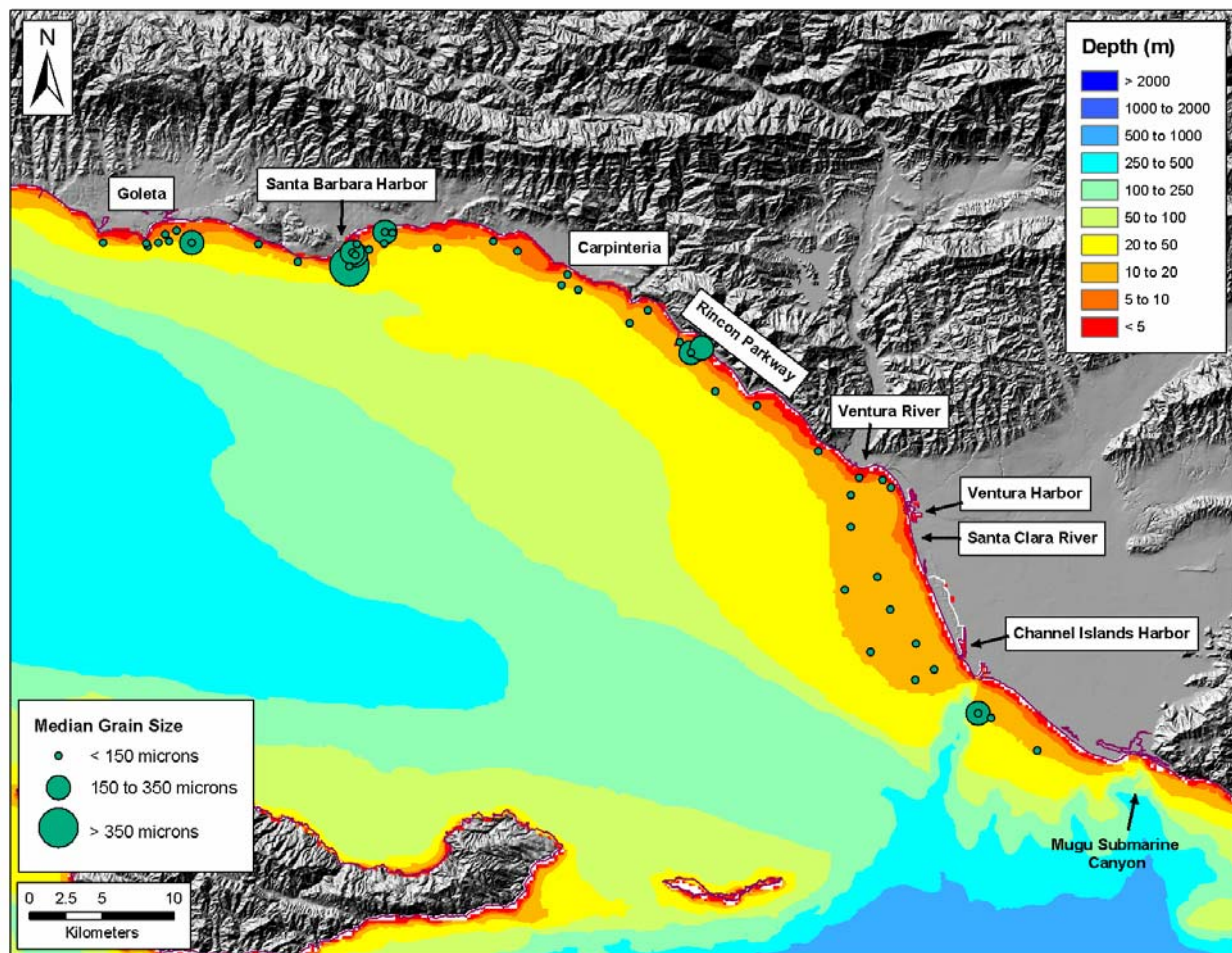


Figure 5.13. Box-core sample results.

Chapter 6— The Impacts of Debris Basins on Sediment Delivery to the Santa Barbara Littoral Cell, California

By Jonathan A. Warrick

Abstract

An assessment was made of the impacts of debris basins in the Santa Ynez Mountain coastal watershed on the littoral-grade sediment discharge into the Santa Barbara littoral cell by using Santa Barbara County Public Works Department records of basin maintenance. These records were also used to calculate and extrapolate sediment-yield estimates from the controlled watersheds to the entire coastal drainage basin. It was found that debris-basin maintenance has removed 1.3 to 2.0 million m³ of sediment between 1969 and 2005, the majority (~85 percent) of which was permanently removed from the downstream fluvial and littoral systems through disposal or reuse. Grain-size samples of debris-basin sediment and of the beaches from the Santa Barbara littoral cell suggest that 60 to 80 percent of the removed sediment is coarser than the littoral cutoff diameter ($D_{50} = 0.125$ mm), suggesting that most of this sediment would be appropriate for the beach. The total average littoral-grade sediment discharge from the entire Santa Ynez Mountain coastal drainage was estimated to range between 110,000 and 300,000 m³/yr; rates that are reduced by ~15 percent, or 15,000 to 40,000 m³/yr, due to debris-basin maintenance. The total littoral-grade sediment discharge from creeks would account for ~40 percent to over 100 percent of the supply of littoral sediment passing the Santa Barbara Harbor. Thus, significant amounts of littoral sediment are produced from the small watersheds of the Santa Ynez Mountains, and debris-basin maintenance has significant effects on these fluxes.

Introduction

Sediment fluxes into littoral systems are important for maintaining coastal sediment budgets, which in turn influence patterns of coastal change (Komar, 1996; Willis and Griggs, 2003). Rivers can be important sediment sources to littoral systems, and modifications to river watersheds can alter the erosion and transport of sediment through and/or from rivers (Trimble, 1981; Meade, 1982; Warrick and Rubin, 2007). Land-use and river-channel modifications can either increase or decrease these fluxes of sediment based on the nature, scale, and duration of the modifications (Trimble, 1999). Global inventories of rivers show that total sediment production from the landscape increased during the 20th century due to land-use modifications and enhanced erosion, while fluxes from rivers decreased due to the effects of large dams (Syvitski and others, 2005).

Physical alterations to river flow, such as dams and debris basins, can reduce sediment fluxes by sedimentation within reservoirs and alteration of the rate and volume of streamflow downstream, which modifies sediment transport capacity (Williams and Wolman, 1984; Graf, 1999). It is clear that large dams have had significant effects on sediment transport in many river systems, and many of these changes are influencing coastal sediment budgets (Willis and Griggs, 2003; Yang and others, 2007; Syvitski and others, 2005). The effects of small control structures, such as debris basins, are generally less well understood than dams, primarily due to a lack of data. Debris basins, unlike large dams, may not be well maintained or monitored, can have a broad range of sediment-trap efficiencies, and may or may not significantly alter downstream streamflow. However, debris basins deserve increased attention due to the large number of these small structures, especially in small coastal drainages (Sherman and others, 2002; Willis and Griggs, 2003).

In this chapter, the effects of debris basins on sediment fluxes are examined for the small coastal watersheds of the Santa Ynez Mountains that drain directly into the Santa Barbara littoral cell (SBLCC),

California (fig. 6.1). Although these structures are generally small, they capture ~13 percent of the total coastal watershed area and reduce sediment inputs to the littoral cell. The purpose of this chapter is twofold. First, using historical records an estimate of the quantity of sediment accumulated within and removed from these structures over time is made. Second, using these rates an assessment is made of the long-term sediment losses by these structures, and of the long-term sediment yield from the entire Santa Ynez Mountain watershed, for which little sediment-yield information exists (Warrick and Mertes, in press). As shown below, much of the data for these analyses has been provided by the Santa Barbara County Public Works Department (SBCPWD).

Santa Barbara Littoral Cell

The SBLC extends along the coastal portion of the Transverse Ranges of southern California (fig. 6.1). Due to the west-east orientation of this portion of coast and the predominant swell direction from the west, littoral transport is strongly eastward, as shown by historical observations and dredging records at the Santa Barbara Harbor (Inman and Frautschy, 1965; Patsch and Griggs, 2006). Although Point Conception may be the northern extent of the SBLC (fig. 6.1B), there is continued debate about the relative influence of sediment transport from northward around the point (Pollard, 1979). Unfortunately, few data currently exist to quantify sediment transport around Point Conception, and few data exist to quantify the relative sediment contributions from the Santa Ynez Mountain creeks, which may or may not provide ample local sediment supplies. On the southern end of the SBLC, large sediment inputs are provided by the Ventura and Santa Clara Rivers. The SBLC ends in the Hueneme and Mugu submarine canyons (fig. 6.1).

In this chapter we will consider the small, coastal creek watersheds that drain the Santa Ynez Mountains, and discharge directly into the SBLC, to evaluate the sediment contributions of these creeks (fig. 6.1B). The Santa Ynez Mountains are part of the larger Western Transverse Ranges (fig. 6.1A),

which are a tectonically-active and semiarid region with high rates of denudation (Scott and Williams, 1978; Inman and Jenkins, 1999; Warrick and Mertes, in press). Rapid uplift, ranging from ~1 to >5 mm/yr, is suggested for the Santa Ynez Mountains and the Western Transverse Ranges, which deforms the Cenozoic sedimentary bedrock of the region (Putnam, 1942; Fall, 1981; Rockwell and others, 1984; Duvall and others, 2004).

Land use in the Santa Ynez Mountain drainages is largely open space, mostly consisting of coastal chaparral. Human uses include rangeland, agriculture, and urban areas, although these activities are generally carried out in the lower, and less steep, portions of the drainage basins. Average annual precipitation ranges from ~60 cm in the upper Santa Ynez Mountains to ~40 cm near sea level, a result of orographic effects, but annual precipitation can vary by many fold and is influenced strongly by the El Niño-Southern Oscillation (ENSO; Andrews and others, 2004; Warrick and Mertes, in press). The seasonal and interannual variation in rainfall produces ephemeral, and occasionally torrential, discharge in the region's creeks (Beighley and others, 2003).

Erosion processes in the Western Transverse Range are complex because they include—in approximate order of importance—mass movements, dry ravel, stream-bank erosion, and sheet flow (Rice and Foggin, 1971; Taylor, 1981; Rice, 1982; Hill and McConaughy, 1988; Raphael and others, 1995; Lave and Burbank, 2004). The alteration of land cover by humans, especially the conversion of native chaparral to nonnative grasses for rangeland, has been suggested to increase soil erosion and rates of landsliding in the region (Cole and Liu, 1994; Gabet and Dunne, 2002; Pinter and Vestal, 2005).

Wildfire has influenced the rates of erosion in the study area, and sediment yield has been shown to increase by more than an order of magnitude during the first winter after a wildfire, with lesser impacts during the subsequent 2–5 years (Rice, 1982; Florsheim and others, 1991; Keller and others, 1997; Warrick and Rubin, 2007). This increased potential for erosion can cause mass movements of soil

and rock, which may induce hazardous debris flows in channels downstream, potentially endangering life and structures in the flow pathway. Although wildfire is known to have dramatic effects on short-term erosion rates and potential for hazards, investigations in the Eastern Transverse Range (fig. 6.1A) have shown that over the long-term (that is, lengths of time greater than the fire recurrence interval of ~40 yrs), wildfire increases sediment yield by only 10-20 percent of unburned yields (Taylor, 1981; Lave and Burbank, 2004).

However, it is the potential for post-wildfire hazards, such as debris flows, that has led to the construction of numerous debris basins in the more populated sections of the Santa Ynez Mountains drainage basins (fig. 6.1C; table 6.1). Although debris basins were largely constructed downstream of wildfires to reduce the risks of debris-flow hazards, none has been removed after vegetation reestablished and risks were reduced (fig. 6.2A). Thus, there are currently 16 debris basins operated and maintained by the Santa Barbara County Public Works Department (SBCPWD) capturing ~104 km² (or ~13 percent) of the Santa Ynez Mountains drainage area. Maintenance includes the removal of sediment following winters with flooding events, as detailed in the Methods and Results sections below.

Methods

The primary method of analysis for this paper is the compilation and synthesis of sediment removal maintenance records for the 16 existing debris basins of the Santa Ynez Mountains. Although sediment removal is commonly termed “desilting,” we will refrain from using this term owing to the general lack of silt in these sediment stockpiles. Sediment maintenance was evaluated from internal SBCPWD management and monitoring documents, such as Santa Barbara County Flood Control and Water Conservation District (SBCFCWCD, 1990; 1996; 2001) and other unpublished documents provided by Karl Treiberg in 1998 and Dana Zertuche in 2008, and personal communication with these two senior staff of SBCPWD.

The sediment that settles in debris basins is excavated to provide maximum protection from subsequent debris-flow hazards as part of the SBCPWD maintenance program. When cleaned, basins are routinely excavated to approximately the original design shape and capacity. However, a 2005 assessment of basin capacities revealed that most were smaller than the original design (table 6.1), suggesting either (1) basin storage was lost with time owing to sedimentation, or (2) the basins were not originally built to design specifications. The actual volumetric capacity of SBCPWD debris basins as of 2005 was approximately 68 percent of the original design capacity.

Records of maintenance activities, including the frequency, approximate amounts, and approximate grain size of the sediment removed, were provided by the SBCPWD. The volume of sediment contained within each debris basin was estimated by either visual estimates by SBCPWD senior staff or, more rarely, from surveys of the extent and height of the sedimentation. Grain-size samples were taken from short hand augers into the basin sediment and evaluated using traditional sieve analyses. The SBCPWD also provided records of sediment excavations from the lower channels of the Goleta and Carpinteria Creek watersheds (fig. 6.1C), and these data are included here to evaluate the implications of these activities. As discussed in the Results section below, most of the sediment removed in these operations is landfilled or used as fill material by private parties.

Results

Sediment Removal from Debris Basins

Annual maintenance of the debris basins occurred until 1987, and as-needed maintenance has occurred since that time (fig. 6.2C). Major sediment-removal projects (that is, removal of near basin-capacity volume of sediment) occurred across all existing debris basins in 1969, 1978, 1983, 1998, 2005, and twice in 1995, which were all years with exceptional precipitation. Many basins were built in

response to upland wildfires as noted above, and post-fire maintenance was performed on basins affected by fires during the 1-2 years after a wildfire (fig. 6.2C).

Unfortunately, detailed records of the amount of sediment removed from each basin were generally not kept, except during the 1996, 1998, and 2005 projects. The 1996 and 1998 estimates were made from visual inspections of the basins and were originally reported in percent of basin volume filled with sediment (K. Treitenburg, SBCPWD, pers. comm.). Using these percent-filled estimates, basin-cleaning projects were estimated to have removed approximately 180,000 to 260,000 m³ of sediment in 1996, and 200,000 to 300,000 m³ of sediment in 1998. The range in these sediment volumes results from the uncertainty in actual basin capacities as reported in the Methods section above. Topographic surveys before and after the basin cleaning in 2005 suggest that 152,000 m³ of sediment was removed (D. Zertuche, SBCPWD, pers. comm.).

The sediment removed following the 1969, 1978 and 1983 seasons was not recorded, but can be assumed to be equivalent to the percentage of basin capacity removed in 1998, owing to the massive flooding and maintenance projects that occurred during these years (K. Treitenburg, SBCPWD, pers. comm.). The amount removed in 1995 is approximately double the 1998 rate, owing to two major cleaning projects during this year (K. Treitenburg, SBCPWD, pers. comm.). The lower estimate of basin capacity (that is, that basins have always been smaller than designed) results in conservative sediment-removal volume estimates of 40,000 m³ in 1969, 170,000 m³ in both 1978 and 1983, and 400,000 m³ in 1995 (fig. 6.2C).

Basins were also cleaned as part of post-fire activities, such as the cleaning of two Maria Ygnacio Creek debris basins in 1991 and 1992. The volume of sediment removed during 1991 was estimated to be 23,000 m³ of primarily fine sand to gravel largely associated with post-fire erosion (Keller and others, 1997). Unfortunately, there is not adequate information to estimate the sediment

volumes removed from the remaining post-fire projects or from the annual maintenance that occurred until 1987 (K. Treitenburg, SBCPWD, pers. comm.).

Fate of Maintenance Material

Much of the sediment removed from the basins is given to local land owners for fill material, although approximately 200,000 m³ of debris-basin sediment was deposited on Goleta Beach in 1995 as a one-time emergency operation (fig. 6.2C). Thus, a highly conservative estimate for the total amount of sediment removed from stream discharge by the debris basins during 1969-2005 is 1.3 million m³, which includes the lower estimates of sediment removal during the 7 years of major maintenance programs, but excludes the sediment removed from all post-fire and annual maintenance programs. Only ~200,000 m³ of the removed sediment was eventually placed into the littoral zone, while the remaining sediment was removed from the fluvial, and hence littoral, systems.

Sediment Grain Size

To evaluate the potential impacts of this sediment removal on the SBLC, grain size must be considered. Unpublished particle-size analyses reveal that 80 to 95 percent of the sediment deposited in the Santa Ynez Mountain debris basins is sand size or coarser (>75 µm, K. Treiburg, SBCWRD, unpub. data). Most of this material is medium to fine sand, consisting primarily of particles passing the No. 30 sieve (600 µm; black bars in fig. 6.3). An integrated sample of the Santa Monica Creek debris-basin sediment by Simon, Li and Associates (1994) is consistent with these unpublished SBCWRD results (red line, fig. 6.3). These samples are consistent with the grain sizes of sediment deposited in the low-gradient channels of the coastal wetlands in the region discussed below (blue shading, fig. 6.3). Thus, sediments deposited into and cleaned from the debris basins are primarily fine sand and coarser, which is consistent with observations by Keller and others (1997). An estimated littoral cutoff diameter (that

is, the approximate lower limit of grain size) for the sediment in the SBLC is 125 μm (Chapter 5; Limber and others, 2008; fig. 6.3), which suggests that 60 to 80 percent of the sediment volume trapped and removed from the debris basins has grain sizes compatible with the region's beaches.

Sediment Removal from Coastal Wetlands

For comparative purposes it is also valuable to describe and synthesize the maintenance projects that remove sediment from the channels of coastal wetlands in the area. This sedimentation in the study area was similarly assessed with published and unpublished reports from the SBCPWD.

The largest coastal-wetland sediment-maintenance program is conducted by SBCPWD in the numerous channels of the Goleta Slough (fig. 6.1C). Most of this work consists of channel maintenance and dredging following winters with high discharge events to restore the channel geometry, and thus to reduce the potential for subsequent flooding. Recent dredging operations removed approximately 120,000 m^3 of sediment in 1991 (following the Painted Cave fire), 50,000 m^3 in 1994, 300,000 m^3 in 1995, and 85,000 m^3 in 1998 (K. Treitenburg, SBCPWD, pers. comm.; Keller and others, 1997).

A compilation of the grain-size distributions of 13 sediment borings taken in 1998 of the sediment deposited in the Goleta Slough channels is shown in figure 6.3. Sediment deposited in these channels is largely fine sand and coarser, which is generally consistent with the sediment removed from debris basins as noted above. Because this sediment is deemed to be roughly consistent with sediment found on Goleta Beach, immediately adjacent to the site, most of the dredged material has been placed into the adjacent littoral zone. Hence, the sedimentation within the slough channels has not reduced inputs to the littoral cell from the Goleta Slough watersheds. Sedimentation rates in the marsh portion of Goleta Slough (that is, outside of the channels) have not been measured, and sediment-removal maintenance does not occur in these areas.

Dredging operations are also employed to reduce sedimentation in the channels of the Carpinteria Salt Marsh (fig. 6.1C). For example, during the 1998 storm season approximately 7,500 m³ of sediment was removed from the marsh channels and placed on Carpinteria Beach. Following the 1998 storm season, 23,000 m³ of additional sediment was removed from the marsh creeks, dried, and given to private land owners for fill material because much of this material did not meet the federal requirements of at least 80 percent sand for beach fill (K. Treitenburg, SBCPWD, pers. comm.).

Discussion

The maintenance of debris basins in the Santa Ynez Mountain coastal watershed impacts sediment delivery to the SBLC by removing sand-sized debris. As noted above, a highly conservative estimate for the total sediment captured by these debris basins between 1969 and 2005 is 1.3 million m³. Assuming that 60 to 80 percent of this sediment would be adequately coarse for the littoral cell, 0.8 to 1.0 million m³ of littoral sediment was captured and removed due to debris-basin maintenance.

During the 37 years of maintenance records (1969-2005), this rate of total-sediment capture is equivalent to an annualized sediment yield of approximately 370 m³ per km² of watershed per year (m³/km²/yr). However, this estimate is biased because the first and last years of the record were flood years and thus had unusually high sediment accumulations. To correct for this bias, the 1930-2005 suspended-sediment discharge estimates from the USGS stream gage at the Ventura River (USGS 11118500) synthesized by Warrick and Mertes (in press; fig. 6.4) were compared to the debris-basin data. The average annual sediment load for the river during 1969-2005 is 1.22 Mt/yr, which is 156 percent higher than the average load for the 1930-2005 record. Correcting for this level of bias produces an average annualized sediment yield for the Santa Ynez Mountain debris basins of approximately 230 m³/km²/yr.

To evaluate the total sediment output of the Santa Ynez Mountains, it is assumed that the remaining Santa Ynez Mountains produce sediment yields equivalent to those interpreted from the debris basins, which is a conservative estimate owing to higher yields measured from some of these basins by Warrick and Mertes (*in press*). Using this assumption, the total sediment production from the Santa Ynez Mountain coastal watersheds is estimated to be 190,000 m³/yr. Noting that 60 to 80 percent of this sediment would be littoral-cell grade sediment, it is calculated that without debris basins, 110,000 to 150,000 m³/yr of littoral sediment would be discharged from these watersheds into the SBLC. This total littoral-grade sediment discharge is likely reduced by an average of 15,000 to 20,000 m³/yr because of debris-basin maintenance.

It must be emphasized that these “long-term” estimates of littoral-grade sediment discharge from the Santa Ynez Mountain coastal watersheds (110,000 to 150,000 m³/yr without debris basins, or 90,000 to 130,000 m³/yr with debris basins) are highly conservative owing to:

- a) the assumption that debris basins have 100 percent trap efficiencies for littoral-grade sediment,
- b) the rate of sediment production captured during the 24 years of annual maintenance was not included in this estimate,
- c) post-fire debris production, which as noted above is estimated to increase long-term sediment yield by 10 to 20 percent (Taylor, 1981; Lave and Burbank, 2004), was not included in these calculations,
- d) the assumption that debris-basin capacities were smaller than the design capacities for the entire record, and
- e) the assumption that sediment yields were constant across the Santa Ynez Mountain drainage basins, even though higher rates are suggested for parts of this area (Warrick and Mertes, *in press*).

It is difficult to assess the uncertainty involved in (a), but debris-basin sedimentation observations and theory (for example, Haan and others, 1994) would suggest that trap efficiencies for sand-sized particles in the types and sizes of structures considered would be less than 100 percent. If assumption (d) is incorrect, and debris-basin capacities were reduced sometime between 1998 and 2005, an additional 700,000 m³ of sediment would have been captured and removed from maintenance projects, resulting in a total capture of 2 million m³ during 1969-2005 and an average annual sediment yield of 600 m³/km²/yr. Under this scenario, the “long-term” average littoral-grade sediment discharge from the Santa Ynez Mountain coastal watersheds would be 190,000 to 250,000 m³/yr. Thus, combining the effects of (a) through (e), a high estimate of littoral-grade sediment discharge would be 200,000 to 300,000 m³/yr, with approximately 25,000 to 40,000 m³/yr lost due to debris-basin maintenance.

These rates of sediment discharge into the littoral cell can be compared to the littoral-transport rate of ~240,000 m³/yr that has been estimated from dredging records of the Santa Barbara Harbor (Patsch and Griggs, 2006; Chapter 2). The actual average littoral-grade sediment discharge (that is, the total supply including debris-basin reductions) was estimated to range between a minimum of 90,000 m³/yr and a maximum of 260,000 m³/yr, values that would account for ~40 to more than 100 percent of the littoral sediment passing the Santa Barbara Harbor. Thus, significant amounts of littoral sediment are produced from the small coastal watersheds of the Santa Ynez Mountains, although it cannot be determined from the data whether these supplies of sediment are the dominant or a secondary source of littoral sediment to the SBLC.

Conclusions

- Maintenance records from debris basins suggest that the Santa Ynez Mountain coastal watersheds discharge 110,000 to 300,000 m³/yr of littoral-grade sediment into the SBLC.
- Debris basins are estimated to have reduced littoral-sediment contributions to the SBLC by 15,000 to 40,000 m³/yr, or about 15 percent of the total littoral-sediment production of the Santa Ynez Mountain coastal watersheds.
- Debris-basin maintenance has removed 1.3 to 2.0 million m³ of sediment between 1969 and 2005, the majority (~85 percent) of which is permanently removed from the downstream fluvial and littoral systems through disposal or reuse.

Acknowledgments

This work could not have been conducted without the assistance and support of Karl Treiberg and Dana Zertuche of the County of Santa Barbara Public Works Department. I thank them for their time digging up old reports and files and answering questions. This work was started when the author was a graduate student at the University of California, Santa Barbara, and funded by a NASA Earth System Science Fellowship, and completed while he was supported by the USGS Western Coastal and Marine Geology Team.

References

- Andrews, E.D., Antweiler R.C., Neiman, P.J., and Ralph, F.M., 2004, Influence of ENSO on flood frequency along the California coast: Journal of Climate, v. 17, p. 337-348.
- Beighley, R.E., Melack, J.M., and Dunne, T., 2003, Impacts of California's climatic regimes and coastal land use change on streamflow characteristics: Journal of the American Water Resources Association, v. 39, no.6, p. 1419-1433.

- Cole, K.L., and Liu, G.W., 1994, Holocene paleoecology of an estuary on Santa Rosa Island, California: Quaternary Research, v. 41, p. 326-335.
- Davis, F.W., Theobald, D., Harrington, R., and Parikh, A., 1990, University of California Santa Barbara Campus Wetlands Management Plan: Part 2 – Technical Report on the Hydrology, Water Quality and Sedimentation of West and Storke Campus Wetlands. Department of Geology. University of California, Santa Barbara, 105 p.
- Duvall, A., Kirby, E., and Burbank, D., 2004, Tectonic and lithologic controls on bedrock channel profiles and processes in coastal California: Journal of Geophysical Research, v. 109, F03002, doi:[10.1029/2003JF000086](https://doi.org/10.1029/2003JF000086)
- Gabet, E.J., and Dunne, T., 2002, Landslides on coastal sage scrub and grassland hillslopes in a severe El Niño winter: The effects of vegetation conversion on sediment delivery: Geological Society of America Bulletin, v. 114, p. 983-990.
- Graf, W.L., 1999, Dam nation: A geographic census of American dams and their large-scale hydrologic impacts: Water Resources Research, v. 35, no.4, p. 1305-1311.
- Fall, E.W., 1981, Sediment management for Southern California mountains, coastal plains and shoreline; Part A, Regional geological history: Environmental Quality Laboratory report No. 17-A. California Institute of Technology, Pasadena.
- Florsheim, J.L., Keller, E.A., and Best, D.W., 1991, Fluvial sediment transport in response to moderate storm flows following chaparral wildfire, Ventura County, southern California: Geological Society of America Bulletin, v. 103, p. 504-511.
- Haan, C.T., Barfield, B.J., and Hayes, J.C., 1994, Design hydrology and sedimentology for small catchments: Academic Press, Inc., San Diego, 588 p.

- Hill, B.R., and McConaughy, C.E., 1988, Sediment loads in the Ventura River Basin, Ventura County, California, 1969-81: U. S. Geological Survey Water-Resources Investigations Report 88-4149. Sacramento, CA. 22 p.
- Inman, D.L., and Frautschy, J.D., 1965, Littoral processes and the development of shorelines. In: Coastal Engineering, Santa Barbara Specialty Conference, ASCE, New York, NY, p. 511-536.
- Inman, D.L., and Jenkins, S.A., 1999, Climate change and the episodicity of sediment flux of small California rivers: *Journal of Geology*, v. 107, p. 251–270.
- Keller, E.A., Valentine, D.W., and Gibbs, D.R., 1997, Hydrological response of small watersheds following the southern California Painted Cave fire of June 1990: *Hydrological Processes*, v. 11, p. 404-414.
- Komar, P.D., 1996, The budget of littoral sediments – concepts and applications: *Shore and Beach*, v. 64, no.3, p. 18-26.
- Lavé, J., and Burbank, D.W., 2004, Denudation processes and rates in the Transverse Ranges, southern California: erosional response of a transitional landscape to external and anthropogenic forcing: *Journal of Geophysical Research-Earth Surface*, v. 109, F01006, 10.1029/2003JF000023.
- Limber, P.W., Patsch, K.B., and Griggs, G.B., 2008, Coastal sediment budgets and the littoral cutoff diameter: A grain size threshold for quantifying active sediment inputs: *Journal of Coastal Research*, v. 24, no.2B, p. 122-133.
- Meade, R.H., 1982, Sources, sinks, and storage of river sediment in the Atlantic drainage of the United States: *Journal of Geology*, v. 90, no.3, p. 235-252.
- Patsch, K.B and Griggs, G.B., 2006, Littoral cells, sand budgets, and beaches: Understanding California's shoreline, Report of the Institute of Marine Sciences, University of California, Santa Cruz, 40 p.

- Pinter, N., and Vestal, W.D., 2005, El Nino-driven landsliding and postgrazing vegetative recovery, Santa Cruz Island, California: Journal of Geophysical Research, v. 110, p.
- Pollard, D.D., 1979, The source and distribution of beach sediments, Santa Barbara County, California. Ph.D. Dissertation, University of California, 188 p.
- Putnam, W.C., 1942, Geomorphology of the Ventura region, California: Geological Society of America Bulletin, v. 53, p. 691-754.
- Raphael, M., Feddema, J., Orme, A.J., and Orme, A.R., 1995, The unusual storms of February 1992 in southern California: Physical Geography, v. 15, p. 442-464.
- Rice, R.M., 1982, Sedimentation in the chaparral: how do you handle unusual events? In: Sediment Budgets and Routing in Forested Drainage Basins. Swanson F.J., Janda, R.J., Dunne, T., Swanston D.N. (Eds.). Pacific Northwest Forest and Range Experiment Station, General Technical Report PNW-141.
- Rice, R.M., and Foggin, G.T. III., 1971, Effect of high intensity storms on soil slippage on mountainous watersheds in southern California: Water Resources Research, v. 7, p. 1485-1496.
- Rockwell, T.K., Keller, E.A., Clark, M.N., and Johnson, D.L., 1984, Chronology and rates of faulting of Ventura River terraces, California: Geological Society of America Bulletin, v. 95, p. 1466-1474.
- Rose, P.B., Countryman, C.M., and Storey, H.C., 1949, Probable peak discharges and erosion rates from southern California watersheds as influenced by fire: United States Department of Agriculture Forest Service Publication, 46 p.
- Santa Barbara County Flood Control and Water Conservation District (SBCFCWCD), 1990, Addenda to 90-EIR-7: Final program environmental impact report for Santa Barbara County flood control routine maintenance activities.

- Santa Barbara County Flood Control and Water Conservation District (SBCFCWCD), 1996, Debris Basin Maintenance Plan.
- Santa Barbara County Flood Control and Water Conservation District (SBCFCWCD), 2001, Addenda to 01-ND-01, Final program negative declaration for Santa Barbara County debris maintenance plan.
- Santa Barbara County Flood Control and Water Conservation District (SBCFCWCD), 2001.
- Scott, K.M., and Williams, R.P., 1978, Erosion and Sediment Yield in the Transverse Ranges, Southern California: U.S. Geological Survey Paper 1030. Palo Alto, CA, 37 p.
- Sherman, D.J., Barron, K.M., and Ellis, J.T., 2002, Retention of beach sand by dams and debris basins in southern California: Journal of Coastal Research, Special Issue 36, p. 662-674.
- Simons, Li and Associates, Inc., 1994, Sediment transport analysis: Carpinteria Salt Marsh enhancement project. Unpublished project report to the Santa Barbara County Flood Control and Water Conservation District.
- Syvitski, J.P.M., Vörösmarty, C.J., Kettner, A.J., and Green, P., 2005, Impact of humans on the flux of terrestrial sediment to the global coastal ocean: Science, v. 308, p. 376–380.
- Taylor, B.D., 1981, Sediment management for Southern California mountains, coastal plains and shoreline; Part B, Inland sediment movements by natural processes: Environmental Quality Laboratory Report No. 17-B, California Institute of Technology, Pasadena.
- Trimble, S.W., 1981, Changes in sediment storage in the Coon Creek basin, Driftless Area, Wisconsin, 1853 to 1975: Science, v. 214, p. 181-183.
- Trimble, S.W., 1997, Contribution of stream channel erosion to sediment yield from an urbanizing watershed: Science, v. 278, p. 1442-1444.
- Trimble, S.W., 1999, Decreased rates of alluvial storage in the Coon Creek basin, Wisconsin, 1975-1993: Science, v. 285, p. 1244-1246.

Warrick, J.A., 2002, Short-term (1997–2000) and long-term (1928–2000) observations of river water and sediment discharge to the Santa Barbara Channel, California. Ph.D. Thesis, Santa Barbara, University of California, 337 p.

Warrick, J.A., and Rubin, D.M. 2007, Suspended-sediment rating curve response to urbanization and wildfire, Santa Ana River, California: Journal of Geophysical Research, v. 112, F02018, doi: [10.1029/2006JF000662](https://doi.org/10.1029/2006JF000662).

Warrick, J.A., and Mertes, L.A.K., in press, Sediment yield from the tectonically active semi-arid Western Transverse Ranges of California: Geological Society of America Bulletin.

Williams, G.P., and Wolman, M.G. 1984, Downstream effects of dams on alluvial rivers: U.S. Geological Survey Professional Paper 1286. 83 p.

Willis, C.M., and Griggs G.B., 2003, Reductions in fluvial sediment discharge by coastal dams in California and implications for beach sustainability: Journal of Geology, v. 111, p. 167– 182, doi: [10.1086/345922](https://doi.org/10.1086/345922).

Yang, S.L., Zhang, J., and Xu, X.J., 2007, Influence of the Three Gorges Dam on downstream delivery of sediment and its environmental implications, Yangtze River: Geophysical Research Letters, v. 34, L10401, doi: [10.1029/2007GL029472](https://doi.org/10.1029/2007GL029472).

Table 6.1. Characteristics of debris basins in the Santa Ynez coastal drainage basin. Totals may not equal sums due to rounding.

Code	Debris basin name	Construction year	Drainage area (km ²)	Design capacity (m ³)	2005 measured capacity (m ³)
A Go	bernador	1971	20.58	36,000	19,000
B Fra	nklin Main	1971	1.82	9,500	4,500
C Sant	a Monica	1977	8.50	160,000	156,000
D Ar	royo Paredon	1971	3.04	19,000	6,300
E Tor	o East	1971	1.62	11,000	4,800
F	Toro Lower West	1971	1.54	43,000	15,000
G	Toro Upper West	1971	2.43	22,000	11,000
H R	omero	1971	4.45	21,000	12,000
I San	Ysidro	1964	6.88	8,400	6,000
J C	old Springs	1964	9.51	15,000	9,600
K Rattlesnake		1964	5.67	6,300	2,200
L M	ission	1964	6.27	11,000	3,100
M San	Roque	1964	8.90	31,000	12,000
N San	Antonio	1964	10.52	26,000	14,000
O	Maria Ygnacio East	1990	4.05	46,000	45,000
P	Maria Ygnacio Main	1990	8.50	23,000	8,900
TOTAL			104.27	487,000	333,000

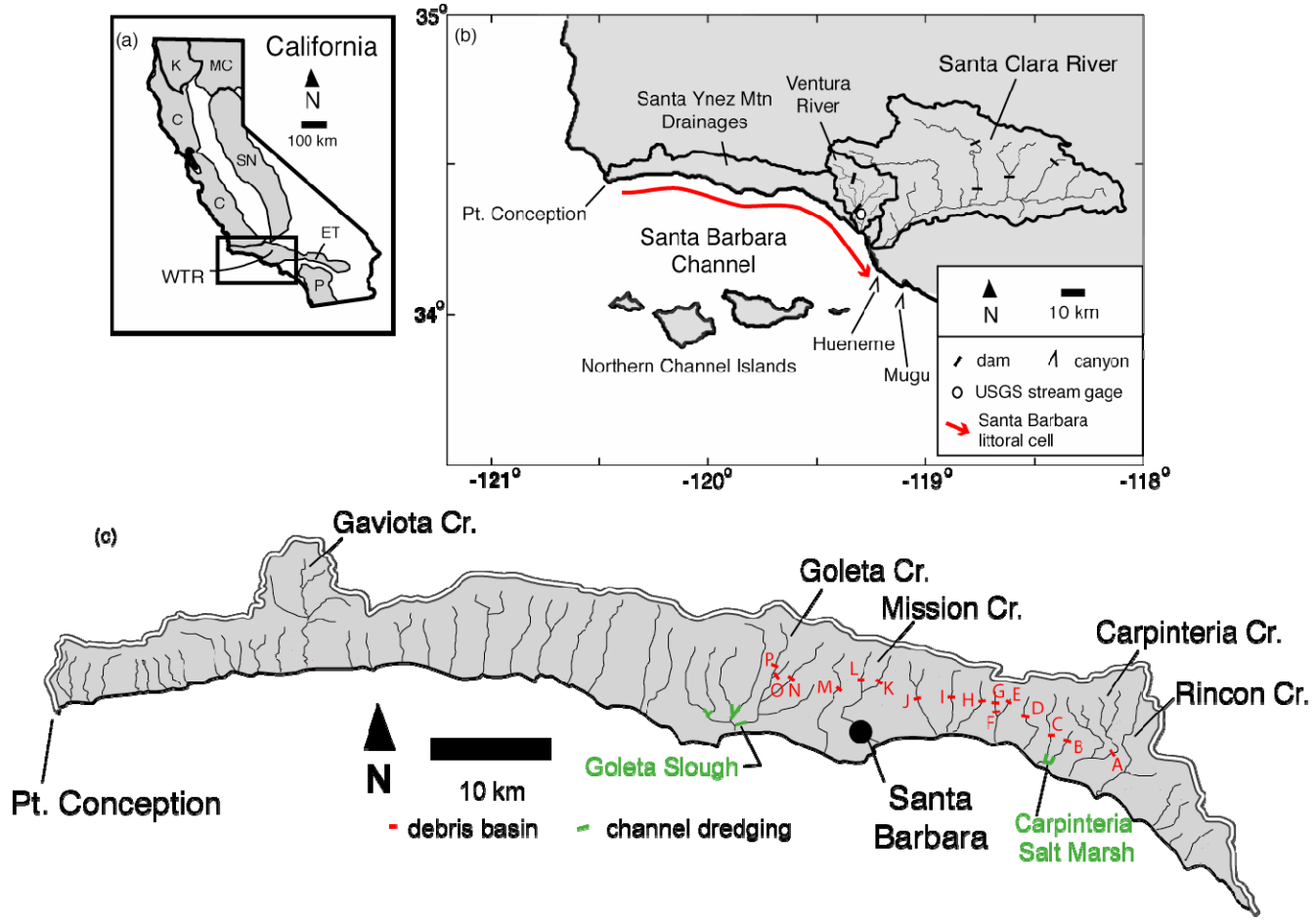


Figure 6.1. Study area maps for the Santa Barbara littoral cell (SBLC) and its watersheds. *A*, California location map with the major mountain ranges identified: Western Transverse Range (WTR), Coastal (C), Eastern Transverse (ET), Klamath (K), Modoc and Cascade (MC), Peninsular (P) and Sierra Nevada (SN). *B*, Watershed map of the SBLC. *C*, Watershed map of the small coastal drainages of the Santa Ynez Mountains, including the locations of debris basins and channel-dredging operations.

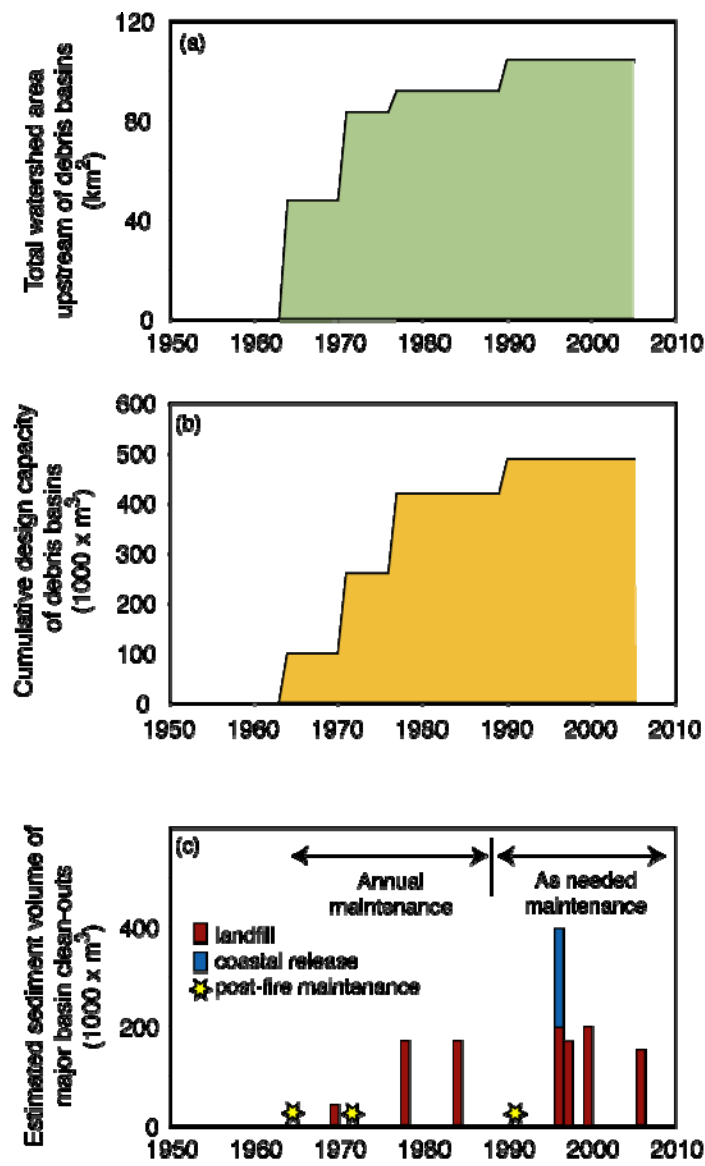


Figure 6.2. Characteristics of the debris basins maintained by the Santa Barbara County Public Works Department in the Santa Ynez Mountains drainage basin. *A*, Cumulative watershed area trapped by debris basins. *B*, Cumulative debris-basin volumetric design capacity. *C*, History of the removal of sediment from these debris basins.

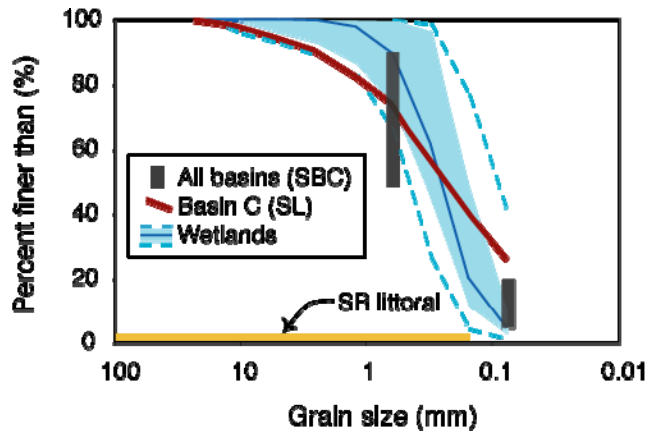


Figure 6.3. Grain-size distribution data from the debris basins and coastal-wetland channels of the Santa Ynez Mountain coastal watersheds. Data include unpublished hand-auger samples from the basins in 1998 by the Santa Barbara County Public Works Department (SBCPWD)(All basins, SBC), a published integrated sample from the Santa Monica Creek Basin (Basin C, SL) after Simons, Li and Associates (1994), and wetland-channel (Goleta Slough) samples from 1998 by SBCWPD (Wetlands). The grain-size cutoff of the SBLC (SB littoral) is after the findings of Limber and others (2008).

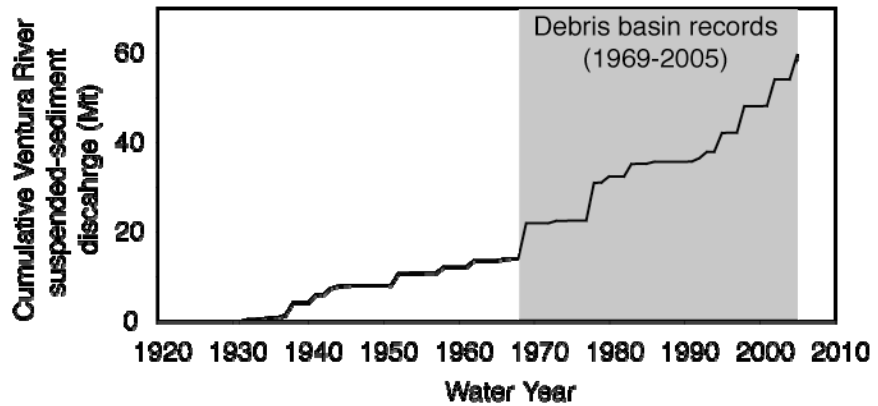


Figure 6.4. The cumulative suspended-sediment discharge during 1930-2005 from the Ventura River as assessed at USGS stream gage 11118500. Data compiled from Warrick and Mertes (in press). The shaded area represents the time for which debris-basin maintenance records are synthesized in this report.

Chapter 7—Multibeam Bathymetry

By Pete Dartnell

Introduction

The coastal waters of the Santa Barbara Channel from Point Conception to Point Mugu have now been completely mapped from the 10-m isobath out to 3 nautical miles using sonar mapping technology (fig. 7.1). This 3-year cooperative mapping effort was completed by researchers from a number of agencies and institutions, including the USGS, California State University, Monterey Bay, and Fugro Pelagos, with support from Federal (USGS and MMS), State (California Coastal Conservancy), and local (BEACON) agencies.

The mapping systems, including multibeam sonar and bathymetric sidescan sonar collected coregistered bathymetry and acoustic-backscatter data at 2-m spatial resolution. These data give unprecedented views of natural features on the sea floor, including large underwater canyons (fig. 7.2), smaller gullies, rock outcrops, and bedform fields, as well as of anthropogenic features such as oil platforms, outfall pipes, supply pipelines, and cables.

These maps are now being used to generate a series of benthic habitat and sea-floor geology maps that will not only be useful in local studies and issues, but will also become part of a larger State wide mapping effort.

Some of the bathymetry and backscatter data and interpreted habitat maps are now publicly available, and more recently collected data and reports are in the process of becoming available. Completed data are available at http://seafloor.csumb.edu/SFMLwebDATA_s2.htm#SBChannel, and a benthic-habitat map for the region offshore of Carpinteria is available at <http://pubs.usgs.gov/of/2007/1271/>. A seamless onshore-offshore geologic map surrounding the Isla Vista area is near completion and should be available in 2009 (figs. 7.3-7.4), and as part of the

California State Waters Mapping Project, sea-floor geology, sea-floor character, benthic-habitat, and sediment-thickness maps are being produced for the entire coastal region of the Santa Barbara Channel.

The full results of the completed multibeam and habitat map off Carpinteria are vetted in Barnard and others (2007). However, a detailed analysis of data from others sites is limited by the final processing schedule. Therefore, only a brief results section follows to summarize the key findings as they relate to sediment transport and management issues that are a focus of this report. BEACON will be apprised of further results when the data is formally released.

Results

The Coal Oil Point region is dominated by thin veneers of sediment and bedrock exposures. In Carpinteria, sand dominates the substrate in water depths < 20 m, where clearly visible wave-induced ripples are present. The only prominent hard-bottom area mapped in the Carpinteria region nearshore is the extension of Rincon Point, which is dominated by boulders and large rocks (fig. 7.5). The mouths of the Ventura and Santa Clara River are generally featureless and dominated by a sandy substrate. At Mugu submarine canyon, large, downward-migrating sand waves are observed in the upper reaches of canyon channels, suggesting the active transport of large volumes of sand-sized sediment from the littoral zone to the canyon system (fig. 7.2).

Conclusions

- During the last several years the entire nearshore zone from the 10-m isobath seaward to the State 3-mile limit has been mapped using multibeam and sidescan sonar.
- Numerous map products are currently in production, highlighted by high-resolution bathymetry, habitat maps, and seamless onshore-offshore geologic maps.
- The Coal Oil Point region is dominated by thin veneers of sediment and bedrock exposures.

- The substrate offshore of Carpinteria and off of the Ventura and Santa Clara Rivers is sand-dominated.
- At Mugu Canyon, abundant, long-wavelength sand waves suggest high rates of down-canyon, sand-sized sediment transport.

References

- Barnard, P.L., Revell, D.L., Eshleman, J.L., and Mustain, Neomi, 2008, Carpinteria coastal processes study, 2005-2007; Final report: U.S. Geological Survey Open-File Report 2007-1412, 129 p., [<http://pubs.usgs.gov/of/2007/1412> (last accessed March 13, 2009)].
- Cochrane, G.R., Golden, N.E., Dartnell, P., Schroeder, D.M., and Finlayson, D.P., 2007, Seafloor mapping and benthic habitat GIS for southern California, v. III: U.S. Geological Survey Open-File Report 2007-1271, [<http://pubs.usgs.gov/of/2007/1271/> (last accessed March 13, 2009)].

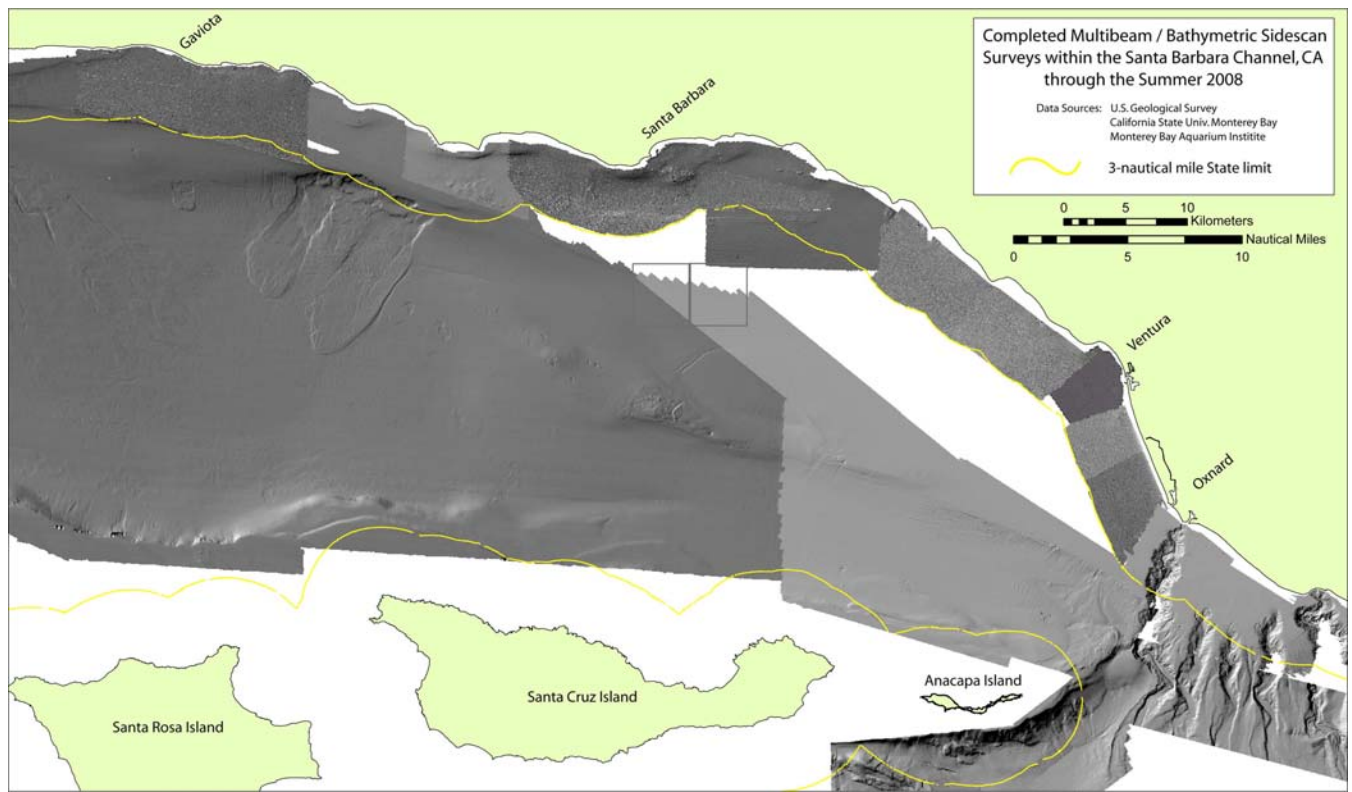


Figure 7.1. All high-resolution bathymetric surveys in the Santa Barbara Channel through summer 2008.

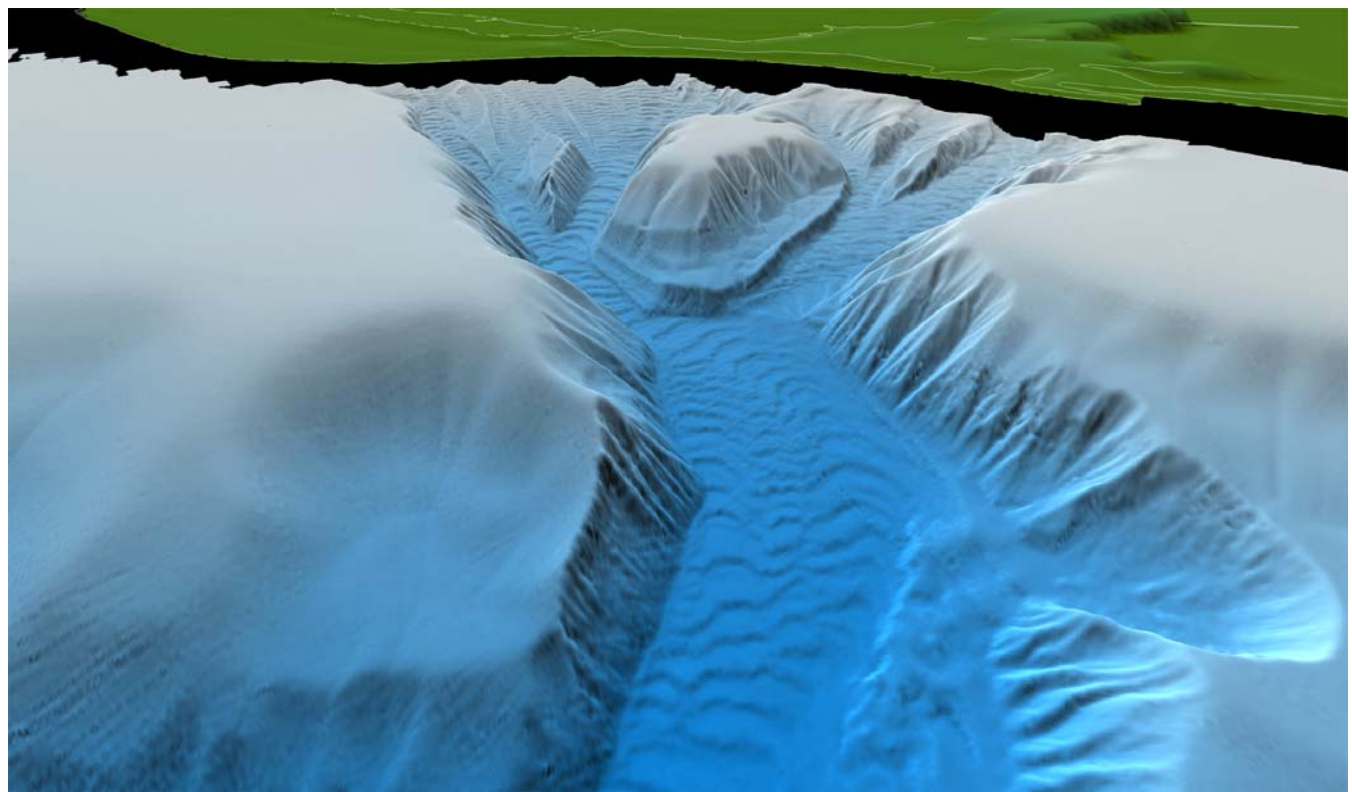


Figure 7.2. Perspective view, looking north, of the Mugu submarine canyon.

Preliminary Sea Floor Character Map -
Coal Oil Point Area, Santa Barbara Channel

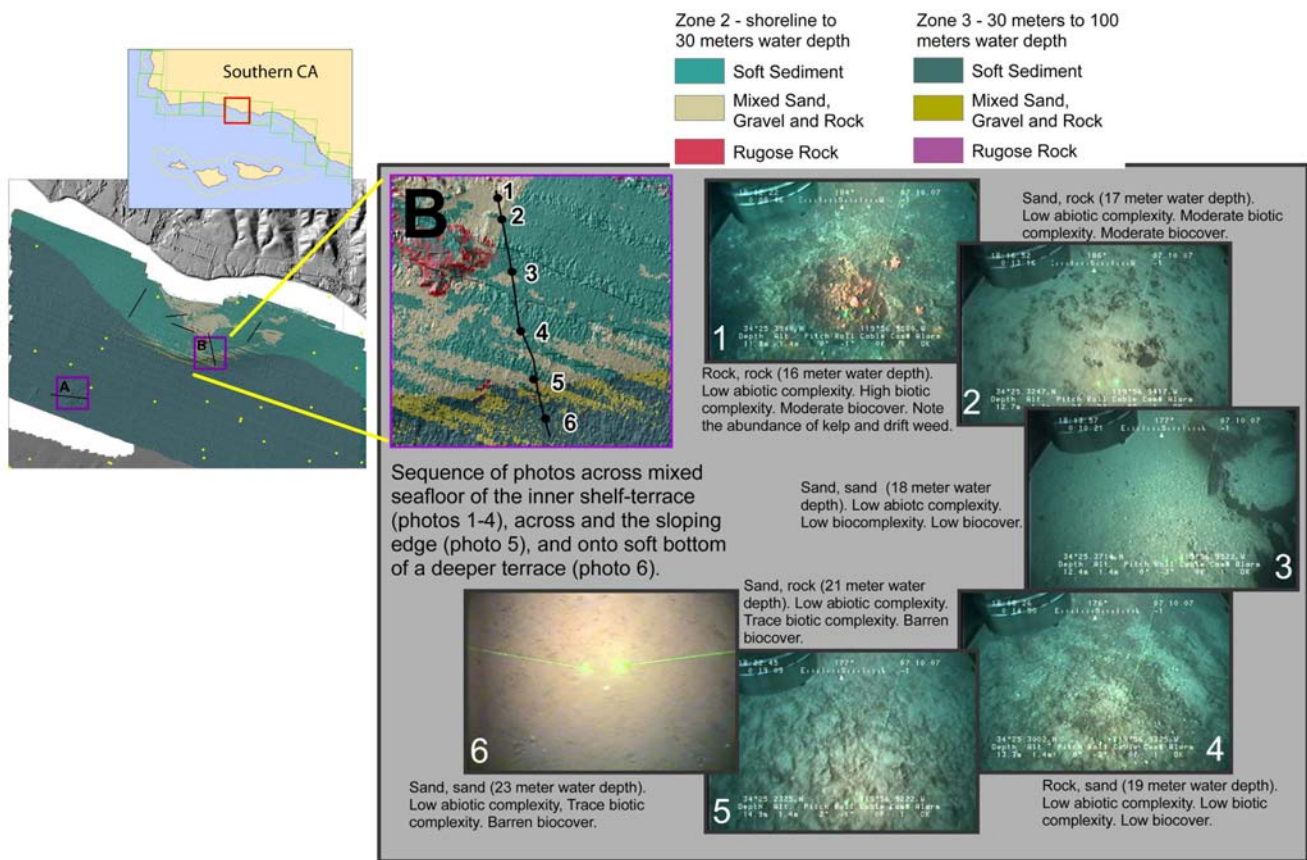


Figure 7.3. Example of sea-floor character map from the Coal Oil Point area.

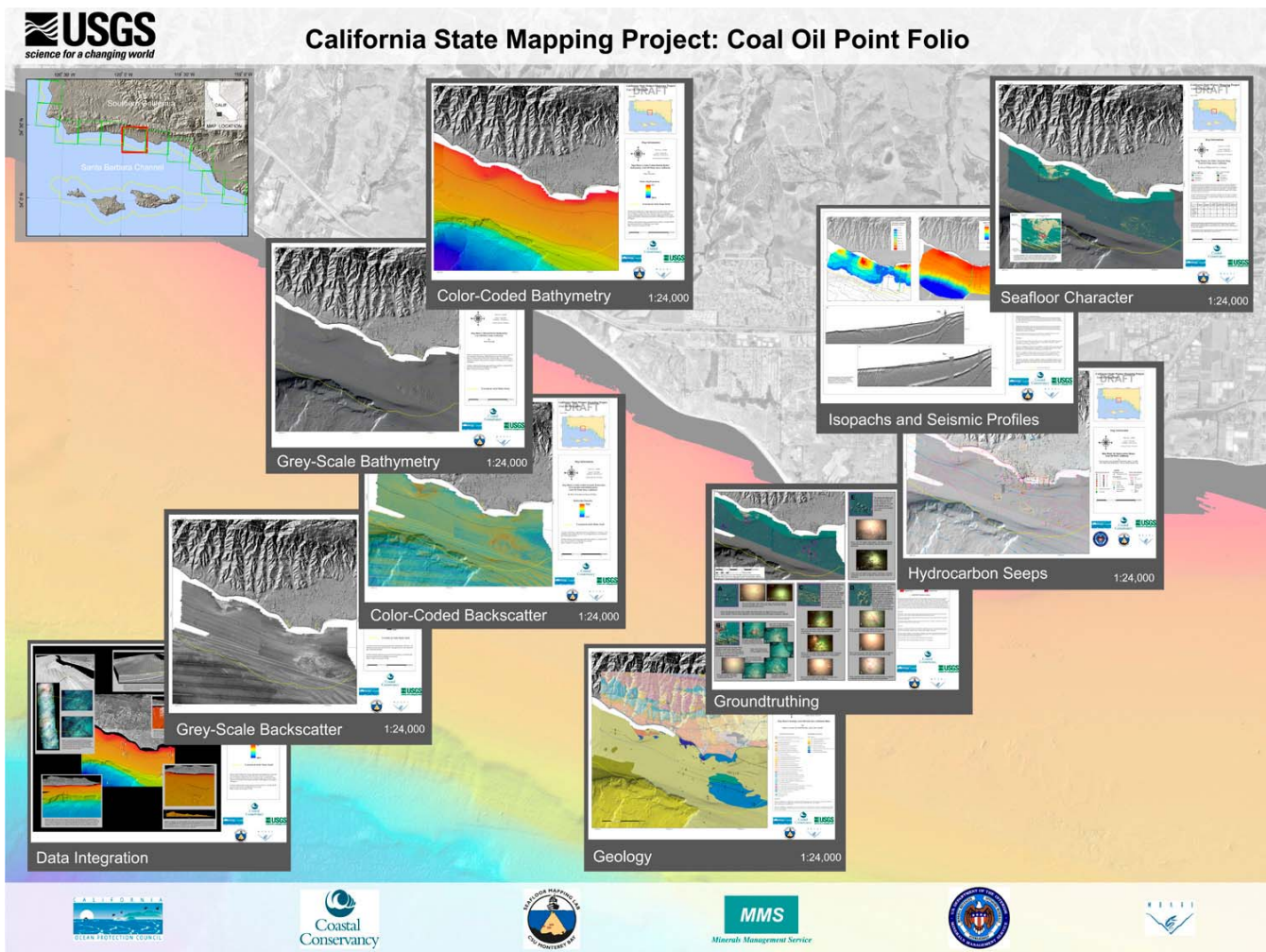


Figure 7.4. Examples of products to be released as part of the California State Waters Mapping Projects.

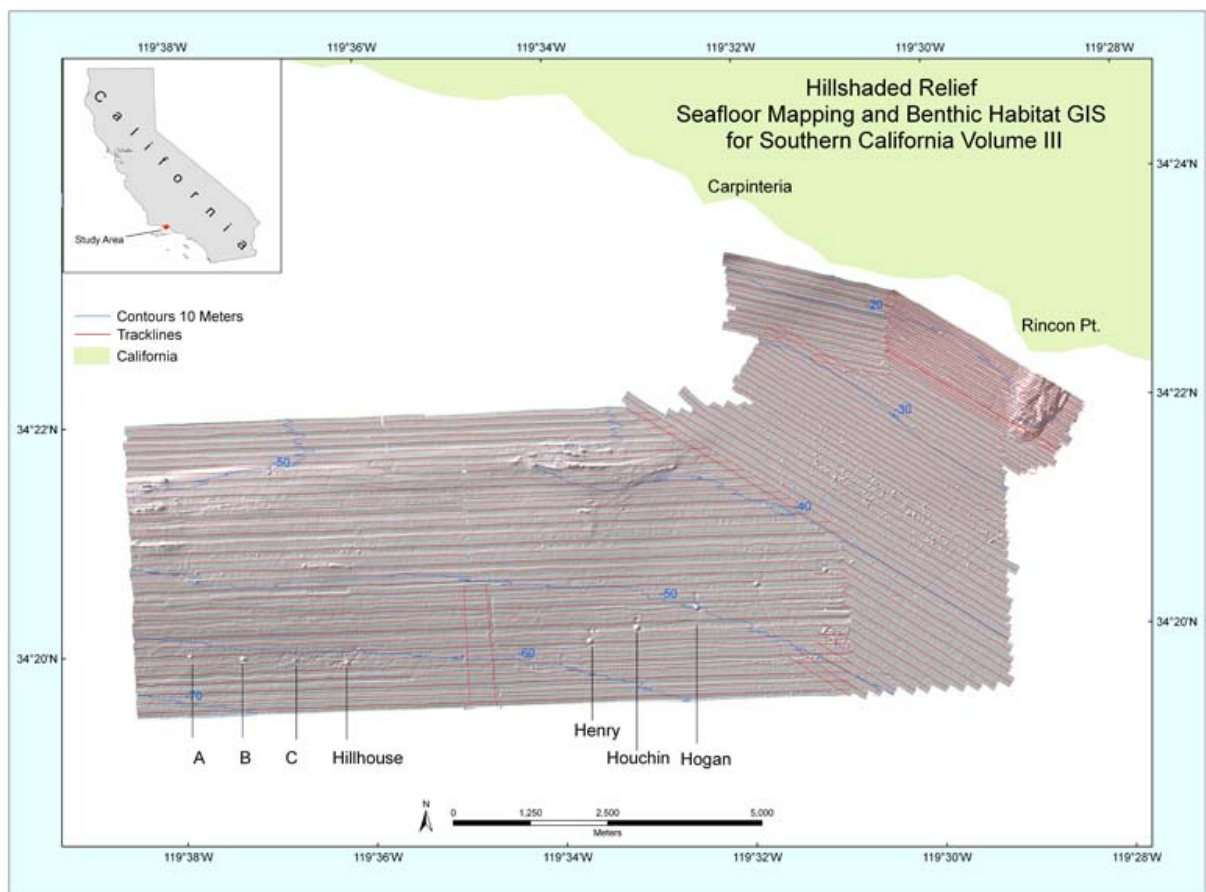


Figure 7.5. Coverage area for the 2005 Carpinteria offshore bathymetric survey .

Chapter 8—Seismic-Reflection Images of Shallow Sedimentary Deposits

By Amy E. Draut, Patrick E. Hart, and Holly F. Ryan

Full details of this USGS seismic-reflection work, including the data, can be found at

<http://pubs.usgs.gov/of/2008/1246/>.

This chapter is only meant to provide a brief summary of this work as it was not directly funded by BEACON.

Introduction

High-resolution shallow seismic-reflection data were collected by the USGS in September 2007 from the continental shelf offshore of Southern California between Goleta and Mugu Canyon (Sliter and others, 2008). These data allow newly refined characterization of the continental shelf and shallow slope, where sediment derived from steep coastal mountain ranges accumulates along a tectonically active continental margin. Interaction of sediment on this shelf and in the Santa Barbara Basin with active faults has generated large landslide features such as the Goleta slide (Fisher and others, 2005), indicating substantial geohazard potential in this area. Sedimentary deposits offshore of Santa Barbara have yielded Late Tertiary and Quaternary paleoclimate records that are among the highest resolution in the world (Behl and Kennett, 1996; Nicholson and others, 2006); additional work by the USGS was completed in 2008 to support paleoclimate research by Nicholson and others.

Data were acquired in 2007 using mini-sparker and Edgetech Chirp 512 instruments aboard the R/V Zephyr. The survey area spanned approximately 100 km of coastline (fig. 8.1) and included shore-perpendicular transects spaced 1–2 km apart that extended offshore as far as the 3-mile limit of State waters, in water depths ranging from 10 to 300 m. Subbottom acoustic penetration spanned tens to several hundred meters, and varied by location.

Images of shallow subsurface geology can be used to identify sites where removal of sediment for applications such as beach nourishment may be feasible. Seismic data alone do not, however, permit distinction between sand and mud, nor do they indicate unequivocally the degree of compaction and induration of the sedimentary deposits. Sediment on the Santa Barbara shelf that may be sufficiently unconsolidated for extraction overlies a regional unconformity representing a sea-level lowstand surface, as shown in figure 8.2. Deposits above this lowstand unconformity are Late Pleistocene to Holocene in age (Dahlen and others, 1990) and thicken toward the southeast, approaching the deltas of the Ventura and Santa Clara Rivers (see also Dahlen and others, 1990; Slater and others, 2002). Figure 8.3 shows an isopach map of sedimentary-deposit thickness above the lowstand unconformity, generated from the chirp and mini-sparker data. To produce this isopach map, the seafloor and unconformity reflection two-way travel times were picked along seismic profiles, and were output to a geographic information system (GIS) mapping program. Location and elevation data were gridded and contoured using an inverse distance-weighted algorithm (Liszka, 1984); two-way reflection times were converted to depth using a sound velocity of 1,500 m/s for the water column and 1,600 m/s for the interval between the seafloor and lowstand unconformity. Where the thickness is mapped as < 0.5 m, bedrock crops out at the seafloor or is covered by a very thin layer of sediment. Preferential accumulation of sediment in areas corresponding to coastal embayments is apparent near Goleta and Santa Barbara, as is thickening of the sedimentary package toward the southeast onto the Ventura River delta.

Conclusions

- Major depositional centers are located off Ellwood, Goleta, Miramar/Summerland, and Rincon toward the Ventura River delta.

- Shallow bedrock (< 1 m) is found off Isla Vista, Arroyo Burro, Santa Barbara Harbor, and Rincon Point.

References

- Behl, R.J., and Kennett, J.P., 1996, Brief interstadial events in the Santa Barbara basin, NE Pacific, during the past 60 kyr: *Nature*, v. 379, p. 243–246.
- Dahlen, M.Z., Osborne, R.H., and Gorsline, D.S., 1990, Late Quaternary history of the Ventura mainland shelf, California: *Marine Geology*, v. 94, p. 317–340.
- Fisher, M.A., Normark, W.R., Greene, H.G., Lee, H.J., and Sliter, R.W., 2005, Geology and tsunamigenic potential of submarine landslides in Santa Barbara Channel, Southern California: *Marine Geology*, v. 224, p. 1–22.
- Liszka, T., 1984, An interpolation method for an irregular net of nodes: *International Journal for Numerical Methods in Engineering*, v. 20, no.9, p. 1599–1612.
- Nicholson, C., Kennett, J., Sorlien, C., Hopkins, S., Behl, R., Normark, W., Sliter, R., Hill, T., Pak, D., Schimmelmann, A., and Cannariato, K., 2006, Santa Barbara Basin study extends global climate record: *Eos, Transactions, American Geophysical Union*, v. 87, no.21, p. 205, 208.
- Slater, R.A., Gorsline, D.S., Kolpack, R.L., and Shiller, G.I., 2002, Post-glacial sediments of the Californian shelf from Cape San Martin to the US–Mexico border: *Quaternary International*, v. 92, p. 45–61.
- Sliter, R.W., Triezenberg, P.J., Hart, P.E., Draut, A.E., Normark, W.R., and Conrad, J.E., 2008, High-resolution chirp and mini-sparker seismic-reflection data from the southern California continental shelf-Gaviota to Mugu Canyon: U.S. Geological Survey Open-File Report 2008-1246, [<http://pubs.usgs.gov/of/2008/1246/> (last accessed March 13, 2009)].



Figure 8.1. Location map of tracklines (from Sliter and others, 2008).

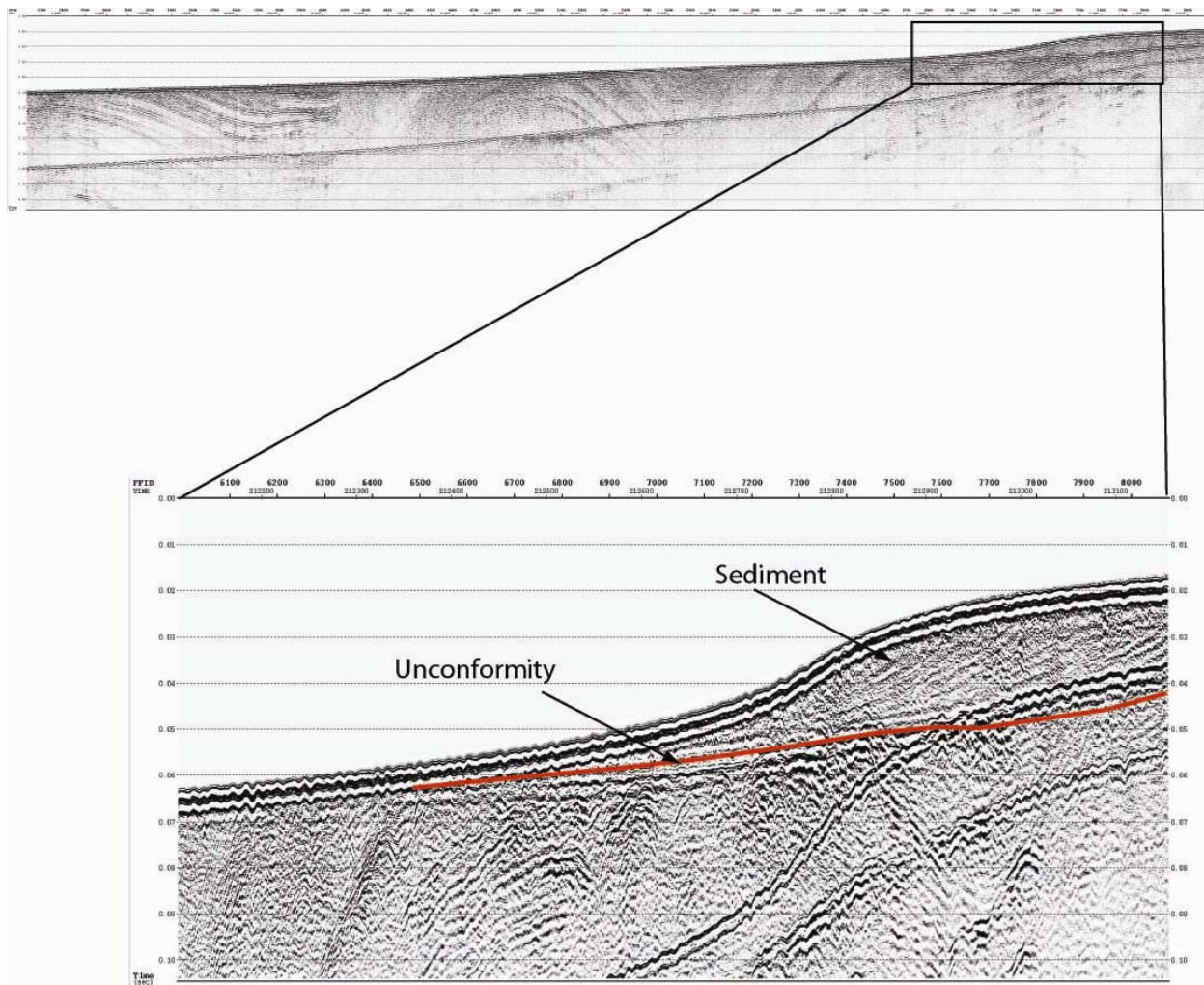


Figure 8.2. Mini-sparker data along Line SB-148 (from Sliter and others, 2008), showing sediment (including clinoforms) overlying regional lowstand unconformity.

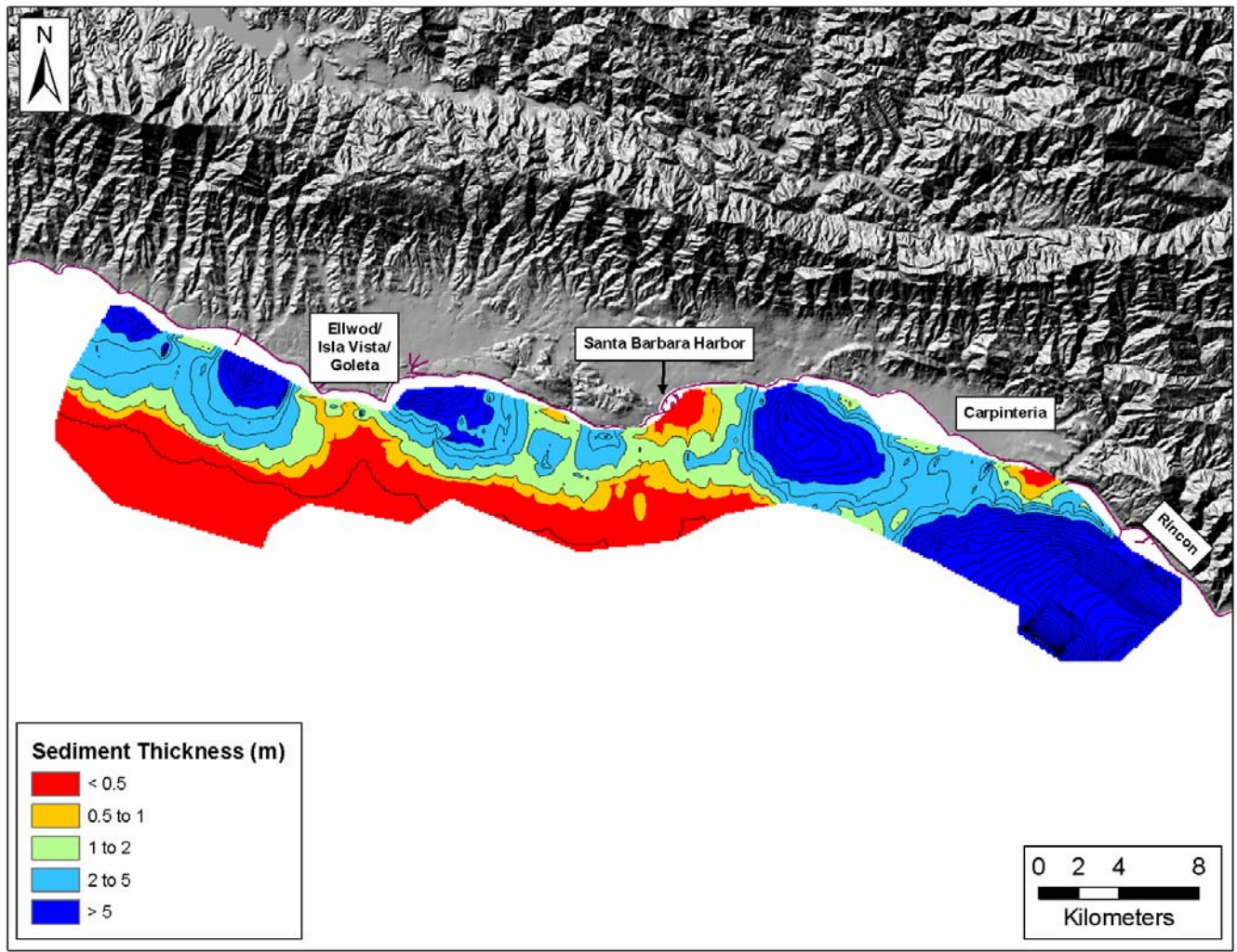


Figure 8.3. Isopach map for the survey region.

Chapter 9—Numerical Modeling Sediment Budget Analysis for the Santa Barbara Littoral Cell using Delft3D

By John Brocatus, Edwin Elias, and Patrick Barnard

This chapter is designed to summarize only the key model findings. The entire modeling report, the master's thesis of John Brocatus, is contained in Appendix E.

Introduction

The main objective of the numerical modeling is to identify and quantify the pathways of average annual sediment transport within the Santa Barbara littoral cell (SBLC), with emphasis on the sites where the shoreline erosion is persistent. The aim is to answer the following research questions: (1) how does the morphological system in the SBLC actually work, and (2) what will the future coastline evolution be in the focus areas of Ellwood/Isla/Vista/Goleta, Carpinteria, and Ventura?

The Delft3D numerical model is used to simulate the hydrodynamic and morphodynamic processes and to calculate the littoral transport rates. Subsequently, a regional sediment budget is proposed to provide insight into the net surplus or deficit of sediment during the modeling period.

To answer these research questions, the main objective is divided into two subobjectives:

- **Determine the hydrodynamic and morphologic interaction within the SBLC**
 - What are the characteristics of the hydrodynamic forcing?
 - What are the characteristics of a reduced set of wave conditions that can replace the full set of wave conditions and still represent the correct alongshore sediment transport?
- **Determine the long-term morphologic behavior within the SBLC.**
 - What are the characteristics of the alongshore sediment transport?

- What is the effect of the alongshore sediment transport on the beaches and what are the short- and long-term erosion and accretion trends?
- Are the littoral-drift rates limited by sediment supply or by wave forcing?

A Delft3D Online Morphology model is used to meet the primary objective of this study.

Another objective of this study is to reduce the computational runtimes of the simulations by simplifying the hydrodynamic input conditions. To increase the model's overall performance and to determine its sensitivity to some model parameters, a sensitivity analysis was performed.

Methods

Delft3D-FLOW Module

The main components in the Delft3D-Online modeling approach are the Delft3D-FLOW module and the Delft3D-WAVE module. The Delft3D-FLOW module (version 3.39.28) is the central module in the Delft3D-Online approach. It solves the nonlinear shallow-water equations that are derived from the three-dimensional Navier Stokes equations for incompressible free-surface flow in two (depth-averaged) or three dimensions. The system of equations consists of the horizontal momentum equations, the continuity equation, and the transport equations. While the water depth is assumed to be much smaller than the horizontal length scale, the shallow-water assumption is valid. Under this assumption, vertical accelerations are assumed to be small compared to the gravitational acceleration, and the vertical momentum equation can be reduced to the hydrostatic pressure equation.. A concise description of the basic flow equations is given in Appendix A of the full modeling report (Appendix E). For a more detailed description reference is made to the Delft3D-FLOW User Manual (WL | Delft Hydraulics, 2006) and Brocatus (2008).

Delft3D-WAVE Module

The effects of waves on flow (from forcing due to breaking, enhanced turbulence, and bed shear stress) and the effects of flow on waves (from set-up, current refraction, and enhanced bottom friction) are taken into account by online coupling of the Delft3D-FLOW and Delft3D-WAVE module. The wave effects are integrated in the flow simulation by executing the third-generation SWAN (Holthuijsen and others, 1993; Booij and others, 1999) wave processor (version 40.51A). The SWAN model solves the action-balance equation in two dimensions of spectral and geographical space and in time, with which the evolution of random, short-crested waves is calculated. SWAN accounts for wave refraction, propagation, wave-wave interaction, wave generation by wind, dissipation due to whitecapping, bottom friction, and depth-induced wave breaking. The results of the wave simulation (significant wave height, peak spectral period, wave direction, mass fluxes) are included in the flow calculations through additional driving terms. If the water level, bathymetry, or flow-velocity field changes significantly during the FLOW simulation, it is desirable to call the WAVE module more than once (van Rijn and Walstra, 2003). The wave field can thereby be updated, accounting for the changing water depths and flow velocities.

Computational Grids

Two different horizontal computational grids are applied to this study area: a low-resolution orthogonal grid and a high-resolution curvilinear grid (fig. 9.1). The first is used within the Delft3D-WAVE module, while the latter is used in both the Delft3D-WAVE and the Delft3D-FLOW module. The low-resolution wave grid has a spatial scale of 90 by 180 km to cover all physical obstacles within the area that might influence the propagation of wave energy into the Santa Barbara Channel. Point Conception and the Northern Channel Islands will refract, diffract, and dissipate incoming wave energy, so these obstacles are incorporated within the low-resolution wave grid. The cross-shore resolution

varies from approximately 550 m (nearshore) to 1,100 m (seaward model boundary). In the region of the Northern Channel Islands, the cross-shore resolution is refined to approximately 550 m to enable correct wave-energy propagation between the islands. The alongshore resolution is about 1,100 m throughout the entire grid domain. In total, the low-resolution wave grid has 22,800 grid cells.

The high-resolution curvilinear flow grid is smaller than the large wave grid and covers the morphologically active zone. The western boundary is located 10 km east of Point Conception, while the eastern boundary is located near Channel Islands Harbor. The seaward boundary stretches about 12 km offshore to ensure that the entire morphologic active zone is captured by the flow grid. The alongshore grid resolution increases from 1,100 m at the western boundary to 500 m at the eastern side of the grid domain. At the seaward boundary, the cross-shore resolution is approximately 550 m (~ the resolution of the coarse wave grid), whereas in the nearshore area it is increased to 20 m. In the alongshore direction the grid consists of 260 grid lines, with 119 grid lines in the cross-shore direction. In total, the high-resolution flow grid consists of 28,600 grid cells.

Schematization of Wave Climate

A method of reducing the run time for the simulation is to force the model with just the wave cases that contribute most to the alongshore sediment transport. To determine the reduced set of wave conditions, rough wave data first has to be classified in a wave-climate table. Primary wave properties such as significant wave height (H_s), peak period (T_p), direction, and probability of occurrence (P), are binned into wave-height and direction classes. Next, a reliable and preferably fast series of sediment-transport computations with all wave conditions has to be performed. According to Steijn (1992), the simulation time of these simulations should preferably be equal to, or a multiple of, the tidal-cycle period. Together, all these computations represent the average annual sediment transport induced by the entire wave climate. This average annual sediment transport is referred to as the target sediment

transport, and forms the basis of the schematization procedure. Parameters in SWAN were tuned such that the modeled littoral-drift rates entering the Santa Barbara and Ventura Harbors approximated the historical dredging rates (U.S. Army Corps of Engineers, unpubl. data).

The tool that takes care of the schematization procedure is the Opti-routine, which is solely based on statistical assumptions (WL|Delft Hydraulics, 2007). The schematization relies on the relative contribution of each wave condition to the target sediment transport. The schematization is not based on the sediment transport within the entire area, but only on the sediment transport through a number of predefined transects (fig. 9.2). The routine starts with the target sediment transport and all wave conditions as determined from the Coastal Data Information Program Harvest Buoy (Station 071; Scripps Institute of Oceanography, 2008). First, with all conditions still participating, the contribution of condition i to the sediment transport target is computed. In an iterative process, the wave condition that contributes least to the target will be eliminated by setting its weight to zero. To what extent the remaining wave conditions resemble the target is based on the relative root mean square error. For each randomly determined new set of weight conditions, the relative root mean square error is again calculated to determine the resemblance with the target. After all iterations, it is determined with which set of weights the target is resembled best by finding for which iteration the root mean square error is lowest. This process continues until an optimal reduced set of wave conditions exists. The selection of a “morphological representative wave climate” is based on (1) the root mean square error between the reduced and the target transport, (2) the ratio between the amount of western and southern swells and (3) the amount of wave conditions left. The 27 transects, which are more or less evenly spread over the domain, are defined to calculate the annual net sediment transport (m^3/year). All offshore points of the transects are located at the sea-boundary of the flow grid to incorporate the entire morphological active zone (fig. 9.2). The transects are oriented perpendicular to the shoreline to incorporate the alongshore

transport and to exclude the cross-shore sediment transport. From an initial set of 97 wave conditions, 10 wave conditions were selected that resemble the target sediment transport with a root mean square error of 5.6 percent. Together, the new weight factors have a probability of occurrence of 62.0 percent or 226 days a year. The final set of reduced wave conditions is listed in table 9.1.

Summary of Results

The driving components of the hydrodynamic forcing are the tide and the prevailing wave climate. The tide is characterized by a diurnal tide with a strong semidiurnal distortion. The water level difference during a single tide can be as high as two meters, with tidal velocities along the coast rarely exceeding 20 cm/s, which is verified by current meters deployed as part of this study at Coal Oil Point (Goleta focus area), Carpinteria, and the Ventura River mouth. About 75 percent of all deep-water waves originate from the west/northwest (270 to 315 degrees), and have significant wave heights ranging from 0.5 to 7.4 m. The peak period is about 10 seconds for wave heights up to 3.0 m, but increases up to 16 seconds or more for wave heights larger than 5.0 m. The south/southeast deep-water swell direction ranges from 135 to 195 degrees and contributes only 12 percent to the wave climate. The wave heights of swells from the south/southeast are, with a peak value of 4.4 m, lower than wave heights from west/northwest swells. The peak periods are relatively higher for south/southeast swells (~15.0 to 18.5 s) than for west/northwest swells (~10.0 to 18.0 s).

The wave climate is reduced to a set of ten wave conditions that (1) resemble the total sediment transport and (2) resemble the ratio between the western and the less frequently occurring southern swell. The relative root mean square error between the total sediment transport and the sediment transport resulting from the reduced set of wave conditions is 5.6 percent. Each wave condition has its own relative contribution to the total sediment transport (figs. 9.3-9.4). Four of the reduced wave conditions originate from the south/southeast whereas the remaining conditions originate from the west.

It is important to note in figure 9.3 that while the southern swell (wave conditions WC 19, 32, 42, and 63) only contributes 12 percent to the overall wave climate, these events can cause significant littoral-drift reversals in the southern/eastern half of the study area (transects 15 to 27), especially in the vicinity of the Santa Clara River mouth (transect 25). As a result gross sediment transport is much greater than net transport in this area. Further, these reversals can have an even greater impact on sediment distribution if they occur during flood events. Significant wave heights vary from 1.67 to 7.08 m, with peak periods ranging from 12.2 to 18.5 s. Together, these ten representative wave cases only occur 30 days a year, but in order to resemble the total transport, their total probability of occurrence is increased to 62.0 percent or 226 days a year. As stated in section 1.4.3 of Appendix E, hypopycnal flows account for nearshore delta formation, whereas hyperpycnal flows deposit sediment in the offshore delta. The mean annual flood discharge (Q_{maf}), which is statistically defined to be the 2.33-yr recurrence interval peak discharge, can be seen as an upper boundary at which hypopycnal flows takes place (Warrick and others, 2003).

In the sensitivity analysis of the flood river discharge, a hypopycnal flow is simulated, while the nearshore delta deposits are subject to wave impact and alongshore transport. Whereas the mean annual flood discharge (Q_{maf}) is a hypopycnal flow, the distribution pattern of the fluvial-sediment fraction is the same as for the simulation in which the average annual river discharge is used. The littoral-drift rates show a slight increase in the region of the Santa Clara River mouth (transects 23 -25). Variation in grain-size diameter does not have any significant impact on the littoral-drift rates.

The alongshore sediment transport is determined by the residual current, which accounts for the combined effect of the tidal and littoral currents. The tidal current flows opposite to the west-eastward directed littoral current that dominates the residual current. The residual current, and consequently the alongshore sediment transport, is almost uniformly directed from west to east/southeast (fig. 9.5).

Changes in coastline orientation (either abrupt or gradual) and alongshore water-depth variations result in significant alongshore sediment-transport gradients (see fig. 9.4). Although the net sediment transport is almost unidirectional from west to east, there is a distinct difference in the magnitude of the sediment-transport rates between the coastline upcoast (transects 10-15) and downcoast (transects 16-28) of Sandyland. Because the Sandyland profiles are hardly affected by southern swell, gross transports are nearly equivalent to the net transport along the coastline west of Sandyland. Downcoast of Sandyland the gross sediment-transport rates are, although dominated by western swell, significantly higher than net sediment-transport rates because of the effect of southern swell on the sediment transport.

The simulated alongshore sediment-transport rates are in good agreement with the annual dredging rates at the Santa Barbara and Ventura Harbors. The error between the simulated littoral-drift rates and the dredging rates is on the order of 10 percent, with the simulated transport rates being underestimated. However, based on the frequency of littoral-drift reversals in the vicinity of Ventura Harbor and slight reversal in the lee of the Santa Barbara Harbor, the modeled rates are likely more in line with true net littoral-drift rates. Due to these reversals, using dredging rates as a proxy for net littoral drift at these harbors could result in a potentially significant overestimation at Ventura and Channel Islands Harbors, and a slight overestimation at Santa Barbara Harbor.

Based on the analysis of the simulated residual current (fig. 9.6) and the patterns of two of the primary wave conditions (fig. 9.7) the main characteristics of the littoral-drift rates at the focus sites within the SBLC are summarized below. The primary modeling findings summarized below strongly agree with long- and short-term shoreline-change patterns determined from the field data presented in Chapters 3 and 4.

- Ellwood/Isla Vista/Goleta—The abrupt counter-clockwise rotation of the coastline at the western side of Ellwood locally increases the residual velocities (fig. 9.6C). Halfway up this beach, the

coastline bends back in the seaward direction, and the velocities decrease up to Devereaux Slough. Consequently, erosion dominates in the western half of Ellwood, and accretion dominates in the eastern half up to Coal Oil Point. While seeking equilibrium, the beach rotates clockwise and disappears around the rocks at Coal Oil Point. Isla Vista shows a similar clockwise rotation. Sediment is transported from west to east and residual velocities decrease in the lee of Coal Oil Point so accretion occurs there when sediment is available. However, the residual current accelerates through the middle of Isla Vista where severe erosion dominates. Just downcoast of Goleta Point (also known as Campus Point), the decline in the residual velocities suggests an accreting trend at UCSB and the western side of Goleta Beach. The lack of sediment being transported around Campus Point, however, prevents the beaches of UCSB and the part of Goleta Beach west of Goleta Slough from accreting. East of Goleta slough, the residual current increases and is dominated by western swell, resulting in a persistent erosion trend of Goleta Beach. The sediment transport at this part of the coastline is dominated by wave condition 24, the most common wave condition in the morphological representative wave climate (table 9.1).

- Carpinteria—There are long- (Chapter 2) and short-term (Chapter 4) trends of erosion at the City of Carpinteria Beach and accretion at the eastern side of Carpinteria State Beach. The revetment along the coastline directly upcoast of the City of Carpinteria Beach and along Sandyland maintains the erosion at the City of Carpinteria Beach by causing an acceleration of littoral drift (fig. 9.6E). While the revetment prevents erosion at Sandyland and fixes Sand Point, rotation of the coastline (which reduces the angle of wave approach and consequent alongshore transport) is restricted to the beaches in front of Carpinteria. The fixed shorelines in Sandyland prevent the

adaptation of the coastline to the prevailing wave condition and maintain the relatively large angle of wave approach associated with the predominant western swells.

- Rincon Parkway—Substantial littoral-drift acceleration around Rincon Point and deceleration in the lee of the point promotes local erosion and accretion, respectively. These model predictions agree with decadal-scale accretion observed locally at La Conchita (see Chapters 3 and 4). Conversely, acceleration of the littoral current at Oil Piers and attendant erosion has led to the implementation of hard stabilization measures there.
- Ventura and Santa Clara River mouths—Gross sediment-transport rates are large in this region because of the orientation of the southwest-facing coastline. Swells, coming from either the west or the south, have maximum impact on the sediment transport, while the deep-water angle of wave approach is on the order of 45 degrees for both directions. Littoral-drift acceleration at Surfer’s Point has led to long-term chronic erosion pressures there, and the south-facing San Buenaventura State Beach encounters erosion as a result of the large angle of wave approach of western swells and associated high littoral-drift gradients. The groin field in this area was designed to trap sediment, slowing littoral drift. A dredging bypass recovers the disruption in the littoral drift of the Ventura Harbor breakwater. The increasing effect of sediment transport from southern swell enlarges the gross, but reduces the net sediment transport, resulting in a long-term accreting trend downcoast of the Ventura Harbor.
- Other Observations—The acceleration of the residual current immediately downcoast of East Beach in Santa Barbara contributes to chronic erosion in front of the Biltmore (see Chapter 3, BEACON line 12). Deceleration of the residual current further downdrift in the vicinity of Summerland and Padaro (see Chapters 3 and 4, BEACON lines 14 and 15) appears to correspond broadly with observed accretion in these areas.

Sediment supply, particularly the anthropogenic reduction of sediment supply to the SBLC by damming, trapping of sediment in debris basins, urbanization of fluvial systems, and armoring, is not the sole control on local, long-term pockets of erosion. Although the Campus Point region at UCSB may be limited by sediment supply, erosion in other areas appears to be heavily influenced by the prevailing wave climate and the local orientation of the coastline. Locally large transport gradients exist due to variability in coastline orientation. Many of the beaches that encounter long-term erosion have a strong increase of the littoral-drift rate at the upcoast side. The littoral drift rate decreases along the beach and consequently accretion occurs at the downcoast side of the beach. Under these conditions the beaches would normally rotate clockwise to decrease the angle of wave approach for the prevailing wave condition. However, the orientation of many beaches in the SBLC is controlled by the underlying, hard-rock geology, so the shoreline has limited ability to rotate in response to littoral drift gradients, resulting in shoreline erosion hot-spots that are largely fixed through time. Therefore, structural controls on shoreline orientation and sediment supply are the critical factors affecting local erosion and accretion in the SBLC.

Conclusions

- Local erosion and accretion patterns in the SBLC are well explained by modeled littoral-sediment transport gradients.
- Significant littoral-drift reversals at the Ventura and Channel Islands Harbors, due to western and southern wave energy, result in dredging rates that may significantly exceed the true net transport rate.
- Littoral-drift acceleration at Goleta, Carpinteria, and Surfer's Point correlates with short- and long-term erosion trends in those areas.

- Deceleration of littoral-drift rates near La Conchita and the Santa Clara River mouth correspond with the decadal-scale accretion noted in those locations.
- Geologically-controlled shoreline orientation and sediment supply are the critical factors controlling local shoreline behavior.
- Rotation of beaches predicted in modeling agrees with observed trends at the Ellwood/Isla Vista/Goleta and Carpinteria focus areas.

References

- Booij, N., Ris, R.C., and Holthuijsen, L., 1999, A third-generation wave model for coastal regions—1. Model description and validation: Journal of Geophysical Research, vol. 104, no. C4, p. 7649-7666.
- Brocatus, J., 2008, Sediment budget analysis of the Santa Barbara Littoral Cell. Deltas University, M.S. Thesis, 105 p.
- Holthuijsen L.H., Booij, N., and Ris, R.C., 1993, A spectral wave model for the coastal zone: Proceedings of 2nd International symposium on ocean wave measurement and analysis, New Orleans, p. 630-641.
- SCRIPPS Institution of Oceanography, 2008, The coastal data information program: San Diego, Integrative Oceanography Division, Scripps Institution of Oceanography, [<http://cdip.ucsd.edu> (last accessed March 13, 2009)].
- Steijn, R.C., 1992, Input filtering techniques for complex morphological models: Report H 824.65, WL|Delft Hydraulics, The Netherlands.
- Van Rijn, L.C., and Walstra D.J.R., 2003, Modelling of sand transport in Delft3D-Online: Report Z 3624, WL|Delft Hydraulics, The Netherlands.
- WL|Delft Hydraulics, 2006, Delft3D-FLOW Manual version 3.13, Simulation of multi-dimensional hydrodynamic flows and transport phenomena, including sediments: Delft, The Netherlands.

WL|Delft Hydraulics, 2007, Schematisation of boundary conditions for morphological simulations -
unpublished report: Delft, The Netherlands.

Warrick J.A., and Milliman, J.D., 2003, Hyperpycnal sediment discharge from semiarid southern
California rivers: Implications for coastal sediment budgets: Geology v. 31, no. 9, p. 781-784.

Table 9.1. Morphological representative wave climate as derived from the Coastal Data Information Program Harvest Buoy (Station 071; Scripps Institute of Oceanography, 2008).

Wave condition	Significant wave height , in meters	Peak period, in seconds	Direction, in degrees	Weight factor	
				Original	New
19 1.	67	15.71	188 0.	0136	0.0080
24 1.	74	12.24	279 0.	0419	0.4637
32 2.	21	15.39	174 0.	0014	0.0391
35 2.	24	15.47	237 0.	0006	0.0014
62 3.	75	18.53	170 0.	0009	0.0002
63 3.	95	18.50	187 0.	0003	0.0002
69 3.	74	13.12	294 0.	0213	0.0911
88 5.	71	15.53	278 0.	0006	0.0053
89 5.	74	12.78	295 0.	0001	0.0080
99 7.	08	14.13	307 0.	0003	0.0027

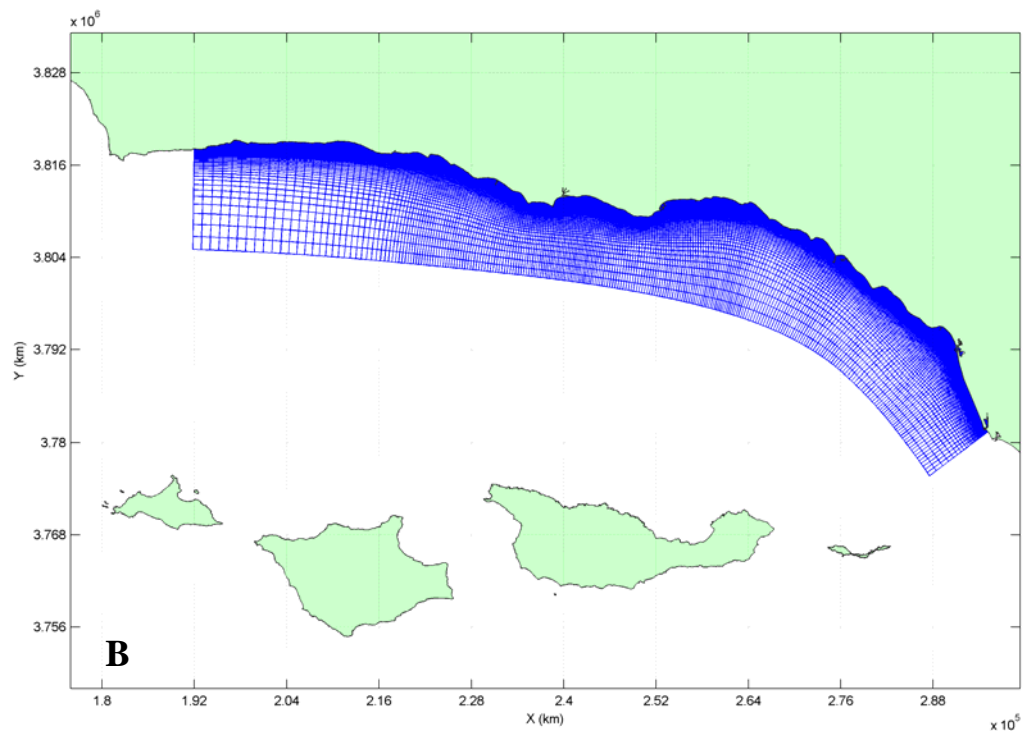
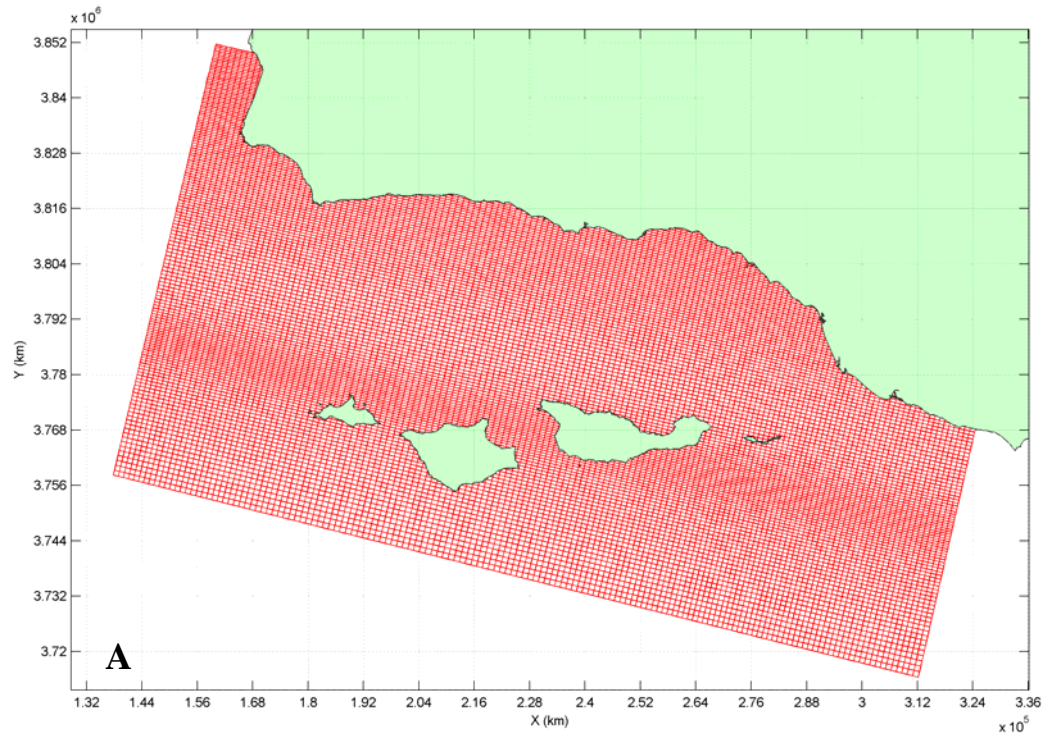


Figure 9.1. Computational grids. *A*, Wave grid. *B*, Flow grid. The flow grid is also used as a nested wave grid to ensure a high grid resolution in the surf zone.

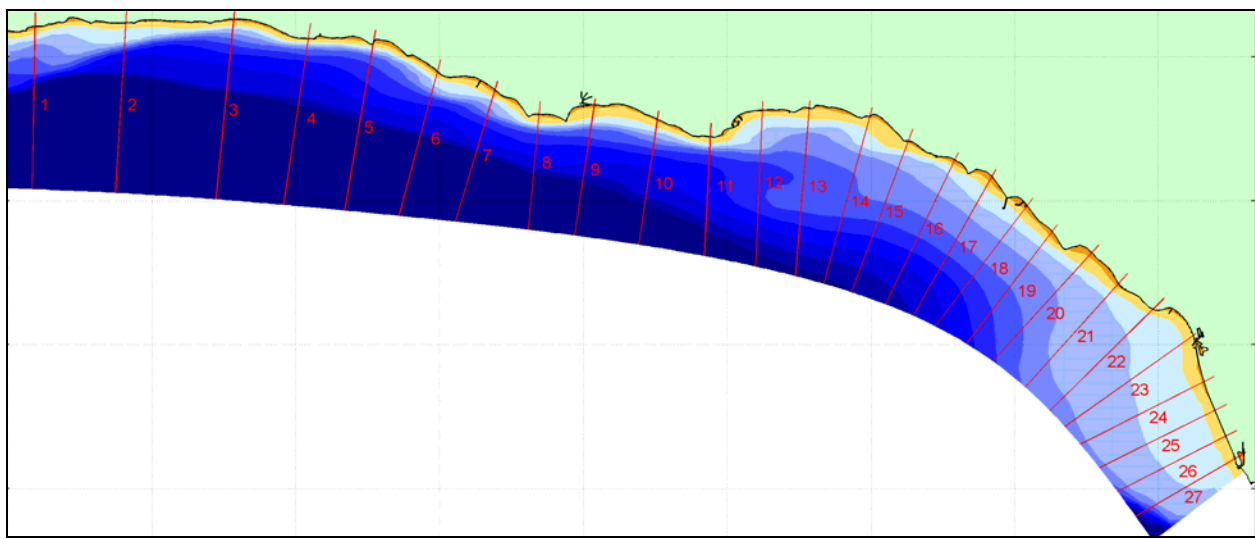


Figure 9.2. Overview of the 27 predefined transects. Bathymetry shading is at 10m intervals.

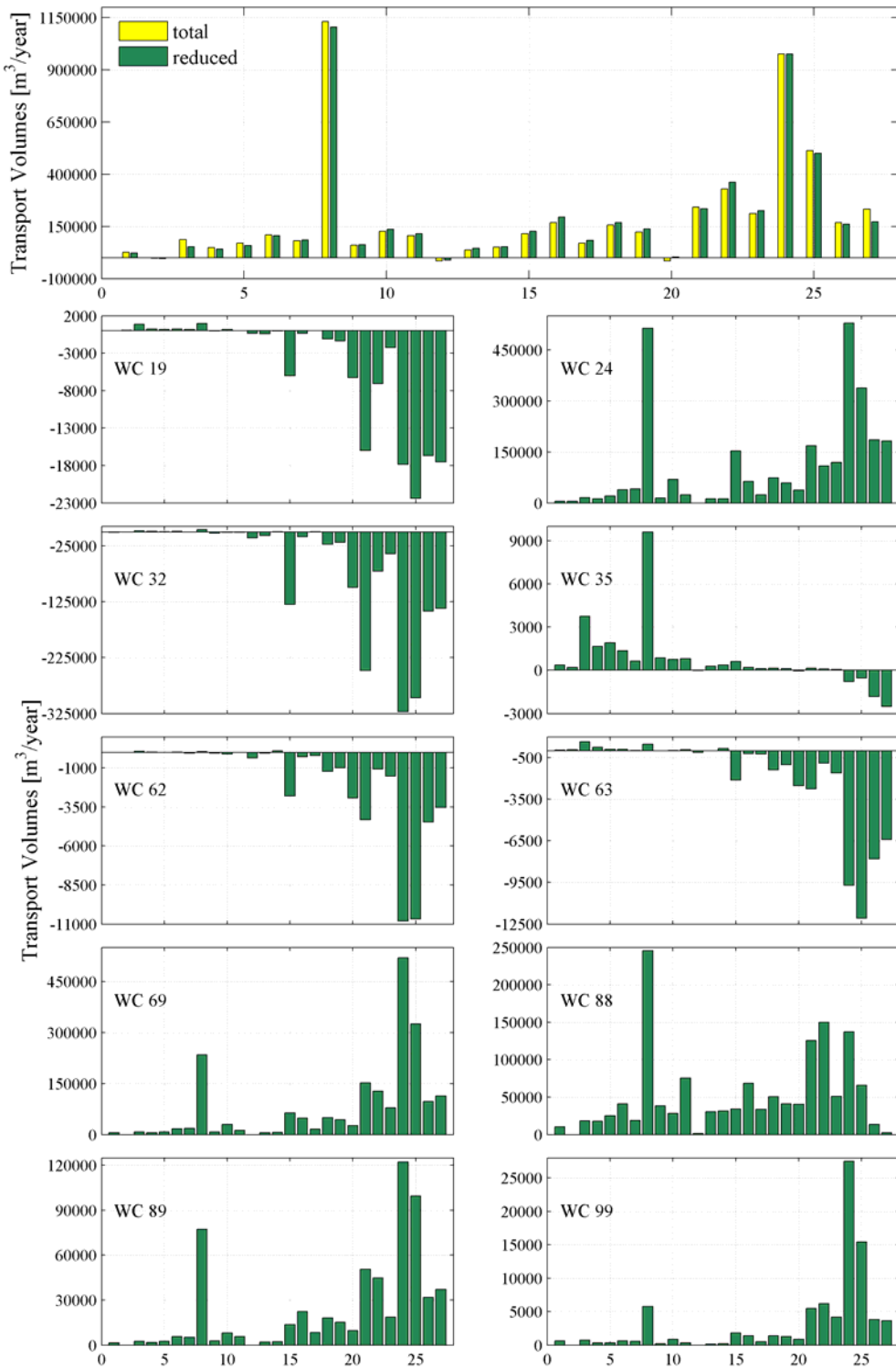


Figure 9.3. *Top panel*, Comparison of the nonvalidated littoral-drift rates for the entire (green) and the reduced (yellow) wave climate. The relative root mean square error is 5.6 percent. *Bottom panels*, Individual sediment-transport contributions for each wave condition (WC) within the reduced wave climate. Negative transport values indicate north and/or westward transport.

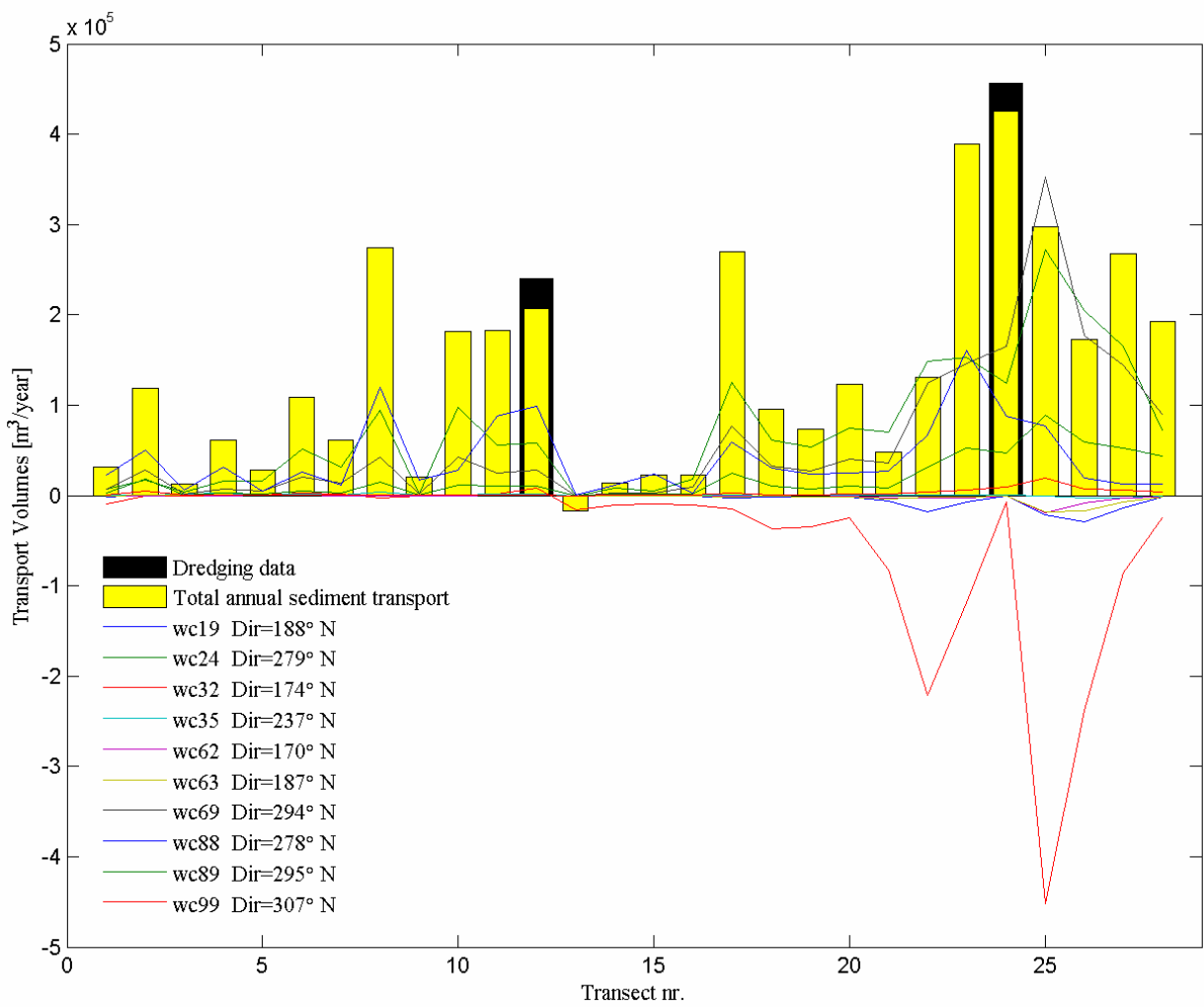


Figure 9.4. Modeled total annual sediment transport (yellow bars), and individual contributions for each wave condition in the morphologically representative wave climate (colored lines). Dredging volumes at Santa Barbara and Ventura Harbors (black bars) are shown for reference. WC, Wave condition.

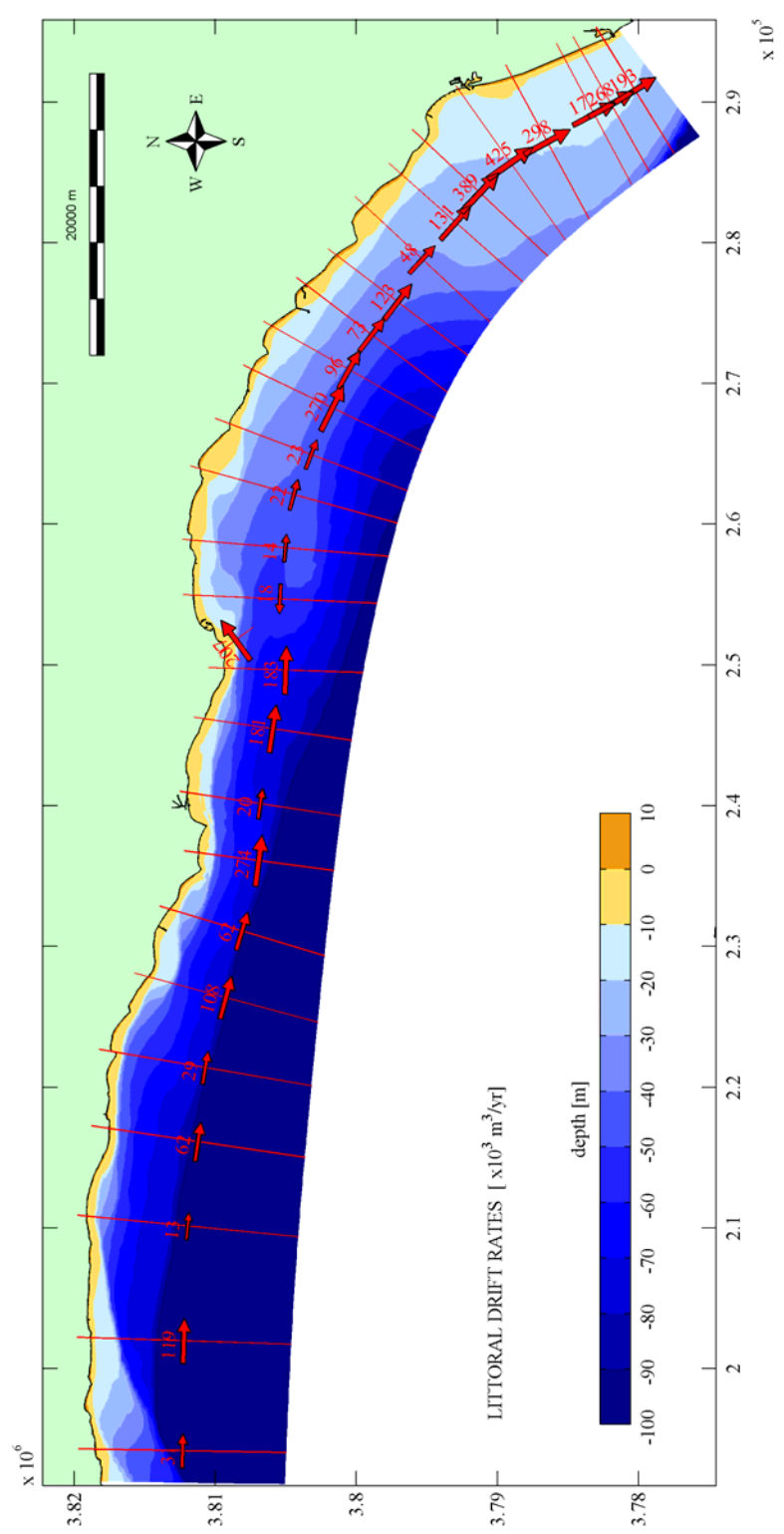


Figure 9.5. Residual sediment-transport vectors for the Santa Barbara Channel.

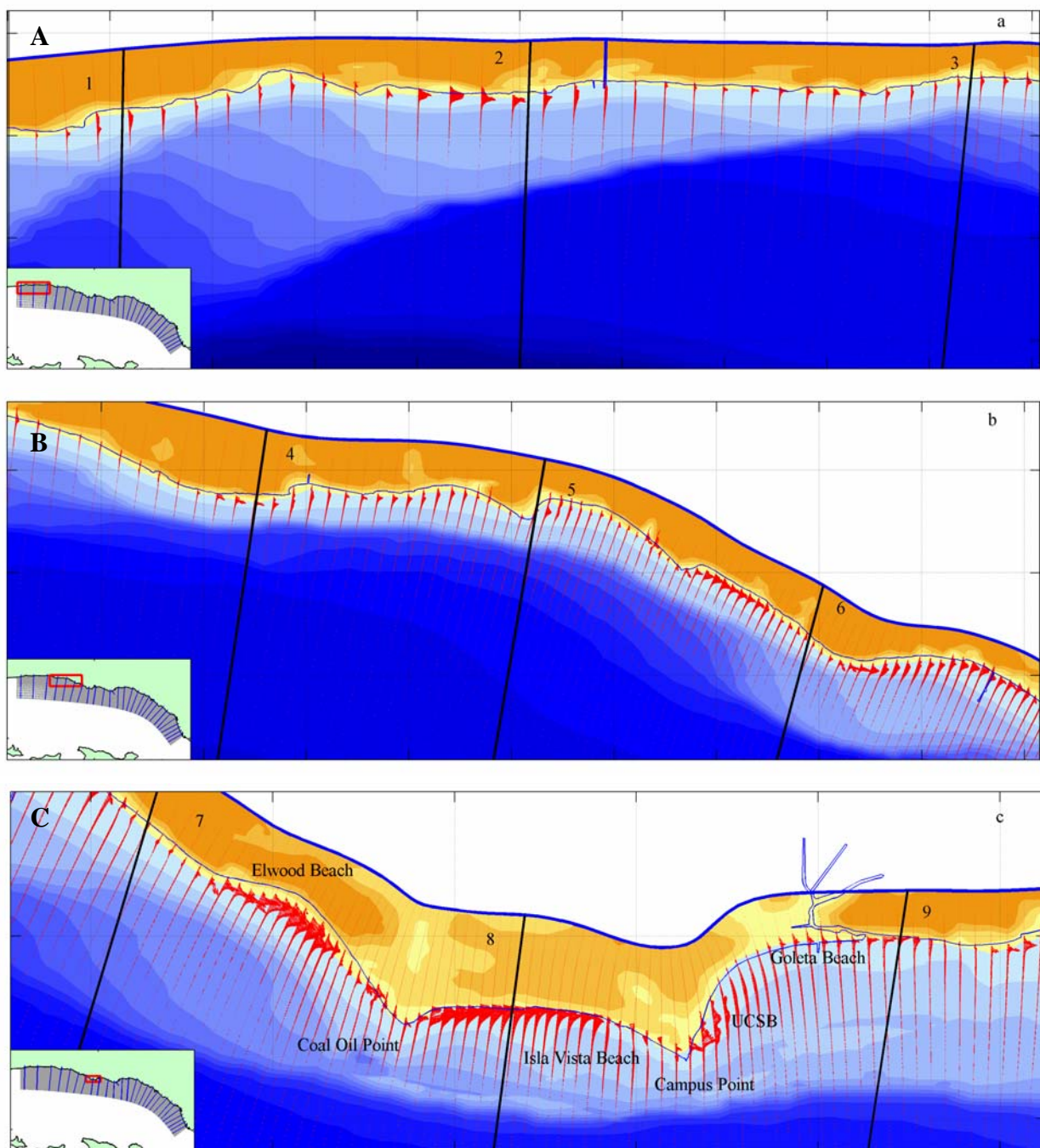


Figure 9.6. Residual current patterns in the Santa Barbara littoral cell along the Gaviota Coast to Goleta Beach. *A*, Updrift segment; *B*, Middle segment; *C*, Downdrift segment. Longer arrows indicate higher potential sediment-transport rates.

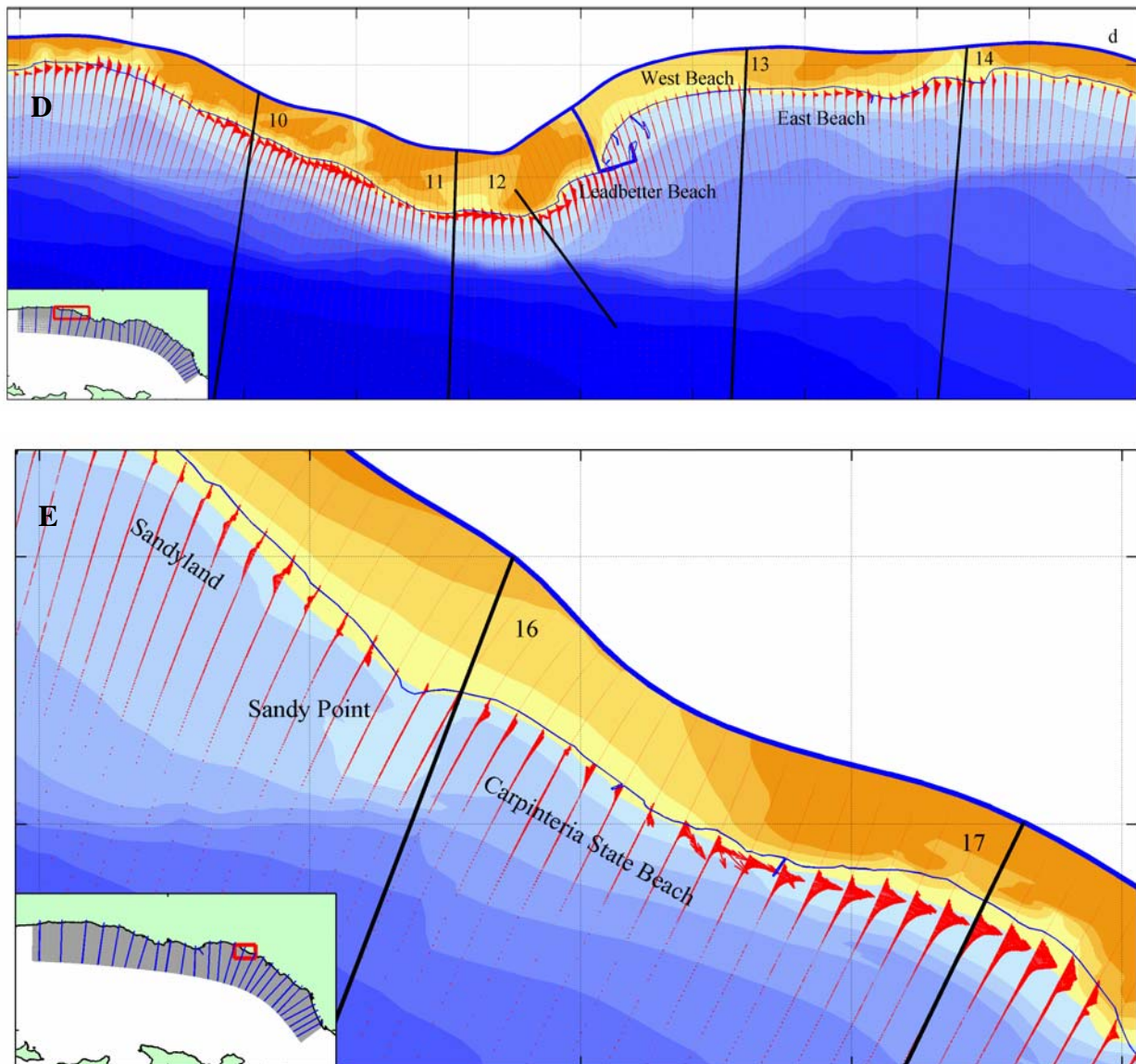


Figure 9.6 (cont.). Residual current patterns in the Santa Barbara littoral cell from *D*, the Santa Barbara area to *E*, Carpinteria. Longer arrows indicate higher potential sediment-transport rates.

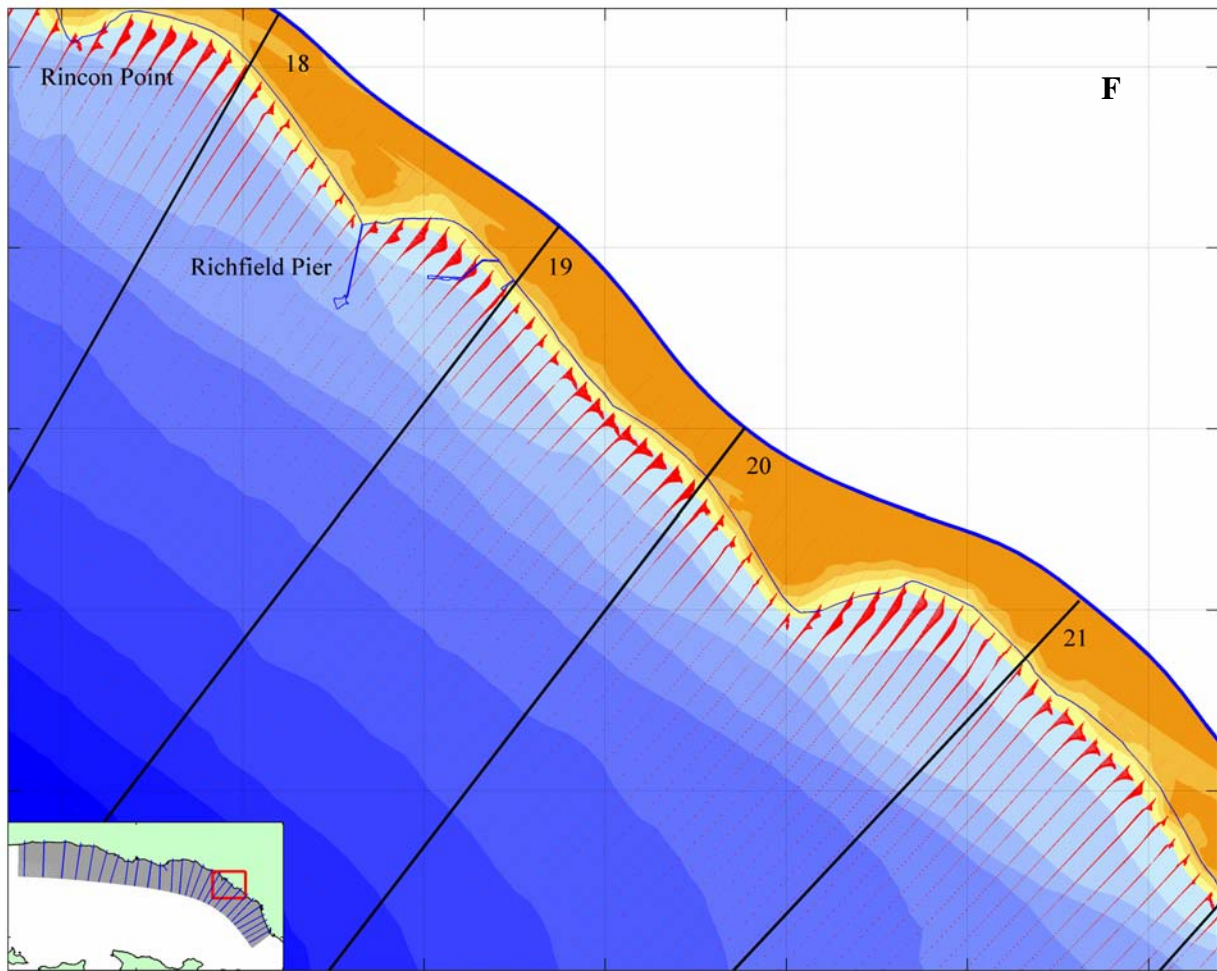


Figure 9.6 (cont.). *F*, Residual current patterns in the Santa Barbara littoral cell along the Rincon Parkway. Longer arrows indicate higher potential sediment-transport rates.

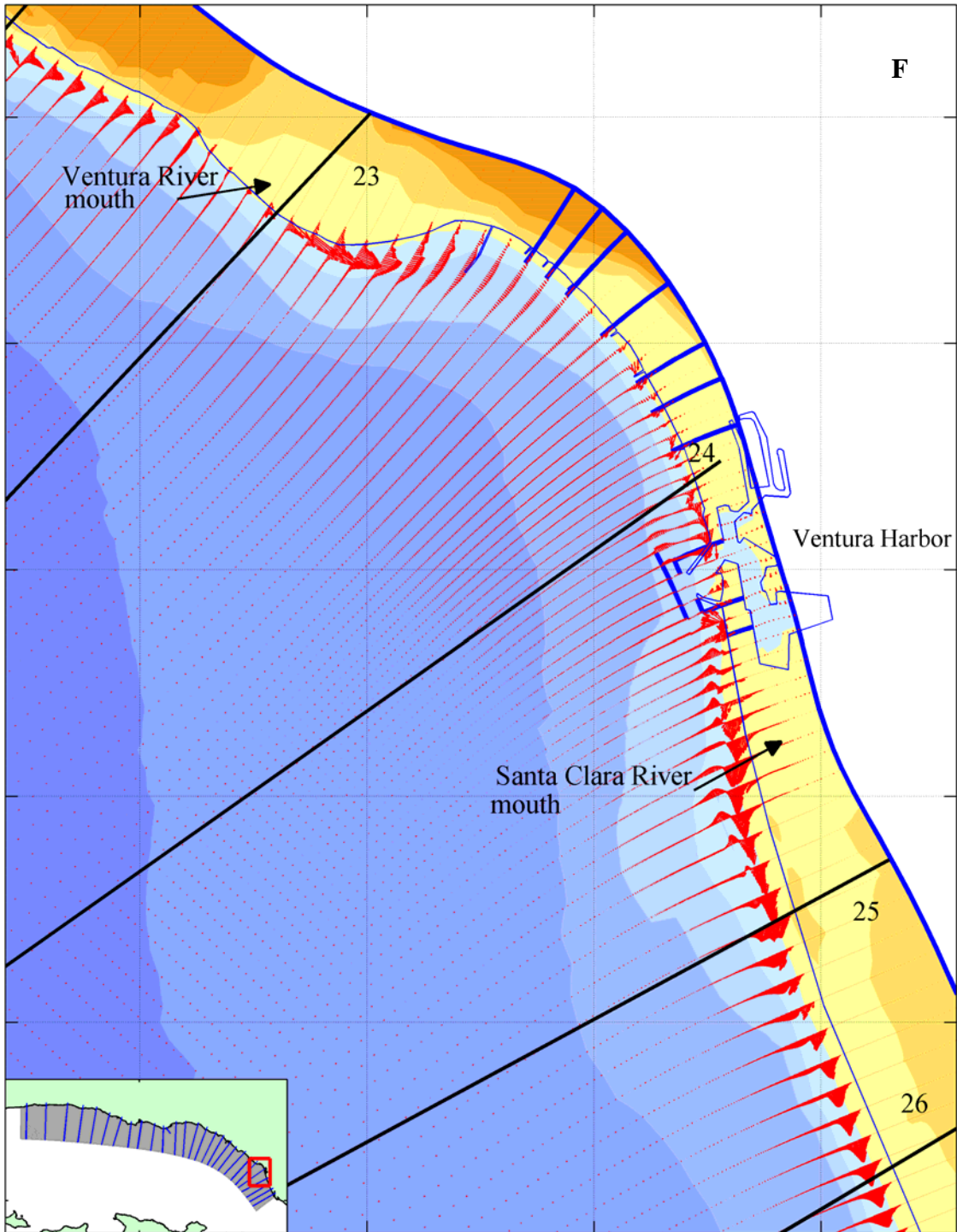


Figure 9.6 (cont.). G. Residual current patterns in the Santa Barbara littoral cell in the Ventura/Santa Clara River mouths focus area. Longer arrows indicate higher potential sediment-transport rates.

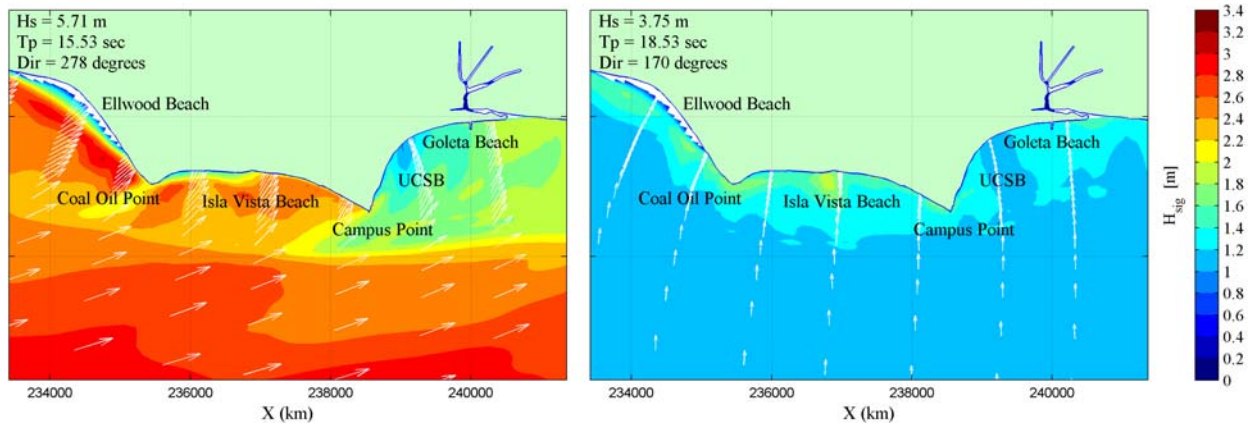
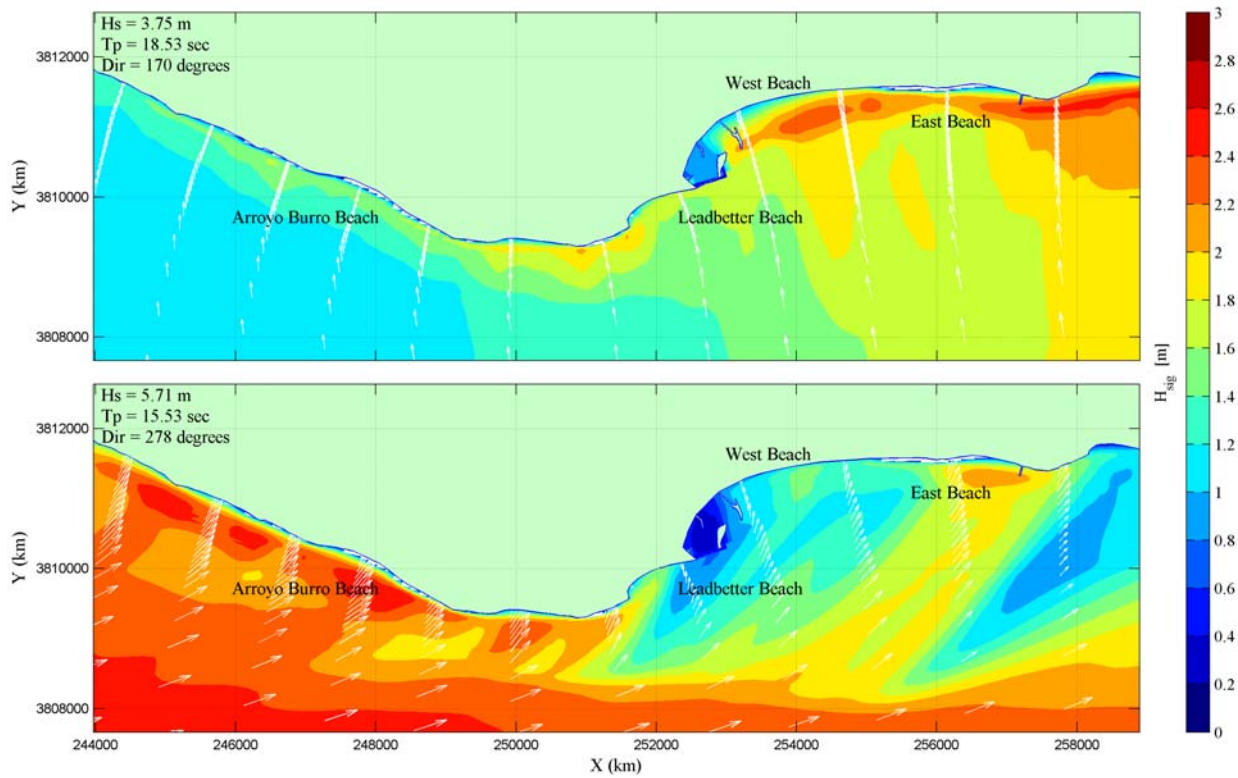
A**B**

Figure 9.7. Significant wave height and direction for wave conditions 88 and 62 at *A*, Ellwood/Isla Vista/Goleta, and *B*, Santa Barbara Harbor. White arrows indicate wave direction.

C

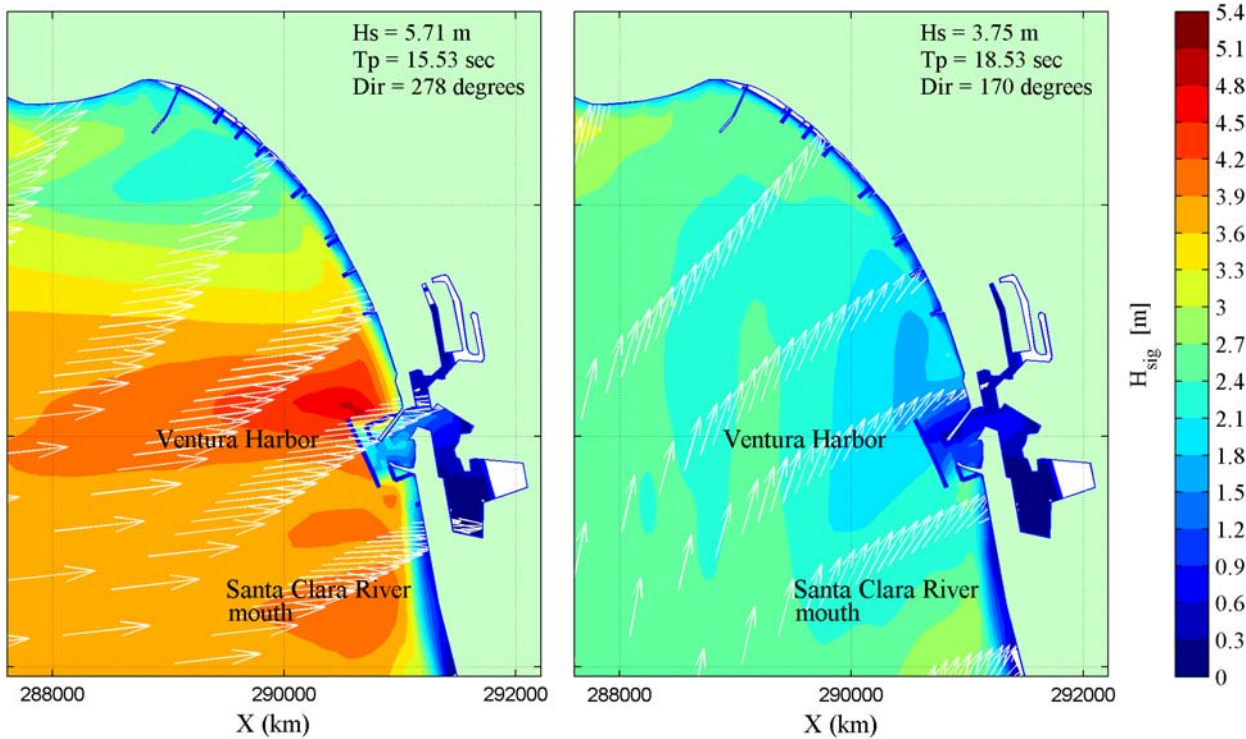


Figure 9.7 (cont.). C, Significant wave height and direction for wave conditions 88 and 62 at Ventura/Santa Clara River mouths. White arrows indicate wave direction.

Chapter 10—Project Synthesis

The Santa Barbara littoral cell (SBLC) is a complex coastal system with significant management challenges. The coastline ranges broadly in exposure to wave energy, fluvial inputs, hard structures, and urbanization. Geologic influence (structural control) on coastline orientation exerts an important control on local beach behavior, with anthropogenic alterations and the episodic nature of sediment supply and transport also playing important roles.

Short- and long-term temporal analyses of shoreline change, beach width, and volume change show no obvious trends in regional beach behavior. Extensive armoring along the SBLC has accreted the back beach, narrowing beach widths and in some cases increasing sediment transport. Unarmored beaches have exhibited mild erosion while maintaining similar widths. Harbor constructions have had notable impacts on downdrift beaches, but once the coastal system has equilibrated the signal becomes strongly damped and littoral-drift gradients driven by natural shoreline orientation again become dominant. Sediment inputs from the Santa Clara River dominate sediment processes on beaches to the south.

The SBLC is dominated by episodic flood and storm-wave events. Exceptionally large accretion signals along this stretch of coastline are closely tied to major flood events when large amounts of sediment are deposited in deltas. These deltas decay over time, supplying downdrift beaches with sediment. Storm-wave impacts and gradients in alongshore transport can lead to beach rotations and migrating erosion hotspots when geological controls are weak. Annual and seasonal rates of cross-shore and alongshore transport are at least 2-3 times higher for the more west- and southwest-facing beaches south of the Ventura River as compared to the more sheltered beaches to the west/north. Gross littoral transports are good approximations of net littoral transports for beaches west/north of Ventura as transport is almost purely unidirectional. However, significant transport reversals occur intermittently in

the east/south, especially adjacent to the Ventura and Channel Islands Harbors. For this reason, and due to the episodic nature of flood and storm wave events, using dredging rates from the harbors at Ventura and Channel Islands as a proxy for drift rates may be invalid.

An extensive grain-size investigation of the surface and shallow subsurface in the nearshore region of the SBLC identified only two sites for potential beach-nourishment material: offshore of Santa Barbara Harbor and Oil Piers. However, seismic-reflection lines offshore of Santa Barbara suggest shallow bedrock (< 1 m), so the volume of coarse material in this area may be limited. Sampling of the Santa Clara River delta was minimal, but this site could be promising.

Numerical modeling shows that local beach behavior is primarily influenced by local littoral-drift gradients, which are in turn controlled by natural shoreline orientation. Given the high rates of net littoral drift and the relatively insignificant cross-shore transport in the SBLC, the SBLC should be considered a sediment-limited system (as opposed to a transport-limited system). Management actions, such as any future beach nourishment, would likely have a severely limited life span without employing additional measures that adequately address local littoral-drift gradients to retain added sand.